



## THE SEISMICITY OF KILAUEA'S MAGMA SYSTEM

By Fred W. Klein, Robert Y. Koyanagi, Jennifer S. Nakata, and Wilfred R. Tanigawa

### ABSTRACT

Earthquake-hypocenter data collected by the Hawaiian Volcano Observatory during 1960–83 provide a wealth of information on the active processes of Kilauea's magma system. The magma conduits produce volcanic earthquakes that occur in episodic swarms often accompanied by tilt changes or eruptions. Tectonic earthquakes in Kilauea's flanks and some parts of the upper mantle occur more continually and are punctuated with mainshock-aftershock sequences. Volcanic earthquakes also have smaller magnitudes, a greater proportion of small events, and frequent association with tremor. Three-dimensional earthquake patterns and separation of volcanic and tectonic seismicity can be visualized in a series of hypocenter depth slices and cross sections. Earthquakes reveal a magma system consisting of a vertical conduit from Kilauea caldera to about 60 km depth, two shallow rift zones radial to the caldera, and a shallow magma reservoir joining these three conduits.

The shallow magma reservoir is an aseismic zone beneath the south edge of Kilauea caldera. The reservoir is surrounded on two sides by intensely active rift conduits centered near 3 km depth, above by a seismically active cap in the caldera mostly between 1 and 2 km depth, and below by the vertical magma conduit having earthquakes as shallow as 7 km. The deformation centers are mostly between 2 and 4 km depth, near the top of the aseismic zone that is between 3 and 7 km depth. Inflation of the reservoir produces earthquakes above and in the adjacent rift conduits by extension in the summit region and slow magma intrusion into the rifts.

The vertical magma conduit, as defined by earthquakes, consists of two parts: a narrow and nearly vertical pipe between 7 and 20 km depth mostly having swarms of volcanic earthquakes, and a zone that widens into a diffuse and south-dipping region between 20 and 60 km depth. Earthquakes in the deeper conduit are larger in magnitude and more continuous in time, as if tectonic in origin. Earthquakes below 40 km depth merge with the Hawaiian hot spot below Kilauea, Loihi and Mauna Loa Volcanoes. Kilauea's deep earthquakes also join a band of seismicity along the island's south coast, which is probably caused by shear stress applied from Kilauea's mobile south flank and by the growing and asymmetrical weight of the Kilauea shield. The number of earthquakes in the vertical conduit dropped dramatically at the time of the  $M=7.2$  Kalapana earthquake in 1975. This decrease indicates that conduit earthquakes are partly driven by regional stresses derived from the seaward push of the south flank.

The vertical distribution of conduit earthquakes shows pronounced gaps near depths of 5, 13 and 20 km. The first gap results from the magma reservoir between 3 and 7 km depth, and the 13-km-depth gap is probably bounded by the Moho and the prevolcanic oceanic sediments. The depth of 20 km is also a

gap for earthquakes in the surrounding lithosphere, marks the change from volcanic-style earthquakes above to tectonic below, and is probably the zone of the neutral stress axis in the lithosphere bending under the island's weight. The vertical magma conduit thus is similar to a passive, weak zone in the lithosphere that triggers earthquakes mainly driven by regional stresses.

Kilauea's rift zones produce shallow swarms of varied intensity and complexity arising from periods of summit inflation, slow intrusions, and rapid intrusions that may also result in eruptions. Slow intrusions may feed the rifts adjacent to the caldera during inflation, send slow pulses of magma (and hence earthquakes) down the rifts, or be aseismic except at the terminus of the intrusion where magma collects. Much of this paper documents earthquakes from swarms during 1962–84. To examine the dynamics of intrusion and dike formation, computer plots for each swarm are designed to show the position, depth, size and shape of the seismic zone, deflation and seismicity with time, and migration of earthquakes along the rift or vertically.

Rapid intrusions generally begin with earthquakes in a small volume near the main rift conduits at 3 km depth and may spread along the rift and upward. Migration and growth speeds are about 0.1 to 6 km/h. An intrusion often loses upward speed as it approaches the surface, or downrift speed as it nears its terminus. Earthquakes occur at and behind the front of the dike as the conduit widens and the walls compress. Barriers within the rifts, where the conduit is pinched shut or stress is concentrated, often generate clusters of earthquakes and act as places where intrusions start and stop. The most prominent barriers are adjacent to the summit magma reservoir and in the east rift zone below Pauahi Crater and Mauna Ulu, but many are present along both rifts. The Pauahi-Mauna Ulu barrier is important because many intrusions start there and move uprift and downrift, and it also marks a bend in the rift, where it intersects the Koaie fault zone. A possible small magma reservoir below Pauahi Crater is recognized by the absence of earthquakes; this reservoir is dammed uprift of the Pauahi-Mauna Ulu barrier.

The most common earthquake migration direction at Kilauea is downrift and is presumably driven by gravity and a pressure gradient along the magma conduit. Upward earthquake migration is visible in many intrusions and reflects ascending magma presumably driven by buoyancy forces. The east rift zone between Kilauea caldera and Mauna Ulu is an anomalous zone of earthquake migration; uprift, downrift and bilateral migration of earthquakes are equally likely. This zone is also unusual in its high degree of activity, its northwest trend oblique to the regional stress, its shallowness of earthquakes, its ability to feed two intrusions simultaneously, and its short 2- to 3-hour interval from the beginning of an intense earthquake

swarm to the start of an eruption. The upper east rift zone thus seems to be a multitiered and complex honeycomb of conduits. The various directions of earthquake migration in this area may result from a complex pattern of stresses and pressure gradients, or from an uplift-traveling pressure pulse within magma flowing downrift. The latter may have caused the reflection of a downrift earthquake migration off a rift barrier back uplift, as observed in many intrusions.

Intrusions occur in larger cycles that alternate between rifts. Intrusions are often grouped in pairs or triplicates within a few weeks of each other—they may retrace the same path or occur adjacent to their predecessors. In addition, four complete cycles of east-rift-zone to southwest-rift-zone shifts, each lasting 3–4 years, occurred during 1968–83. A basic cycle consists of several east-rift-zone intrusions (beginning near Mauna Ulu), a period of inflationary swarms at the summit, a major intrusion usually in the southwest rift, and about one year of no new intrusions before beginning the cycle again. This cycle may be an oscillatory tectonic process involving the south flank. A series of intrusions in one rift apparently helps trigger other intrusions and also compresses the adjacent flank. This compression inhibits additional intrusions and hinges open the other rift until a switch occurs. The Kalapana earthquake in 1975 may have disrupted the basic pattern set by the first two cycles: periods of inflationary swarms did not occur in 1977 and 1980–81, no southwest-rift intrusions occurred in 1977–78, and the switch from the southwest rift zone to the east rift zone in 1982–83 occurred without a pause.

## INTRODUCTION

Few volcanoes in the world are as seismically active and as extensively monitored as Kilauea has been since 1960. The Hawaiian Volcano Observatory (HVO) has steadily expanded its seismic network and data-processing effort, and routinely analyzes several thousand earthquakes each year. This paper draws heavily on a catalog of about 70,000 earthquakes of all types carefully gathered by the past and present staff of HVO during 1962 through 1983.

Kilauea is a tholeiitic shield volcano, and eruptions occur in the summit caldera or from either the east rift zone (ERZ) or southwest rift zone (SWRZ) (fig. 43.1). The basic model of Kilauea has been refined by HVO through the years, but is not fundamentally changed from that stated by Eaton and Murata (1960) and Eaton (1962). The key feature of the Kilauea model is a magma reservoir beneath the caldera. The basic eruption cycle begins with gradual inflation of the magma reservoir as it fills via feeder conduits from below. The inflation is revealed by a bulge of the ground surface and by an increase of small earthquakes within the caldera. The summit becomes unstable when the barriers holding back the magma give way and magma rapidly intrudes the caldera or the rifts. Formation of vertical dikes appears to be the dominant process in rift-zone intrusion (for example, see Macdonald, 1956; Fiske and Jackson, 1972; Swanson and others, 1976a; Pollard and others, 1983). The intrusion may take a few hours or days and is revealed by a rapid deflation of the summit, inflation or extension above the new dike, an intense earthquake swarm caused by stress surrounding the new dike, harmonic tremor, and an eruption if the dike reaches the surface.

## THE SUMMIT MAGMA RESERVOIR

Deformation data provide the best evidence for the location and depth of the magma reservoir beneath Kilauea caldera. Using tilt data from 1960, Eaton (1962) determined a center of deflation 3–4 km beneath the southern part of the caldera. Fiske and Kinoshita (1969) obtained similar depths and a migrating pattern of uplift deformation centers using leveling data from 1966 and 1967. Dieterich and Decker (1975) used level and trilateration data from 1967 to infer a vertically elongate zone of inflation extending from about 1 to 3 km depth. Ryan and others (1983) modeled several subsidence events as magma withdrawal from a sill-like body. Careful inversions of tilt, level and trilateration data from several inflation and deflation episodes during 1966–70 produced a set of about 26 deformation centers within and just outside of the southern part of the caldera (Dvorak and others, 1983). The deformation centers scattered within a radius of about 2 km from a point 2 km south-southeast of Halemaumau Crater. Depths were mostly between 2 and 4 km, but occasional deformation centers may have been as deep as 7 km. The buried centers of deformation coincide with the seismically defined magma reservoir.

The above papers inferred that the magma reservoir is in fact a honeycomb of interconnected fluid pockets from the many different deformation centers. The top of the reservoir complex is about 2 km beneath the southern part of the caldera, and it extends at least to 4 km depth. The nature of magma storage below 4 km is difficult to determine from deformation measurements, because surface displacements are dominated by the shallowest active parts of the reservoir and because parts of the reservoir below 4 km may be too weak to partake in large elastic changes.

The magma reservoir was delineated seismically and was spatially related to the dynamics of intrusions and earthquake swarms (Koyanagi and others, 1976a, 1976b). Using selected summit earthquakes during 1971–73, they identified several regions: (1) a vertical conduit below about 7 km depth delineated by mostly long-period earthquakes, (2) a region of relatively low seismicity between about 3 and 6 km depth that they interpreted as the magma reservoir, (3) a seismically active cap above the magma reservoir, and (4) two seismic zones that form the uppermost parts of the rift zones adjacent to the reservoir. Their study also related the temporal activity of these regions to the eruption cycle. The cap above the magma reservoir is mainly active during periods of inflation and prior to eruptions and intrusions. The rift zones adjacent to the reservoir are mainly active when magma intrudes the rift zones and deflates the reservoir.

The three-dimensional distribution of hypocenters beneath Kilauea's summit and upper ERZ was clarified by a transparent model and series of perspective figures by Ryan and others (1981). Using the same 1971–73 data as Koyanagi and others (1976a), Ryan and others expanded the discussion of magma storage and transport and identified the same seismic and aseismic regions. In addition, the latter paper identified a vertical pipe below the upper ERZ and inferred a feeder conduit connecting its base with Kilauea's main conduit. The pipe was about 3 km downrift of Kilauea caldera (1 km southwest of Kokoolau) and was defined by

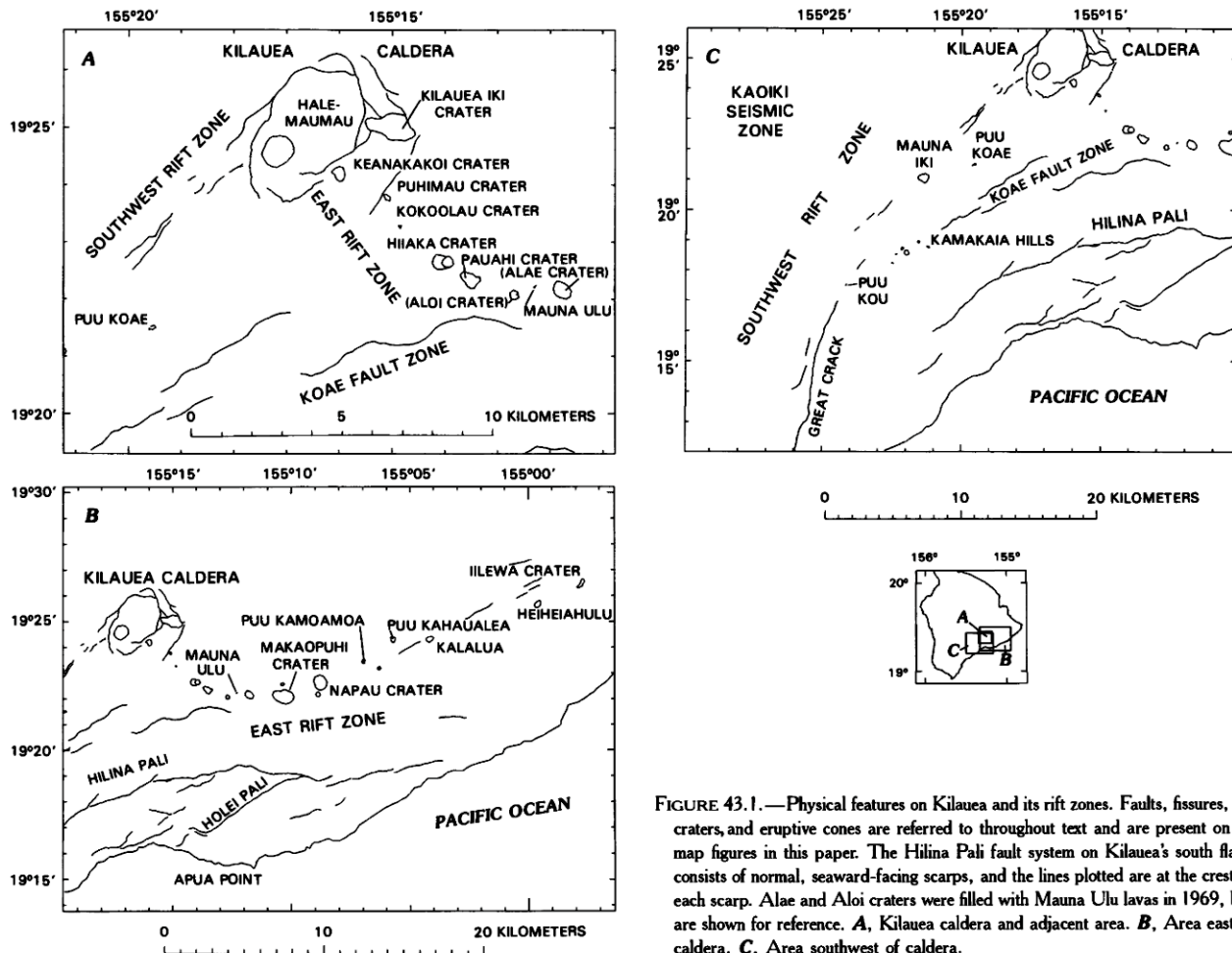


FIGURE 43.1.—Physical features on Kilauea and its rift zones. Faults, fissures, pit craters, and eruptive cones are referred to throughout text and are present on all map figures in this paper. The Hilina Pali fault system on Kilauea's south flank consists of normal, seaward-facing scarps, and the lines plotted are at the crest of each scarp. Alae and Aloi craters were filled with Mauna Ulu lavas in 1969, but are shown for reference. *A*, Kilauea caldera and adjacent area. *B*, Area east of caldera. *C*, Area southwest of caldera.

hypocenters between 1.9 and 5.7 km depth. This ERZ pipe is not visible in the present study, which uses a much expanded and revised data set.

In addition to seismicity, the newer technique of three-dimensional seismic-velocity inversion reveals the presence and location of Kilauea's magma reservoir (Thurber, chapter 38; 1984). The reservoir is recognized as a zone at least 0.5 km/s slower than the surrounding rock, and its position coincides with that obtained from other methods within the resolution of the technique.

#### INFERRING MAGMA FROM EARTHQUAKES

Ideally Hawaiian earthquakes could be used to infer the positions and dynamics of magma conduits and storage reservoirs, but several precautions must be heeded when doing this. Most importantly, earthquake generation requires rock that is both stressed and brittle. In addition, rock that already contains fractures

or faults is far more likely to be seismically active than an equivalent perfectly homogeneous region. Aseismic regions, however, may be either unstressed, unfractured or hot and ductile. Direct associations, therefore, cannot always be made between seismicity and magma. In addition, pressured magma as a source of stress can generate earthquakes in brittle rock that is adjacent to or intermixed with the magma conduit. Earthquakes may occur on systems of fault planes between echelon tips of active dikes (Hill, 1977). Thus, two possible lines of thought could lead one to infer that magmatic zones are either seismic or aseismic. Thus, other factors such as earthquake time behavior, their relation to deformation measurements and geology must be considered. Relating seismicity to magma is not a simple process, but requires a fabric of related observations and assumptions.

We generally interpret regions of swarm seismicity to be zones of dike intrusion or magma conduits (the rift zones or vertical feeder conduit). An aseismic region adjacent to volcanically related seismicity is either an inferred zone of primary magma storage (the

summit magma reservoir) or a stable block (such as Kilauea's north flank).

Earthquake locations have both systematic and random errors, and give a somewhat blurred view of the magma system. Largely because of a finite number of stations and an inability to perfectly model the true three-dimensional velocity structure, the earthquake location error and hence resolution in the summit region is typically several hundred meters and sometimes more. Therefore, resolving structures of meters to tens of meters in size is hopeless, although determining and using a three-dimensional velocity model offers some improvement locally (Thurber, chapter 38; Thurber and others, 1984).

All earthquakes in Hawaii are ultimately attributable to volcanism, but several characteristics of seismicity can be used to infer the closeness of its relation to magma. We use the term "volcanic" earthquake for those that are in or immediately adjacent to magma conduits. By "tectonic" earthquake, however, we mean those that are at least one step removed from a magma conduit: although deriving their driving stress from dike intrusion or volcano growth, they may be several kilometers from any magma. Kilauea's volcanic earthquakes occur beneath its mappable rift zones and summit caldera, where they are less than 5 km deep. Volcanic seismicity is also typical of the vertical conduit below the reservoir, which extends to 55–60 km depth. Tectonic seismicity occurs on Kilauea's active flanks, such as south of the rift zones (for example, Koyanagi and others, 1972; Crosson and Endo, 1982), and in the Kaoiki seismic zone between Mauna Loa and Kilauea's SWRZ (for example, Endo and others, 1978; Koyanagi and others, 1984; Endo, 1985). These flank earthquakes typically occur between about 5 and 13 km depth. Location and depth are thus good discriminants of volcanic and tectonic earthquakes.

The time behavior of a sequence, seismic  $b$ -value, maximum magnitude and association with tremor also are significantly different in volcanic and tectonic earthquake source areas. Volcanic earthquakes at Kilauea typically occur in swarms (a sequence more or less isolated in time and without a single dominating mainshock). The swarm may last for hours or days if it accompanies rapid dike intrusion in the summit or rift zones, or it may be days or weeks long if driven by the gradually inflating magma reservoir. Tectonic earthquakes, however, occur both continuously and in mainshock-aftershock sequences. Mogi (1963) interpreted earthquake swarms as characteristic of concentrated sources of stress and heterogeneous material properties (such as magma conduits and dike swarms), and mainshock-aftershock sequences as typical of more homogeneous regions (such as volcano flanks). Swarms are also typical of geothermal regions. Because intrusions and eruptions generally produce both earthquake swarms and tremor, their frequent association implies that moving magma is a direct cause for both.

In addition to swarm character, volcanic earthquakes on Hawaii have other distinguishing characteristics. As will be discussed later, volcanic events generally show higher seismic  $b$ -values, which is the slope of the statistical frequency-magnitude distribution. The maximum magnitudes of tectonic events are larger because these regions can sustain higher stress over a larger volume and because the

faults or other stressed structures that can slip in a single event are larger than in volcanic earthquake regions. The  $M=7.2$  Kalapana earthquake in 1975 (for example, Ando, 1979) ruptured nearly the entire length of Kilauea's south flank. The Kaoiki seismic zone broke with a  $M=6.6$  event in 1983 (Koyanagi and others, 1984). By contrast, the largest volcanic events located near Kilauea's magma system are about magnitude 4.

The differing behavior of earthquake sequences in time, the  $b$ -values and maximum magnitudes of volcanic and tectonic earthquakes are all expressions of the differing regimes in which they occur: the magmatic zones are heterogeneous and highly fractured, and have concentrated sources of stress; the tectonic flanks are more homogeneous in stress and material properties. Kilauea's earthquakes are somewhat analogous to those on plate boundaries on a larger scale around the world: the characteristics of volcanic earthquakes are typical of spreading ridges, and tectonic events bear resemblance to those at transcurrent faults and subduction zones.

Note that many of the differences we infer between volcanic and tectonic earthquakes are statistical or based on a property of a group of events. These methods will of course not work for a single earthquake. No difference may be apparent in individual seismograms between the two event types, but discrimination occurs only after it is located and assigned to a region known to be volcanic or tectonic. One may thus use either location or group behavior to determine the type of a group of events, and only one type of information may be available at a sparsely monitored volcano or one whose magma system has a poor surface expression.

Earthquakes elsewhere in Hawaii are analogous to those at Kilauea. The submarine volcano Loihi generates earthquakes of both types, indicating that it is an active volcano with mobile flanks (Klein, 1982a). Mauna Loa's summit and rifts produce volcanic seismicity (for example, Decker and others, 1983), and tectonic earthquakes are characteristic of its southeast flank to the west of Kilauea. Earthquakes scattered elsewhere around the island appear to be mostly tectonic and may often be generated by deformation of the lithosphere and subsidence of the island under its own weight. Seismicity of Kilauea's vertical conduit below about 25 km depth displays some characteristics of both volcanic and tectonic regimes. At this depth the seismic zone is much wider than those above and may represent a distributed network of magma channels. The broad conduit complex may then experience more uniform stresses associated with lithospheric flexure.

The remainder of this paper will explore some aspects of Kilauea's volcanic earthquakes in space and time. We will begin with a description of the earthquake data and how it is processed. Then we examine the three-dimensional seismicity structure of Kilauea through a series of earthquake depth slices. The physical relations and time histories of the seismic zones seen in the depth slices provides a basis for their classification as volcanic or tectonic. The following sections explore the size and shape of Kilauea's shallow reservoir and vertical magma conduit using maps and cross sections of earthquakes. We then examine the chronology of shallow earthquake swarms in Kilauea's rift zones as one expression of magma flow and storage. This section does contain interpretations of

individual swarms, but casual readers may wish to skip it owing to its length and chronological format. The paper concludes with a summary and discussion of various types of rift swarms and what they reveal of the intrusion process, the structure of the rifts, and large-scale interactions of intrusions with each other.

#### ACKNOWLEDGMENTS

The vast amount of earthquake data summarized here is the work of many of the past and present staff of the Hawaiian Volcano Observatory. People whose persistence in the face of boredom contributed to the completeness and continuity of this data set include Karen Meagher, Pat Stevenson, Irene Takayesu, Alvin Tomori and many others. George Kojima's dedication to maintaining and recording the seismic network over the years made it all possible. We are grateful to Elliot Endo and Michael Ryan for their thoughtful reviews, and to Bob Decker for his editorship and determined coaxing to get the manuscript ready for this volume.

#### EARTHQUAKE DATA GATHERED BY THE HAWAIIAN VOLCANO OBSERVATORY

A network of high-gain seismometers has operated on Kilauea since the 1950's, and its steady improvement brought an explosion in both quantity and quality of earthquake data. The number and sensitivity of stations, their recording and timing accuracy, and the effort devoted to reading records and locating earthquakes have all greatly improved. The growth of the seismic network operated by HVO is clear from figure 43.2, which shows the station sites operating in 1963, 1973 and 1983. The greater number and improved accuracy of located earthquakes means that small swarms during the 1980's often can be studied in greater detail than larger sequences in the 1960's. The characteristics and growth of the network are documented by Klein and Koyanagi (1980), but we briefly summarize a few milestones here:

- 1958–60 Network of six Kilauea summit stations centrally recorded at HVO on smoked paper with telemetry by overland wire. Five distant stations independently timed and recorded.
- 1962–63 Increase in seismic staff (R. Y. Koyanagi) resulted in daily analysis and more earthquakes systematically timed and analyzed. Addition of 3 smoked-paper recorders.
- 1968–71 Rapid increase in number and sensitivity of stations. Introduction of telemetry by radio and recording on a Develocorder permit a reading precision of 0.10–0.05 s. Additional staff increase.
- 1974–75 Growth in number of stations, especially on Mauna Loa.
- 1978–79 Arrival of Eclipse computer at HVO for all seismic processing. Timing precision now 0.01–0.02 s.
- 1985 Network consists of 50 station sites on the Island of Hawaii. Increased numbers of 3-component stations.

The improvements in the seismic network resulted directly in increases in numbers of Kilauea earthquakes (a smaller magnitude

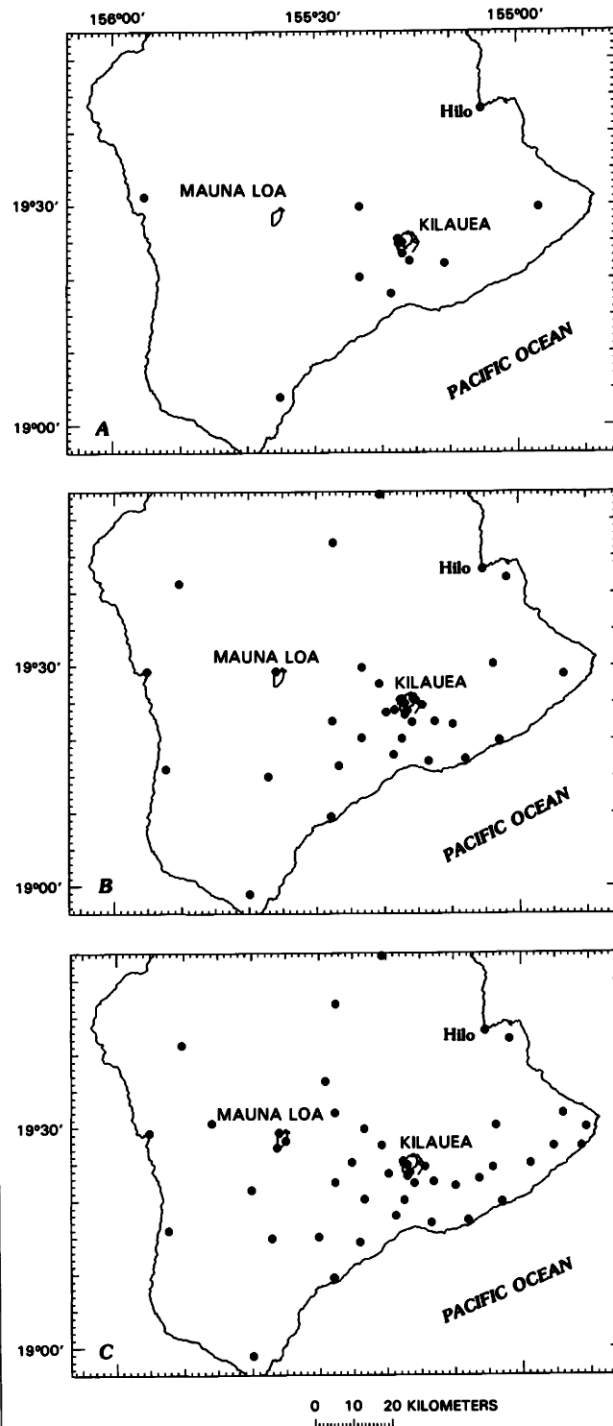


FIGURE 43.2.—Growth and coverage of network of seismic stations operated by the Hawaiian Volcano Observatory. *A*, December 1963, 13 station sites. *B*, December 1973, 34 station sites. *C*, December 1983, 47 station sites. Faults, fissures, and pit craters are as shown in figure 43.1.

above which events are complete) and in the precision of locations. Shallow Kilauea earthquakes in the early 1960's were often only located if larger than about magnitude 2, but the level of completeness in the early 1980's is now about 1. This means roughly a tenfold increase in the number of events with which to study swarms and other features, and smaller magma intrusions can now be identified. The number of seismic stations used for earthquake location by computer was often less than 10 in the 1960's, but was usually more than 20 in the 1980's. The level of completeness of Kilauea events deeper than about 13 km and flank earthquakes more than about 10 km from the caldera has been about magnitude 2 in the 1970's and 1980's. Structures such as magma conduits revealed by earthquakes can now be resolved and associated reasonably well with geologic features. In the early 1960's location and depth errors of 2–5 km meant swarms looked like formless clouds, but errors of 0.5–1 km in the 1980's give swarm clusters internal detail.

All earthquake data presented in this paper have been reprocessed using the same procedures currently used to locate earthquakes at HVO. Thus no bias occurs to the earlier hypocenters other than larger errors resulting from sparser station coverage and poorer timing precision. The earthquake data presented in this paper are more systematically located and slightly more accurate than those used in previous papers (for example, Koyanagi and others, 1976; Ryan and others, 1981). Annual seismic summaries (for example, Nakata and others, 1982) list earthquake hypocenters and other seismic data together with a description of the analysis procedure. The computer program HYPOINVERSE (Klein, 1978) locates all events. A crustal velocity model incorporating linear gradients within velocity layers (Klein, 1981) was used. Earthquake depths determined by this method are referred to the land surface above the hypocenter. In the Kilauea summit region the depth datum is about 1 km above sea level. Both the velocity model and two sets of station corrections were designed to minimize the residuals between observed and calculated arrival times and were derived using numerous earthquakes under south Hawaii. The stations which operated during the year, and their locations and timing corrections are listed in the annual seismic summaries. The space, time and magnitude coordinates of earthquakes are plotted for this paper using the program QPLOT (Klein, 1983).

### A THREE-DIMENSIONAL OVERVIEW OF KILAUEA SEISMICITY

Representing the three-dimensional distribution of earthquakes is difficult on any two-dimensional plot. Klein and Koyanagi (1985) produced a seismicity map of the south side of Hawaii, but depths are only indicated by one of four symbol colors. One of the easiest ways to visualize earthquakes is by depth slices using only a narrow, horizontal layer of events plotted on each map. Depth slices suit Kilauea very well because patterns change with depth and an earthquake's depth is often useful in discriminating it as volcanic or tectonic. The intent of this section is to present an overview; later sections of this paper will explore the magma system in more detail.

A series of depth slices for Kilauea from the surface to 40 km depth is shown in figure 43.3. Because the vertical magma conduit broadens with depth, deeper slices should cover a broader area. Figure 43.4 thus includes the entire south side of Hawaii and covers depths from 20 to 60 km. Figures 43.3 and 43.4 include data from 1970 through 1983. Figure 43.5 duplicates the slices of figure 43.4, but covers the 1960–69 period. The earlier data is plotted separately because it differs somewhat in pattern and is poorer in quality. The layers plotted thicken from 1 km at the surface to 4 km at depth, thus compensating for both spatial patterns that change less rapidly at depth and the slightly larger location errors associated with deeper events. Typical location errors for each depth range are about one-half the cutoffs chosen, which only eliminate the poorest events. Thus, an error in depth could possibly place a given event in an adjacent layer from where it actually occurred. Descriptions of the main features in different depth ranges follow.

### THE SHALLOW CRUST BETWEEN 0 AND 5 KILOMETERS DEPTH

Events in the depth range 0–5 km are mostly volcanic earthquakes at Kilauea's caldera, rift zones and the Koae fault zone. Caldera seismicity extends mainly from 0 to 4 km depth. The aseismic magma reservoir beneath the southern part of the caldera is indistinguishable at this scale. Earthquakes in the northern and central parts of the caldera are most intense between 1 and 3 km depth and thus are mainly in the rocks of the caldera floor capping the summit reservoir. Southern caldera seismicity occurs both above and to the side of the reservoir and thus is active during periods of inflation and during rapid intrusions of dikes connected to the reservoir.

The most active part of the ERZ is between 2 and 4 km depth, at which nearly all of the 25 km of rift just east of the caldera has experienced some seismicity during 1970–83. Most of these earthquakes were produced during rapid intrusions or eruptions. The main ERZ magma conduit is most active at about 3 km depth. Unlike the SWRZ and the rest of the ERZ, the 6 km of ERZ adjacent to the caldera is seismically active nearly to the surface (fig. 43.3A). This shallow part of the ERZ may form a secondary conduit system that is intruded repeatedly and is a region brittle and stressed enough to generate earthquakes. This shallow earthquake zone could also be the result of tensile deformation when the main conduit below is intruded.

The SWRZ seismicity also forms a narrow and nearly continuous band. It does not exactly follow the course of the rift at the surface, but heads south from the caldera for about 3 km before bending to the southwest. The center of the ERZ earthquake band is displaced about 0.5 km south of the surface axis of the rift (defined by pit craters and eruptive centers), whereas the SWRZ seismic axis is displaced as much as 2 km south of the surface rift. The buried SWRZ magma conduit active during the last decade thus has no obvious surface expression. The SWRZ probably consists of a 3-km-wide zone of parallel dike systems that are active

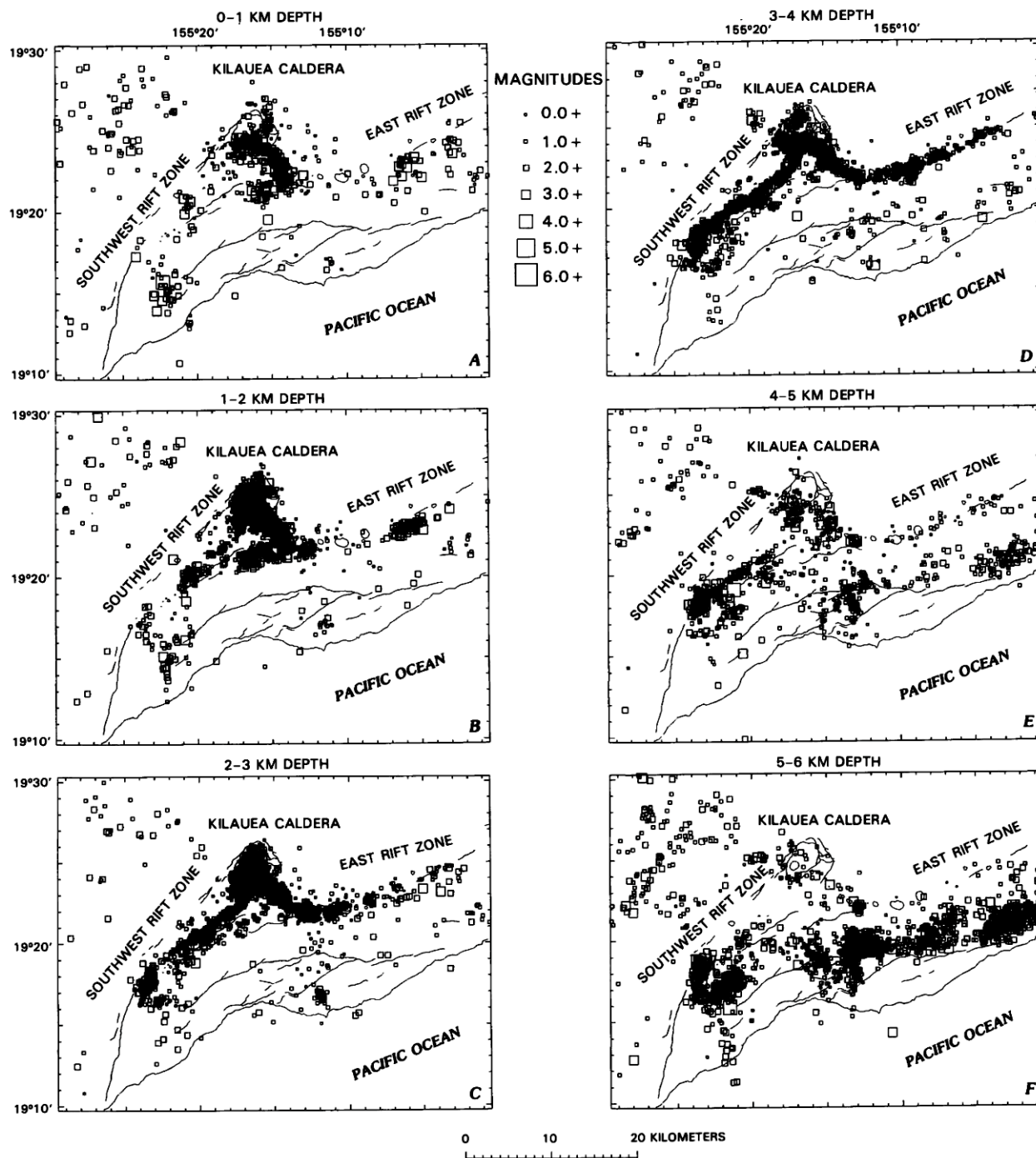


FIGURE 43.3.—Depth slices from 0 to 40 km showing hypocenters of Kilauea earthquakes, 1970–83. Earthquake symbols are squares whose size depends on magnitude. Maximum horizontal error of plotted hypocenters is: *A–O*, 2 km; *P–T*, 4 km. Maximum vertical error is: *A–J*, 2 km; *K–O*, 3 km; *P–T*, 5 km. Faults, fissures, and pit craters are as shown in figure 43.1.

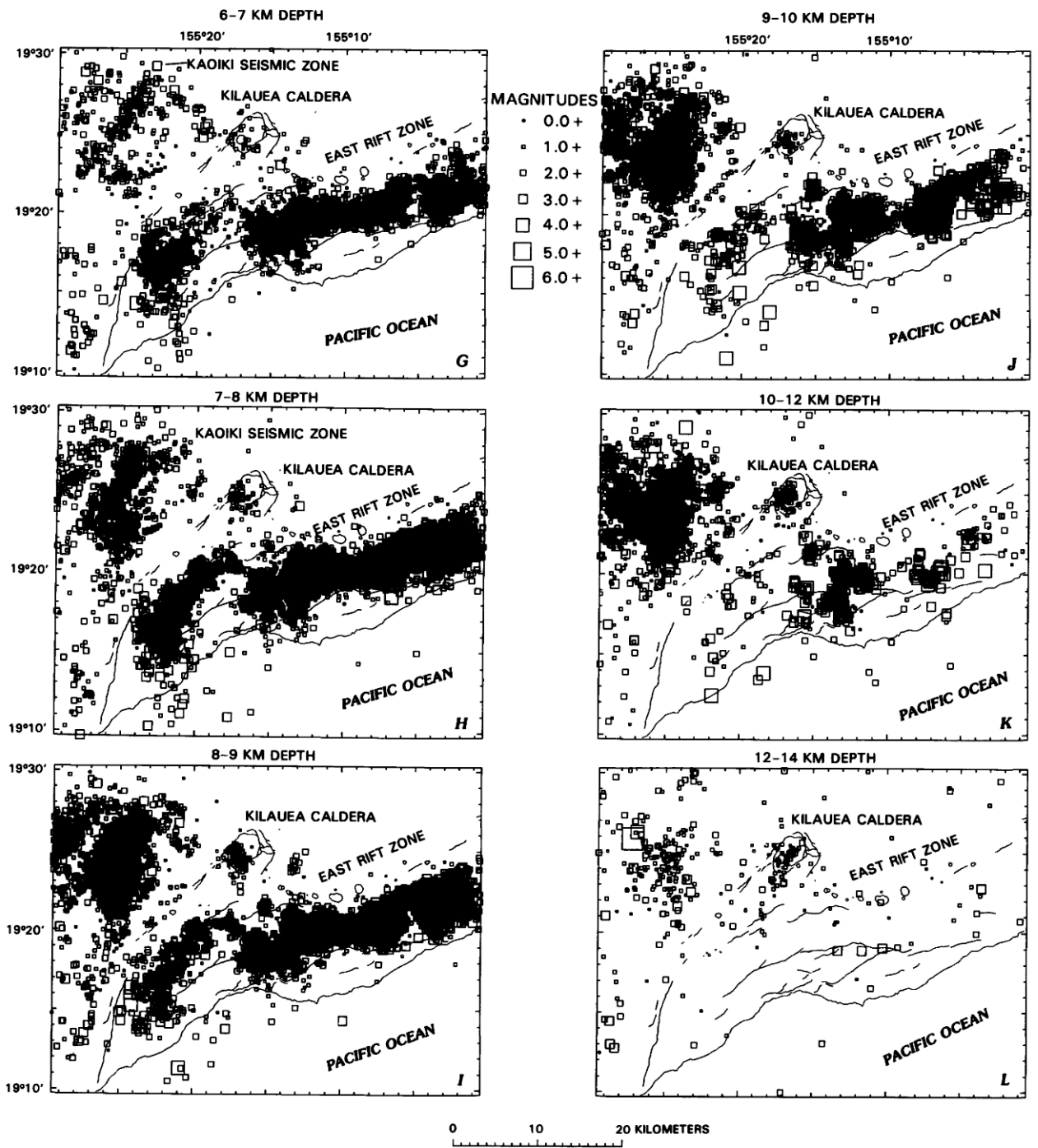


FIGURE 43.3.—Continued.

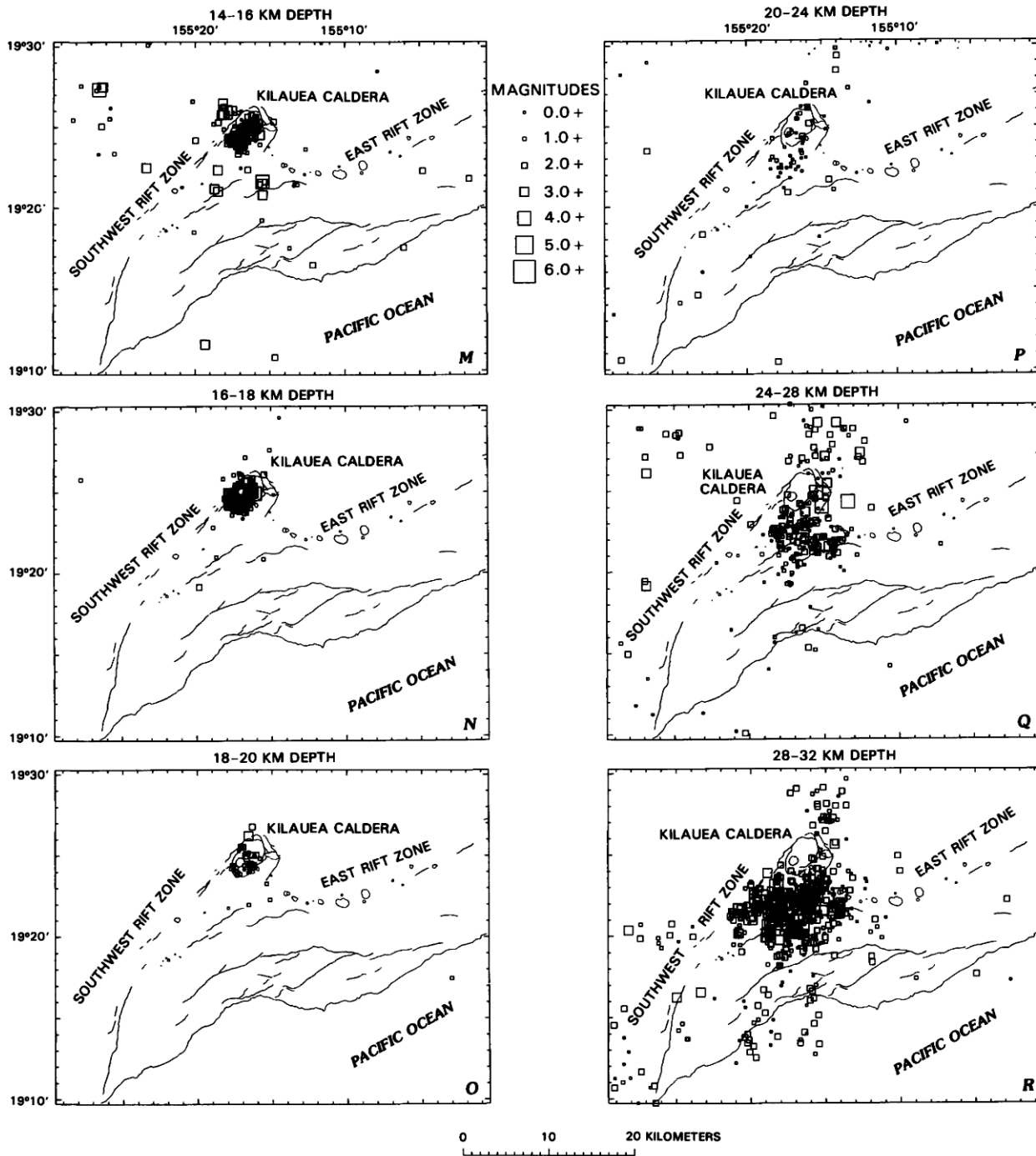


FIGURE 43.3.—Continued.

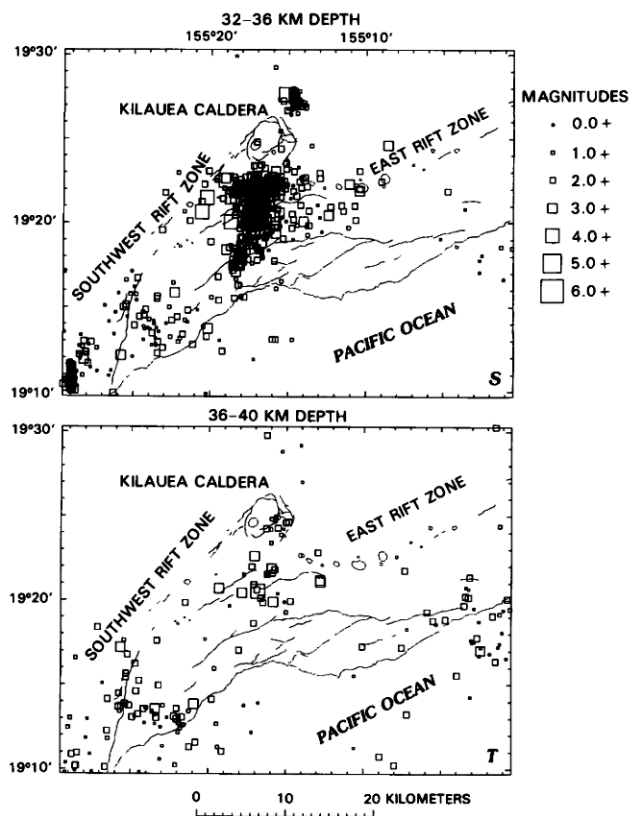


FIGURE 43.3.—Continued.

at various times and that evolve with time. Because the contemporary magma conduits of both the ERZ and SWRZ are south of the established surface features, the vertical dike trajectories must dip southward. The offset of earthquakes and surface geology could be a consequence of southward migration of the rifts with time (Swanson and others, 1976a).

Like the ERZ, the primary conduit of the SWRZ is at about 3 km depth, with seismicity extending for about 1 km above and below. A notable exception is the shallow clump just downrift of Puu Koaie ( $19^{\circ}20' \text{ N.}, 155^{\circ}20.5' \text{ W.}$ ; fig. 43.3A, B). Surface cracks appeared in this area during the August 1981 SWRZ intrusion and were probably caused by a dike branching upward from the main conduit. A similar shallow extension occurs above the ERZ conduit near Mauna Ulu ( $19^{\circ}22' \text{ N.}, 155^{\circ}12.5' \text{ W.}$ ; fig. 43.3B). Much of the shallow seismicity near Puu Kamoamoa and Puu Kahaualea ( $19^{\circ}23' \text{ N.}, 155^{\circ}06' \text{ W.}$ ; fig. 43.3A, B), however, occurred in a series of extended swarms that coincided with inflation of the rift near

the earthquake epicenters. The very shallow seismicity thus appears to be over a part of the rift conduit that was accumulating magma and is analogous to the seismic cap over the summit magma reservoir. The rift inflation occurred cyclically and coincided with times of slow summit deflation.

The linear part of the SWRZ active during 1970–83 extends only to the north end of the Great Crack ( $19^{\circ}17' \text{ N.}, 155^{\circ}25' \text{ W.}$ ; figs. 43.1C, 43.3A–E), where the rift bends to a more southerly trend. The seismicity in this lower southwest rift (LSWR) region is somewhat complex and diffuse. Earthquakes scatter south of the rift over a wide range of depths. Between 0 and 3 km depth this area is active most of the way to the coast, and below 2 km the seismically active rift branches into parallel segments just south of the main rift axis. Unlike the rest of the SWRZ, the LSWR can be intensely active below 4 km depth, and seismicity merges with the region of tectonic earthquakes in Kilauea's south flank. In addition, LSWR earthquakes accompany both the larger SWRZ intrusions and major tectonic events on the south flank, such as the November 1975 Kalapana earthquake. The LSWR thus seems to be a weak but brittle zone extending from 0 to 10 km depth in which activity can be triggered either by intrusions in the SWRZ to the north or by tectonic events to the east.

Other scattered events at 0–4 km depth occur away from the volcanic conduits. The events distributed broadly through the upper part of Kilauea's south flank occurred both as aftershocks of the  $M=7.2$  Kalapana earthquake and as induced events associated with larger ERZ intrusions (Dvorak and others, 1985). This area thus responds both to large scale slip in the lower crust (tectonic events) and to compressional stress generated by dike intrusion to the north (volcanic events). The Kaoiki seismic zone also produces some shallow tectonic earthquakes even though most activity lies below 5 km depth. Small isolated clusters of tectonic earthquakes also occur near Apua Point (0–4 km depth) and 4 km west of Kilauea caldera (3–8 km depth).

#### TECTONIC EARTHQUAKES BETWEEN 5 AND 14 KILOMETERS DEPTH

The vast majority of Kilauea earthquakes at 5–14 km depth are tectonic events on the south flank and in the Kaoiki seismic zone. The tectonic events plotted in figure 43.3F–L are composed of both continuous seismicity and aftershocks of larger earthquakes. The majority of earthquakes on the portion of the Kaoiki seismic zone included in figure 43.3 show right-lateral slip on northeast striking planes (Endo and others, 1978). Lineations of earthquakes also follow this trend. The typical focal mechanism of south-flank events is low-angle faulting with the upper block slipping seaward (Crosson and Endo, 1982). Unlike the Kaoiki seismic zone, no clear alignment of hypocenters on fault planes is apparent, and many slip planes are active.

#### THE MAGMA CONDUIT BETWEEN 5 AND 20 KILOMETERS DEPTH

The vertical magma conduit below Kilauea caldera is clearly defined by hypocenters below about 6 km depth. In the depth slices of figure 43.3G–O, the seismic conduit is centered below Halemaumau and Kilauea's summit magma reservoir. The shape and size of the seismic conduit varies only slightly with depth, and typically is about 3 km in diameter. The earthquake location errors from both random and systematic sources means that small variations in cross-sectional shape and a precise diameter probably are not significant within about 1 km. It is tempting to interpret the ring of seismicity in figure 43.3N surrounding an aseismic magma conduit, but the precision of hypocenter position does not justify the interpretation. The earthquakes represent a zone of deformation in brittle rock surrounding the conduit itself, which is probably much smaller than the seismic zone and may even be multiple. An upper limit to the diameter of the seismically active conduit complex is thus about 3 km. Magnitudes of these events are small and seldom exceed 3.0.

#### THE MAGMA CONDUIT BETWEEN 20 AND 40 KILOMETERS DEPTH

The seismicity of the magma conduit changes character in several ways below 20 km: (1) the earthquake zone broadens to about 13 km in diameter (fig. 43.3R–S) (2) the seismic pipe plunges southward, unlike its vertical direction above 20 km; (3) the activity is more intense, with more events as large as magnitude 4.5; and (4) events are more continuous in time and generally not in swarms like the seismicity above. Earthquakes in the upper conduit are thus typically volcanic, whereas those between 20 and 40 km are mostly tectonic. The broadening with depth and southward plunge of the seismic conduit were plotted but not interpreted by Koyanagi and Endo (1971).

Inversion of teleseismic *P*-times for lateral velocity variations (Ellsworth and Koyanagi, 1977) showed another change in the conduit that occurs near 20–30 km depth. Although the resolution was limited by the 8-km wavelength, the average velocity is a few percent low directly below and to the south of Kilauea caldera at 28–58 km depth, suggesting a laterally extensive conduit system. Conduit velocities above that depth, however, are several percent higher than their surroundings (Ellsworth and Koyanagi, 1977; Thurber, 1984). These inversion studies also demonstrate high seismic velocities in the upper crust below the rifts, suggesting that a narrow conduit lies within a high-velocity intrusive complex in both the rifts and upper vertical conduit.

The narrow finger of earthquake hypocenters between 5 and 20 km depth is adjacent to the magma conduit and is thus seismically somewhat analogous to the shallow rift zones. The stress causing earthquakes in the upper pipe is thus partly derived from magma pressure within the conduit. The stress driving the earthquakes centered near 30 km depth, however, seems to be more than just that from magma pressure within the conduit complex. The magma

conduit apparently passes through the 30-km-deep seismic zone and may have triggered its formation initially. But the size and intensity of the 30-km-deep seismic zone indicate a more regional stress source. Possibilities include flexure of the lithosphere under the gravitational load of the island or response to tractional stress applied from the volcanic edifice. Depletion of mass near this depth could also cause intense local seismicity. The behavior of these earthquakes in time (see next section) provides additional evidence bearing on the cause of these earthquakes.

Kilauea's magma conduit seismicity below 20 km must be examined in the context of a wider seismic region. Figure 43.4 plots depth slices below 20 km and includes deeper earthquakes from Mauna Loa and Loihi Volcanoes. The main seismic root of Kilauea is the prominent feature between 20 and 40 km, but a smaller funnel-shaped zone between 24 and 34 km is recognized just north of the caldera (figs. 43.3Q–S, 43.4B–D).

#### THE MAGMA CONDUIT AND HOT SPOT BELOW 40 KILOMETERS DEPTH

Earthquakes below about 30 km depth mostly occur in a wide band roughly coincident with the south coast of Hawaii (fig. 43.4C–J). The deep seismic zone consists partly of dense earthquake clusters (fig. 43.4F–H). The small clusters do not extend vertically more than about 8 km, so they cannot clearly be identified with long magma conduits. The clusters may occur at places weakened by past and present magma flow, or simply at points having a high density of fractures. Seismicity concentrates in the triangle with corners at Kilauea, Mauna Loa and Loihi, but also extends to the northeast and southwest. Kilauea loses its narrow seismic root at about 40 km depth in this diffuse cloud. Earthquakes become sparse below about 50 km (fig. 43.4I–J) and none are located reliably below 60 km depth.

Earthquakes mark an isolated, narrow conduit beneath Mauna Loa that can be traced between about 28 and 48 km depth (fig. 43.4C–G). The earthquakes north of Hilo around 40 km depth are mostly aftershocks of the April 1973 Honoumuli earthquake (Unger and Ward, 1979).

Most deep earthquakes occur continually, which suggests a relatively uniform stress by analogy with crustal events. A few deep earthquakes are in swarms, which may be associated with pulses of ascending magma. The part of the seismic zone equidistant from Kilauea, Mauna Loa and Loihi is a frequent source of deep harmonic tremor, and magma certainly is present there. Tremor originating in this region can be quantitatively related to Kilauea's magma supply and transport to the shallow reservoir (Aki and Koyanagi, 1981). The coincidence of tremor, of the center of the deep seismic zone, and of the major earthquake cluster shown in figure 43.4E–G suggests that the contemporary Hawaiian hot spot is centered there (Klein, 1982a).

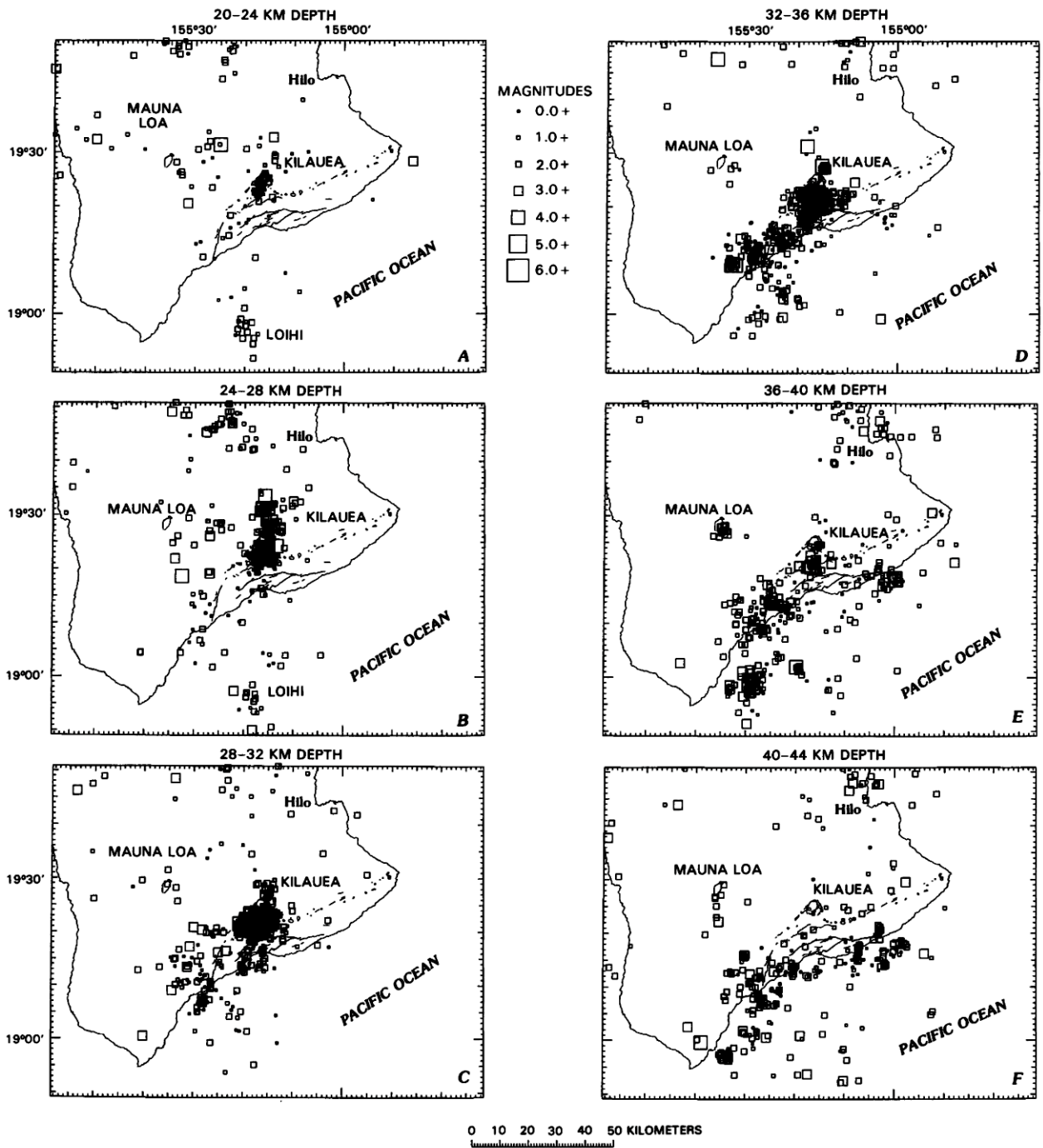


FIGURE 43.4.—Depth slices from 20 to 60 km showing hypocenters of south island earthquakes, 1970–83. Earthquake symbols are squares whose size depends on magnitude. Maximum horizontal and vertical errors for A–J are 5 and 7 km, respectively. Note that J includes hypocenters to 99 km depth, but those below 60 km are not reliably located. Faults, fissures, and pit craters are as shown in figure 43.1.

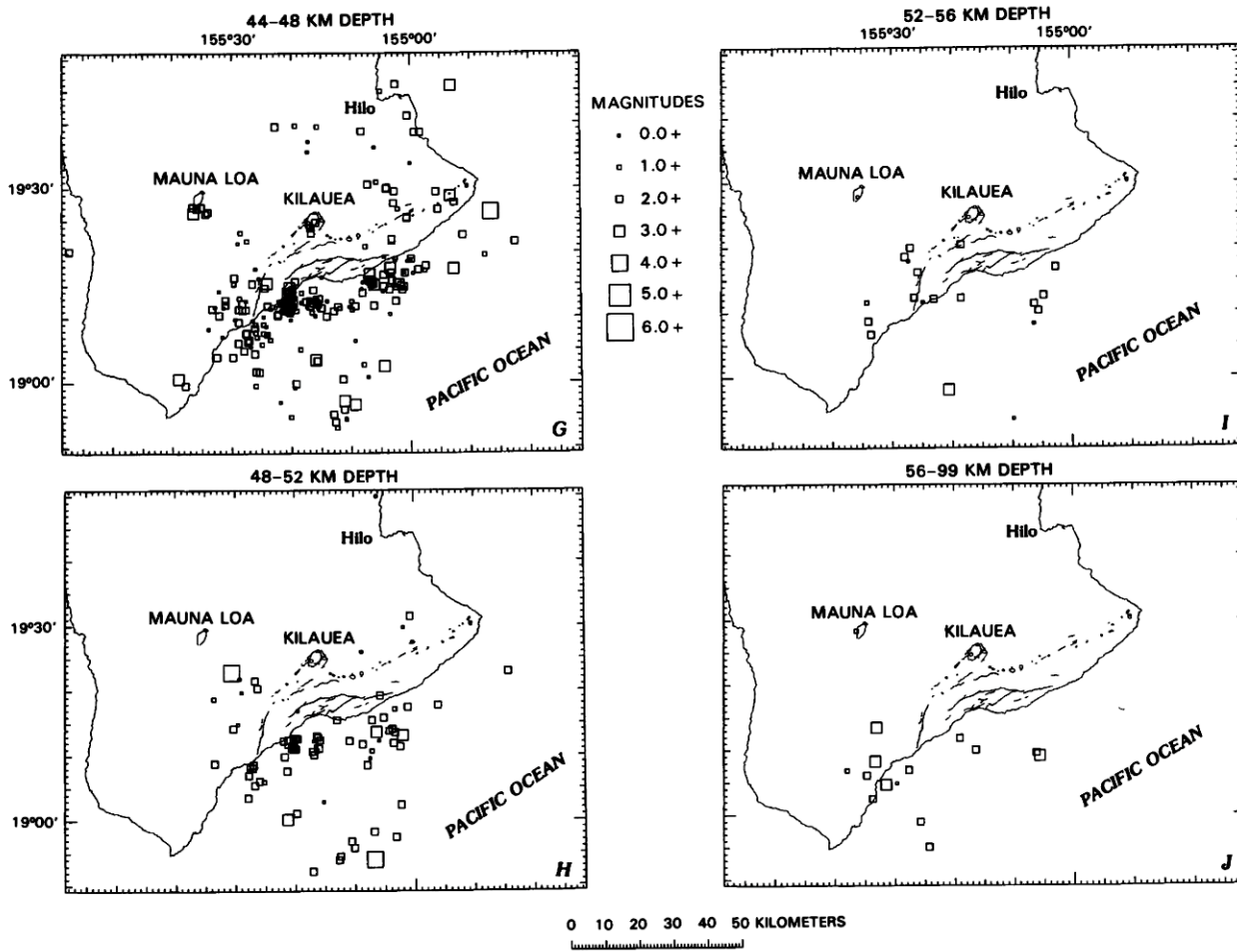


FIGURE 43.4.—Continued.

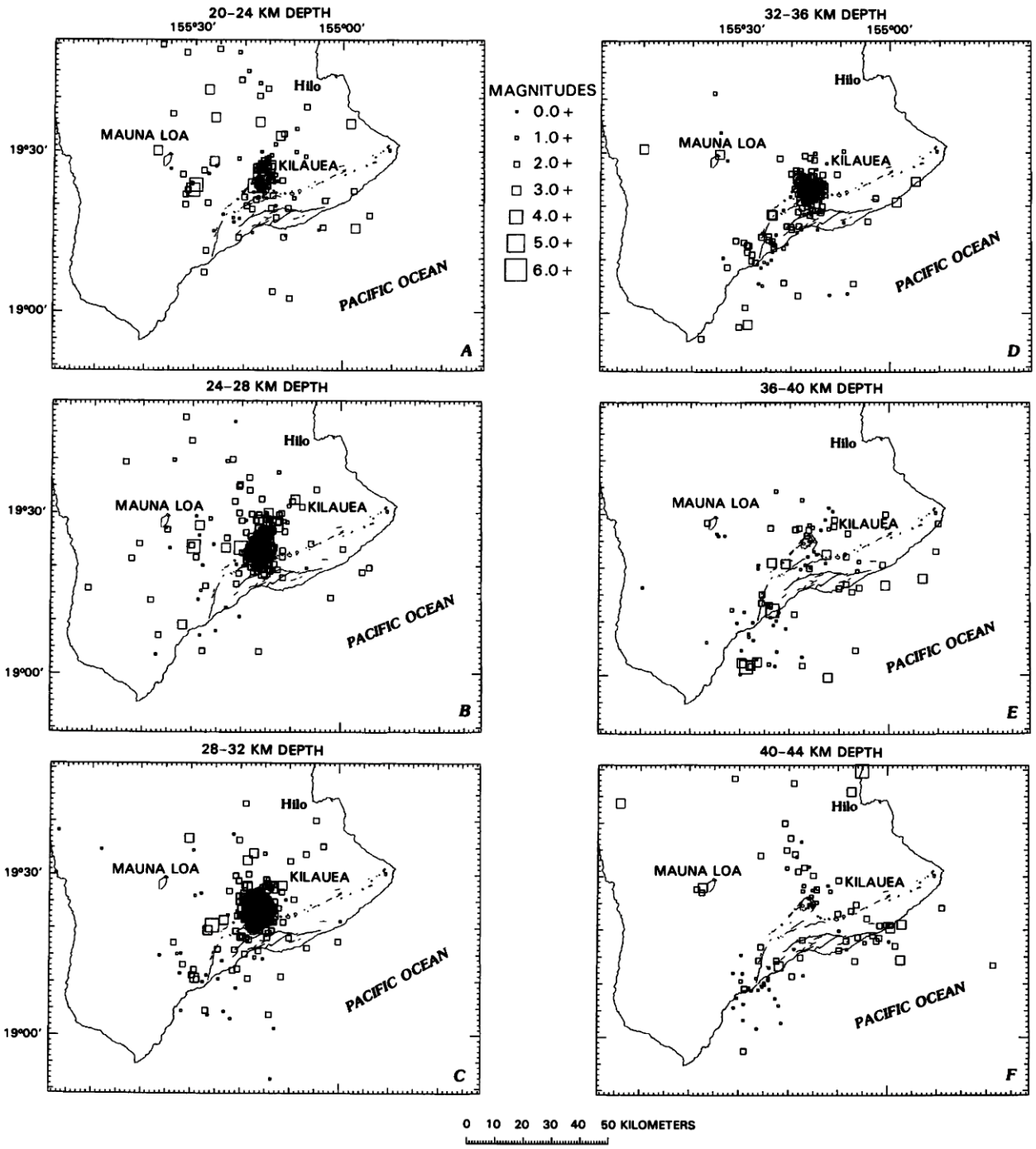


FIGURE 43.5.—Depth slices from 20 to 60 km showing hypocenters of south island earthquakes, 1960–69. Earthquake symbols are squares whose size depends on magnitude. Maximum horizontal and vertical errors for A–J are 10 and 15 km, respectively. Note that J includes hypocenters to 99 km depths, but those below 60 km are not reliably located. Faults, fissures, and pit craters are as shown in figure 43.1.

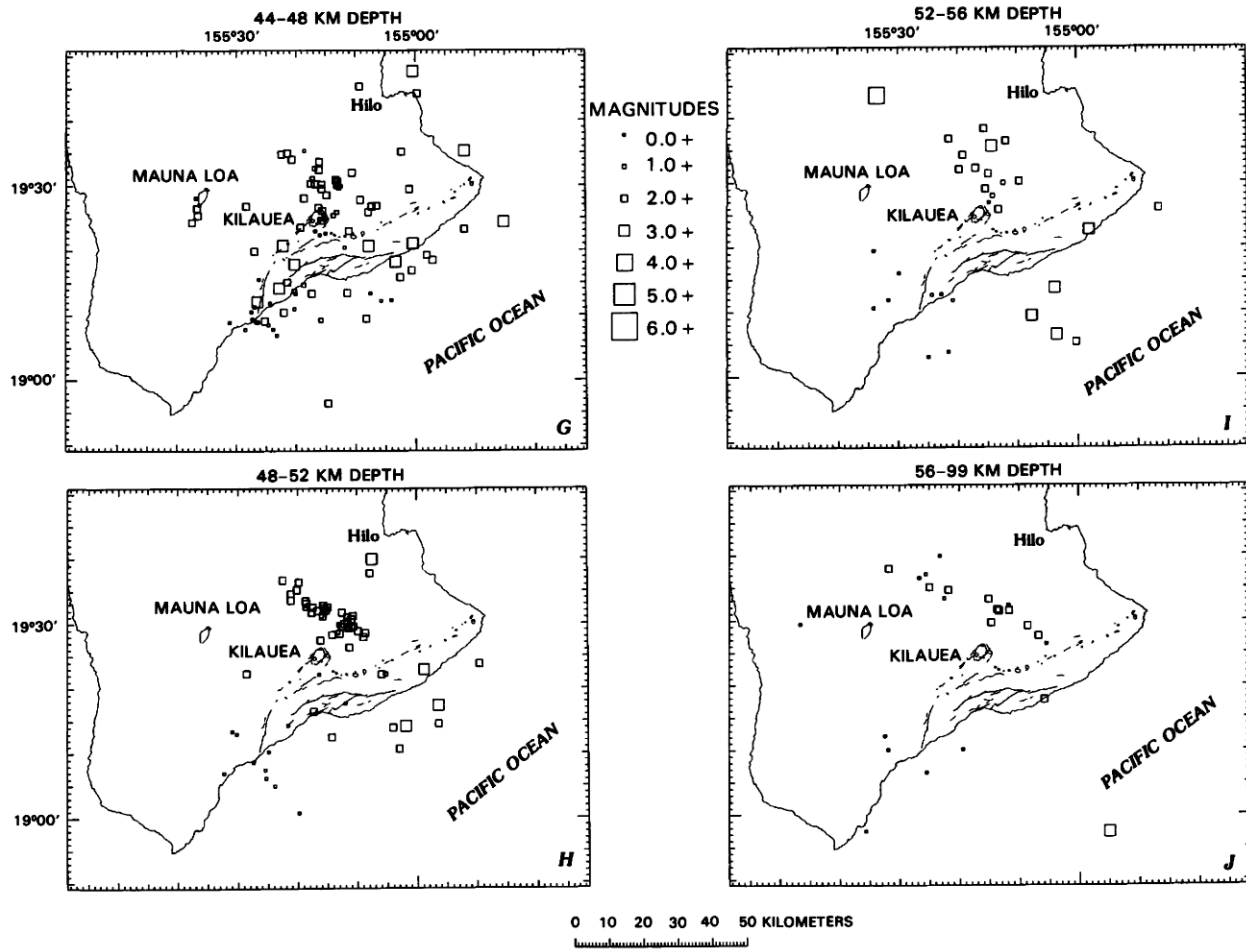


FIGURE 43.5.—Continued.

### THE MECHANISM OF DEEP EARTHQUAKES

The deep seismic band roughly coincides with the mobile and growing south flank of the island. This coincidence suggests that the stress causing the earthquakes is related to the dynamics of the volcanic pile above. In recent decades, the south side of the island has been most active volcanically, seismically and tectonically, and the three phenomena are related. Stress at depth could arise in three main forms: (1) the unbuttressed and mobile south flanks of Kilauea and Mauna Loa exert a lateral shear on the lithosphere as they are pushed seaward by their growing rift zones and gravitational slumping; (2) the added weight of new lava and dikes continually increases the normal gravitational stress on the lithosphere, and its nonuniformity causes earthquakes near the additional load; and (3) the mantle beneath the seismicity is being melted and depleted, and mass from above slumps down along active faults to replenish the lost volume.

The circumstantial evidence favors some combination of shear and normal stress applied from the volcanic pile above as a driving mechanism of Kilauea earthquakes below 13 km. First, the fact that most deep earthquakes do not occur in swarms argues against the close association of earthquakes and partial melting. If widely distributed pockets and conduits of magma were present, then local stress concentrations would result in swarms, as it does in the shallow rift and conduit systems. Seismicity resulting from settling to compensate for much deeper melt depletion would produce continuous seismicity essentially similar to the effects of applying stress from above. The stress and geometry of magma distribution at 20–40 km depth may change with time, as suggested by the absence of earthquakes at this depth prior to 1961, and the fact that some swarms did occur in the early 1960's (Eaton and others, chapter 48).

Second, the time behavior of Kilauea's deep earthquakes (13–60 km) is linked to the stress state of Kilauea's south flank. The rate of Kilauea's deep seismicity dropped markedly at the time of the 1975 Kalapana earthquake (see next section). The effect of the  $M=7.2$  earthquake was to relieve compressional stress stored in the mobile south flank by slipping seaward, thus also releasing shear stress that had been applied to the mantle below. The sudden drop of applied stress could have caused the drop in rate of Kilauea's deep earthquakes. The occurrence of the Kalapana earthquake suppressed the seismicity of Kilauea's vertical magma conduit from 6 to 60 km, and its effect on earthquake rates diminished with depth. The Kalapana earthquake, however, had little influence on the deep and broad band of earthquakes along Hawaii's south coast. Apparently the effects of relieving stress in 1975 did not extend beyond Kilauea's immediate vicinity.

Third, the position of the band of earthquakes below 36 km along Hawaii's south coast argues that stress applied from volcanic and tectonic activity is a causative mechanism. Growth of the island's volcanic pile is on the south half of the island, but was primarily under Kilauea during recent decades. Addition of mass is far greater on land north of the band of deep earthquakes than to the south offshore. This differential loading produces a stress gradient under

the coastline. The unbuttressed seaward coasts of both Kilauea (Ando, 1979; Crosson and Endo, 1982) and Mauna Loa (for example, the  $M=5.6$  and  $M=5.4$  Ninole Hills earthquakes of January 21, 1982) are mobile and experience large tectonic earthquakes in which the upper block slips seaward. The stress build-up which causes these earthquakes also exerts a shear on the lithosphere that is greatest along the south flank of the island.

Lithospheric flexure also appears to play a part in the distribution and cause of deep earthquakes. It is a complex problem, with varying shear and normal stresses applied to the top of a rigid lithosphere containing weaker magma conduits. Kilauea's deep seismicity thus seems to result from a combination of tectonic and gravitational stress applied from above, perturbation from its magma conduit, flexure of the lithosphere, and interaction with the Hawaiian hot spot.

### EARTHQUAKES AT 20–60 KILOMETERS DEPTH DURING 1960–69

Earthquakes during 1970–83 are more accurately located and more complete than those before, but earlier events are important because some changes of spatial pattern occur with time. The seismic coverage during 1960–69 was not good for resolving fine details in shallow seismicity, but was adequate for larger patterns of deeper earthquakes. Figure 43.5 plots the same depth slices and map area as figure 43.4, but contains only 1960–69 data.

Kilauea's seismic root above 36 km depth appears the same during both periods (compare fig. 43.4A–D with fig. 43.5A–D), but differences are obvious in other areas. The band of earthquakes that coincides with the island's south coast was better developed during 1970–83 (fig. 43.4C–H). Although the many small earthquake clusters cannot be resolved by the sparser network during 1960–69, the band itself had roughly the same size and shape (fig. 43.5C–H). Most Loihi earthquakes occurred during swarms in 1971–72 and 1975 (fig. 43.4A, B; Klein, 1982a). The absence of Loihi events during 1960–69 is a combination of its inactivity and reduced network sensitivity to distant earthquakes.

The greatest seismicity differences are deeper than 40 km (compare fig. 43.4F–J and fig. 43.5F–J). The area about 20 km north of Kilauea caldera was very active in 1960, but during 1961–83 the southwest corner of Kilauea was most active. This shift is not a result of changing seismic network geometry, but stems from deep swarms in July and October 1960 that did not recur in the subsequent 23 years. Earthquakes in 1959 similar to those in 1960 were interpreted by Eaton and Murata (1960) as originating from Kilauea's magma conduit. The apparent northwest trend of epicenters in this deep 1960 zone (fig. 43.5H–J) is partly real and partly an artifact of the station geometry: this is the direction of poorest control by the stations to the southwest. By looking at only 1960 data one might conclude that Kilauea's main seismic root plunged north rather than southwest as current evidence suggests. No seismic pattern should be considered permanent, and our view of the vertical magma conduit will surely be modified in subsequent decades.

### THE *b*-VALUES OF SHALLOW EARTHQUAKES

The earthquake regions discussed in this "Three-dimensional overview" section differ in their time history, maximum magnitude and a statistical parameter called earthquake *b*-value. The log-number of events is generally a linear function of magnitude when the sample of earthquakes is complete. The constant of proportionality is the *b*-value and usually ranges from about 0.5 to 1.5 (Richter, 1958). Higher *b*-values are often characteristic of volcanic areas and should be typical of regions with lower and heterogenous stress (Mogi, 1962; Wyss, 1973). A detailed survey of *b*-values is beyond the scope of this paper, but preliminary results suggest that *b*-values are higher in Kilauea's volcanic earthquake regions. Earthquake *b*-values were computed for each region shown in figure 43.6 using events shallower than 20 km depth during 1970–79. Major swarms and aftershock sequences were removed, but their inclusion would not significantly change the results. The regions with *b*-values larger than 1.1 include Kilauea's rift zones and parts of the immediately adjacent south flank, Mauna Loa and Loihi: these are volcanic areas where magma presumably produces concentrated stress and larger *b*-values. Lower *b*-values are characteristic of Kilauea's flanks more distant from rift zones. These flank areas apparently can sustain higher and more uniform stresses.

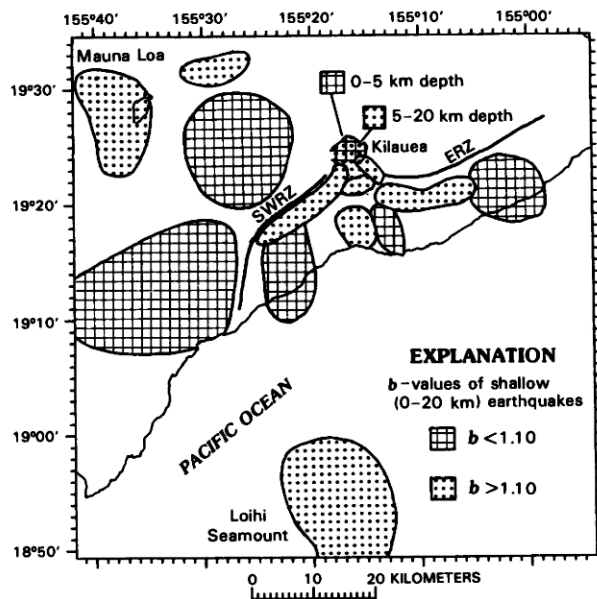


FIGURE 43.6.—Kilauea and part of Mauna Loa, differentiating areas of higher *b*-values (>1.1, dot pattern) from areas of lower *b*-values (<1.1, grid pattern). The *b*-values were only calculated for the regions shown. Earthquake data from 1970 to 1979 were used, but swarms and aftershock sequences were excluded.

### GENERALIZED HISTORY OF KILAUEA EARTHQUAKES

A key discriminant between volcanic and tectonic earthquake regions is whether seismicity occurs in episodic volcanic swarms or combines continual activity with mainshock-aftershock sequences as in tectonic regions. Changes in the rate of earthquake occurrence also indicate times when stress is changing. We divided Kilauea into several regions (fig. 43.7) and plotted the cumulative number of earthquakes versus time for each (fig. 43.8). Only events larger than a particular cutoff magnitude were chosen so that the detection would be complete or at least consistent. For shallow earthquakes at Kilauea, coverage is reasonably complete to magnitude 1 except during the most intense swarm periods. Kilauea's deep and flank events are mostly complete to about magnitude 2, except during times of exceptionally high seismicity, such as aftershocks of the 1975 Kalapana earthquake. For present purposes, it is better to choose a cutoff magnitude low enough to provide sufficient events to characterize an area's behavior, than to choose it high to be sure of an absolutely complete sample above the cutoff magnitude.

### SHALLOW VOLCANIC EARTHQUAKES

The cumulative plots of shallow earthquakes in volcanic areas have a characteristic sawtooth pattern resulting from episodic swarms. For shallow caldera earthquakes (fig. 43.8A), the curve for a typical eruption cycle begins as a plateau with few earthquakes following an intrusion and deflation. During reinflation seismicity gradually increases, resulting in an upward curving line. The cycle ends with an upward jump in the graph whose length is the number of events in the swarm larger than magnitude 1. Because figure 43.8A includes both caldera and some adjacent rift zone events, we see both the gradually building earthquakes related to inflation (in the caldera and upper rifts) and the rapid swarms (usually in the rift zones). The prominent increase in the rate of seismicity beginning in 1979 appears not to be just an artifact. The lower rate prior to 1979 is not a simple result of incomplete reporting of events larger than magnitude 1 because cumulative curves with magnitude cutoffs larger than 1 show the same increase. The beginning of a new procedure based on computer processing at HVO occurred in 1979, so the apparent increase arises from a combination of changes in event selection and magnitude calculation.

Seismicity of the upper ERZ and middle ERZ (fig. 43.8B, C) also shows a sawtooth pattern. The background rate is typically low, but is punctuated by short swarms that cause the curve offsets. Many of the larger swarms contributed earthquakes to both ERZ regions and hence to both curves of figure 43.8B and C. Some immediate aftershocks of the  $M=7.2$  Kalapana earthquake contribute to figure 43.8C, but this is the only earthquake large enough to have caused aftershocks in this region. During 1979 and 1980, the middle ERZ experienced several cyclic intrusions that occurred too slowly to produce an intense swarm or eruption. Drops in summit tilt and seismicity were coupled with periods of inflation and intermittent earthquakes at shallow depth below the rift.

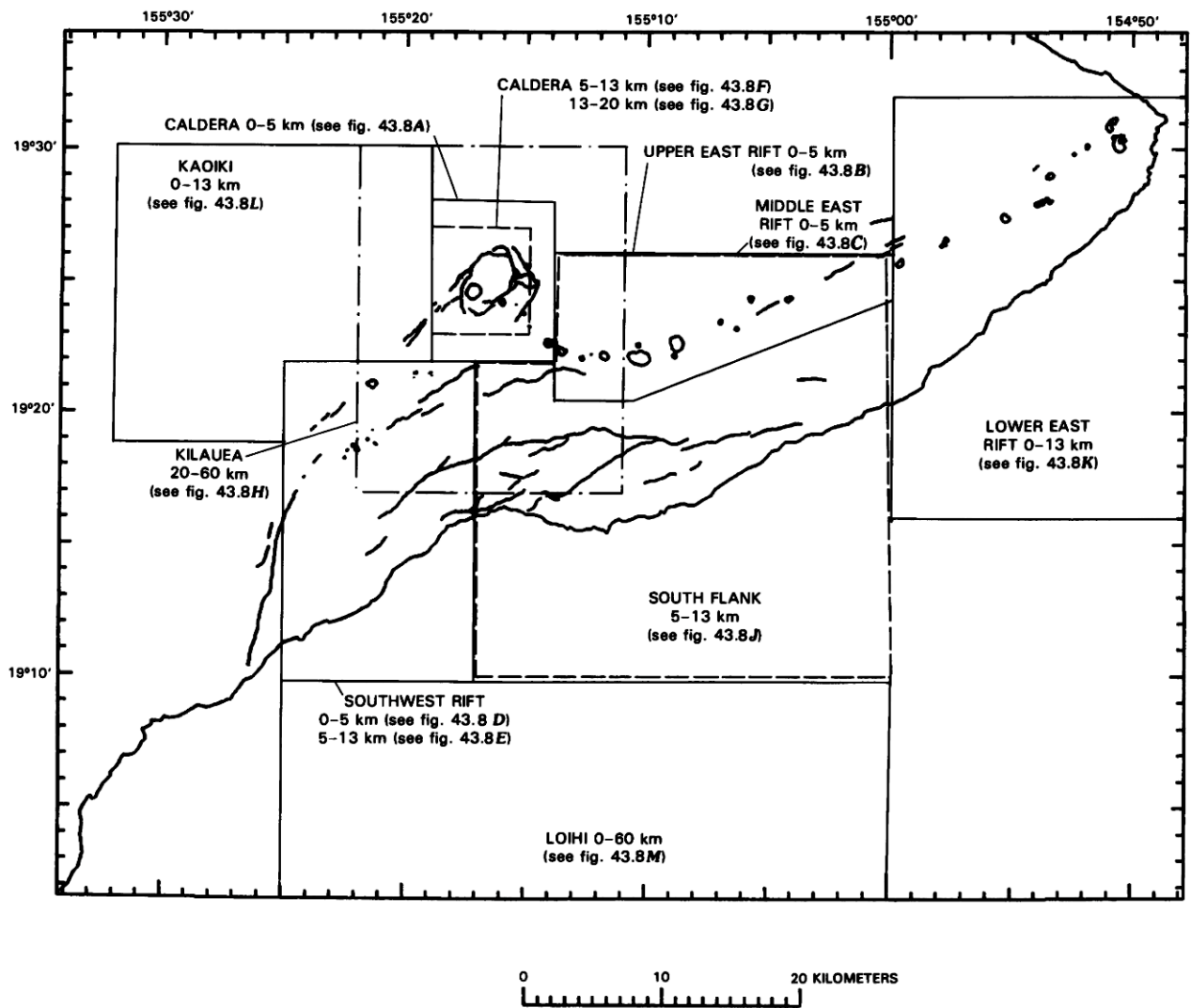


FIGURE 43.7.—Locator map of regions used to select earthquakes for cumulative seismicity curves shown in figure 43.8. Boundaries were chosen to enclose approximately homogeneous seismic regions, but seismicity is certainly not distributed uniformly in each region. Solid lines are used for boundaries that extend up to the surface, dashed lines for regions between 6 and 20 km depth, and a dash-dot line for Kilauea's root below 20 km. The Loihi region between 155° 00' and 155° 25' W. longitude extends south (beneath the figure) to 18° 40' N. latitude.

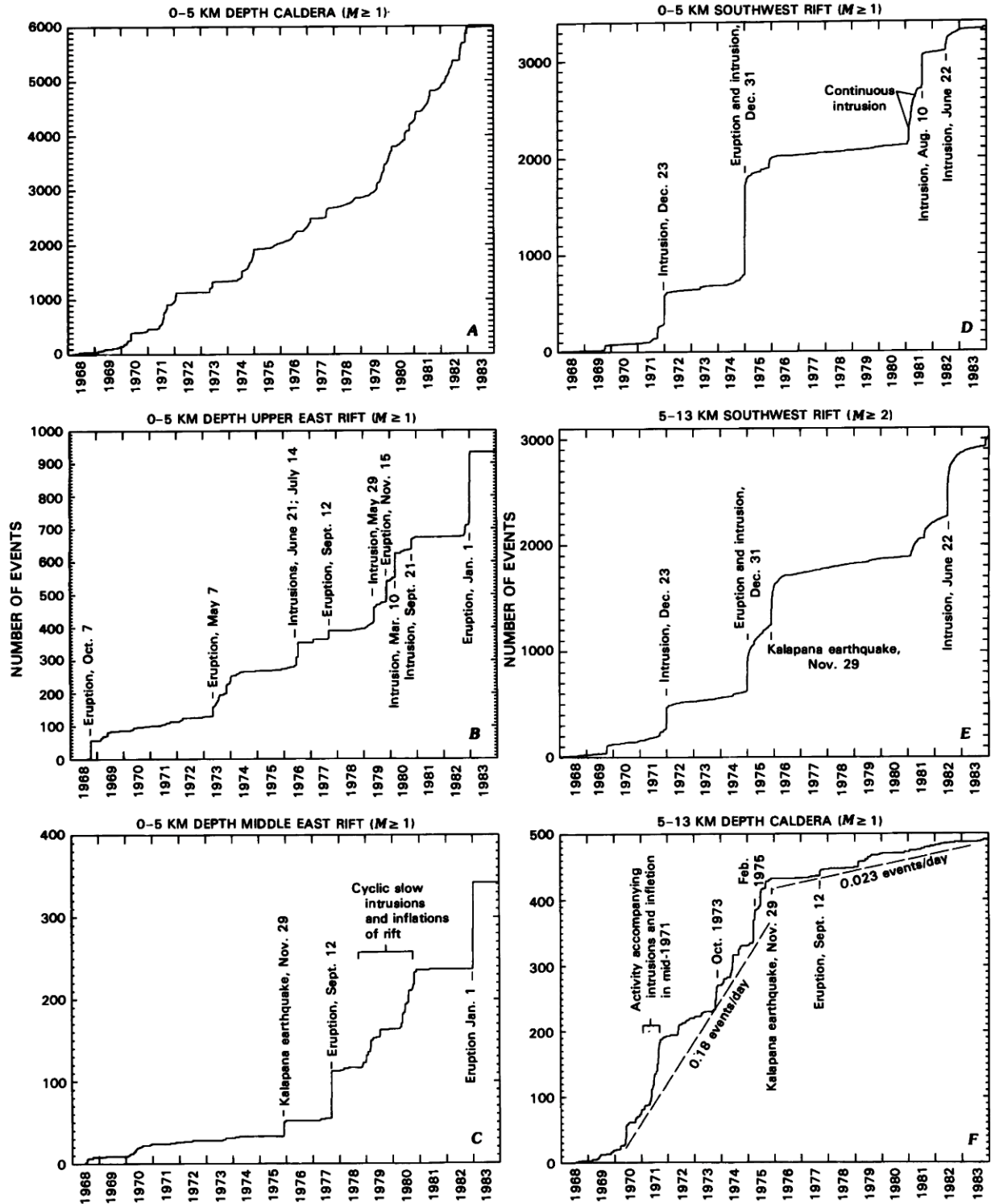


FIGURE 43.8.—Cumulative numbers of earthquakes plotted versus time. **A–M**, Regions outlined in figure 43.7. The “south island” region of figure 43.8/ includes the entire area of figure 43.7. Curve shape indicates how episodic or continuous seismicity is. Only events larger than indicated magnitude are included in count, in an attempt to maintain uniform completeness. Apparent increase in activity after 1969 in some areas may be an artifact of network improvements at about that time. Some large earthquakes, eruptions and intrusions are noted. Dashed lines are labeled with their slopes in events per day.

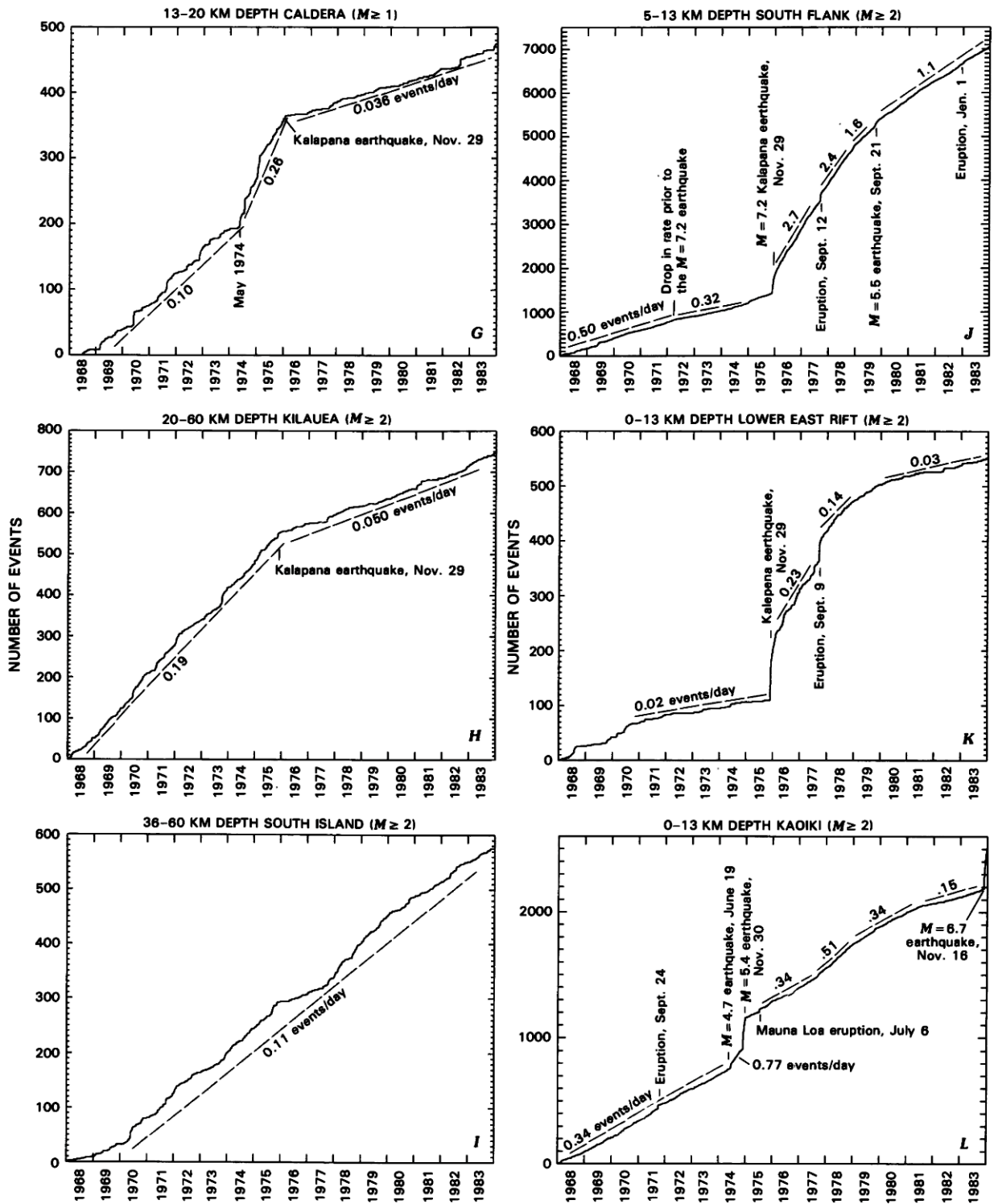


FIGURE 43.8.—Continued.

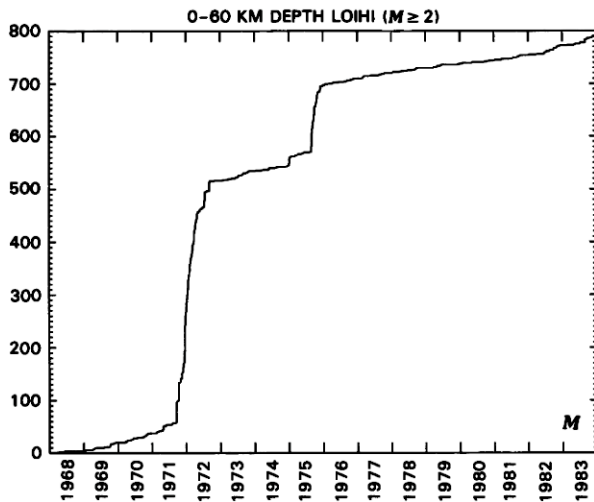


FIGURE 43.8.—Continued.

Shallow SWRZ seismicity (fig. 43.8D) is composed mostly of major intrusions in 1971, 1974 and 1981. The pattern is similar to that of the ERZ but with fewer and more seismogenic intrusions. Similar to the ERZ in 1979 and 1980, the SWRZ experienced a prolonged and continuous intrusion in the first half of 1981. This intrusion was marked by continuous but low-level seismicity of 5–10 events of magnitude 1 or larger per day. Summit tilt was nearly constant, suggesting that Kilauea's magma supply was being diverted into the rift without accumulating in the summit reservoir. At 5–13 km depth beneath the same region (fig. 43.8E), most earthquakes were in swarms and were south of the rift axis. Note that seismicity following the intrusions of 1974 and 1982 wanes gradually, as expected for tectonic earthquakes within the south flank produced indirectly by stress generated at the rift zone. The region of figure 43.8E also includes part of the Kalapana aftershock zone, so both south flank (tectonic) and rift (volcanic) events induce earthquakes here. The seismicity between intrusions in figure 43.8D and E comes mostly from the region's inclusion of small portions of the constantly active south flank and Kaoiki seismic zones.

#### KILAUEA'S MAGMA CONDUIT BELOW 5 KILOMETERS DEPTH

Seismicity rate curves for Kilauea's vertical magma conduit below 5 km depth are shown in figure 43.8F–H. Most of the events in the upper region (fig. 43.8F) occurred in swarms, but deeper activity becomes more continuous in time (fig. 43.8H). This change apparently is caused by a shift from volcanic earthquakes and concentrated stress in the shallow system to more uniform stress in the deeper conduit.

Earthquake data prior to 1968 is incomplete, but was not as continuous in time as the 1968–83 period of figure 43.8G–H. The 30-km-depth source was relatively inactive in the years prior to January 1961 (Eaton and others, chapter 48). In addition, several major swarms from 40–60 km depth occurred in late 1959 and 1960 (Eaton and others, chapter 48). The change from swarms to continuous seismicity may have been associated with the major subsidence of the summit of Kilauea during the 1960 Kapoho eruption, which was twice as large as any subsidence since.

Many swarms at 5–13 km depth (fig. 43.8F) occur in the days or weeks following major subsidence of the summit during large intrusions or eruptions. Examples include January–February 1975 and September 1977. The post subsidence swarms often consist of events having a long period seismic signature and are probably related to rapid refilling of the magma reservoir from below. This intermediate-depth seismicity was also high accompanying a series of swarms at the summit during 1971 (Koyanagi and others, 1976a). The summit seismicity was associated with both slow and rapid intrusions into the upper parts of both rifts. Other swarms in figure 43.8F, such as October 1973, are not obviously related to shallow volcanic or seismic activity.

The most prominent characteristic of the vertical conduit seismicity (fig. 43.8F–H) is the sharp drop in rate following the November 1975 Kalapana earthquake. The long-term drop in rate is not the result of masking by Kalapana aftershocks. The aftershocks interfered with the analysis of other earthquakes in two ways: (1) the intense seismicity for several days after the Kalapana earthquake masked most everything on the seismograms; and (2) the magnitude threshold for reading all events was raised to 2.6 for most of 1976 owing to the intense activity.

The drop in earthquake rate after the Kalapana earthquake was most pronounced between 5 and 13 km depth where it dropped by a factor of 8. The earthquake rate fell less for deeper events: there was a factor of 5 decrease between 13 and 20 km, and a factor of 4 below 20 km depth. Because the slip plane of the earthquake was at 10 km depth and displaced the entire block above, its effect on conduit seismicity was greatest in the crust.

As discussed above in the section "The Mechanism of Deep Earthquakes," the Kalapana earthquake relieved stress on both the magma conduit and upper mantle as the south flank moved seaward and expanded. The south flank had been compressed by numerous dike intrusions into the rifts during the century preceding the magnitude-7.2 earthquake (Swanson and others, 1976a). The sudden decompression and slip of the south flank caused the immediate intrusion of about 100 million cubic meters of magma into the ERZ (Dzurisin and others, 1980). The earthquake also triggered a shift in volcanic behavior from mostly eruptions to mostly intrusions, because the reduced stress near the rift accommodated magma below the surface without sufficient pressure to come to the surface and erupt (Klein, 1982b). The 1975 earthquake, however, apparently did not cause a drop in Kilauea's magma supply rate (Dzurisin and others, 1984). The Kalapana earthquake thus relieved stress on Kilauea's shallow magma system, and the rate drop of vertical conduit earthquakes indicates stress relief on the deeper

system as well. A future study of fault-plane solutions and history of vertical conduit earthquakes is planned to help constrain the space and time changes in stress.

The effects of the Kalapana earthquake on volcanic seismicity suggest that the stresses driving rift and vertical conduit earthquakes are slightly different. At depths below 5 km, the earthquake both relieved elastic stress and reduced seismicity in distributions that diminish with depth, thus suggesting that vertical conduit seismicity and tectonic earthquakes on the flanks are driven by interacting regional stresses. The conduit seismicity occurs because this stress is geometrically concentrated around the zone weakened by the presence of magma. In contrast, the Kalapana earthquake had no obvious effect on either the earthquake occurrence rate or intensity of individual swarms in the shallow summit and adjacent ERZ where swarms are frequent (fig. 43.8A, B). Seismicity was unchanged even though the shallow conduit system should have experienced stress and displacement changes larger than in the deeper conduits. Earthquakes in the shallow conduit system must therefore result more directly from very local stress generated by magma pressure than by regional or tectonic stress. This difference in the local versus regional scale of driving stress is in perfect agreement with the contrast in magnitude, time and space characteristics of shallow and deeper earthquakes.

The magnitude-2 or larger earthquakes below 36 km depth and under the entire south side of the island occur at a nearly constant rate of about 0.11 per day (fig. 43.8I). A few of the deepest events directly below Kilauea are plotted in both figure 43.8H, I, but they are a small percentage and do not dictate the behavior of either plot. The Kalapana earthquake appears to have caused a temporary drop in rate that is probably not real; for much of 1976, aftershocks were so numerous that processing of all smaller events was not completed. The recovery of rate indicates that the Kalapana earthquake had no lasting effect (either real or artificial) on the deepest seismicity. Earthquakes below about 36 km thus depend on the long-term mantle processes discussed earlier, and not on stress or volcanic changes in the crust.

#### TECTONIC EARTHQUAKES ON KILAUEA'S SOUTH FLANK

Kilauea's south flank seismicity is nearly continuous (fig. 43.8J), unlike the swarms that characterize the adjacent ERZ. Earthquake rates vary as the mechanical state of the flank changes. The 1968-71 period probably represents the most normal time in figure 43.8J and has a background rate of 0.50 events per day. The rate for the entire south flank dropped to about 60 percent of its prior value in early 1972. The change was localized to a few areas of the south flank and was interpreted by Wyss and others (1981) as premonitory to the 1975 Kalapana earthquake. The drop in rate presumably resulted from partial stress release adjacent to areas that remained locked and seismically active, but that showed different precursory anomalies.

The November 29, 1975 earthquake caused both immediate aftershocks and a massive seismic excitation of the south flank that

persists a decade later. The upward step in figure 43.8J is from immediate aftershocks. The step should be larger than plotted because data during December 1975 and most of 1976 is incomplete between magnitudes 2.0 and 2.6. The bending over of the seismicity curve to a constant rate of about 2.7 events per day (which is a reliable value in 1977) signified the end of immediate aftershocks. This immediate aftershock sequence diminished with a time constant of weeks to months, but the value is difficult to determine with the presently incomplete data. For seismicity to continue at a rate about 5 times above background level more than a year following the earthquake is unusual for a magnitude 7.2 event. South-flank seismicity in this extended aftershock sequence is diminishing very slowly, as shown in figure 43.8J. The rate of decrease is approximately exponential with a time constant of about 6 years. One possibility for the high south-flank seismicity is simply relaxation of localized stress changes caused by the earthquake, but at an unusually low rate. In addition, the south-flank seismicity is above the nearly horizontal slip plane of the Kalapana earthquake. These aftershocks are thus not simple in the sense of being confined to the mainshock fault plane, and may thus have a more complex history.

Earthquakes in the south flank are ultimately driven by stress applied from repeated intrusions into the ERZ to the north. The largest events, such as September 1977 and January 1983 (fig. 43.8J), induce south-flank earthquakes that decrease after a few days or weeks (Dvorak and others, 1985). It is difficult to reconcile the rate of decrease of intrusions (days to weeks) and immediate Kalapana aftershocks (weeks to months) with the prolonged decrease of the extended aftershocks. Additional magma intrudes the rift steadily and between the rapid intrusions at rates difficult to estimate (Dzurisin and others, 1984). Stress was therefore applied incrementally but often to the south flank, at least during the period plotted in figure 43.8J. The cause of the extended aftershocks may therefore lie not in response to incremental stress from the Kalapana earthquake, but in a fundamental change in the mechanical behavior of the flank as it responds to stresses applied more or less steadily. For example, the creation of many new fractures by the Kalapana earthquake may shift the flank's response from elastic compression and aseismic creep to seismic slip on new faults. The new faults could then heal or become locked on a several-year time scale and eventually shift the balance back to aseismic deformation. This difficult problem needs more detailed work.

Kilauea's lower ERZ experienced a similar dramatic increase in seismicity at the time of the Kalapana earthquake (fig. 43.8K). From a pre-1975 rate of 0.02 events per day for magnitude-2 and larger earthquakes, the rate jumped by an order of magnitude even after the immediate aftershocks decreased. The rate diminished steadily and in the early 1980's was close to the pre-earthquake value. The decay time constant is roughly one-half that of the central south flank to the west. Earthquake swarms related to volcanic processes also occur in this section of rift (Koyanagi and others, 1981), such as in 1970, 1977 and 1982 (fig. 43.8K). The earthquakes determining the basic shape of the cumulative event curve, however, are primarily tectonic.

### TECTONIC EARTHQUAKES IN THE KAOIKI SEISMIC ZONE

The Kaoiki seismic zone is the second most active region of tectonic flank earthquakes in Hawaii, and the cumulative curve shows continuous activity punctuated by aftershock sequences (fig. 43.8L). A background rate of 0.34 events per day is characteristic of 1968–73 and appears to be typical for the years following the two aftershock sequences of 1974. Between the aftershock sequences of June and November 1974 the rate is nearly constant at 0.77 events per day.

The Kaoiki seismic zone, however, cannot be considered in isolation from Kilauea and Mauna Loa. Mauna Loa's seismic reawakening in 1974 was in preparation for its July 1975 eruption (Koyanagi and others, 1975), and its accompanying inflation added stress to the Kaoiki seismic zone and may have helped trigger the  $M=4.7$  (June 19, 1974),  $M=5.4$  (Nov. 30, 1974) and  $M=4.7$  (Dec. 15, 1974) earthquakes. The November Kaoiki earthquake was followed one month later by a large intrusion into Kilauea's SWRZ. The earthquake probably did not cause the intrusion, but may have caused Kilauea to shift its attention away from the ERZ, where eruptions and intrusions occurred during the previous three years. The strike-slip mechanism of the November 1974 earthquake (Endo and others, 1978) would have relieved confining stress on the SWRZ permitting an easier intrusion path than before. Seismic shaking of Kilauea's magma system may also have changed the magma conduit of least resistance and led to the shift from the ERZ to the SWRZ.

The variations in seismic rate of the Kaoiki seismic zone after 1974 are also significant. The drop in rate in mid-1981 to one-half its former value is readily identifiable and can be interpreted as the onset of seismic quiescence precursory to the November 1983 earthquake (M. Wyss, written commun., 1985). The variations in rate during 1975–80 are real, but it is harder to identify breaks in slope and the three periods of varying seismicity whose rates are indicated in figure 43.8L. The origin of the high seismicity of 1977–78 has not been identified.

### SEISMICITY NEAR KILAUEA'S SHALLOW MAGMA RESERVOIR AND RIFT ZONES

Kilauea's summit region produces its most intense seismicity, which is detailed in a series of depth slices only 0.5 km thick in figure 43.9. Several earthquakes per minute can be generated within volumes smaller than a few cubic kilometers during rapid intrusions. Most active are the short sections of the two rifts within about 4 km of the summit caldera (fig. 43.9E–G). Events are highly concentrated both in time and space, indicating that the source of stress producing them is nearby, produces large gradients and can change rapidly. The most intense and linearly continuous seismicity is between 2.5 and 3.5 km depth (fig. 43.9F, G), and the main magma conduits are presumably centered at about 3 km depth.

Most seismicity between intrusions is caused by inflation of the magma reservoir. The reservoir is capped by brittle rock within the

caldera, which produces earthquakes when the reservoir inflates. As stated in the previous section, a gradual buildup of caldera earthquakes lasting several days to months often precedes an intense swarm and intrusion. The pre-intrusion activity is not only within the caldera and reservoir cap, but may include slow intrusions of the sections of rift adjacent to the reservoir. Portions of the rifts thus appear at times to be magma-filled and directly connected to the inflating summit reservoir.

### THE SUMMIT MAGMA RESERVOIR

The summit magma reservoir, as defined by a gap in seismicity, is at the intersection of the active conduits of the two rifts. The seismic gap coincides with the geodetic deformation center and is part of a zone of low rigidity (fig. 43.9F, G). The rift conduits constrain the reservoir's position on its south and east sides near 3 km depth. The clusters of earthquakes in the north-central caldera and just southwest of Halemaumau apparently form other parts of an incomplete ring of brittle deformation surrounding the magma reservoir. Some earthquakes do plot within this region identified with the magma reservoir, however: these may either be slightly mislocated owing to the large lateral and unmodeled velocity gradients, or actually inside brittle slivers within a magma storage complex. All of the limitations of location precision discussed earlier apply here and mean that we cannot resolve detail within this 1- to 2-km-diameter void.

These relations can be seen from a different perspective by examining vertical cross sections taken through the summit magma reservoir. Figure 43.10A is a map showing the rectangular areas included in the four sections of figure 43.10B–E. The cross sections intersect at summit magma reservoir. Only earthquakes with both horizontal and vertical errors less than 1 km are plotted in figure 43.10, so structures of about this size should be resolvable. This also means that proportionally more earthquakes below about 4 km than above this depth are eliminated from the plots, because errors increase somewhat with depth.

A zone with few or no earthquakes below the caldera contains the magma reservoir complex. The dashed oval in figure 43.10B–E is not meant to portray its exact size or shape, but only to sketch the outer limits of sparse seismicity. Its position is constrained by four zones of seismicity: a cap of earthquakes mostly between 1 and 2 km depth directly above the reservoir, the intensely active segments of the ERZ and SWRZ adjacent to the reservoir's upper part near 3 km, and the top of the vertical conduit at a depth of about 7 km.

The reservoir's seismic cap is centered and most intense beneath Halemaumau, but extends across most of Kilauea caldera (fig. 43.10). The greater intensity of seismicity between 1 and 2 km compared to just above is probably a result of its proximity to the source of stress below. The reduced activity above 1 km may also be a result of lessened confining stress on the shallowest fault planes or a concentration of seismicity in very small-magnitude events that are detected but are not locatable with the seismic network. The northern half of the caldera produces events most intensely near 2 km

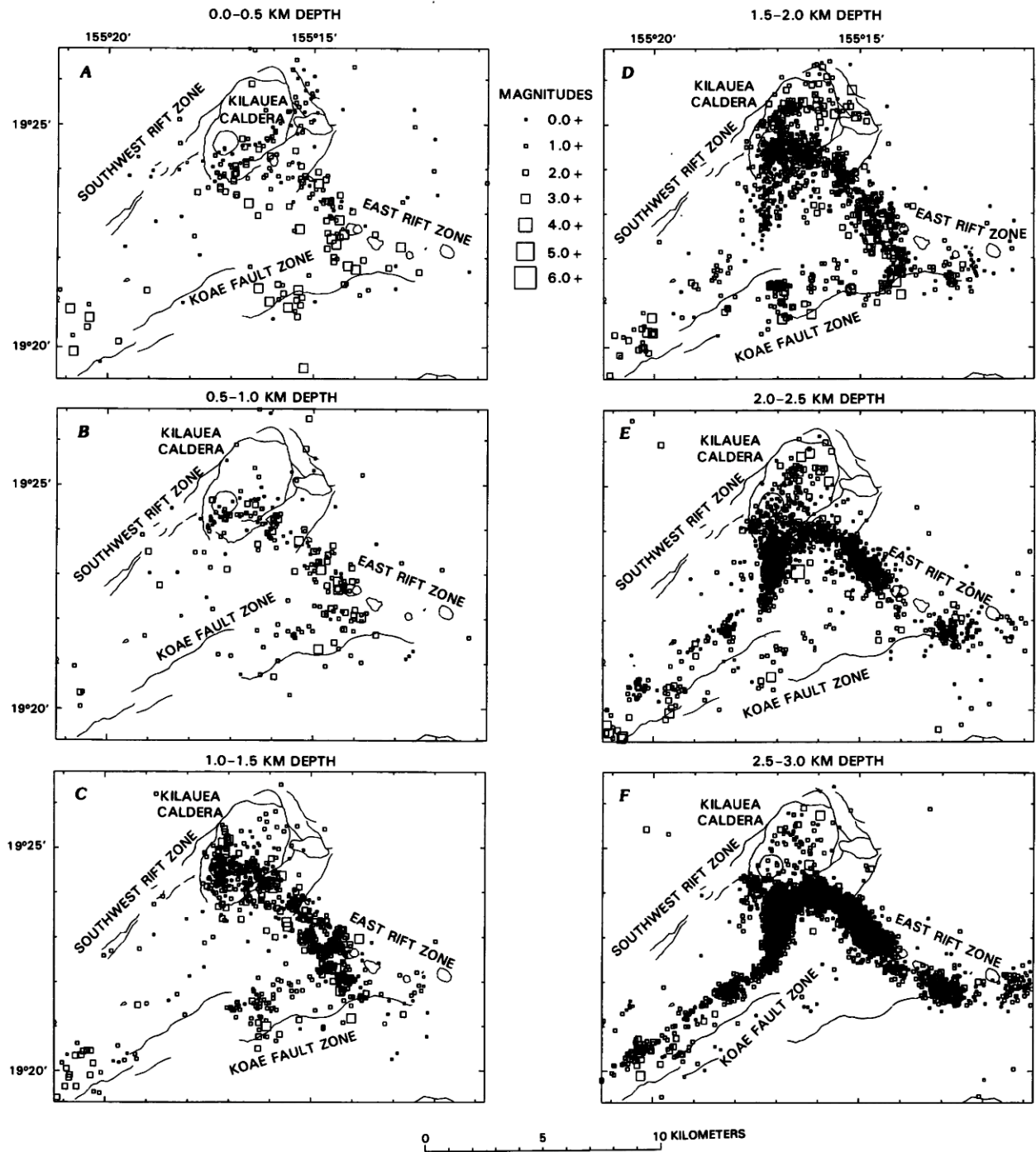


FIGURE 43.9.—Depth slices, 0.5 km thick, of 1970–83 earthquakes near Kilauea caldera between 0 and 5 km depth. Maximum location error of plotted events is 3 km horizontally or vertically. Earthquake symbol size scales with magnitude. Faults, fissures, and pit craters are as shown in figure 43.1.

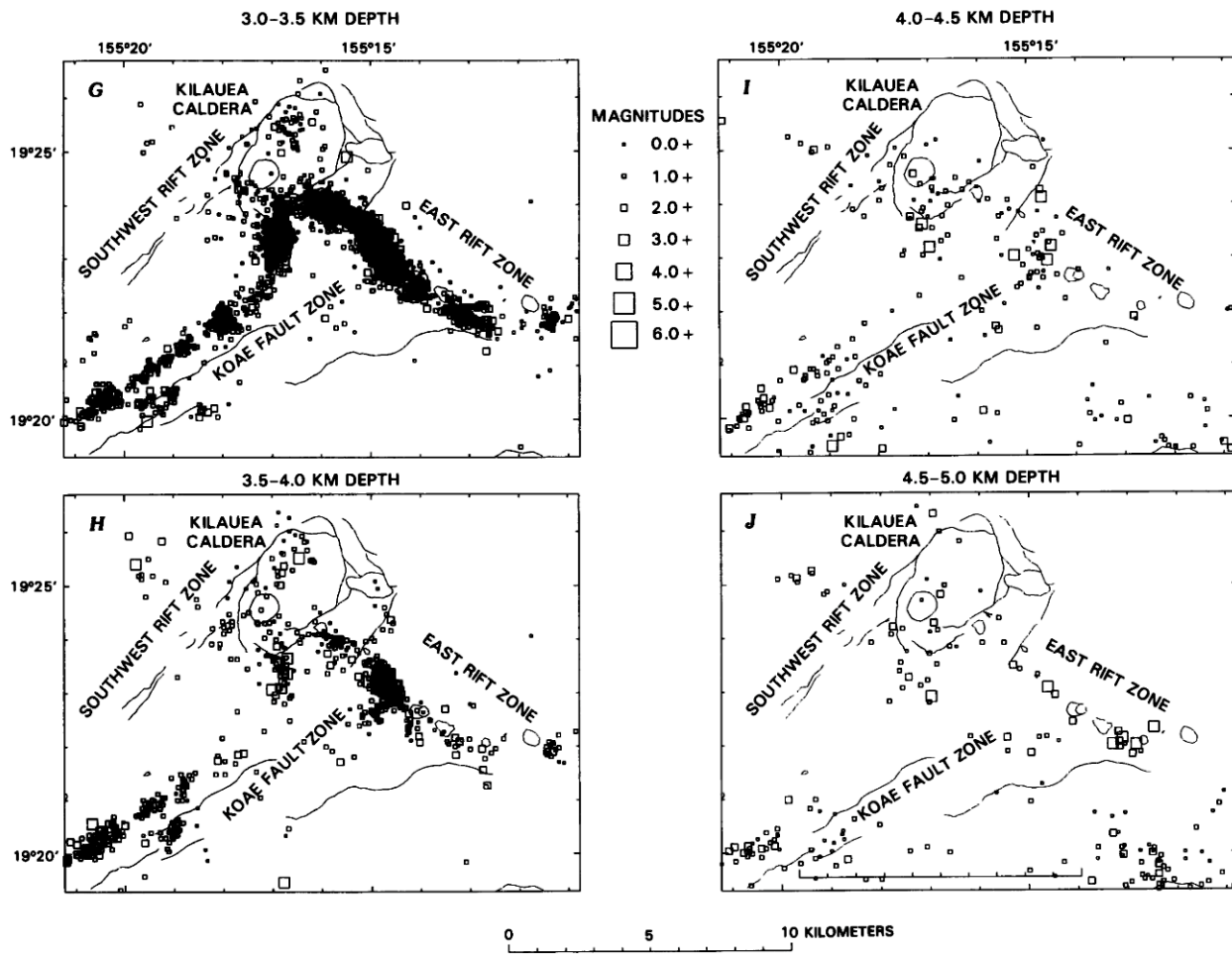


FIGURE 43.9.—Continued.

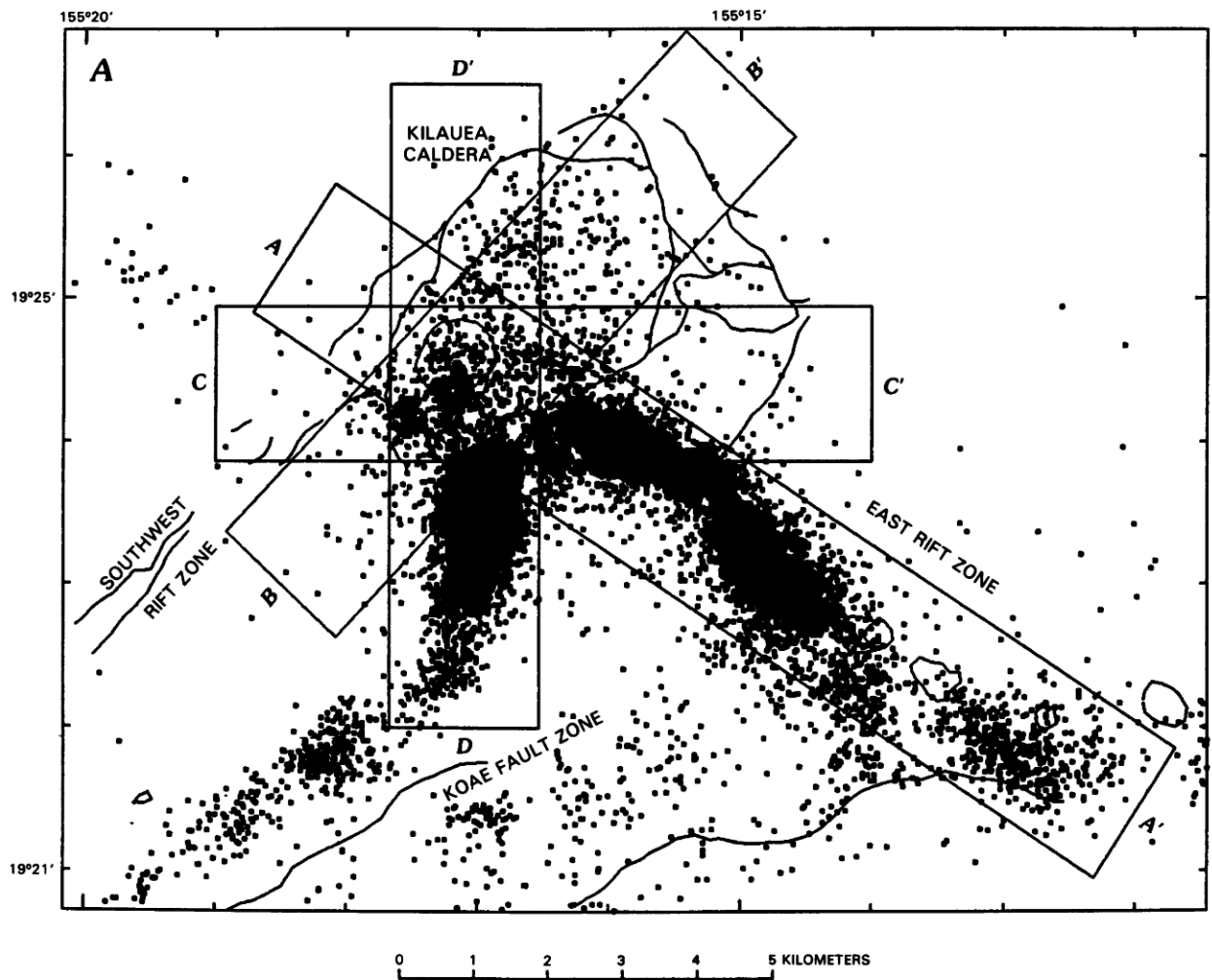


FIGURE 43.10.—Epicenters and hypocenters of shallow 1970–83 earthquakes near Kilauea caldera. *A*, Epicenter map showing positions of cross sections. Sections cross over buried magma reservoir. Endpoints of sections are labeled with letters keyed to the distance axes of figure 43.10*B–E*. Only earthquakes inside the 2-km-wide rectangular areas of figure 43.10*A* are plotted on figure 43.10*B–E*. *B–E*, Cross sections of 1970–83 hypocenters. Position of magma reservoir is approximated by dashed oval. Horizontal and vertical errors of all hypocenters plotted is 1 km or less. Datum for sections is ground surface. When comparing earthquake patterns in map and sections note that sections extend to 12 km depth, but map only plots events in upper 5 km for clarity. Faults, fissures, and pit craters are as shown in figure 43.1.

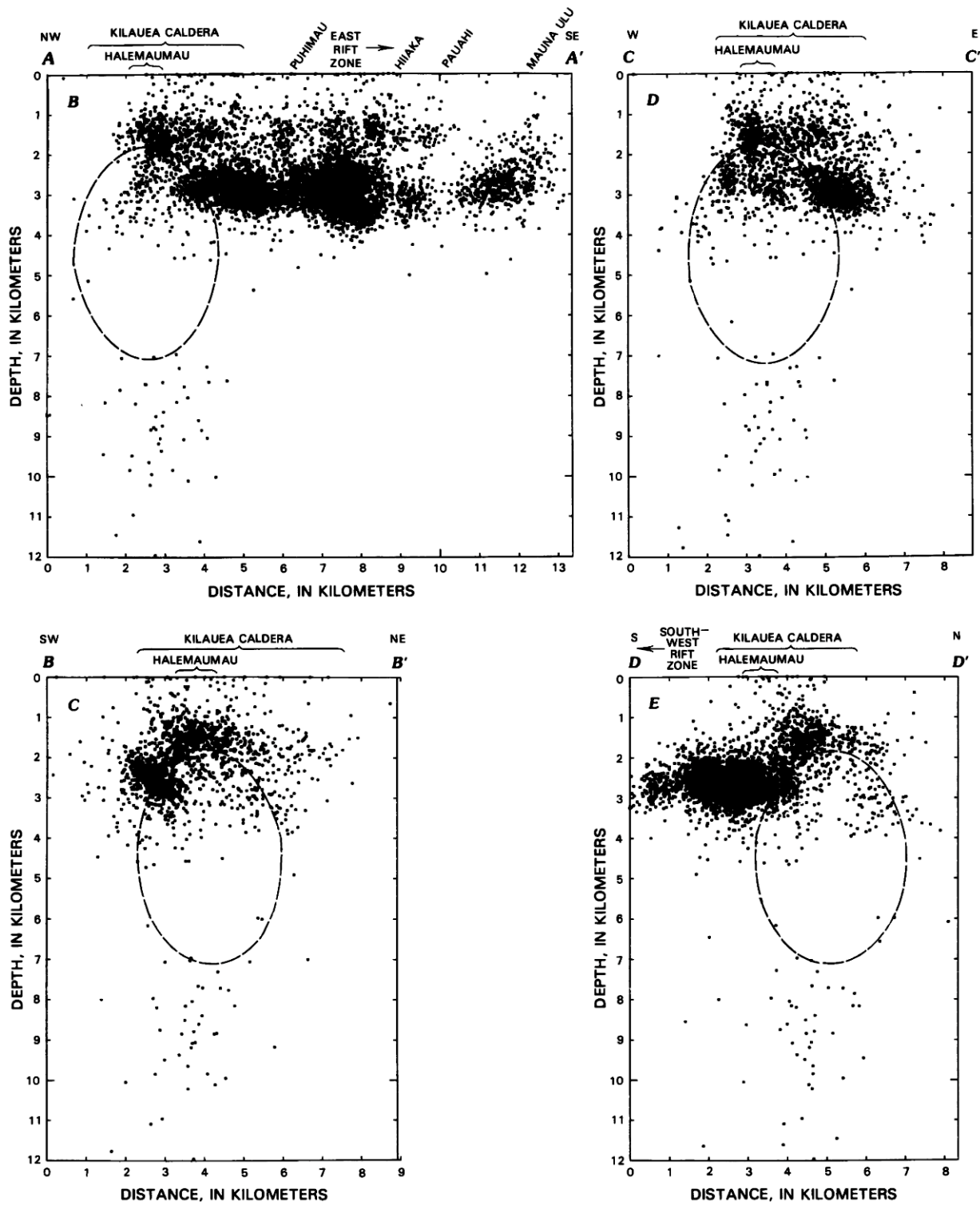


FIGURE 43.10.—Continued.

depth (fig. 43.9D, E). Most of these earthquakes occur at times of rapid inflation and probably are triggered by lifting and extension of the brittle cap over the magma reservoir. Seismicity above the reservoir also accompanies major and rapid deflations such as in September 1977, August 1981 and January 1983. The band of very shallow events north of Kilauea Iki (fig. 43.9A) parallels the caldera rim and appears to be caused by movement on rim faults during periods of inflation.

The upper and lower parts of the magma reservoir behave differently. The buried centers of inflation and deflation of Dvorak and others (1983) are mostly in the upper half of the dashed oval shown in figure 43.10B–E. These deformation centers are below the base of the seismic cap at 2 km, but above the completely aseismic region between 4.5 and 7 km depth. The upper section of the magma storage complex is thus the active portion: it produces some seismicity, the changes in magma volume near the deformation centers occur there, and it is surrounded by the zones in which seismicity and intrusions occur. The lower section of the reservoir is passive and has low rigidity, however: it is aseismic and seldom supports centers of elastic deformation. Any deformation of the lower half of the reservoir would probably be masked by that in the upper half, to which surface measurements are most sensitive. The reservoir can also be viewed as the upper part of a fluid column whose top level fluctuates with changes in stored magma volume. Variations in level then change the pressure on the confining cap where the seismicity and uplift occur. The magma reservoir is apparently a connected network of liquid and solid segments, as indicated by the limited seismicity and the fact that different centers of deformation are active at different times (Fiske and Kinoshita, 1969; Ryan and others, 1983; Dvorak and others, 1983).

#### THE SUMMIT SECTION OF THE EAST RIFT ZONE

Unlike the SWRZ, the ERZ between Halemaumau and Pauahi (fig. 43.1) generates seismicity above its main conduit and essentially to the surface (fig. 43.9A–D). During the last few decades the ERZ has been more active magmatically than the rest of the rift system. This high magmatic activity may extend the ERZ dike network vertically and stress the upper 2 km to such a degree that it deforms seismically. The shallow seismicity usually occurs at the same times and places as the earthquake swarms in the more intense zone centered at 3 km. There is thus a close seismic and probably magmatic coupling to the main conduit. We interpret the shallow seismicity and patterns of shallow intrusions as evidence of a multitiered and complex honeycomb of magma conduits in the upper ERZ.

Internal structures in the ERZ appear to control seismically active and inactive regions. There is a major cluster of earthquakes about 1 km uprift of Mauna Ulu (fig. 43.10B, C). The earthquakes that plot below this cluster at 5 to 8 km depth (fig. 43.10B) mostly occur just after intrusions and are immediately adjacent to tectonic earthquakes in the south flank. The ERZ bends eastward and the Koaie fault zone meets the rift there. This area is thus structurally complex. Migrating swarms (and by inference also propagating dikes) often begin between Pauahi and Mauna Ulu.

We interpret this cluster as a barrier or pinched zone that sometimes blocks downrift magma flow at this point. Earthquakes are then generated by the formation or rejuvenation of dikes that break through the barrier.

Just uprift of the Mauna Ulu cluster is a seismically inactive zone beneath Pauahi (fig. 43.10A, B). A break in continuity of earthquakes is at 3 km depth, and the 1- to 2-km-deep seismicity essentially ends there. This apparently is a low stress or low rigidity zone of relatively unobstructed magma passage. The magma conduit here is possibly very similar to the rest of the ERZ, but for some structural reason such as proximity to the Koaie fault zone, it does not accumulate stress to be released seismically. We favor an alternative interpretation of this seismic gap as a small magma storage reservoir within the rift. Magma stored there would be held in place by the barrier just downrift. In addition to times of intrusion, this Pauahi reservoir could easily receive magma during periods of summit inflation when the rift between it and the summit reservoir is seismically active and is slowly being fed magma. This possible magma reservoir will be treated below in the section "Discussion of Rift Zone Intrusions." The total volume of magma stored below Pauahi may be small, but if it is consistently kept hot and low in rigidity, seismic stresses will never accumulate to be released in earthquakes.

#### EARTHQUAKE HYPOCENTERS IN THE SOUTHWEST RIFT AND CENTRAL EAST RIFT ZONES

The SWRZ and the ERZ downrift of Mauna Ulu (fig. 43.11) are in some ways simpler than the uprift section of the ERZ: they are less frequently active and have simpler earthquake patterns. Longitudinal cross sections of earthquakes during 1970–83 from both rifts are plotted in figure 43.12. The main magma conduit at about 3 km depth is prominent in each section. The conduits of both rifts plunge from about 2.5 km depth below the surface at their uprift end to about 3.5 km downrift. The apparent 3.7-degree plunge of the ERZ conduit must be added to the 1.3-degree surface slope to give a plunge of about 5 degrees. The SWRZ is somewhat steeper, with apparent and surface slopes of about 5.0 and 1.7 degrees respectively for a total of about 7 degrees. The apparent plunges are probably real, although unmodeled seismic velocity variations are a source of error in the apparent slopes.

The quantity of ERZ earthquakes diminishes with distance from the caldera owing to the reduced frequency and intensity of intrusions. The ERZ conduit cannot be defined seismically farther than 30 km from the caldera. Major intrusions of the SWRZ, however, produce earthquakes in most of the 20 km of rift between the caldera and Puu Kou in a way that does not diminish with distance along the rift.

Considerable rift-zone structure is visible in the sections of figure 43.12. We associate the prominent and persistent clusters of events along both rifts with barriers or blockages of the magma conduit that resist penetration by dikes and produce high stresses during intrusions. The major SWRZ barrier near Puu Kou, for example, has produced an intense cluster of earthquakes and prevented any intrusion from continuing downrift during the period

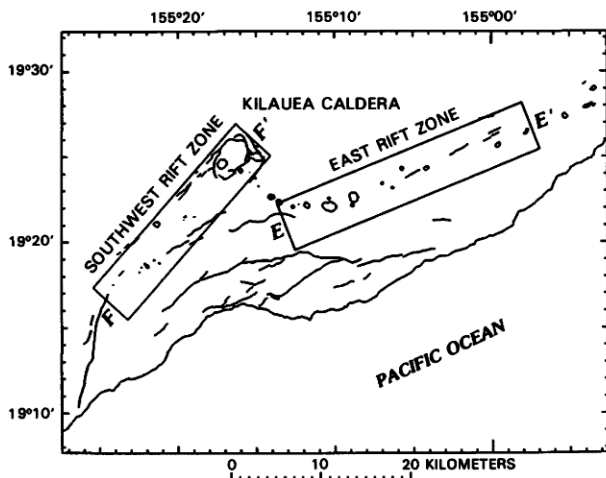


FIGURE 43.11.—Areas included in longitudinal cross sections of rift zones. Only earthquakes within rectangles are plotted in sections. Section *E-E'* is shown in figure 43.12A and *F-F'* in figure 43.12B. Faults, fissures, and pit craters are as shown in figure 43.1.

of historical observation. This barrier also coincides with a bend in the rift (fig. 43.1A). The earthquake gaps between clusters are apparently places of unstressed magma passage, and some may be secondary magma storage pockets. The most prominent gap just northeast of Puu Kamoamoia is such a storage reservoir. This section of rift was geodetically observed to inflate during the slow intrusions of 1978–80. In addition, the earthquakes above the main conduit (0–2 km depth in figure 43.12A occurred during these intrusive pulses, much as shallow caldera earthquakes occur above the summit magma reservoir when it inflates.

Earthquakes in Kilauea's flanks are separated from the rift magma conduits in both map position and depth. Most of the events shown deeper than 5 km in figure 43.12 are tectonic earthquakes from the south flank that fall within the cross-section regions. The base of the zone of tectonic earthquakes is near 10 km and is the approximate depth of the prevolcanic layer of ocean sediments on which the mobile south flank slips seaward (for example, Crosson and Endo, 1982). A series of transverse sections, whose positions are shown in figure 43.13, will make this clear. Figures 43.14A–D are sections successively downrift along the ERZ. The main magma conduit at 3 km depth and north of the deeper south-flank seismicity is visible in each section. The detailed cross-sectional shape of the magma conduit cannot be determined owing to errors in earthquake hypocenters. The sections uprift of Mauna Ulu (fig. 43.14A, B) and near Puu Kamoamoia (fig. 43.14D) include seismicity above the main conduit. Shallow events plotted at the south end of figure 43.14A are in the Koae fault zone. Only the section including Pauahi and Mauna Ulu (fig. 43.14B) reveals significant activity beneath the main magma conduit.

The relation between rift and flank seismicity is very similar in the SWRZ. Figures 43.14E–G are transverse cross sections successively downrift along the SWRZ (fig. 43.13). The main magma conduit is visible at about 3 km depth in each section, defined largely by the major intrusions of December 1974 and August 1981. The scattered earthquakes northwest of the main conduit near the caldera (fig. 43.14E) are partly from the September 1971 intrusion into the northern portion of the SWRZ. The shallow earthquakes southeast of the conduit in the same section are from the west end of the Koae fault zone. The conduit near Mauna Iki (fig. 43.14F) splits into two strands. The shallow (0–2 km depth) earthquakes in this area were generated by an apparent upward branch of the dike formed in the August 1981 intrusion, which also produced surface cracks in this area. Considerable seismicity also occurs southeast of the rift near Puu Kou in Kilauea's mobile south flank (fig. 43.14G).

The rift and adjacent flank earthquakes are spatially better separated at the ERZ than at the SWRZ (compare fig. 43.14B–D with fig. 43.14F, G). The greater distance of flank events from the ERZ correlates with their greater independence from the times of rift intrusions. Earthquakes adjacent to the SWRZ, however, are more closely coupled to the rift in both time and space. The greater separation of rift and flank earthquakes in the ERZ may also result from the narrowness of the surface expression of the ERZ: the wider SWRZ at the surface may be related to the multiple seismic strands and closely coupled flank earthquakes at depth.

The rift zones below about 5 km depth are mostly aseismic. Rifting must extend to about 10 km depth where the volcanic pile is decoupled from the prevolcanic oceanic crust. The lack of seismicity then means the deep rifts are too hot and too ductile to support earthquakes, and the timing of deep rifting relative to the episodic shallow intrusions is unknown. There are, however, some deep rift earthquakes. The main SWRZ magma conduit downrift of Mauna Iki directly overlies a deeper but somewhat diffuse seismic zone (figs. 43.12B, 43.14F, G). This deep zone was active in the intrusion of June 1982, in which rifting apparently extended downward through the crust. A few hypocenters 5 to 10 km beneath Mauna Ulu in the ERZ (fig. 43.10B) are also produced by rifting. These deep ERZ events occurred during and immediately after several shallower swarms and apparently represent a locally brittle zone that responds to intrusions above.

#### THE KOAE FAULT ZONE

The Koae fault zone is seismically active, though far less so than either rift zone. The Koae consists of noneruptive fissures and north-facing normal fault scarps and is interpreted as a tear-apart zone linking the ERZ and SWRZ (Duffield, 1975; Unger and Koyanagi, 1979). Nearly all Koae earthquakes occurred during a few short swarms apparently caused by magma intrusions from the ERZ into an otherwise dry fault zone. No recent eruption from the Koae is known, however, and confining stress is probably so low that magma can be accommodated underground without building enough

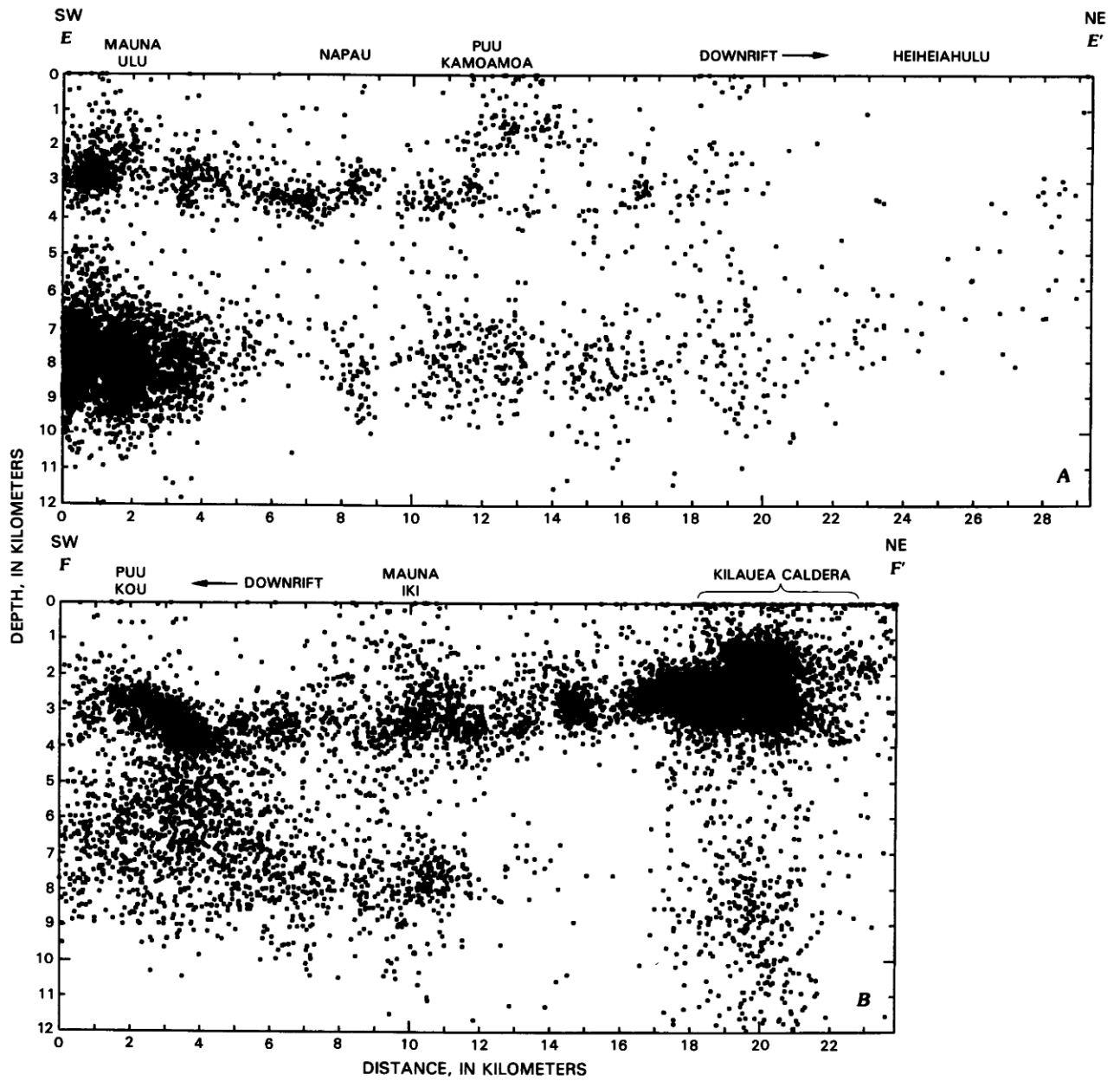


FIGURE 43.12.—Longitudinal cross sections of earthquakes below east rift zone (A) and southwest rift zone (B). Positions and areas of sections are shown in figure 43.11. Main magma conduits are at about 3 km depth.

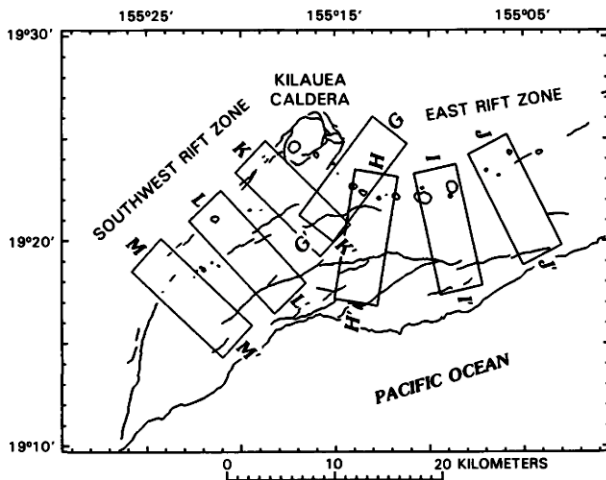


FIGURE 43.13.—Areas included in transverse cross sections of rift zones. Only 1970–83 earthquakes within rectangles are plotted in sections. Sections G–G' through J–J' are plotted in figure 43.14A–D, K–K' through M–M' in figure 43.14E–G. Faults, fissures, and pit craters are as shown in figure 43.1.

hydrostatic pressure to erupt. Earthquakes generally migrate rapidly from east to west as intrusions penetrate the Koa'e. The immediate source of magma might be the suspected magma reservoir in the adjacent ERZ below Pauahi.

Figure 43.15 shows a map and cross section of shallow Koa'e earthquakes. The seismicity extends about 6 km from the ERZ in a linear band that underlies the zone of faults and fissures. Earthquake depths are mainly between 1 and 2 km, the same as the shallow seismic conduit system in the uprift part of the ERZ (figs. 43.10B, 43.15B). The Koa'e intrusions may thus be related to the shallow ERZ conduit system. The main ERZ conduit at 3 km depth, however, is not seismically expressed in the Koa'e. The earthquakes below 6 km depth in figure 43.15B (not plotted in figure 43.15A) are part of the tectonic seismicity in Kilauea's south flank. Very shallow earthquakes are seen in a small area of the SWRZ (fig. 43.9C, D, lower left corner). These earthquakes apparently result from an upward-branching dike within the rift zone, which may be influenced by the intersection of the SWRZ magma conduit with the Koa'e.

#### KILAUEA'S VERTICAL MAGMA CONDUIT AND THE PATTERN OF DEEP EARTHQUAKES

Kilauea's magma conduit is clearly recognized in the earthquake depth slices discussed earlier. Although depth slices show the size and position of the conduit at a particular depth very well, variations in seismicity with depth are more easily seen in a vertical cross section. The map positions of three sections are shown in figure 43.16, along with epicenters of earthquakes below 13 km depth.

The three sections (fig. 43.17) extend from the surface to 60 km depth and all include the seismically defined magma conduit. Enlargements of the central parts of each section restricted to 0–25 km depth (fig. 43.18) clarify the dense seismicity in the upper part of the conduit. Most plotted earthquakes between 0 and 5 km depth are related to Kilauea's summit and rifts, and those between 5 and 13 km occur mostly under the south flank and Kaoiki seismic zones. The magma conduit earthquakes are most clearly separated from shallow seismicity when viewed from the east (figs. 43.17A, 43.18A).

An important geometrical feature of the seismicity associated with the conduit is its unevenness with depth. Earthquakes tend to cluster near depths of 9, 16 and 30 km with reduced activity centered near 5, 13 and 20 km (figs. 43.17A, 43.18A). Several possible reasons exist for the seismic gaps based on either low rigidity, low stress or a low fracture density relative to the conduit above or below. As has been inferred, the gap at 4–7 km results from the low rigidity of the summit magma reservoir. The possibility of magma storage near 13 or 20 km is much more difficult to determine, however: (1) a deeper reservoir may not accumulate enough magma to swell elastically and deform the surface, but merely transmit magma passively; and (2) it would be difficult to detect because of its greater distance from the surface and because of the much larger deformation from the shallow reservoir. The present gradation from volcanic seismicity in the shallow parts of the conduit to more tectonic earthquakes at depth argues against a deep magma reservoir large enough to influence seismicity.

The gaps in seismicity near 13 and 20 km probably result from differences in lithology or stress within the lithosphere, and not necessarily magma reservoirs. The base of the south flank zone of tectonic earthquakes at about 10 km depth (fig. 43.18A) and the basal slip during the 1975 Kalapana earthquake may coincide with the layer of ocean sediments at the base of the Hawaiian volcanic pile (Furumoto and Kovach, 1979; Crosson and Endo, 1982). The depth and landward dip of the oceanic Moho beneath the island's south coast (Hill and Zucca, chapter 37; Zucca and Hill, 1980) if projected, should intersect the vertical magma conduit around 15 km near the base of the seismic gap. The gap in seismicity near 13 km would then roughly coincide with the old oceanic crust and be bounded by the old Moho and sediment layers. The low-rigidity sediment layer could be viewed as a low-stress zone that partially decouples the stresses above and below.

One must consider the interaction between the lithosphere and the whole volcanic system to determine the cause of the very clear absence of earthquakes in the volcanic conduit near 20 km depth. Note that very few events occur at this depth anywhere beneath Kilauea (figs. 43.30, P, 43.17). This observation suggests that stresses are low at this depth in the lithosphere beneath Kilauea. The lithosphere beneath Hawaii can be modeled as an elastic plate flexing downward under the weight of the volcanic pile (for example, Watts and Cochran, 1974; Watts and others, 1985). More detailed modeling of the lithosphere as an elastic-plastic plate suggests that its neutral stress axis (relative extension above and compression below) may lie at a depth of about 23 km (Liu and Kosloff, 1978). The

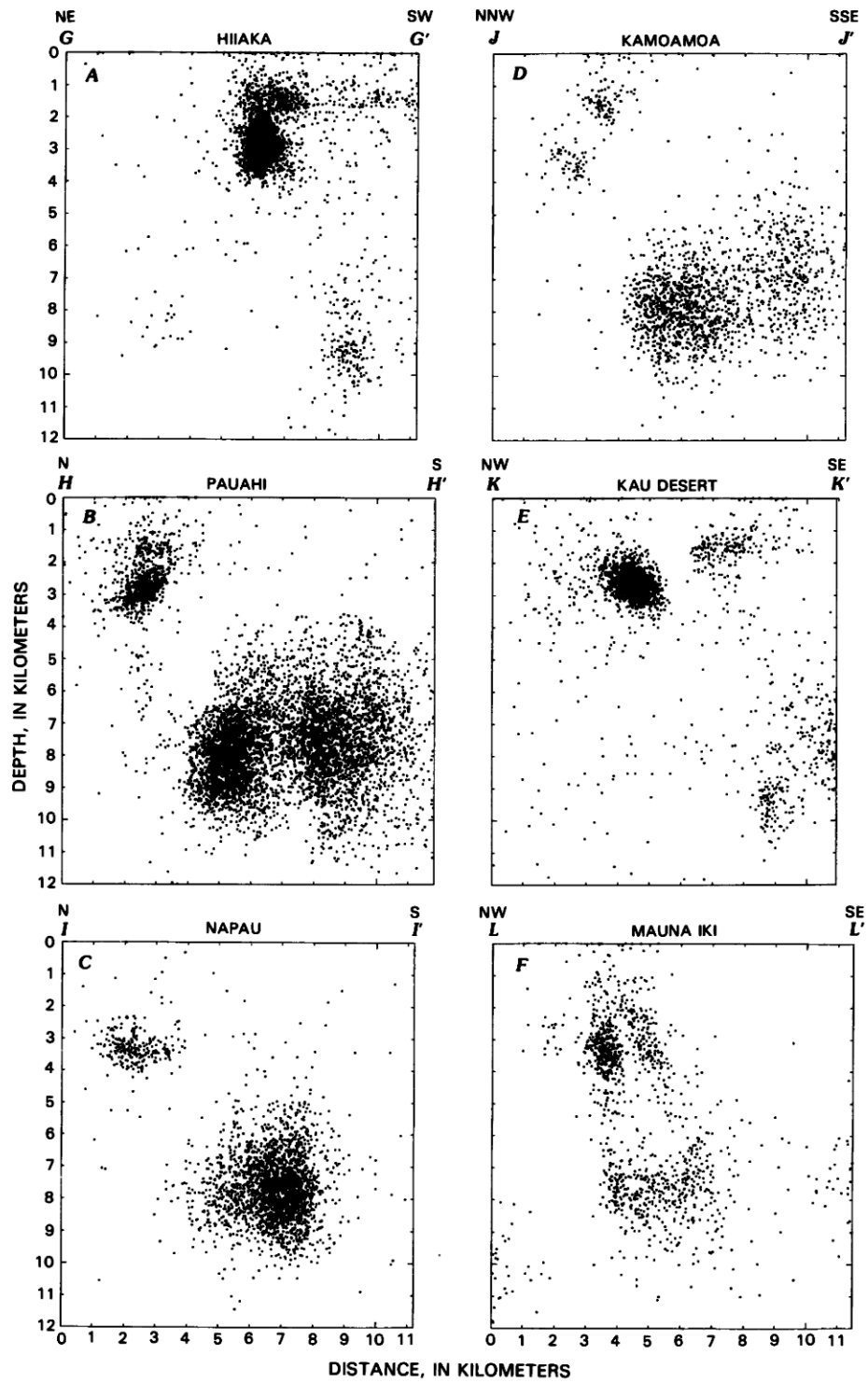


FIGURE 43.14.—Transverse cross sections of earthquakes beneath east rift zone (A–D) and southwest rift zone (E–G). Positions and areas of sections are shown in figure 43.13. Main magma conduits are at about 3 km depth.

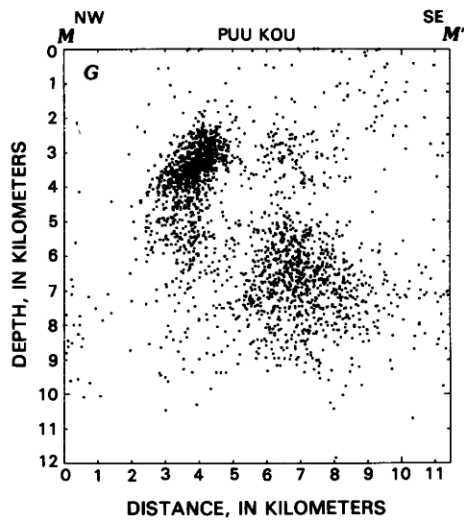


FIGURE 43.14.—Continued.

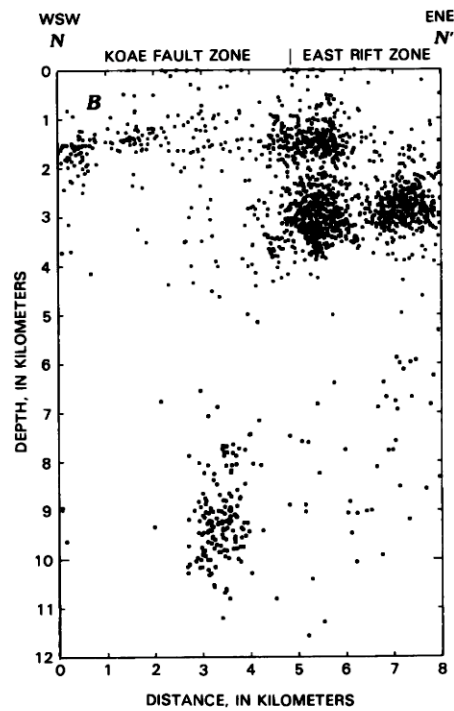
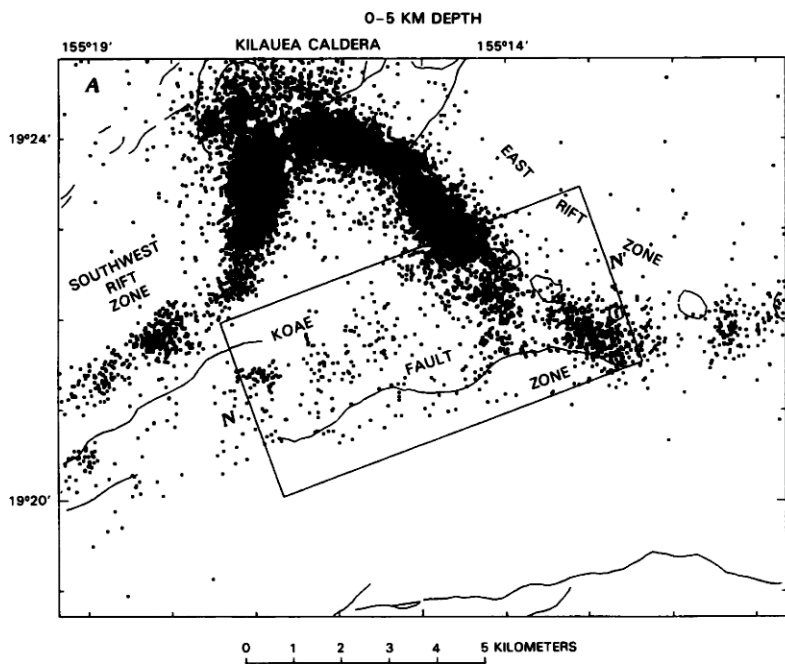


FIGURE 43.15.—Locations of shallow 1970–83 earthquakes south of Kilauea caldera in Koae fault zone. *A*, Map view showing rectangular area of seismicity plotted in cross section *N-N'*. Faults, fissures, and pit craters are as shown in figure 43.1. *B*, Cross section *N-N'* showing earthquakes to 12 km depth, but *A* only plots earthquakes to 5 km depth for clarity.

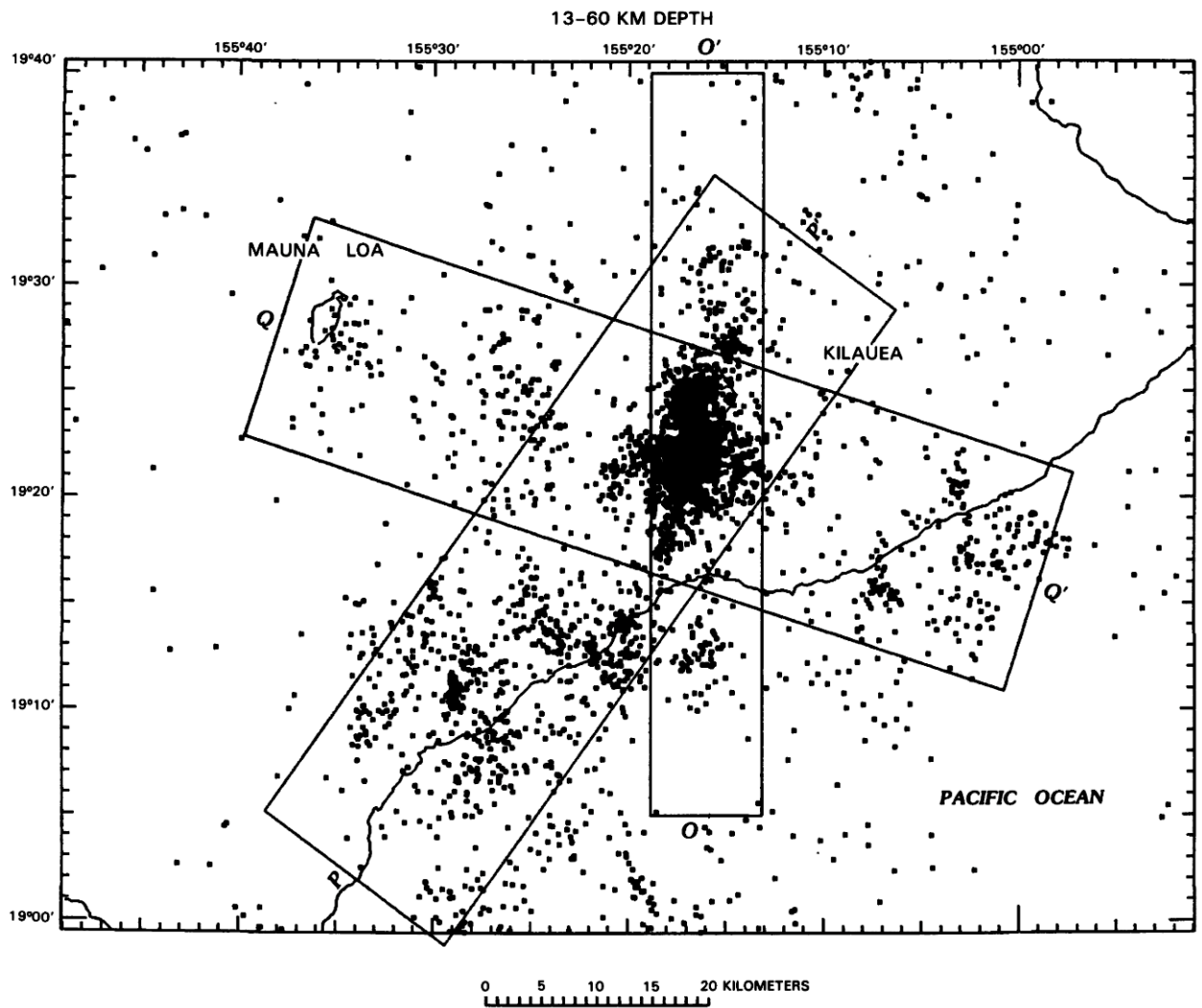
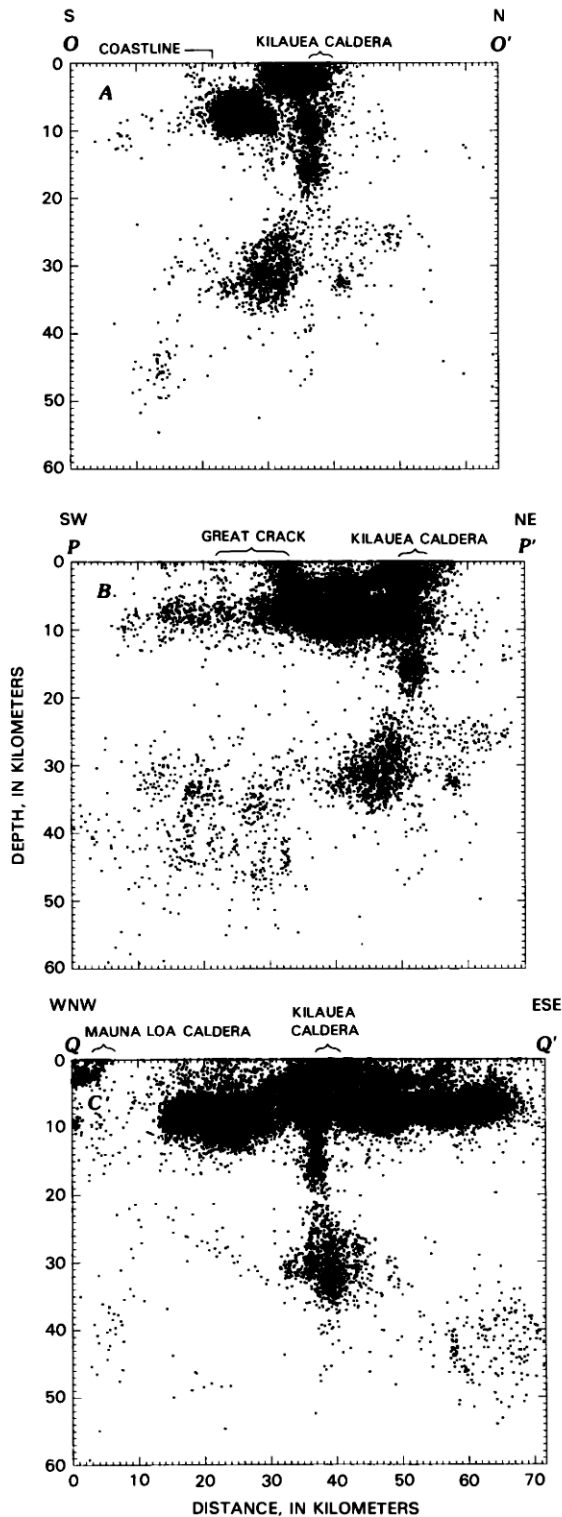


FIGURE 43.16.—Locations of 1970–83 earthquakes from 13–60 km depth beneath south side of Hawaii. Cross sections *O-O'* through *Q-Q'* are shown at different scales in figures 43.17A–C and 43.18A–C. Only earthquakes within rectangular areas are plotted on sections. Although events above 13 km are plotted on sections, they are omitted from map for clarity. All three sections include Kilauea's vertical magma conduit. Faults, fissures, and pit craters are as shown in figure 43.1.



relative absence of earthquakes near 20 km depth thus may mark the lithosphere's neutral stress axis and locally help constrain flexure models. The earthquake gap also means that it is lithospheric stress, and not the magma pressure at this depth, that is the driving stress for these earthquakes. The fault plane solutions of a large set of Kilauea earthquakes deeper than 27 km have compressional axes radial to a point below Hawaii and thus may be oriented by flexure stress below the neutral axis (Elliot Endo, written commun., 1977). The seismic gap at 20 km depth and focal mechanisms of events below that thus suggest that regional stresses arising from lithospheric flexure play a dominant part in Kilauea's deeper seismicity.

The 20-km-depth point not only is a seismic gap, but also marks other differences in earthquake patterns: (1) a change occurs at 20 km from a conduit that is narrow and vertical above and broad and south-plunging below; (2) few events other than near the magma conduit are seen between 13 and 20 km, but earthquakes scatter widely under the south side of Hawaii below 20 km depth; and (3) earthquakes between 13 and 20 km are small and seldom exceed magnitude 2, but those below often exceed magnitude 4. These differences suggest that different lithospheric stresses prevail above and below 20 km. If the neutral stress depth is at 20 km, then the compressive regime below appears to favor earthquake production whereas the relatively extensional conditions above do not generate seismicity except where stresses are perturbed by the magma conduit or active rifts and flanks.

As discussed earlier, the seismically defined magma conduit merges with a diffuse cloud of hypocenters southwest of Kilauea that apparently marks the Hawaiian hot spot at 40–50 km depth. This cloud also lies centrally between Kilauea, Mauna Loa and Loihi, and is commonly a source of volcanic tremor and long-period earthquakes. Kilauea's deepest seismicity and conduit system thus become involved with the diffuse hot spot itself and become difficult to trace.

Not all deep seismicity is as readily interpreted as the major cloud southwest of Kilauea caldera. A smaller but similar cluster is southeast of Kilauea near 40–50 km depth (figs. 43.4E–H, 43.17C). These earthquakes are tectonic and do not appear to be related to tremor or to another volcano. This earthquake cluster can also be considered a part of the band of seismicity that underlies Hawaii's active south coast. The south coast is where the greatest amount of mass has been added to the island as lava flows and intrusives in recent decades and where seaward slip of the south flank occurs. Shear stress in the deep seismic zone is produced both from asymmetric loading by Kilauea growth to the north and southward motion of the flank driven by intrusive growth of the ERZ. Thus,

FIGURE 43.17—Cross sections through Kilauea taken from the surface to deepest seismicity at 60 km. Events from 1970–83 within areas of rectangles shown on figure 43.16 are projected onto sections. A, Section O-O'. B, Section P-P'. C, Section Q-Q'.

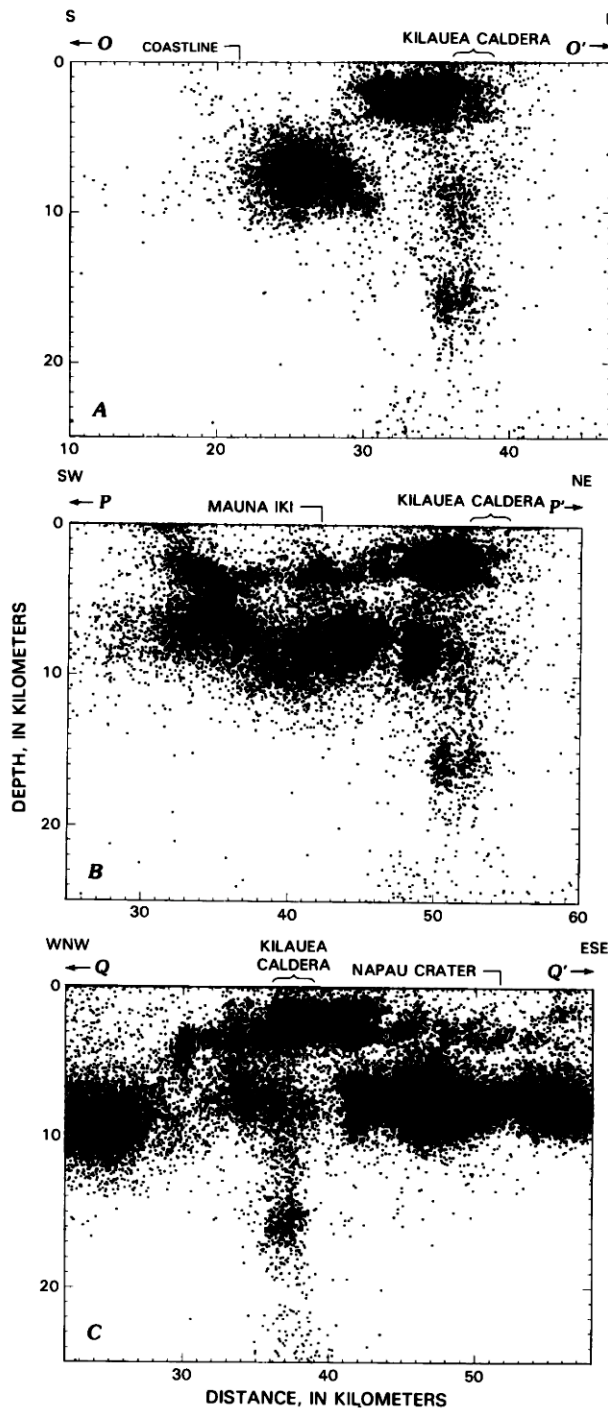


FIGURE 43.18—Enlargements of central portions of cross sections of figure 43.17A–C showing finer detail in upper part of Kilauea's vertical conduit system. A, Section O-O'. B, Section P-P'. C, Section Q-Q'.

rapid loading and stress on the lithosphere possibly produces this concentration of events. The fact that earthquakes do not diminish smoothly with depth in the mantle means that the distribution of stress and material properties is more complex than for a simple halfspace.

Other noteworthy concentrations of seismicity are: (1) the northward extension of the major cluster at 25 to 35 km beneath Kilauea (fig. 43.17A, B); (2) a deep seismic root of Mauna Loa Volcano (fig. 43.17C)—although far less active than Kilauea's, the Mauna Loa conduit is nearly vertical to a depth of almost 50 km; and (3) a diffuse thread of earthquakes linking Kilauea's conduit at 35 km with Mauna Loa's near 20 km depth (fig. 43.17C). Whether this thread represents a magmatic connection between the two volcanoes is not known, but it emphasizes the complex and multi-zoned web of upper mantle seismicity. Also note that the tectonic events under the south flank (right side of fig. 43.18C) extend to about 10 km, but the Kaoiki zone is active to 12–13 km (left side of fig. 43.18C). If these boundaries are both controlled by the layer of prevolcanic sediments below the volcanic pile, then it deepens toward the interior of the island as expected from the observed dip of the Moho (Zucca and Hill, 1980).

To make some of the major seismic zones easier to see, we present in figure 43.19 some paired hypocenter plots to view with a pocket stereoscope. The earthquakes plotted were selected to represent each major seismic zone with enough events to define it, but not so many as to obscure other features. Figure 43.19A shows most of the island and includes Loihi Submarine Volcano south of the island. Figure 43.19B, C show boxes including nearly all of Kilauea, the summit of Mauna Loa and part of Loihi. The vertical magma conduit with its southward plunge into the zone of deepest earthquakes is clearly visible. Note the prominent cloud centered near 30 km depth. The shallow earthquakes below the ERZ and their distinct separation from the south flank zone at 6–10 km depth can also be seen. Figure 43.19D zooms in for a closer look at the central part of Kilauea and includes earthquakes to a depth of 35 km. Figure 43.19E is a close-up of the shallow magma system beneath the caldera to a depth of 18 km. The very active sections of both rift zones are adjacent to the summit magma reservoir. The earthquakes in the foreground between 6 and 10 km depth are tectonic events in the south flank.

We have examined the depth distribution of Kilauea's vertical magma conduit and found three zones of low or no seismicity: the summit magma reservoir causes an absence of earthquakes between 3 and 7 km; the reduced activity near 13 km may be an effect of the buried oceanic crust and sediment layer; and the absence of earthquakes near 20 km depth under all of Kilauea might be associated with the neutral stress level within a lithosphere flexing under the load of the volcanic pile. The vertical conduit thus looks like a passive intruder in the lithosphere: it is a zone weakened by magma in which earthquakes seem to be ultimately driven by regional lithospheric stresses. The low-rigidity conduit both concentrates regional stress and fails more easily than its surroundings. The conduit thus does not need to produce enough magmatic stress to cause earthquakes by itself. If the conduit produced magma pressures much higher than

stress in the adjacent mantle, one would probably see major swarms of volcanic earthquakes and a depth distribution different from its surroundings. The reduction in deep seismicity caused by the stress change during the 1975 Kalapana earthquake also argues for regional rather than magmatic stress as driving the deep earthquakes. A planned examination of earthquake statistics, depth and time history, and earthquake focal solutions will better address the interaction of magma ascent and lithospheric stress.

### THE HISTORY OF KILAUEA'S SHALLOW EARTHQUAKE SWARMS, 1963-83

This section presents a summary of the basic data on two decades of Kilauea's summit and rift-zone earthquake swarms. The emphasis here is on a consistent treatment of basic earthquake patterns, not detailed chronologies. Particular attention will be paid to migration of earthquakes with time as an indicator of magma flow or dike propagation. We will be looking for characteristics common to many swarms and what they reveal of rift-zone dynamics. This section is thus complementary to the traditional treatment of a few well-studied examples. We feel the benefits of this survey approach outweigh the necessary omissions in dealing with so much data.

One benefit of treating two decades of swarms at once is the ability to classify swarms into similar groups, make comparisons and look for simple evolutionary trends. Shallow Kilauea swarms can be loosely divided into fast, intense swarms lasting for a few hours to a couple of days and slow swarms lasting several days to a few weeks. The fast swarms accompany rapid intrusions, which are presumably either the opening of an older magma conduit or the emplacement of a new dike. An eruption occurs if the dike reaches the surface, so nearly all eruptions are accompanied by intrusions and fast swarms. Except for harmonic tremor generated near an erupting vent, intrusions and eruptions are seismically indistinguishable. Summit tilt generally falls rapidly during fast swarms because of the high rate of magma flow. If the eruption or intrusion is within the caldera, however, the superposition of the deformation fields of the deflating reservoir and the nearby dike may cause rapid tilt changes in any direction.

Slow swarms occur between eruptions and intrusions, and are generally related to resupply of magma from depth. The most common slow swarms are within the caldera or immediately adjacent rift zones and result from gradual extension of the caldera during inflation or pressure increase of the magma reservoir. Summit tilt will usually be high and slowly rising during inflationary swarms. Seismicity and tilt levels are often closely correlated, as many examples will show. During some of the intereruption periods, the new magma supply partly or completely flows into a rift zone as a slow intrusion. These slow intrusions are generally accompanied by little or no gain in summit tilt and by a long-lived but low-intensity earthquake swarm in the part of the rift where magma accumulates. These four types of swarms will be referred to as eruptions, intrusions (fast), inflationary swarms and slow intrusions.

Most of the information in this section is contained in a series of figures, one set per swarm. The basic characteristics of all but the

smallest swarms will be presented in four types of earthquake plots: map, cross section, hourly number of earthquakes versus time and downrift position versus time. Because most of the larger swarms form linear seismic zones, the distance axis for both cross sections and position versus time plots will be the same and along the appropriate section of rift zone. When different rift segments are active during the same swarm, more than one set of cross section and position versus time plots may be presented. For a particular swarm, all of the distance and depth scales will be the same on the maps and distance axes. The time scales, however, will vary as appropriate to the swarm.

Time on the position versus time plots proceeds from top to bottom. Significant migrations of earthquakes are noted by lines whose slope is the inverse of the migration speed. Solid lines are used where the migration and speed are clearest, dashed lines where the continuity and speed are uncertain, and a small arrow where a general migration is only suggested. Formal errors of the migration speeds cannot be given, but can be judged qualitatively from the scatter of earthquakes in the distance versus time plots used to determine speeds. For eruptions, the eruptive vents are shown for comparison by red lines on maps, cross sections and distance versus time plots. Vent positions are approximate and not plotted accurately. The position versus time history of vents refers only to the eruption start time of the earliest episode. The time histories of vents are particularly approximate and are usually sketched from limited observations like the beginning times of lava emission at only a few places.

The basic data for all swarms are listed in table 43.1, including the time period for each figure. Each of the several cross sections are identified with a set of letters ( $T-T'$  for the upper ERZ, for example). The endpoints and halfwidths of all sections are listed in table 43.2.

### INTRUSIONS AND ERUPTIONS OF 1963

The seismic network and recording during the early and mid-1960's were not adequate to resolve fine spatial details in the swarms. The 1963 sequences are good examples of swarms whose approximate positions are known, but with no resolvable internal structure. Depth control may also not be adequate for some of the early swarms. Therefore, we cannot assume that events with calculated depths below 5 km are tectonic earthquakes, as is reasonable for most sequences after the late 1960's. Open squares are used in some swarm figures for events between 5 and 13 km depth and may include both tectonic and mislocated swarm earthquakes.

The first swarm for which adequate seismic data exists began on May 9, 1963 (fig. 43.20). This swarm was apparently a SWRZ intrusion, because the shallow swarm cloud is centered at a part of the SWRZ seismically active in later, better located intrusions. Earthquakes began at the time of summit deflation (fig. 43.20B), which is typical for earthquakes caused by rapid magma flow. The swarm's location may have been controlled by the intersection of the SWRZ magma conduit and the west end of the Koa'e fault zone. Ground cracking and inflation were observed in the

TABLE 43.1.—Data for individual Kilauea swarms during 1963–83

[The date the main part of the swarm started is not necessarily same date as an accompanying eruption. Event type is classified: Inf, swarm accompanying inflation; SI, slow intrusion; I, intrusion; E, eruption; Defl, caldera swarm accompanying major deflation. Main swarm locations are Cald, caldera; UERZ upper east rift zone; ERZ, east rift zone; USWR, upper southwest rift zone; SWRZ, southwest rift zone; LSWR, lower southwest rift zone; Koae, Koae fault zone. Swarm location may not coincide with eruptive vents. Seismic zone size refers to map view, parentheses imply epicenters are diffuse and poorly located. Query (?) for earthquake migration speed indicates migration appears to have occurred but with a speed too uncertain to measure. Map and cross-section plots include earthquakes from number of days listed. Delay times are between start of swarm beneath a vent and eruption at vent. Tilt changes are at Uwekahuna and are negative for deflation and positive for inflation. Tilt rates are computed at same time(s) as earthquake migration speed(s). Conduit area is obtained by dividing tilt rate by earthquake migration speed (for example see section "Southwest Rift Zone Intrusions and Caldera Eruption, January through August 1981")]

Figure number	Swarm start date	Swarm type	Swarm location	Swarm duration	Seismic zone size (km)	Downrift speed (km/h)	Uprift speed (km/h)	Upward speed 1-3 km (km/h)	Upward speed 0-1 km (km/h)	Plot duration (days)	Swarm-eruption delay (hours)	Tilt change (mrad)	Tilt rate (mrad/h)	Conduit area (m)
43.20	May 9 63	I	SWR	3 d	(9 by 5)	--	--	--	--	8	--	-32	--	--
43.21	Jul 2 63	I	Koae	3 d	(6 by 4)	east?	--	--	--	6	--	-20	--	--
43.22	Aug 21 63	E	UERZ	1 h?	--	--	--	--	--	2	--	-11	--	--
43.23	Oct 5 63	E	ERZ	3 d	(8 by 3)	--	--	--	--	8	--	-79	--	--
			Koae		(2 by 2)									
43.24	Mar 5 65	E	ERZ	3 d	(8 by 4)	--	--	--	--	5	--	-84	--	--
43.25	Aug 24 65	I	ERZ	1.5 d	(15 by 5)	--	--	--	--	8	--	-3	--	--
43.26	Dec 28 65	E	Koae	2 d	(5 by 5)	--	--	--	--	5	--	-45	--	--
43.27	Nov 5 67	E	Cald	1 h?	--	--	--	--	--	3	--	-11	--	--
43.28	Aug 22 68	E	Koae	4 h	2 by 2	west	--	--	--	3	3	-54	--	--
43.29	Oct 7 68	E	ERZ	2.5 d	11 by 2	3.4	--	--	--	5	3	-60	--	--
43.30	Feb 18 69	Inf	Cald	2.5 d	1 by 1	--	--	--	--	6	--	+11	--	--
43.31	Feb 22 69	E	ERZ	10 h	(11 by 3)	--	--	--	--	5	5	-46	--	--
43.32	Mar 21 69	I?	UERZ	2 h	2 by 2	--	14	--	--	3	--	<3	--	--
43.33	May 20 69	Inf?	ERZ	2.5 d	(8 by 4)	--	--	--	--	4	--	<3	--	--
43.34	May 24 69	E	ERZ	13 h	6 by 6	--	4.4	--	--	6	1	-24	--	--
43.35	Jul 3 69	I	UERZ	18 h	7 by 3	1.3	1.4	--	--	4	--	<3	--	--
43.36	Oct 7 69	SI	LSWR	4 d	7 by 4	--	--	--	--	6	--	+5	--	--
43.37	Nov 3 69	I	ERZ	1 h	1 by 1	6	--	--	--	3	--	-6	--	--
43.38	Dec 22 69	Inf	USWR	7 d	1 by 1	--	--	--	--	8	--	+5,-23	--	--
43.39	Jan 22 70	I	Cald	4 h	2 by 2	--	2.2	--	--	3	--	<3	--	--
43.40	Feb 3 70	Inf	UERZ	8 d	5 by 1	.13,.02	--	--	--	9	--	+3	--	--
			USWR		2 by 1	?	--	--	--					
43.41	Mar 17 70	Inf	USWR	6 d	2 by 1	?	--	--	--	7	--	+5	--	--
43.42	Apr 2 70	Inf	UERZ	7 d	2 by 2	--	--	--	--	8	--	+6,-10	--	--
			USWR		2 by 2									
43.43	May 15 70	I	UERZ	3 d	5 by 2	4.2	.13	--	--	8	--	-8	--	--
43.44	Dec 12 70	Inf	Cald	2 d	5 by 3	--	--	--	--	3	--	<3	--	--
43.45	Dec 22 70	Inf	Cald	19 d	11 by 3	.02	(1.3)	--	--	20	--	+4	--	--
43.48	Jun 6 71	Inf	Cald	9 d	3 by 3	--	--	--	--	10	--	+2	--	--
43.49	Jun 11 71	Inf	USWR	5 d	3 by 1	.35,.05	--	--	--	5	--	-2	.01	70
43.50	Jul 19 71	Inf	UERZ	12 d	2 by 2	.17,.008	--	--	--	12	--	+3	--	--
			USWR		3 by 1	?	--	--	--					
43.51	Aug 8 71	Inf	UERZ	7 d	6 by 1	.22	--	--	--	8	--	+12	--	--
			USWR		4 by 1	.02	--	--	--					
43.52	Aug 14 71	E	Cald	12 h	1 by 1	--	--	--	--	1	--	-16	--	--
43.53	Sep 6 71	Inf	UERZ	8 d	6 by 1	--	--	--	--	8	--	+3	--	--
			USWR		4 by 1									
43.54	Sep 17 71	Inf	UERZ	6 d	3 by 1	--	--	--	--	7	--	+5	--	--
			USWR		4 by 1	?	--	--	--					
43.55	Sep 24 71	E	SWRZ	7 d	13 by 3	.53,.31	--	--	--	7	4-18	+12,-23	.44	280
43.56	Dec 23 71	SI	LSWR	7 d	8 by 6	.29	--	--	--	8	--	<3	--	--
			UERZ		4 by 1	?	--	--	--					
43.57	Jan 19 72	Inf	UERZ	9 d	4 by 1	.08	.15,.15	--	--	10	--	+5	--	--
43.58	Feb 1 72	E	UERZ	5 d	2 by 1	--	--	--	--	7	.5-2 d	<3	--	--
43.59	May 5 73	E	Koae	25 h	8 by 2	.36 west	--	3	1	2	6	-23	1.7	1500
			ERZ				3.6							
43.60	Jun 9 73	I	Koae	23 h	3 by 1	1.0 west	--	--	--	1	--	-7	2.2	700
43.61	Nov 10 73	E	UERZ	16 h	3 by 1	?	--	1.6	?	2	5	-25	--	--
43.62	Mar 24 74	I	UERZ	3 h	1 by 1	?	--	--	--	1	--	-2	--	--
43.63	Jul 19 74	E	UERZ	10 h	3 by 1	--	.16	.55	.18	1	2	-18	--	--
43.64	Sep 16 74	Inf, E	USWR	3 d	7 by 1	?	--	--	--	4	--	+12	--	--
43.66	Dec 24 74	Inf	UERZ	7 d	4 by 1	.06	--	--	--	7	--	+4	--	--
			USWR		3 by 1	.03	--	--	--					
43.67	Dec 31 74	E	SWRZ	>14 d	20 by 2	1.3,.67	?	--	--	14	--	-128	5.3	1400
			USWR		3 by 1	.08	.17	5	.3	2	2	--	--	--
43.68	Jun 21 76	I	UERZ	19 h	5 by 1	?	1.3	.5	--	2	--	-7	--	--
43.69	Jul 14 76	I	UERZ	17 h	6 by 1	?	?	.7	--	2	--	-13	--	--
43.70	Jan 22 77	Inf	UERZ	26 h	4 by 1	.7	--	--	--	2	--	+2	--	--
43.71	Feb 8 77	I	UERZ	7 h	4 by 2	.37	?	--	--	2	--	-6	--	--
43.72	Sep 12 77	E	ERZ	5.5 d	17 by 3	1.23,.23	--	--	--	8	11	-91	3.2	870
			Koae		4 by 2	.09 east	--	--	--					
			Cald		4 by 4									
43.73	Sep 27 77	Defl	Cald	5 d	2 by 1	.01	--	--	--	16	--	-7	--	--
43.75	May 29 79	I	ERZ	8 h	5 by 2	.65	.67	6	--	2	--	-3	--	--
43.76	Aug 12 79	I	UER	5 h	5 by 1	1.6	--	--	--	5	--	-2	--	--
43.77	Sep 22 79	Inf	Cald	3 h	2 by 2	--	--	--	--	1	--	<2	--	--
43.78	Nov 15 79	E	UERZ	21 h	5 by 2	3.8	4.0	1.2	.09	7	11	-8	0.5	44
43.79	Mar 2 80	I	UERZ	4 h	3 by 2	--	?	--	--	3	--	-2	--	--
43.80	Mar 10 80	E	ERZ	30 h	6 by 2	?	1.8	4.3	--	3	--	-16	--	--
			Koae			.22 west	--	--	--					
43.81	Jul 30 80	I	UERZ	1 h	2 by 1	.30	--	--	--	1	--	<2	--	--
43.82	Aug 27 80	I	UERZ	12 h	5 by 1	1.6	.75	3	3	2	--	-9	2.6	860
43.83	Oct 21 80	I	ERZ	27 h	6 by 2	--	--	--	--	3	--	<1	--	--
43.83	Oct 22 80	I	UERZ	3 h	2 by 2	2.7	--	2.1	--	3	--	-3	--	--
43.84	Nov 2 80	I	UERZ	4 h	2 by 2	.7	?	?	?	3	--	-6	2.2	740
43.86	Jan 20 81	SI	USWR	1.2 d	2 by 1	--	.04	--	--	3	--	<3	--	--
43.87	Jan 24 81	SI	USWR	5 d	4 by 1	--	--	--	--	5	--	-5	--	--
43.88	Feb 9 81	SI	LSWR	8 d	4 by 1	?	--	?	--	8	--	-12	--	--
43.89	Aug 2 81	SI	USWR	8 d	5 by 1	?	--	--	--	8	--	-2	--	--
43.90	Aug 10 81	I	SWRZ	3.5 d	22 by 2	2.6,.28	.14	.46	--	9	--	-107	11	1500
			USWR		4 by 1	2.6	3.5	--	--					
43.91	Mar 23 82	I	USWR	1 h	2 by 1	?	--	--	--	1	--	<2	--	--
43.92	Apr 30 82	E	Cald	4 h	2 by 2	--	14	--	--	2	--	+5	--	--
43.93	Jun 22 82	I	SWRZ	5 d	12 by 2	.2	--	?	--	3	--	-45	.83	1400
43.94	Sep 25 82	E	UERZ	1.6 d	5 by 1	1.4	--	1	1	7	2	+18	--	--
			USWR		2 by 1	1.4	--	--	--					
43.96	Dec 9 82	I	UERZ	2 d	5 by 1	6.4	--	.8	--	3	--	-3	--	--
43.97	Jan 1 83	E	ERZ	6 d	16 by 2	.62	.06	?	?	9	21	-120	1	540
			ERZ			.025,.61	--	--	--					

TABLE 43.2.—Endpoints and widths of cross sections

[Half-width of each cross section is distance from cross-section plane within which earthquakes are included on plot. Latitude and longitude are given in degrees and minutes]

Cross Section	Left endpoint		Right endpoint		Half-width (km)
	Latitude	Longitude	Latitude	Longitude	
A-A'	19 25.35	155 18.4	19 21.4	155 12.0	0.8
B-B'	19 23.0	155 18.5	19 26.5	155 15.0	0.8
C-C'	19 24.4	155 19.0	19 24.4	155 14.0	0.8
D-D'	19 22.0	155 17.1	19 26.5	155 17.1	0.8
E-E'	19 20.9	155 13.1	19 26.8	154 57.5	2.7
F-F'	19 16.4	155 24.3	19 26.0	155 15.2	2.6
G-G'	19 25.4	155 12.1	19 20.6	155 16.0	2.0
H-H'	19 23.3	155 12.8	19 17.0	155 13.9	2.0
I-I'	19 23.5	155 9.7	19 17.6	155 8.3	2.0
J-J'	19 24.7	155 6.9	19 19.3	155 4.0	2.0
K-K'	19 24.1	155 19.5	19 20.0	155 15.0	2.0
L-L'	19 21.7	155 21.9	19 17.2	155 17.4	2.0
M-M'	19 19.3	155 25.0	19 15.1	155 20.2	2.0
N-N'	19 20.9	155 17.0	19 22.4	155 12.7	1.7, 2.1
O-O'	19 5.0	155 16.0	19 40.0	155 16.0	5.0
P-P'	19 2.0	155 34.0	19 32.0	155 11.0	10.0
Q-Q'	19 28.0	155 38.0	19 16.0	154 59.0	10.0
R-R'	19 21.0	155 18.8	19 26.0	155 15.9	1.6
S-S'	19 20.9	155 17.9	19 22.4	155 12.7	1.7, 2.1
T-T'	19 24.8	155 17.5	19 21.3	155 12.0	1.3
U-U'	19 23.5	155 18.5	19 23.5	155 2.5	4.3
V-V'	19 21.8	155 15.2	19 22.4	155 9.5	1.3
W-W'	19 21.3	155 16.0	19 21.3	155 5.8	3.8
X-X'	19 22.3	155 20.3	19 26.6	155 14.6	1.6

Koae, and magma may also have intruded the fault zone (Kinoshita, 1967). Some downrift earthquake migration appears to have occurred (fig. 43.20D), but location accuracy is not sufficient to be sure. All subsequent large SWRZ intrusions have shown clear downrift migration of earthquakes.

Another intrusion involving the Koae occurred two months later on July 2, 1963. Earthquakes occurred east of the previous swarm in the central and eastern Koae (fig. 43.21A). Many earthquakes were sharply felt and heard as cracking and booming sounds by observers in the epicentral area on July 1 and 2. Ground cracking was also noticed in the epicentral area and was confined to the eastern Koae fault zone. These observations suggest that many hypocenters were shallow and above about 2 km depth. The deflation indicates that magma left the summit reservoir, though the relative amounts of magma emplaced in the ERZ, SWRZ and Koae are uncertain. Two more accurately located and more clearly paired Koae intrusions occurred in May and June 1973. Earthquake migration (and presumably magma flow), however, was westward from the ERZ in the latter intrusions.

Relatively few earthquakes were located during the August and October 1963 ERZ eruptions (figs. 43.22A, 43.23A). This decrease is more an effect of inadequate instrumentation than failure of the volcano to produce earthquakes. No seismic stations were in this area of the ERZ (fig. 43.2A), and the masking of earthquakes by harmonic tremor is a more serious problem on the smoked-paper records then used to measure earthquakes. The recently active Koae experienced earthquakes during the October event (fig. 43.23A). Geologic and seismic descriptions are given by Moore and Koyanagi (1969).

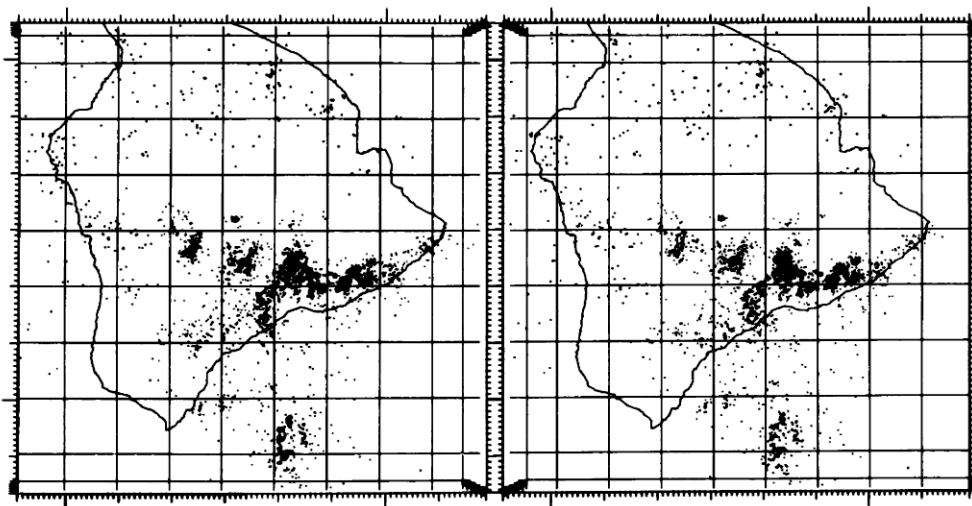
### THE ERUPTIONS AND INTRUSION OF 1965 AND 1967

The ERZ eruption of March 5, 1965 (fig. 43.24; Wright and Kinoshita, 1968) and the August 24, 1965 intrusion (fig. 43.25) were both accompanied by swarms with many earthquakes exceeding magnitude 2. As before, seismic-station geometry did not permit accurate locations. Inaccuracy may account for the scattering of earthquakes away from the rift and into the south flank. Shallow south-flank earthquakes are seen accompanying more recent, better recorded ERZ intrusions and eruptions, but only as events clearly secondary to the main swarm beneath the rift. These 1965 earthquakes must be considered poorly located. Earthquakes during the August event apparently migrated eastward at a speed of 12 km/h, but concluding anything more than the possibility of a migration is ruled out by the location inaccuracies.

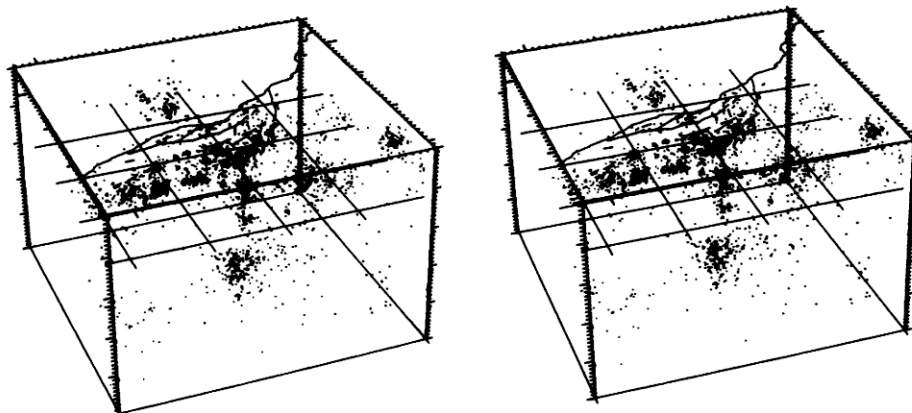
Seismic data from the ERZ eruption of December 1965 (fig. 43.26) and the caldera eruption that began on November 5, 1967 (fig. 43.27) are incomplete. None of the events in the first 3 days of the December 1965 eruption (and intrusion) were initially timed and located owing to their quantity and intensity. Although the eruption was on the ERZ, earthquakes were generated by an intrusion into the Koae (fig. 43.26A). Boscher and Duennebier (1985) timed many small events not plotted here and concluded that the Koae hinged apart in response to stresses in the volcano. The eruption, seismicity and ground cracking in the Koae are described by Fiske and Koyanagi (1968). The migration direction of major ground cracking and earthquakes was westward, as it was for earthquakes in later events combining ERZ eruptions with Koae intrusions. Only two earthquakes accompanying the November 1967 summit eruption were located, owing to the brevity of the swarm prior to the eruption and the intensity of harmonic tremor. The location of the two earthquakes suggests that an intrusion of the adjacent SWRZ initially accompanied the eruption (fig. 43.27A). The eruption that episodically continued until July 1968 is documented in detail by Kinoshita and others (1969).

### THE EAST RIFT ERUPTIONS OF 1968 TO MARCH 1969

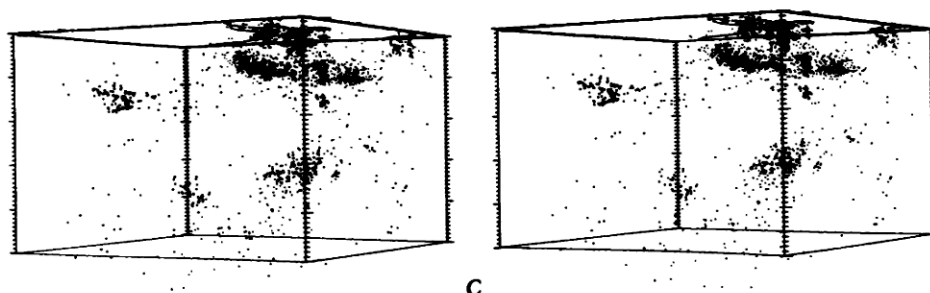
The period from August 1968 to March 1969 was active for the central ERZ between Hiiaka and Puu Kamoamo, which experienced three eruptions and one intrusion. The ability to adequately record and locate earthquakes improved markedly during this period. The eruptions of August 22 and October 7, 1968, are fully described by Jackson and others (1975). No earthquakes in the immediate vicinity of the August 1968 eruptive vents were large enough to time and locate, but events did occur to the southwest in the adjacent section of the Koae fault zone (fig. 43.28A). The Koae earthquakes anticipated the onset of eruption by about 3 hours and also apparently began an eastward migration of vent opening (fig. 43.28D). This eruption was seismically complex, because it began with small and unlocatable earthquakes near Makaopuhi (Jackson and others, 1975) and involved a Koae intrusion at the opposite end of the eruptive zone.



A



B



C

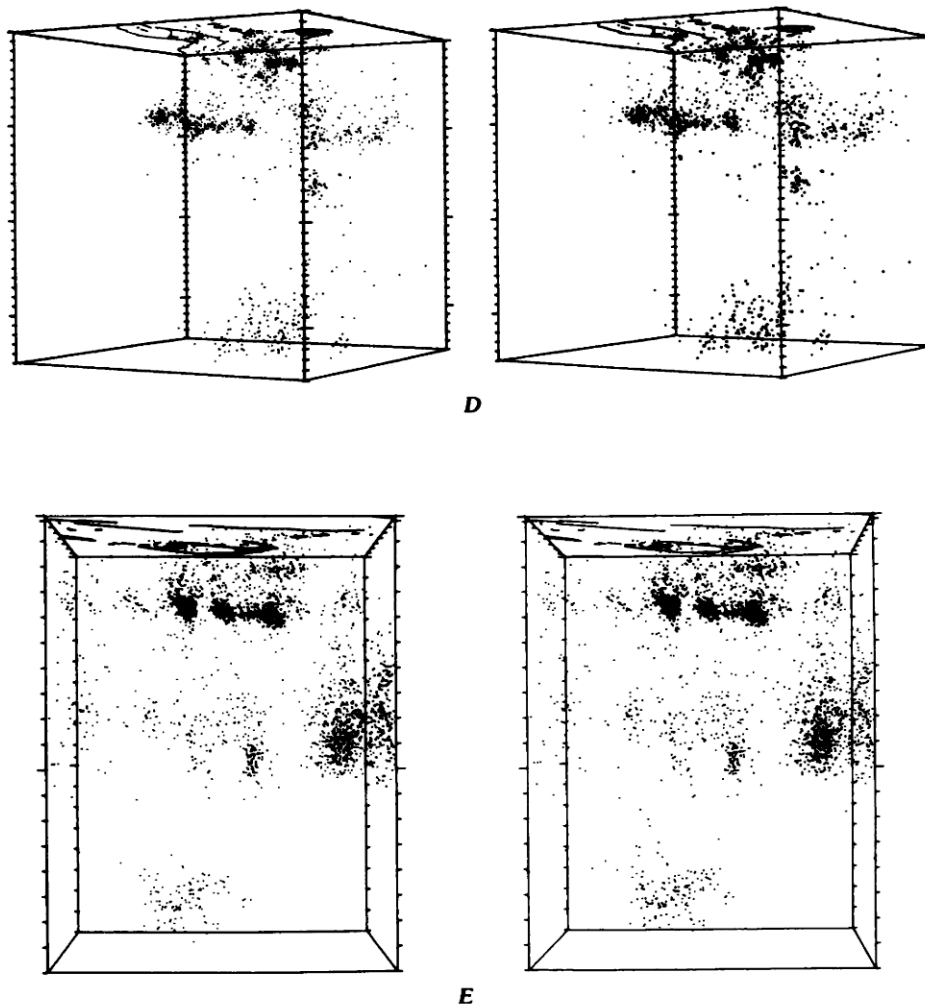


FIGURE 43.19—Stereopair views of 1970–81 Kilauea earthquakes showing major seismic zones. Tick marks on horizontal axes are plotted every minute of latitude and longitude, and those on depth axes are every kilometer. *A*, View from above Hawaii. Loihi Volcano is to south. Coastline is at surface, and grid of lines is at 13 km depth and approximates Moho. *B*, Closer view of Kilauea from north. Grid is plotted at 13 km depth near Moho, and box is 50 km high. Most of shallowest seismicity is below rift zones. Tectonic earthquakes below Kilauea's south flank are mostly between 6 and 10 km depth. Vertical magma conduit and major cluster near 30 km are clearly visible. *C*, Same box as in *B* viewed from northeast at depth of 25 km. Magma conduit merges with diffuse cloud of seismicity in far lower corner, which marks present Hawaiian hot spot. Earthquakes from Loihi are to left and from Mauna Loa in upper right corner. *D*, Closer view of Kilauea from northeast at depth of 17 km. Box is 35 km high. Low seismicity associated with summit magma reservoir is below caldera between about 3 and 7 km. *E*, Close-up view of Kilauea summit region from south at a depth of 9 km. Unlike other stereopairs, essentially all available earthquakes are plotted in *E*. Intense seismic zones at 3 km depth are rift conduits that abut magma reservoir behind and beneath them. Foreground events between about 6 and 10 km depth are tectonic earthquakes in south flank.

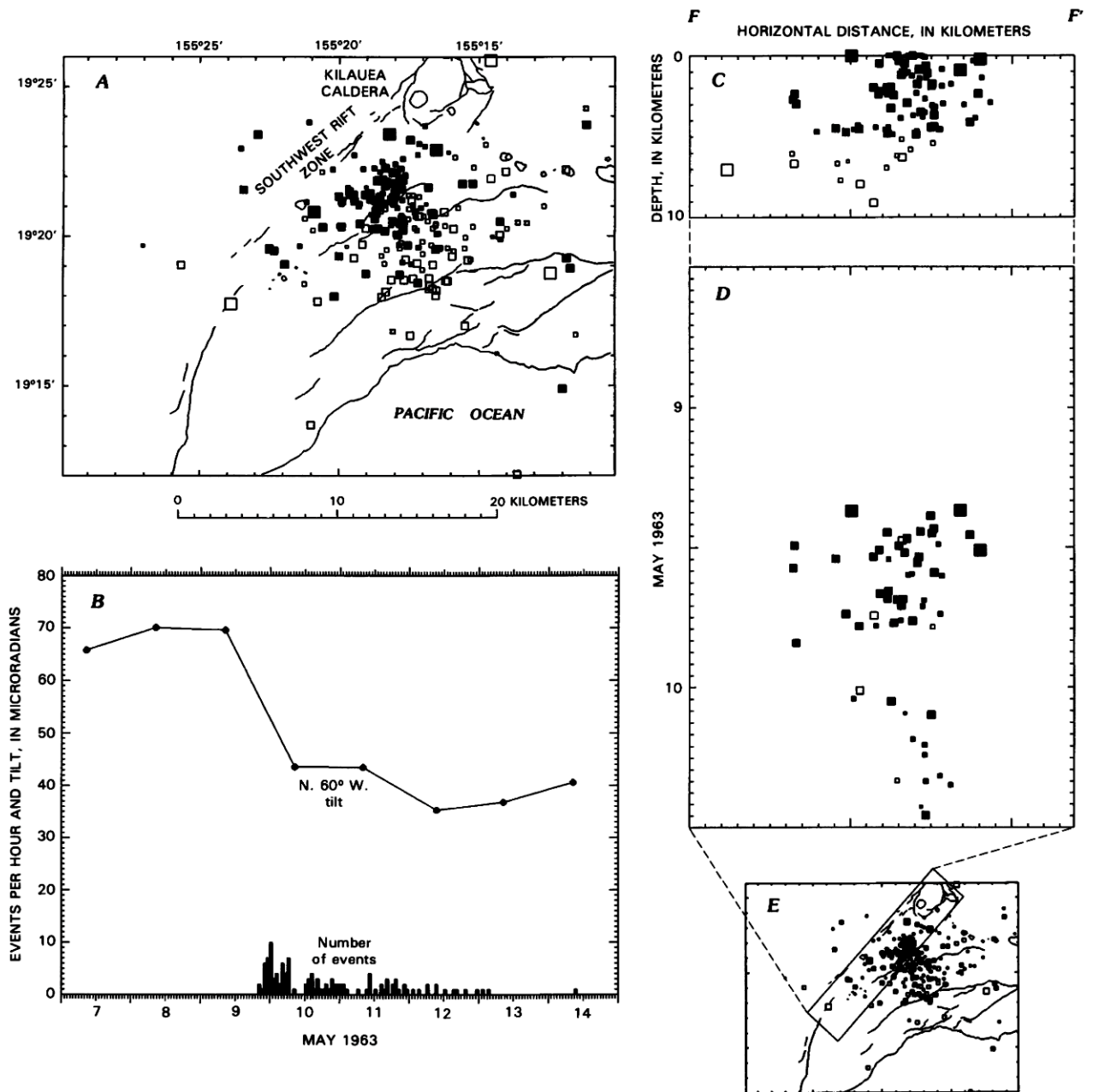


FIGURE 43.20.—Earthquake swarm (and presumed magma intrusion) beginning on May 9, 1963. Only earthquakes that were timed and located are plotted. **A**, Map of earthquake epicenters. Solid squares, earthquakes in depth range 0–5 km; open squares, 5–13 km below surface. Faults, fissures, and pit craters are as shown in figure 43.1. **B**, Plot of tilt at Uwekahuna and hourly number of earthquakes on same time base. Decreasing tilt values correspond to tilt down to east and south and generally to deflation of summit magma reservoir. Connected points are readings from two-component water-tube tiltmeter rotated to N. 60° W., approximately in line with deformation center. Continuous line, beginning with figure 43.49, is from east-west Ideal Aerosmith tiltmeter. **C**, Cross section of hypocenters. End points of cross section and half-width distance from cross section plane are presented in table 43.2. Ticks on horizontal axis at 1-km intervals. Beginning date of earthquakes included in **A** and **C** is the starting swarm date unless otherwise noted. The number of days included in **A** and **C** is given as plot duration in table 43.1 and is not necessarily the same as time axis of tilt and seismicity graph. **D**, Horizontal position of earthquakes versus time; time increases downward, ticks at hourly intervals. Lateral migration of epicenters is recognized as diagonal bands of points. **E**, Rectangular area within which earthquakes are plotted on **C** and **D**.

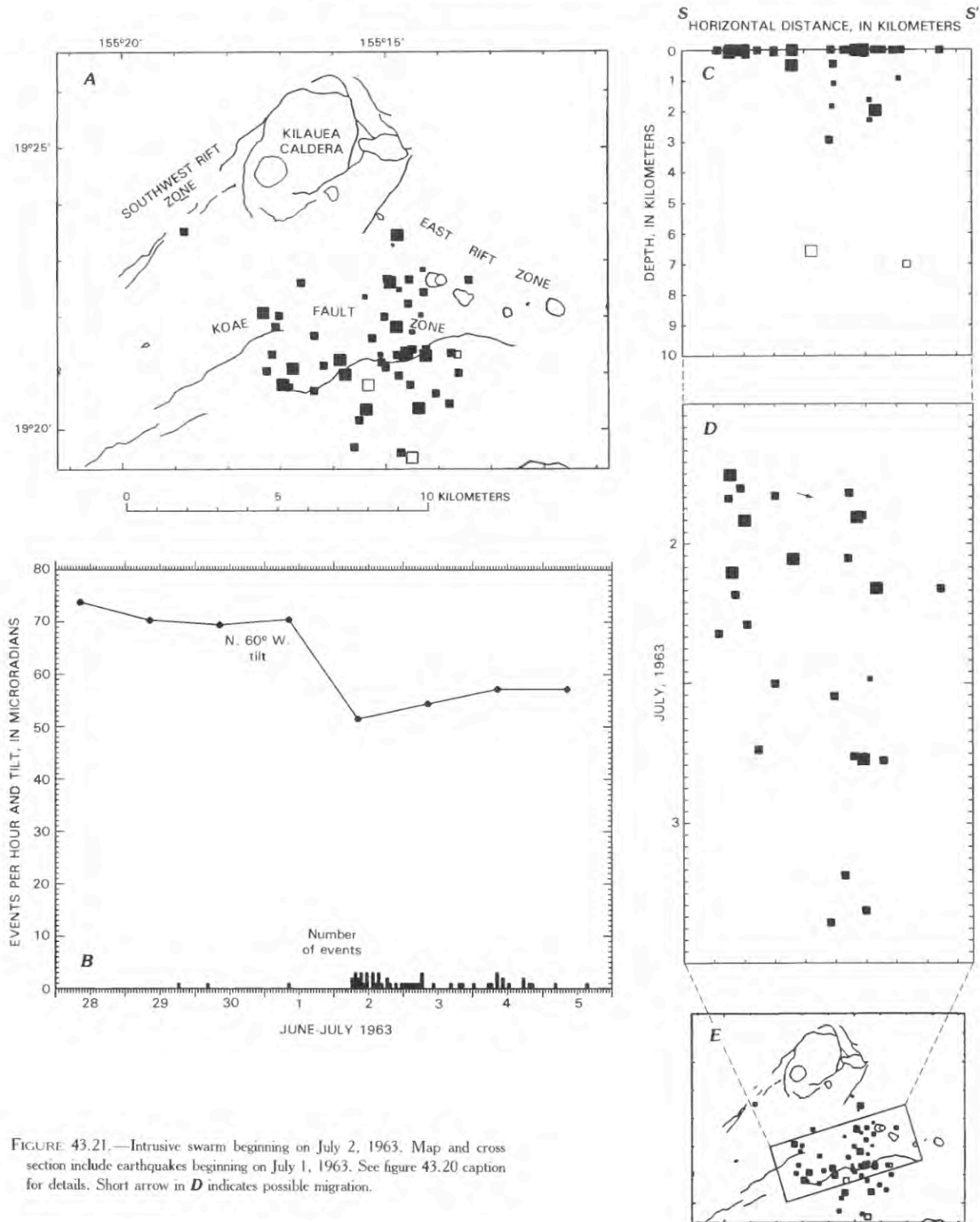


FIGURE 43.21.—Intrusive swarm beginning on July 2, 1963. Map and cross section include earthquakes beginning on July 1, 1963. See figure 43.20 caption for details. Short arrow in *D* indicates possible migration.

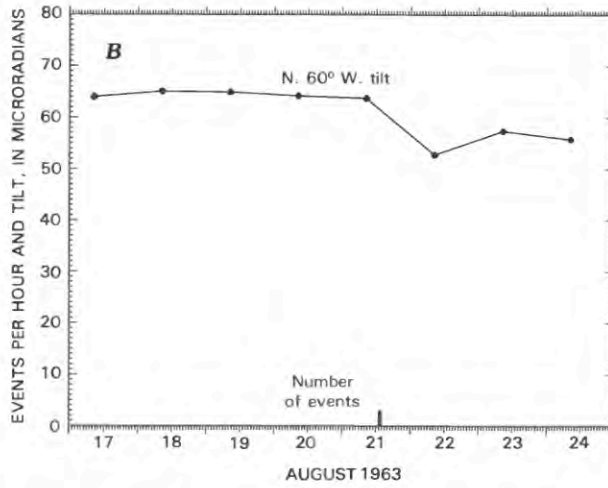
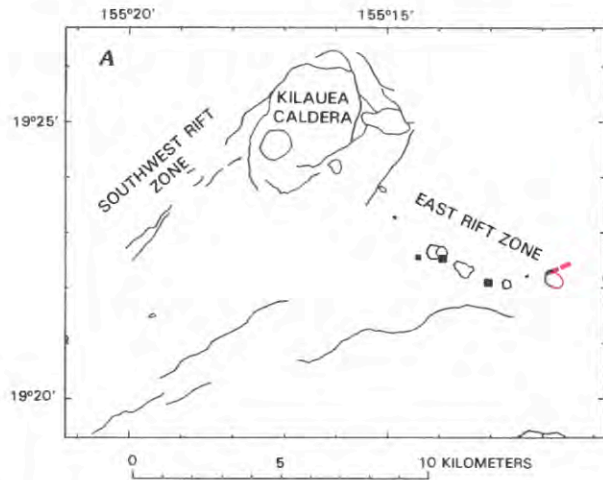


FIGURE 43.22.—Eruptive swarm beginning on August 21, 1963. See figure 43.20 caption for details. Red, eruptive vents.

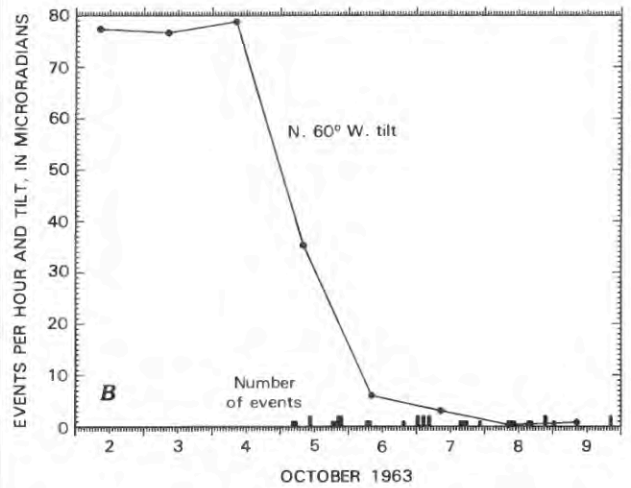
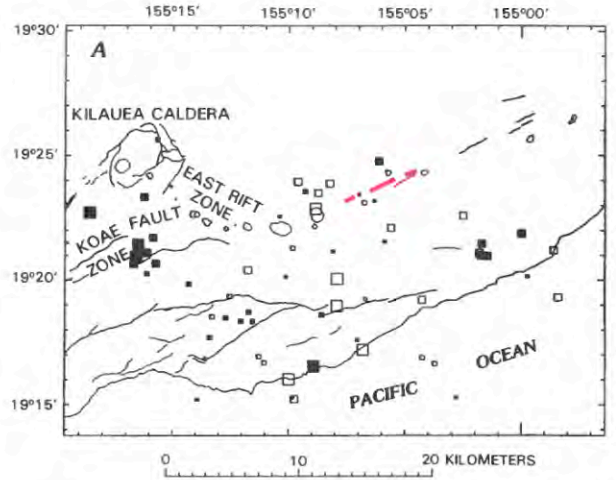


FIGURE 43.23.—Eruptive swarm beginning on October 5, 1963. See figure 43.20 caption for details. Red, eruptive vents.

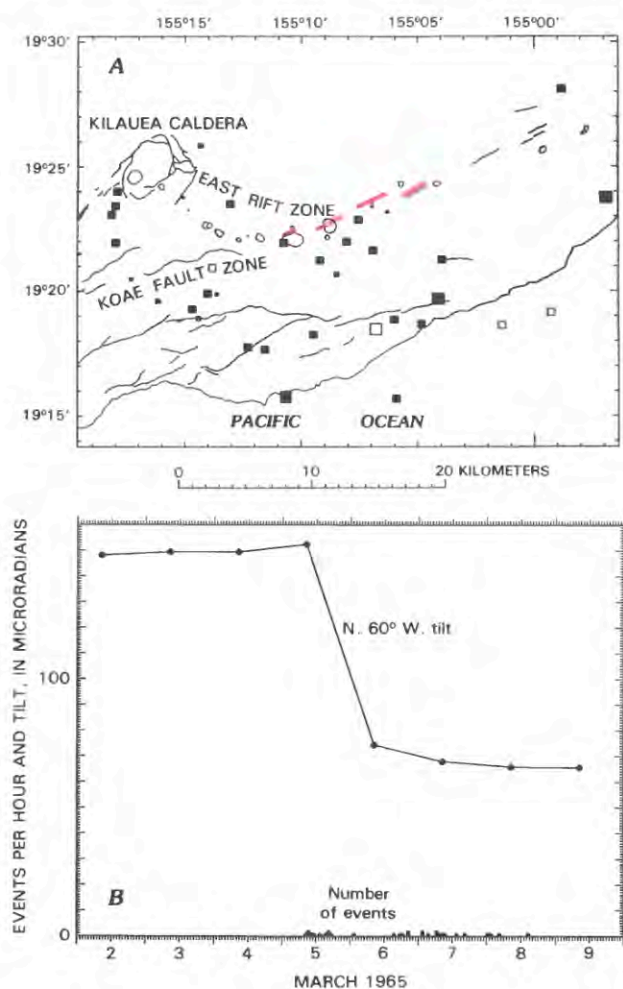


FIGURE 43.24.—Eruptive swarm beginning on March 5, 1965. See figure 43.20 caption for details. Red, eruptive vents.

Earthquakes and volcanism were much more clearly related during the October 1968 eruption. The length and position of the eruptive vents and seismic zone coincide very closely (fig. 43.29A). The displacement of the seismic zone slightly south of surface rift and eruptive vents is typical of later ERZ swarms, but may partly be a result of a biased distribution of seismic stations. A clear downrift migration of earthquakes at about 3–4 km/h occurred uprift of Puu Kamoamo (fig. 43.29D). The speed then slowed to about 1 km/h. Eruptive vents opened in the same direction and at comparable speed, and followed the earthquakes in a given place by about 3 hours. The dike thus grew downrift at 1–3 km/h and upward at about 0.6 km/h simultaneously. Passage of magma upward from the main conduit at 3 km depth was essentially aseismic, as seen by the absence of earthquakes within 2 km below the vents (fig. 43.29C).

The ERZ eruption of February 22, 1969, is associated with two swarms. The first preceded the eruption by several days and was in the southern part of the caldera (fig. 43.30A). It occurred gradually over several days and was concurrent with a premonitory rise in Uwekahuna tilt (fig. 43.30B). The earlier swarm was thus caused by summit inflation. This pulse of inflation may have also triggered the eruption by incrementing magma pressure just above a critical level. The eruption itself was immediately preceded by a swarm located mostly south of the ERZ eruptive vents (fig. 43.31A). Most of these earthquakes are probably mislocated too far south of the rift zone and vents. The first vents to erupt were near Alae crater, and vents opened rapidly to the east and slowly to the west (Swanson and others, 1976b). In each part of the vent system, earthquakes essentially ceased when the vent began erupting (fig. 43.31C). This cessation could result from masking of smaller earthquakes by strong vent-related tremor, by stress and pressure release when the dike reached the surface, or both.

A small swarm lasting less than three hours occurred on March 21, 1969. It was concentrated in a small cluster 1–2 km uprift of the future site of Mauna Ulu and preceded the Mauna Ulu eruption by two months. The March swarm may have been associated with small-scale magma movement in some sense preliminary to the later eruption. Any summit deflation associated with this small intrusion was below the tilt noise level (fig. 43.32B). An apparent and very rapid westward migration of epicenters (fig. 43.32D) is not well seen since the swarm is so small.

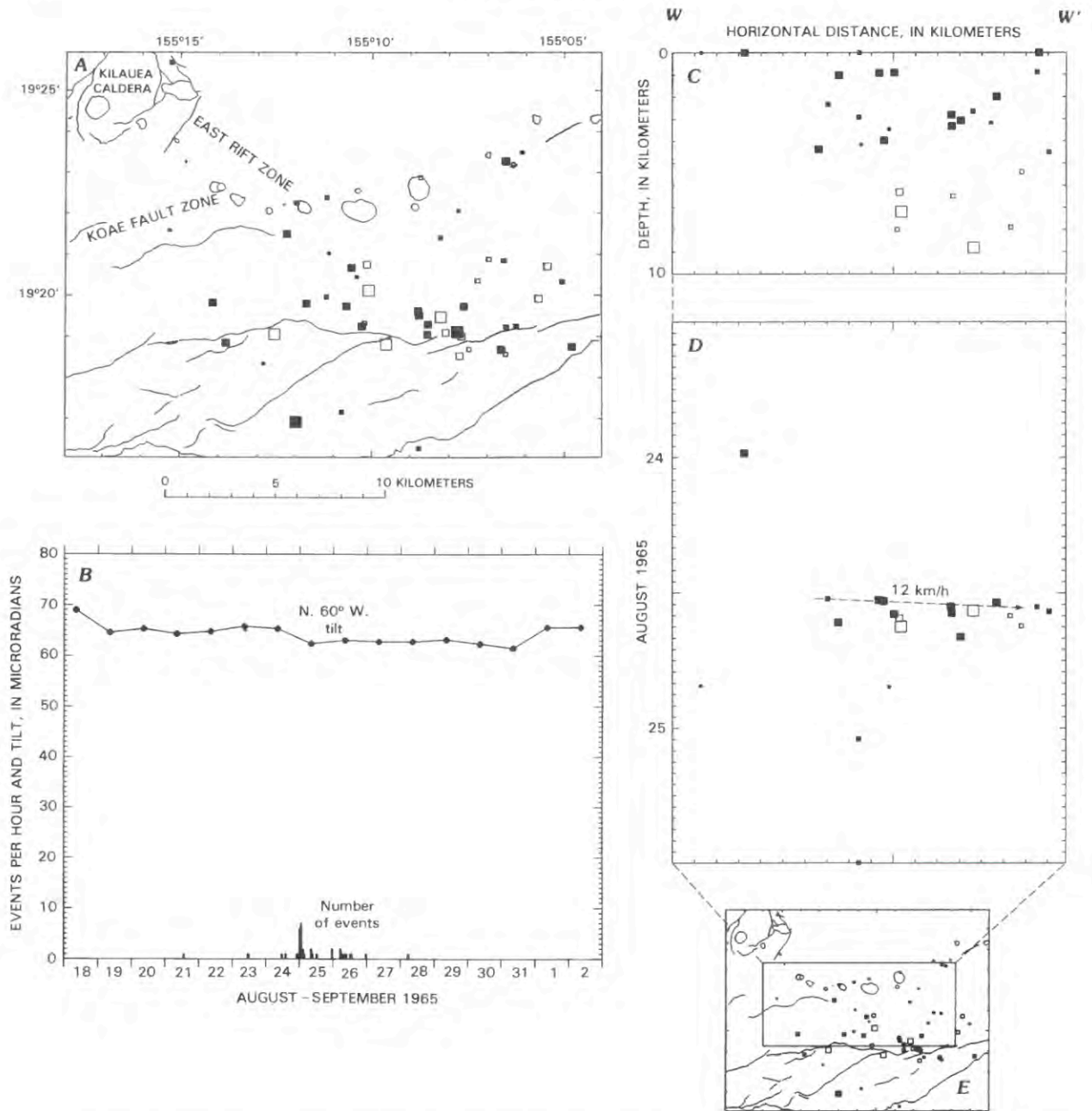


FIGURE 43.25.—Intrusive swarm beginning on August 24, 1965. Map and cross section include earthquakes beginning on August 21, 1965. See figure 43.20 caption for details. Dashed line in *D*, poorly resolved shift in seismicity.

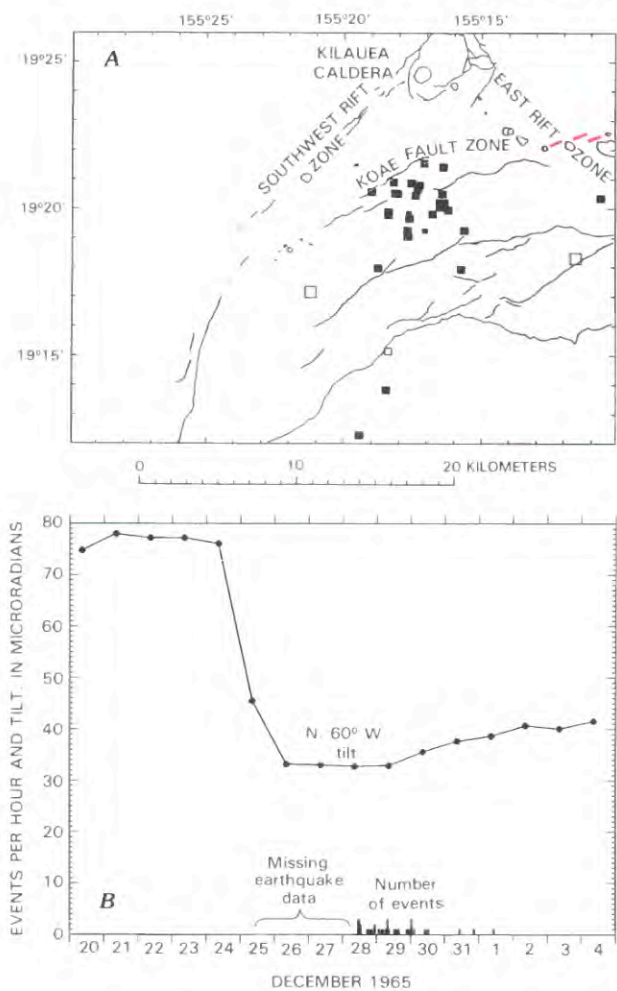


FIGURE 43.26.—Eruptive swarm beginning on December 28, 1965. Map and plot include earthquakes beginning on December 27, 1965. See figure 43.20 caption for details. Red, eruptive vents.

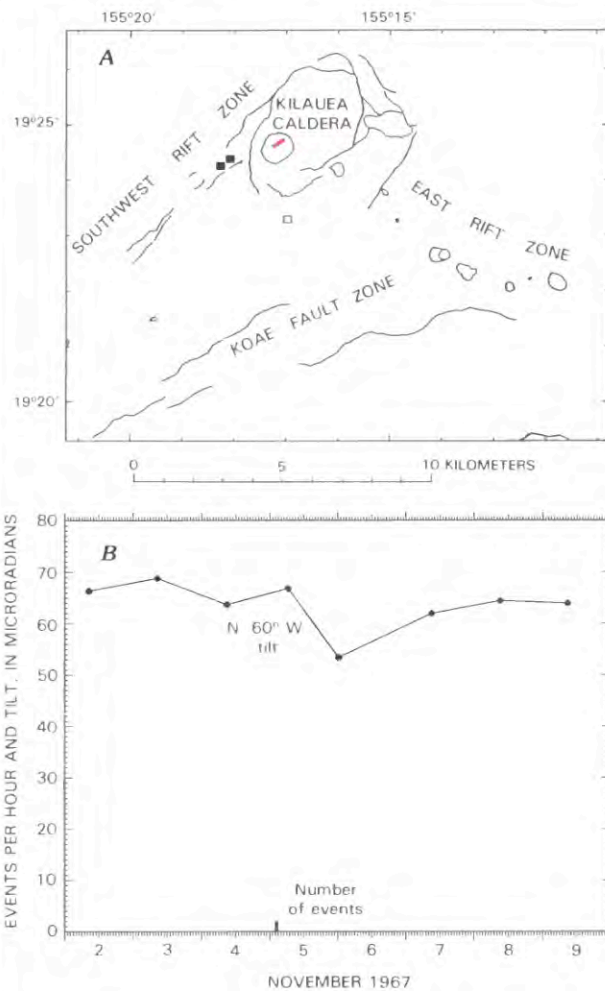


FIGURE 43.27.—Eruptive swarm beginning on November 5, 1967. Map and plot include earthquakes beginning on November 4, 1967. See figure 43.20 caption for details. Red, eruptive vent.

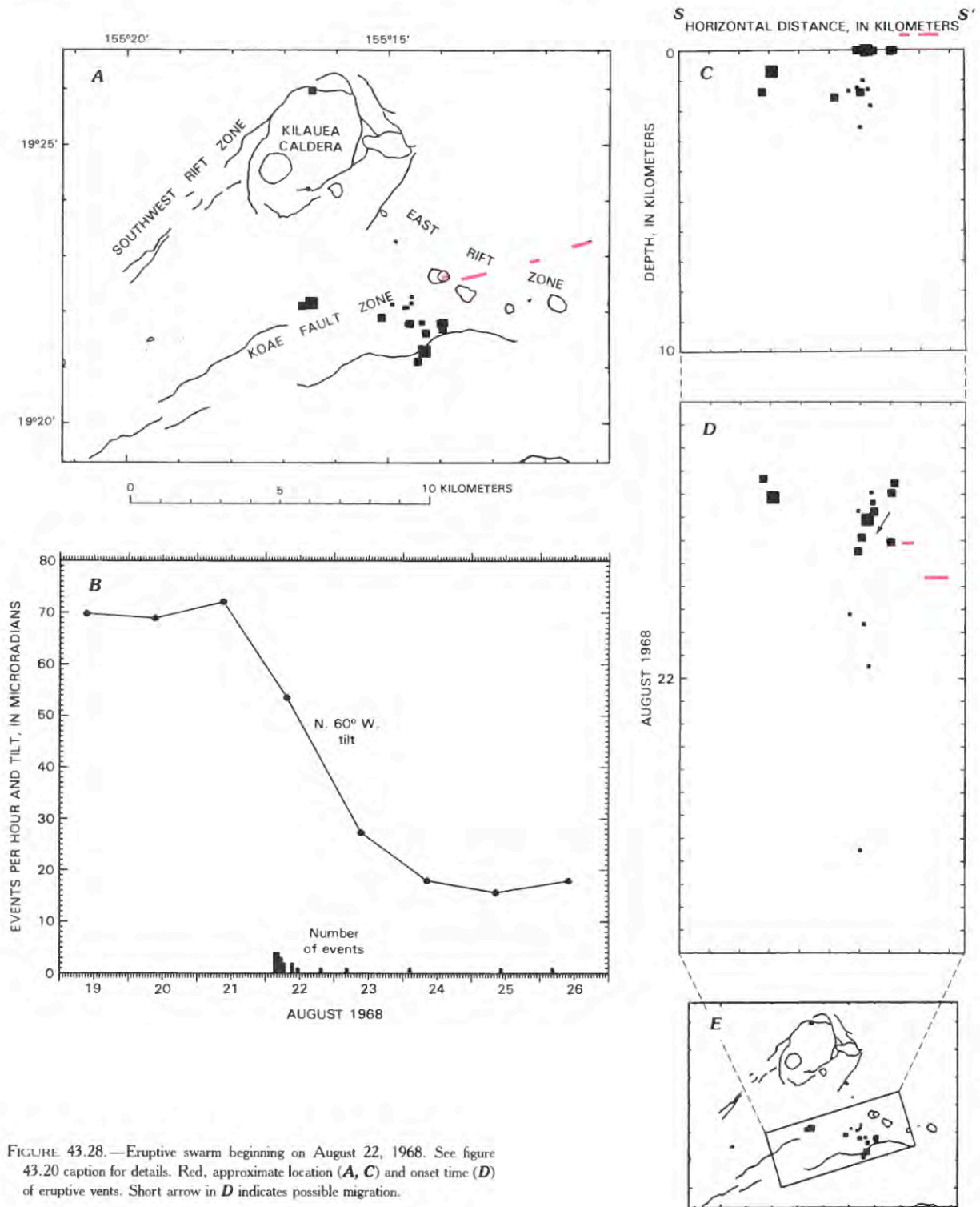


FIGURE 43.28.—Eruptive swarm beginning on August 22, 1968. See figure 43.20 caption for details. Red, approximate location (*A*, *C*) and onset time (*D*) of eruptive vents. Short arrow in *D* indicates possible migration.

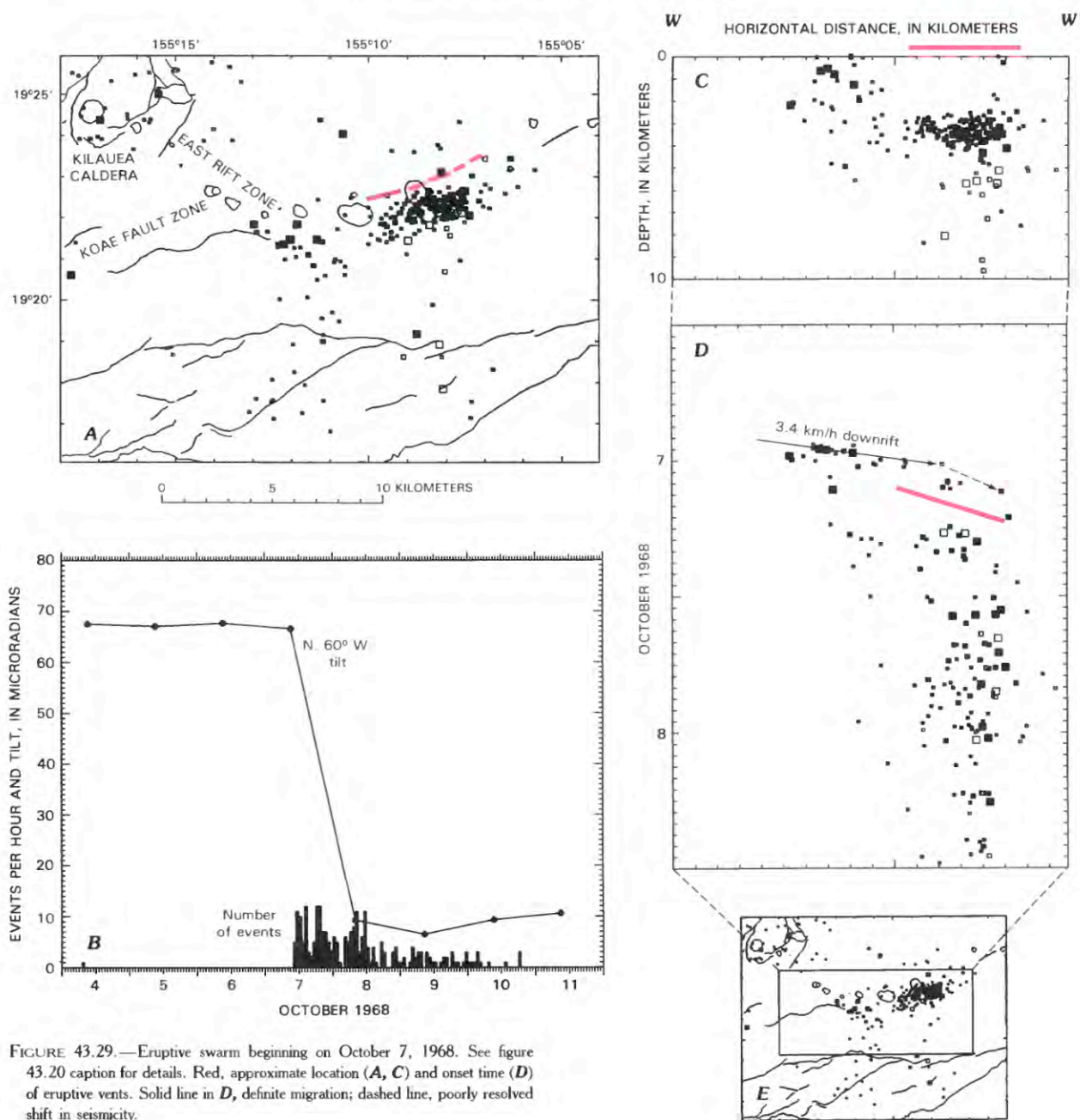


FIGURE 43.29.—Eruptive swarm beginning on October 7, 1968. See figure 43.20 caption for details. Red, approximate location (*A*, *C*) and onset time (*D*) of eruptive vents. Solid line in *D*, definite migration; dashed line, poorly resolved shift in seismicity.

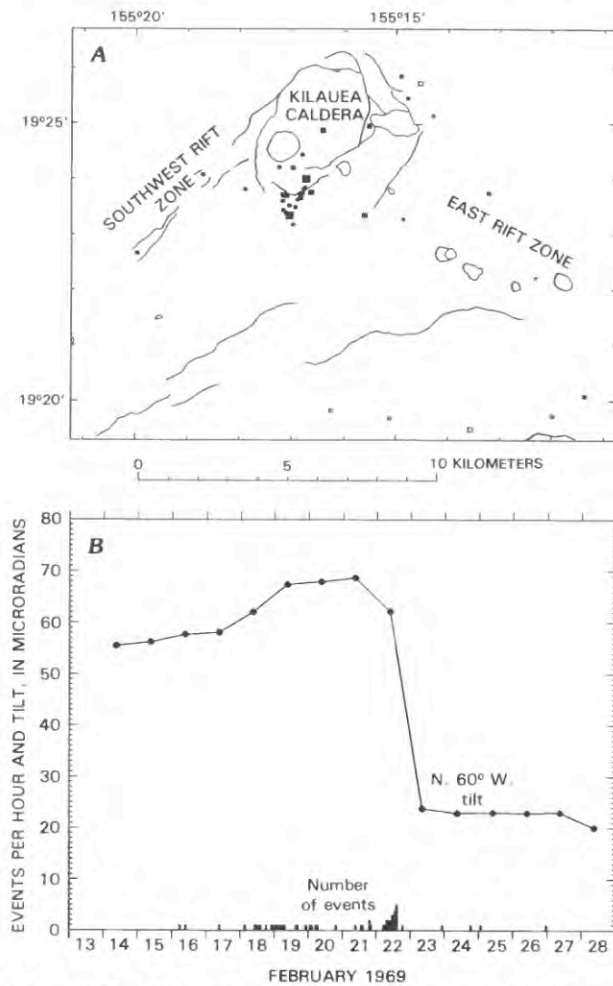


FIGURE 43.30.—Inflationary swarm beginning on February 18, 1969, immediately preceding eruption of February 22, 1969. Map and plot include earthquakes beginning on February 16, 1969. See figure 43.20 caption for details.

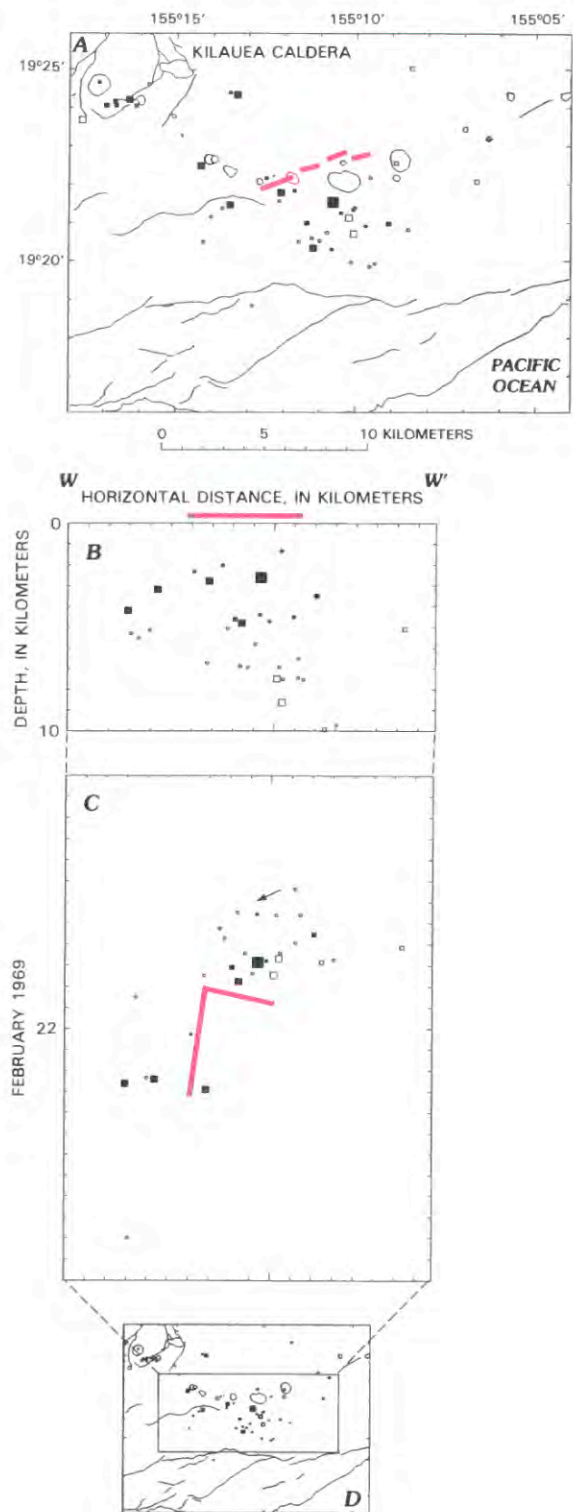


FIGURE 43.31.—Eruptive swarm beginning on February 22, 1969. See figure 43.20 caption for details and figure 43.30B for tilt and hourly earthquake rate. Red, approximate location (A, B) and onset time (C) of eruptive vents. Short arrow in C indicates possible migration.

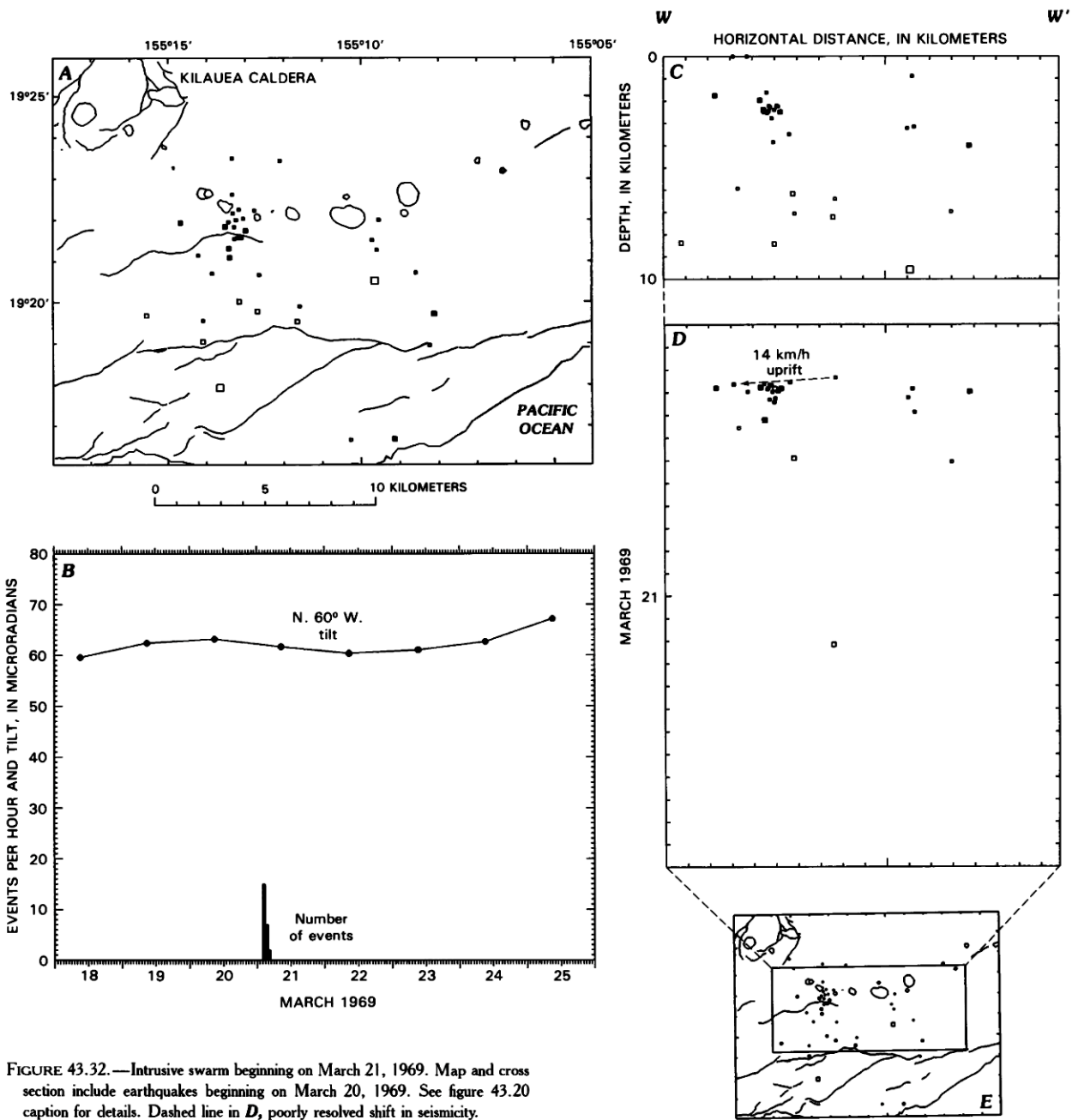


FIGURE 43.32.—Intrusive swarm beginning on March 21, 1969. Map and cross section include earthquakes beginning on March 20, 1969. See figure 43.20 caption for details. Dashed line in *D*, poorly resolved shift in seismicity.

### THE MAY 1969 MAUNA ULU ERUPTION AND INTRUSIONS THROUGH NOVEMBER 1969

Like the February 1969 eruption, the Mauna Ulu eruption commencing on May 24, 1969, was preceded by about three days of low-level seismicity. The pre-Mauna Ulu seismicity, however, appears to emanate from Kilauea's flank south of Makaopuhi and Napau (fig. 43.33A). This swarm was very unusual in that it was not in or near the summit caldera and thus not clearly related to inflation prior to the eruption. The shallow earthquakes were in the south flank near the areas active during the March and August 1965 and February 1969 swarms. This precursory swarm was possibly caused by some sort of south-flank instability that triggered the Mauna Ulu eruption. Because later volcanic swarms seen with an improved seismic network have all been located much closer to the ERZ, the May 20–23, 1969 swarm is probably mislocated too far south.

The swarm accompanying the onset of the Mauna Ulu eruption scatters within about 3 km of the eruptive vent (fig. 43.34A). These earthquakes are shallower than 4 km and locate very close to the surface in the vent area (fig. 43.34B). The intense seismicity began soon after 0300 H.s.t. on May 24 and rapidly migrated westward at an apparent speed of about 4 km/h (fig. 43.34C). This event was apparently a minor intrusion into the east end of the Koaie fault zone about one hour before magma reached the surface. This intense seismicity ended about the time the eruption began. The vents opened nearly simultaneously in the eastern half of the fissure, but opened gradually westward (Swanson and others, 1979). This westward vent progression can be extrapolated to a later burst of earthquakes southwest of Mauna Ulu (fig. 43.34C). A dike or pulse of magma possibly moved westward at about 0.3 km/h into the Koaie, extending the initial vent and causing earthquakes before it stopped. During the next several hours, scattered earthquakes occurred at depths between about 6 and 9 km to the southeast of Mauna Ulu (figs. 43.33D, 43.34). These events apparently were tectonic and were induced by rifting during the onset of the eruption. They also occurred directly beneath the zone of premonitory earthquakes (compare figs. 43.33C and 43.34B). The relations between pre-eruption and posteruption south-flank earthquakes and the eruption itself are unclear.

While Mauna Ulu continued with a series of its own eruptive episodes, a sequence of intrusions took place in July, October and November 1969. None coincided with Mauna Ulu eruptive episodes, and Kilauea apparently went about the business of generating intrusions between episodes of supplying Mauna Ulu with magma. The shunting of magma to Mauna Ulu during 1969–71 was the apparent cause of the increased frequency of intrusions relative to eruptions at Kilauea (Klein, 1982b). The ongoing Mauna Ulu eruption may have robbed the other intrusions of the magma supply and pressure they needed to erupt themselves.

The July 3, 1969 intrusion was near Hiiaka on the upper ERZ (fig. 43.35A). Earthquakes clearly define an east-west

lineation about 7 km long that is oblique to the rift axis. The seismic trend is aligned with the local direction (N. 75° E.) of eruptive vents and fissures, and hence the axis of greatest compressive stress. In this unusual case the shallow stress orientation typical where vents form was also dominant at the 2- to 4-km earthquake depth. The swarm began at the intersection of the seismic lineation and the rift magma conduit. Earthquakes rapidly progressed bilaterally east and west at nearly the same speed of about 1.8 km/h, when projected along the lineation (fig. 43.35D). We interpret this event as the intrusion of a new dike whose direction is controlled by regional stress rather than the pre-existing ERZ magma conduit. Only a small volume of magma was intruded, because no detectable summit deflation was recognized (fig. 43.35B). The intruded magma had likely all been stored within the ERZ near Hiiaka. The observed earthquake migration speed is very typical of other intrusions that propagate along the axes of the rift zones. The processes of intrusion either parallel or oblique to the rift axis must therefore be fairly similar, although dikes off the rift axis may be thinner and not accommodate or store much magma.

Two other small intrusions also occurred between eruptive phases at Mauna Ulu in October and November 1969. The swarm that began on October 7 lasted for about 4 days and was accompanied by slow inflation then deflation (fig. 43.36B). All earthquakes were in the south flank 5 to 8 km southeast of Puu Kou (fig. 43.36A). This swarm is thus puzzling because there was no seismicity beneath the SWRZ. As discussed earlier, the October earthquakes were in a region frequently activated by large SWRZ intrusions. The October swarm may thus have resulted from a slow and aseismic SWRZ intrusion or some sort of rifting episode that stressed the south flank and triggered the swarm. The earthquakes are not a tectonic aftershock sequence: their time history is like a volcanic swarm with no mainshock. The swarm is similar to that of February 1981 (see below), which is more obviously a slow intrusion, owing to its location directly beneath the rift, to the larger deflation and to other associated SWRZ intrusions in 1981. We tentatively interpret the October 1969 swarm as resulting from a slow SWRZ intrusion or a related south flank adjustment.

The November 3, 1969 ERZ intrusion was small and lasted less than one hour (fig. 43.37). It was accompanied by a small summit deflation (fig. 43.37B) and is thus clearly an intrusion. It occurred beneath Mauna Ulu (fig. 43.37A), but did not coincide with a major eruptive episode there (see Swanson and others, 1979). The sparse earthquakes rapidly moved downrift at about 6 km/h (fig. 43.37D), though the speed is not well defined. This swarm appears to have accompanied the emplacement of a small dike below Mauna Ulu, rather than a new pulse of magma to Mauna Ulu itself. No significant earthquake swarms or new seismic intrusions accompanied any of the later Mauna Ulu eruptive episodes. The independence of Mauna Ulu eruptions and the many other intrusions emphasizes the fact that the upper ERZ is really a network of distinct magma conduits, different segments of which can be active simultaneously.

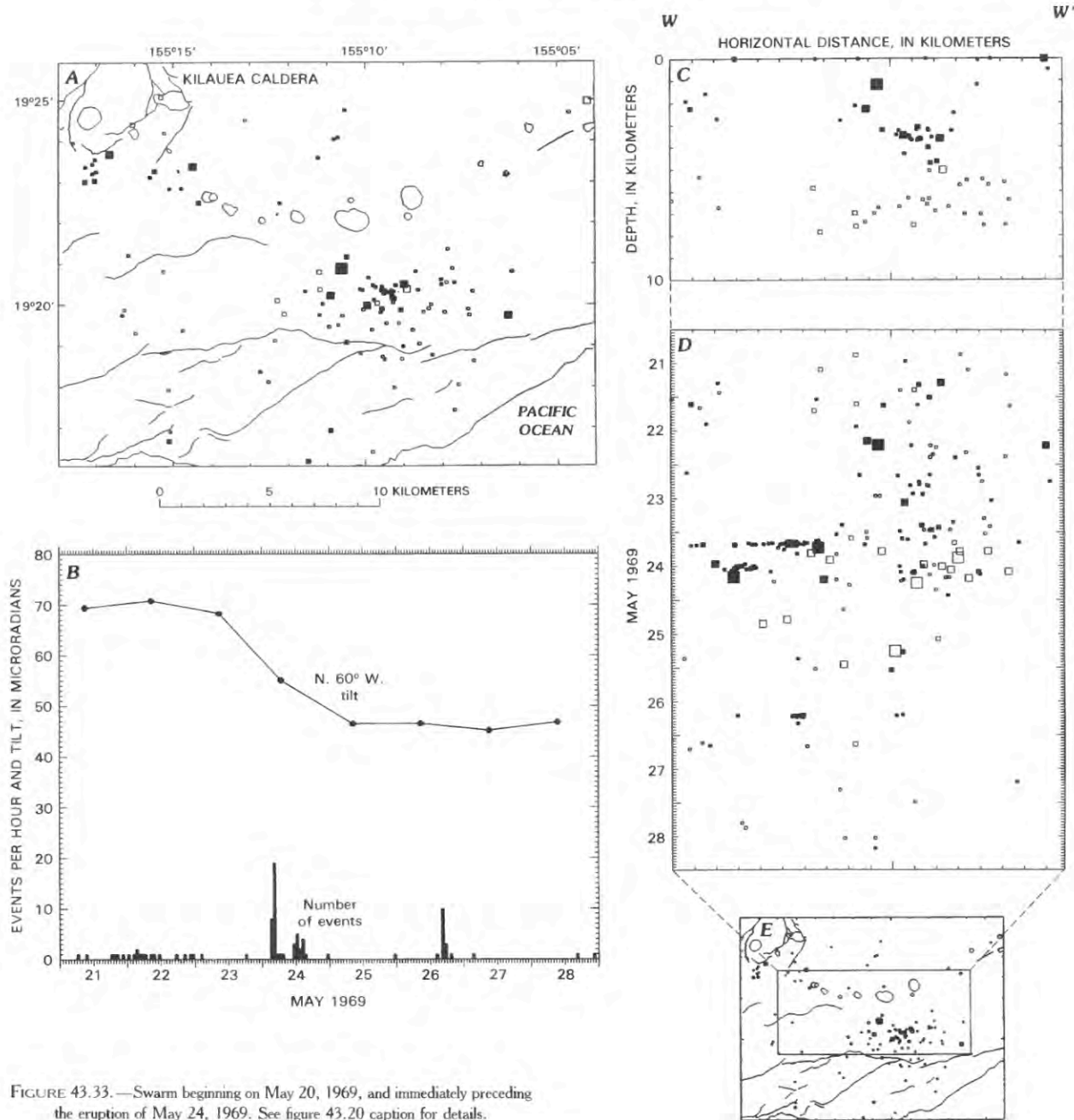
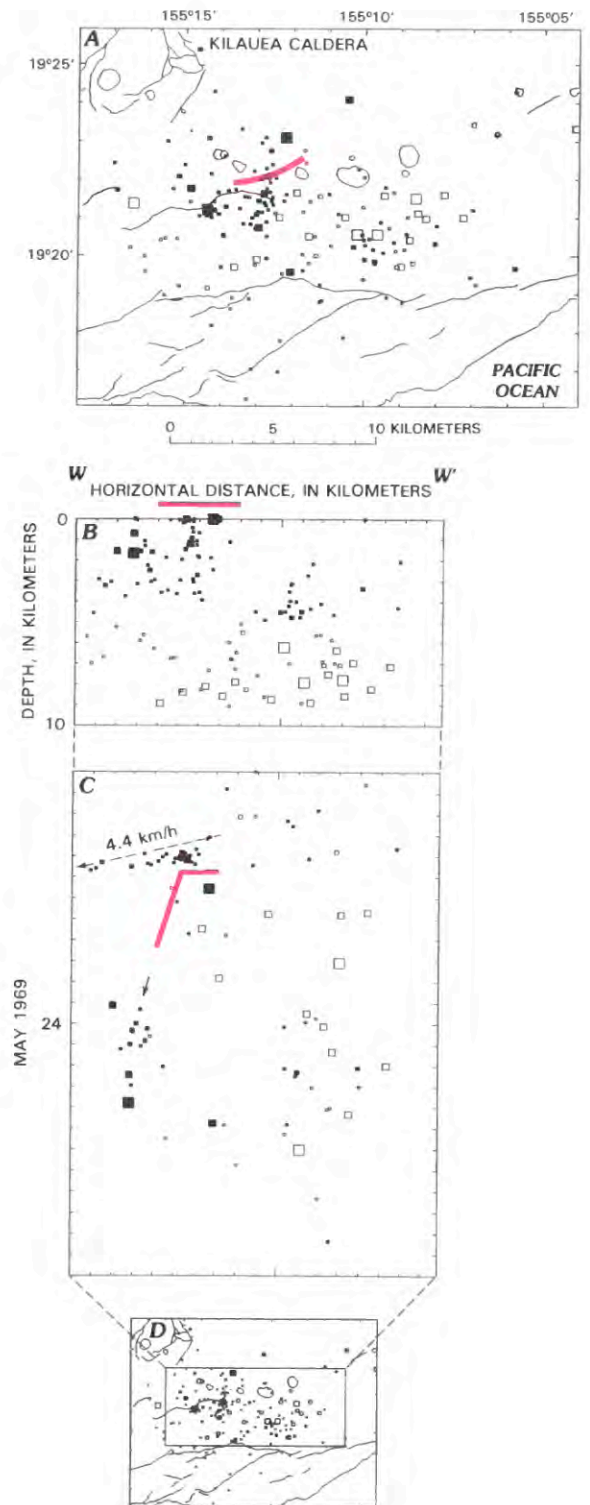


FIGURE 43.33.—Swarm beginning on May 20, 1969, and immediately preceding the eruption of May 24, 1969. See figure 43.20 caption for details.

FIGURE 43.34.—Eruptive swarm beginning on May 24, 1969. See figure 43.20 caption for details, and figure 43.33*B* for tilt and hourly earthquake rate. Red, approximate location (*A*, *B*) and onset time (*C*) of eruptive vents. Dashed line in *C*, poorly resolved shift in seismicity.



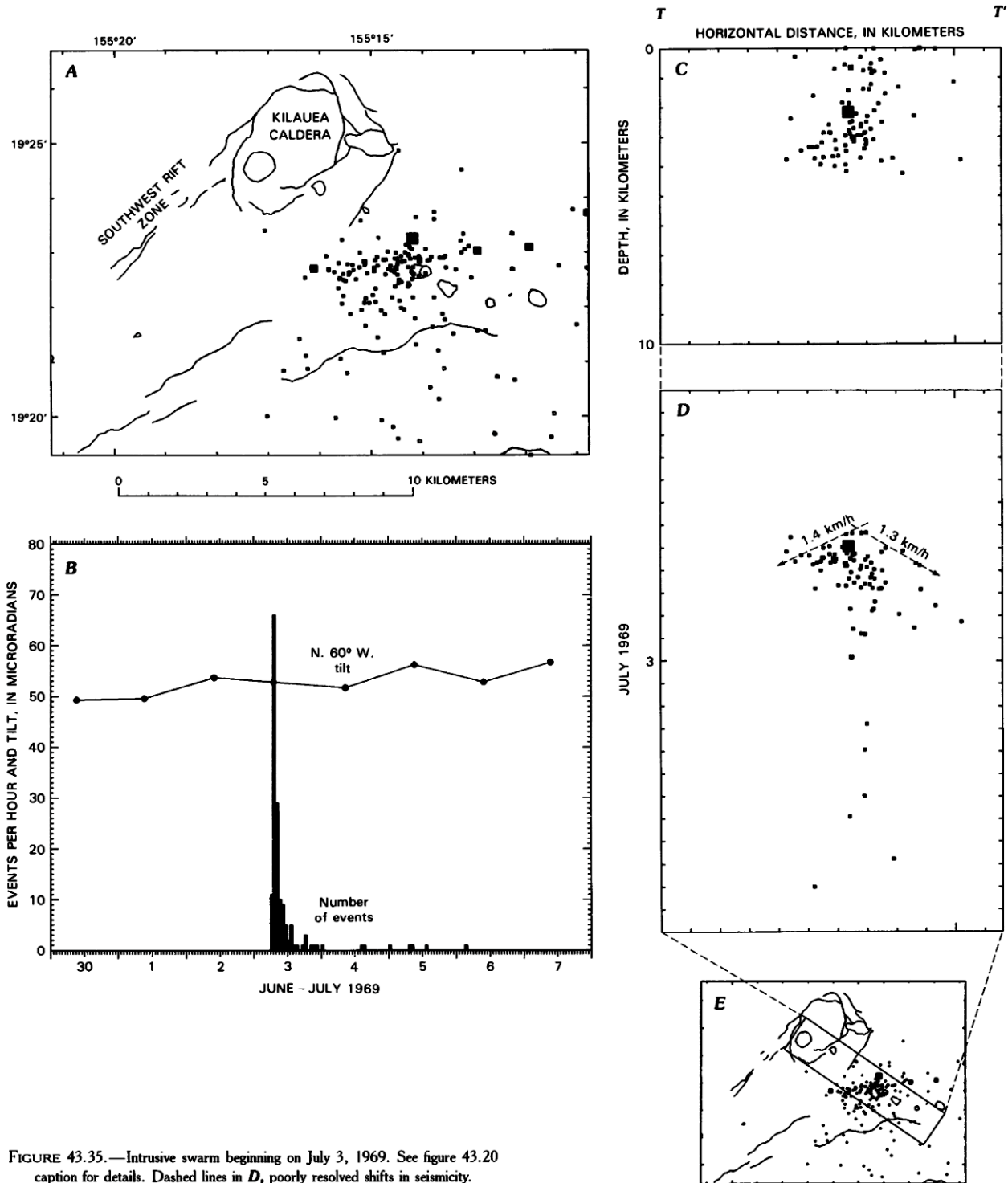


FIGURE 43.35.—Intrusive swarm beginning on July 3, 1969. See figure 43.20 caption for details. Dashed lines in *D*, poorly resolved shifts in seismicity.

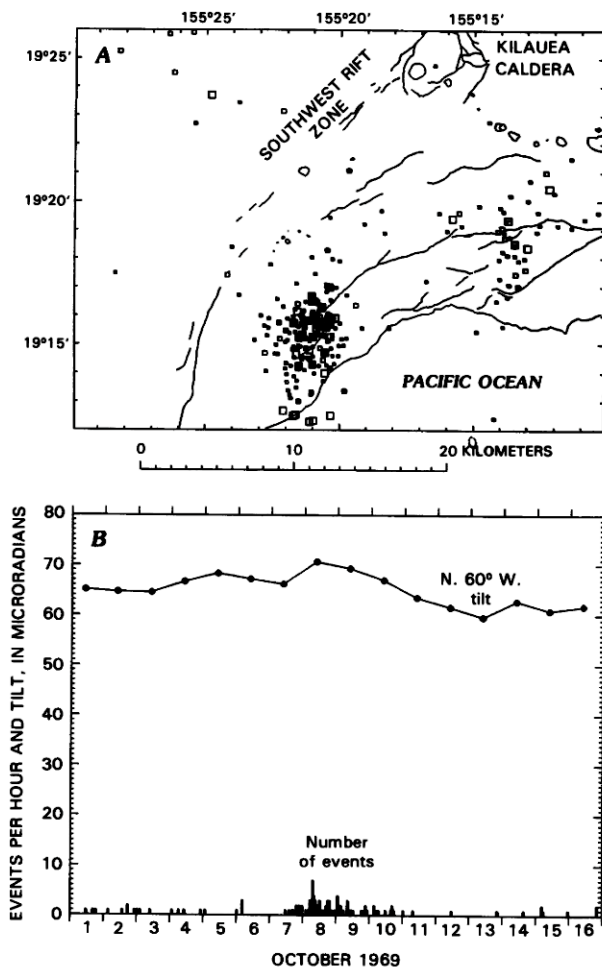


FIGURE 43.36.—Intrusive swarm beginning on October 7, 1969. Map and plot include earthquakes beginning on October 6, 1969. See figure 43.20 caption for details.

#### INFLATION-RELATED SWARMS AND INTRUSIONS, DECEMBER 1969 TO DECEMBER 1970

Uwekahuna tilt rose steadily during 1970 and most of 1971 as magma accumulated in the summit reservoir. Mauna Ulu's eruption was waning, so that more magma was available for summit storage. An additional consequence of the summit inflation during this period was a series of slow swarms within and adjacent to the caldera. The fluctuating tilt and seismicity were often well correlated, since both are consequences of inflation. The division of these inflation earthquakes into swarms is somewhat arbitrary, because summit seismicity fluctuated between a few and a few dozen locatable earthquakes per day for long periods. We have identified the most active intervals and called them slow swarms. The period from December 1969 through

September 1971 contains 11 such slow swarms that last several days each, but only 4 rapid swarms accompanying intrusions or eruptions.

Many of the inflation-related swarms appear to also involve intrusion of magma into the rifts. As with the rapid swarms, earthquakes during inflation often penetrate into the uppermost sections of rift in addition to the caldera. As discussed earlier, the inflation earthquakes and hence the accumulating magma appear to stop at blockages within the rifts. Earthquakes sometimes migrate along the rift conduits. The migration speed of earthquakes and hence the rate of intrusion is generally much slower than during the intrusions that generate intense swarms. The summit tilt changes slowly during these slow intrusions and may either rise, fall or remain unchanged. The 1970–71 period of inflationary seismicity and slow intrusions occurred when tilt values were much higher than average. Inflation swarms generally begin and end gradually, unlike the sharp onset of most swarms accompanying eruptions and rapid intrusions. These contrasts leave the impression that magma leaks or spills over into the rifts during slow intrusions, but pours through a ruptured barrier during rapid intrusions.

Inflationary swarms began on December 22, 1969 (fig. 43.38), February 3, 1970 (fig. 43.40), March 17 (fig. 43.41), and April 2 (fig. 43.42). In each case, tilt and seismicity were correlatable. Each swarm was limited to 2 or 3 km of the ERZ and SWRZ just outside the caldera. The seismicity apparently reached barriers within the rift conduits that could not be overcome by the slow pace of intruding magma. The Mauna Ulu eruptive episode on December 30 and its rapid deflation abruptly ended all earthquakes (fig. 43.38B). The eruption phase itself was aseismic, as were all Mauna Ulu episodes except the first. After the initial swarm, the conduit to Mauna Ulu was mostly open, and no new dike growth or rupture of rock was required. Of these inflationary swarms, only the one on February 3 showed a clear migration of earthquakes. Earthquakes penetrated the SWRZ first (fig. 43.40G). The ERZ soon followed with a more rapid migration that soon slowed (fig. 43.40D). The final downrift speed was only about 0.02 km/h into both rifts. The slow earthquake migration demonstrated that an intrusion occurred even while magma accumulated in the summit reservoir.

Rapid intrusions occurred on January 22 (fig. 43.39) and May 15, 1970 (fig. 43.43). The first was near Keanakakoi, only lasted for three hours, and produced no recognizable deflation (fig. 43.39B). Apparently the volume of magma was small, or it merely shifted position such that no tilt change at Uwekahuna resulted. The swarm moved rapidly toward the caldera (fig. 43.39D). The May swarm was clearly an ERZ intrusion accompanied by about 9 microradians of deflation (fig. 43.43A, B; Duffield and others, 1976). Pollard and others (1983) used a profile of surface displacements to constrain an elastic model of deformation surrounding a new dike. They inferred a dike dipping 86° NW., extending between 0.4 and 0.8 km depth, and 80 cm thick. The numerous earthquakes close to the surface (fig. 43.43C) emphasize the shallow nature of this event. The initial burst of earthquakes may have moved rapidly downrift from Puhimau at about 4.2 km/h (fig. 43.43D). Activity

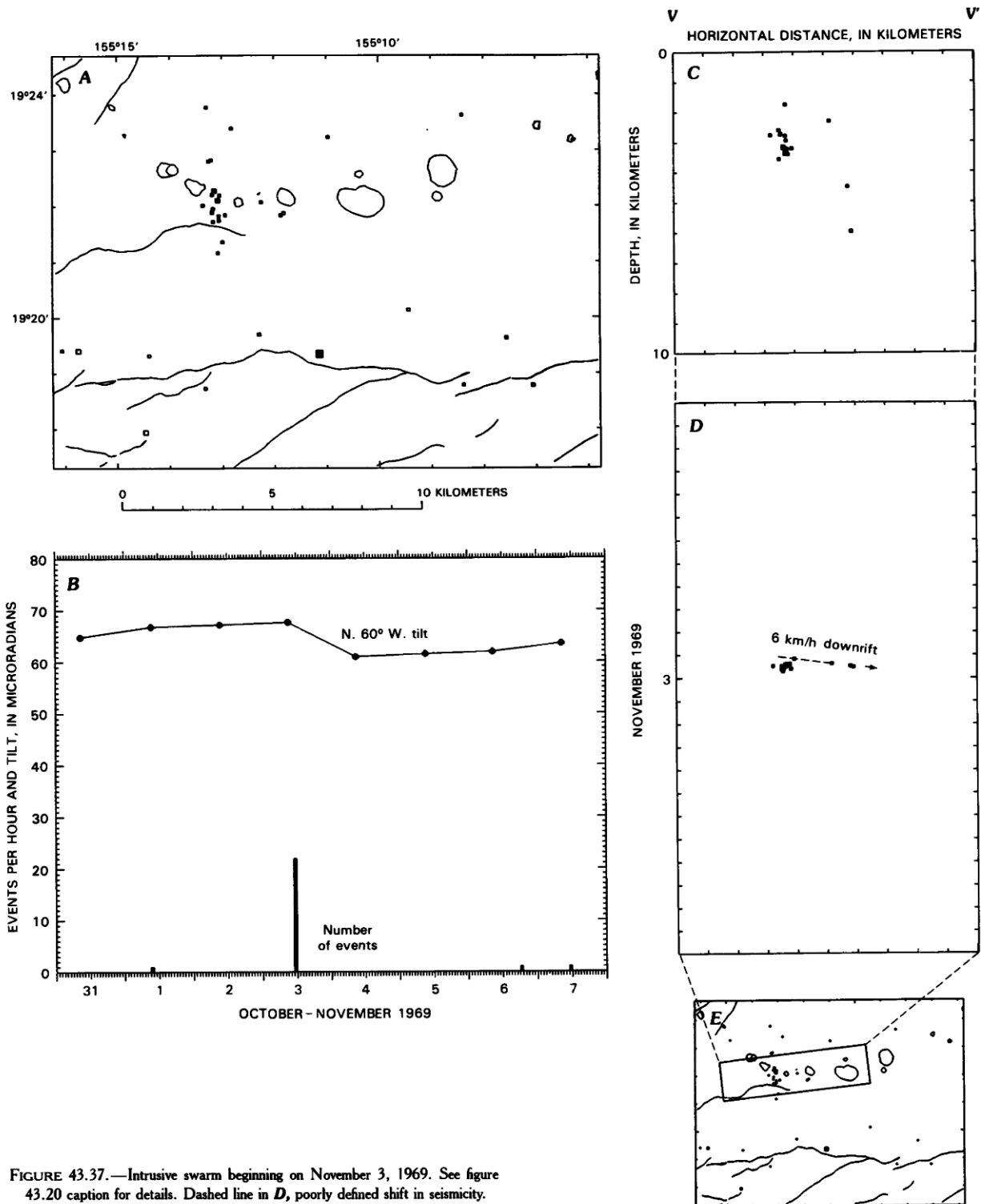


FIGURE 43.37.—Intrusive swarm beginning on November 3, 1969. See figure 43.20 caption for details. Dashed line in *D*, poorly defined shift in seismicity.

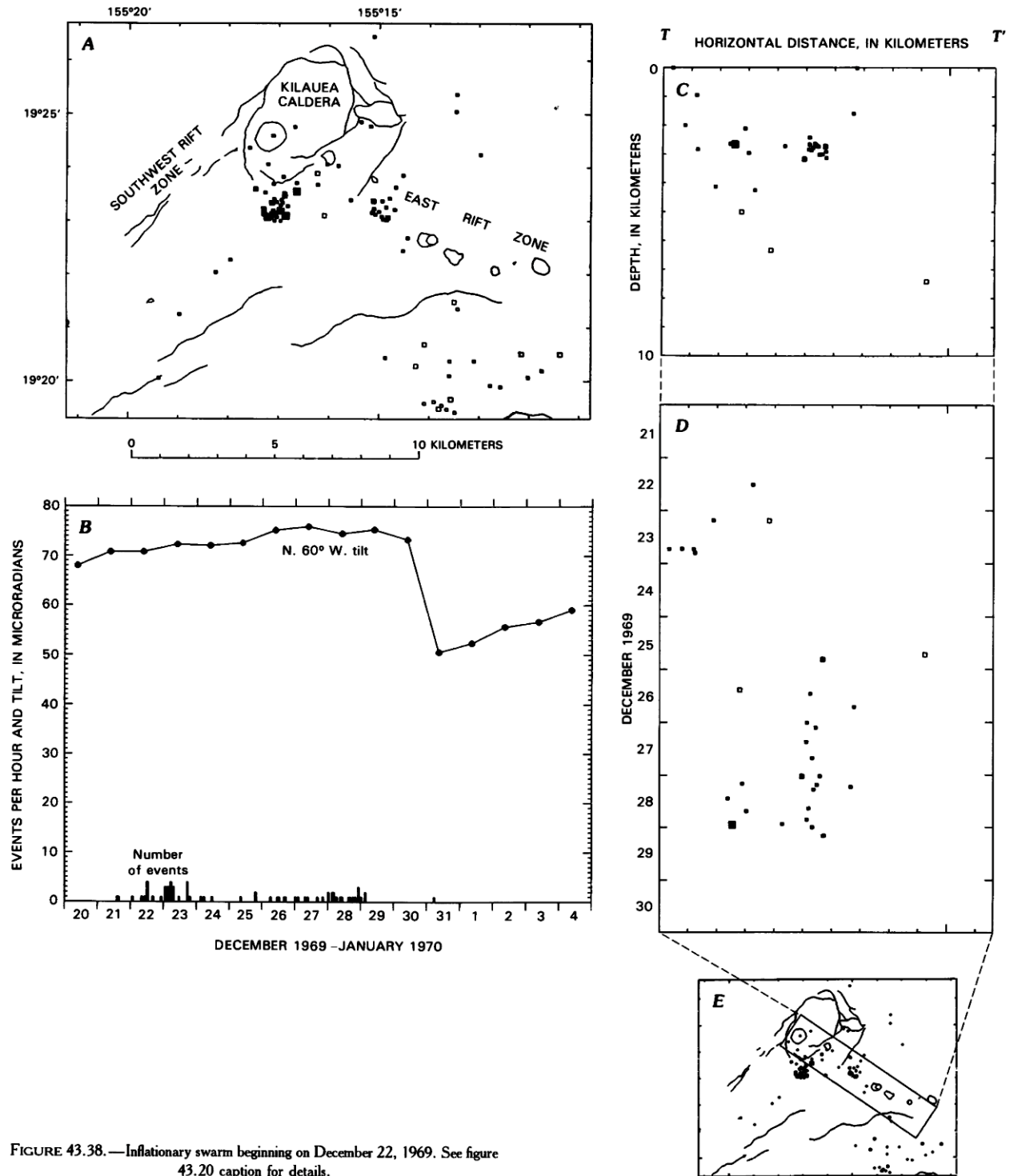


FIGURE 43.38.—Inflationary swarm beginning on December 22, 1969. See figure 43.20 caption for details.

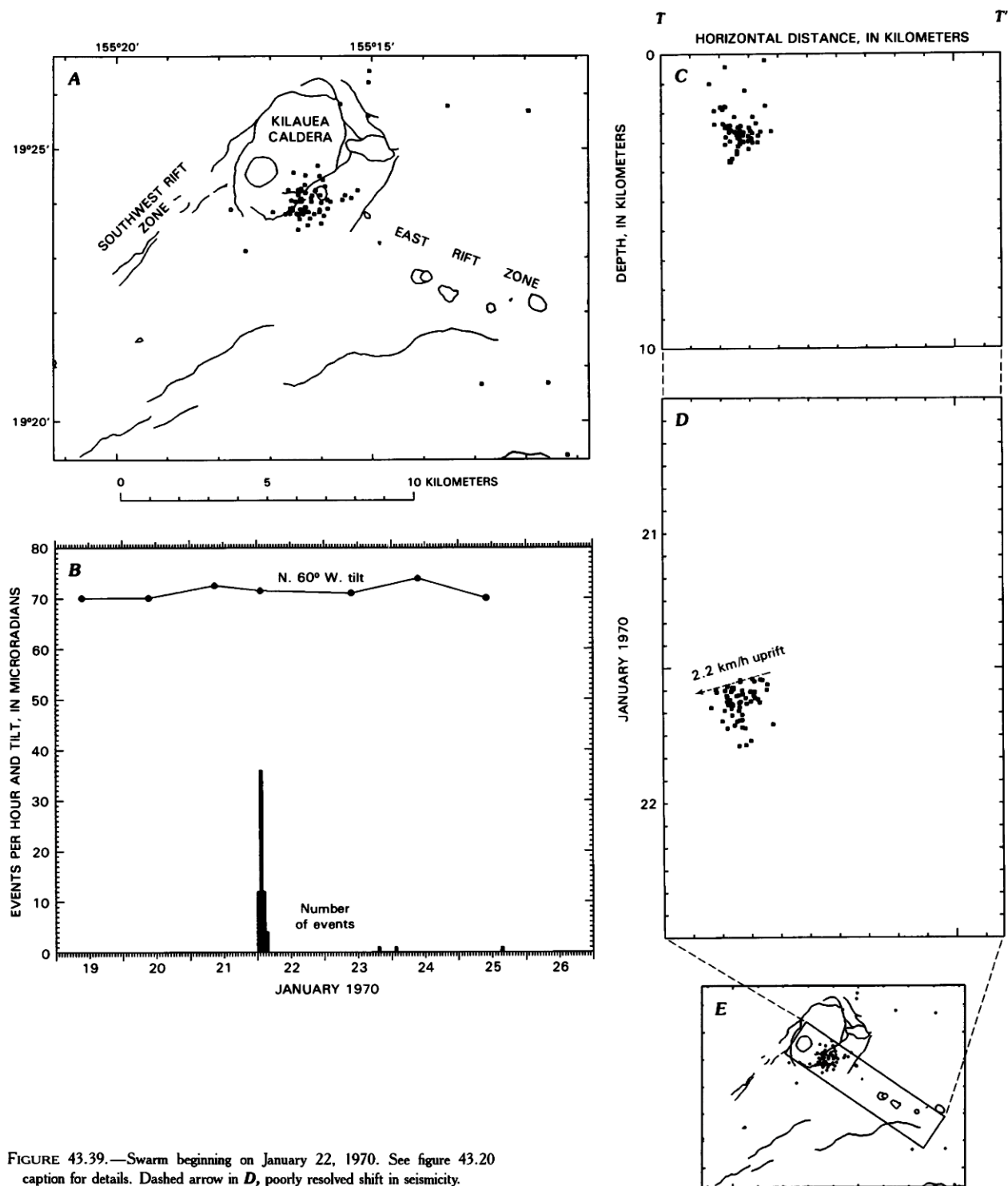


FIGURE 43.39.—Swarm beginning on January 22, 1970. See figure 43.20 caption for details. Dashed arrow in *D*, poorly resolved shift in seismicity.

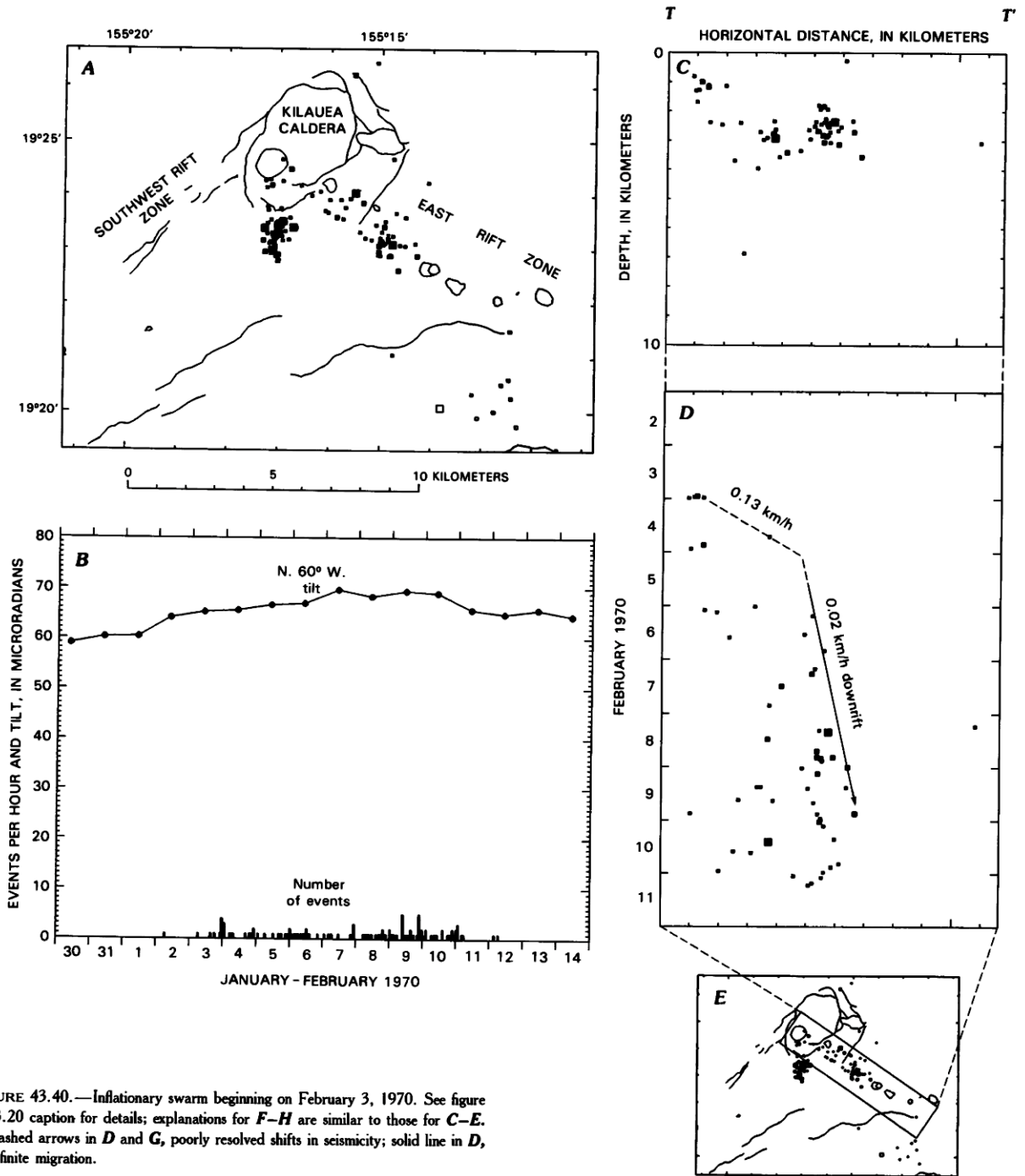


FIGURE 43.40.—Inflationary swarm beginning on February 3, 1970. See figure 43.20 caption for details; explanations for *F–H* are similar to those for *C–E*. Dashed arrows in *D* and *G*, poorly resolved shifts in seismicity; solid line in *D*, definite migration.

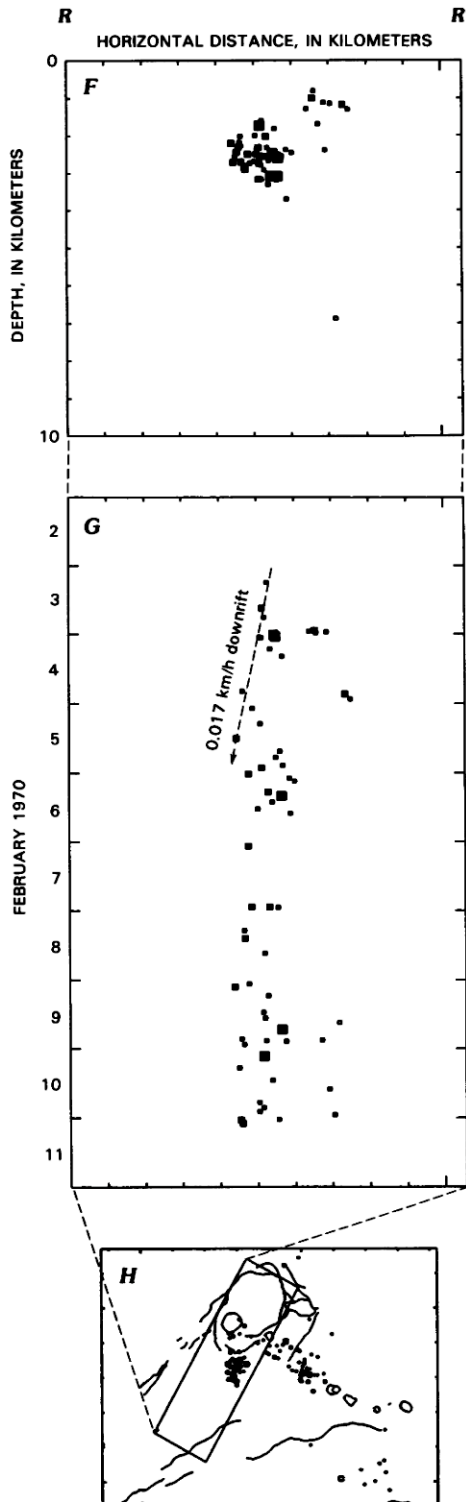


FIGURE 43.40.—Continued.

also moved uprift at about 0.13 km/h and culminated in the second burst about one day later. A few scattered earthquakes near the ERZ between Puu Kamoamo and Heiheiahulu (fig. 43.43F) may have been coincidental.

The inflationary swarms during December 1970 were unlike their predecessors, in that earthquakes occurred throughout the caldera and in particular at its northeast end (figs. 43.44A and 43.45A). The first swarm began on December 12 as tilt slowly rose and fell synchronously with the earthquakes (fig. 43.44B). As tilt rose steadily, the second phase became noticeable on December 22 (fig. 43.45B), began in the southwest caldera, and spread rapidly northward into the entire caldera (fig. 43.45D). Also note the slow migration and intrusion into the SWRZ at the same 0.2 km/h speed as the February 1970 swarm. The path taken by the December 1970 earthquakes on the northern branch of the SWRZ (fig. 43.45A) anticipated the location of the September 24, 1971 eruption.

Another view of these swarms is given by figure 43.46, which superimposes summit tilt and position of earthquakes along the upper ERZ versus time. Figure 43.46A plots the entire November 1969 through February 1972 time interval. Figure 43.46B–D expands the time scale for this period. Moderate inflation and several swarms (3 intrusions and 4 inflationary swarms) with relative seismic quiet between them characterize the period of figure 43.46B. As noted above, the slow swarms are generally at the times of the most rapid inflation. The July 1970 to April 1971 period (fig. 43.46C) saw no net inflation and relatively low summit seismicity. A nearly continuous eruption at Mauna Ulu tapped most of Kilauea's magma supply during this period. By contrast, the next 10 months (fig. 43.46D) saw rapid inflation and considerable caldera and rift seismicity, including 2 eruptions, 2 rapid intrusions, 6 inflationary swarms and a high background of seismicity. This graph illustrates the close correlation between inflation and summit seismicity, and the difficulty of identifying discrete inflationary swarms during such active periods.

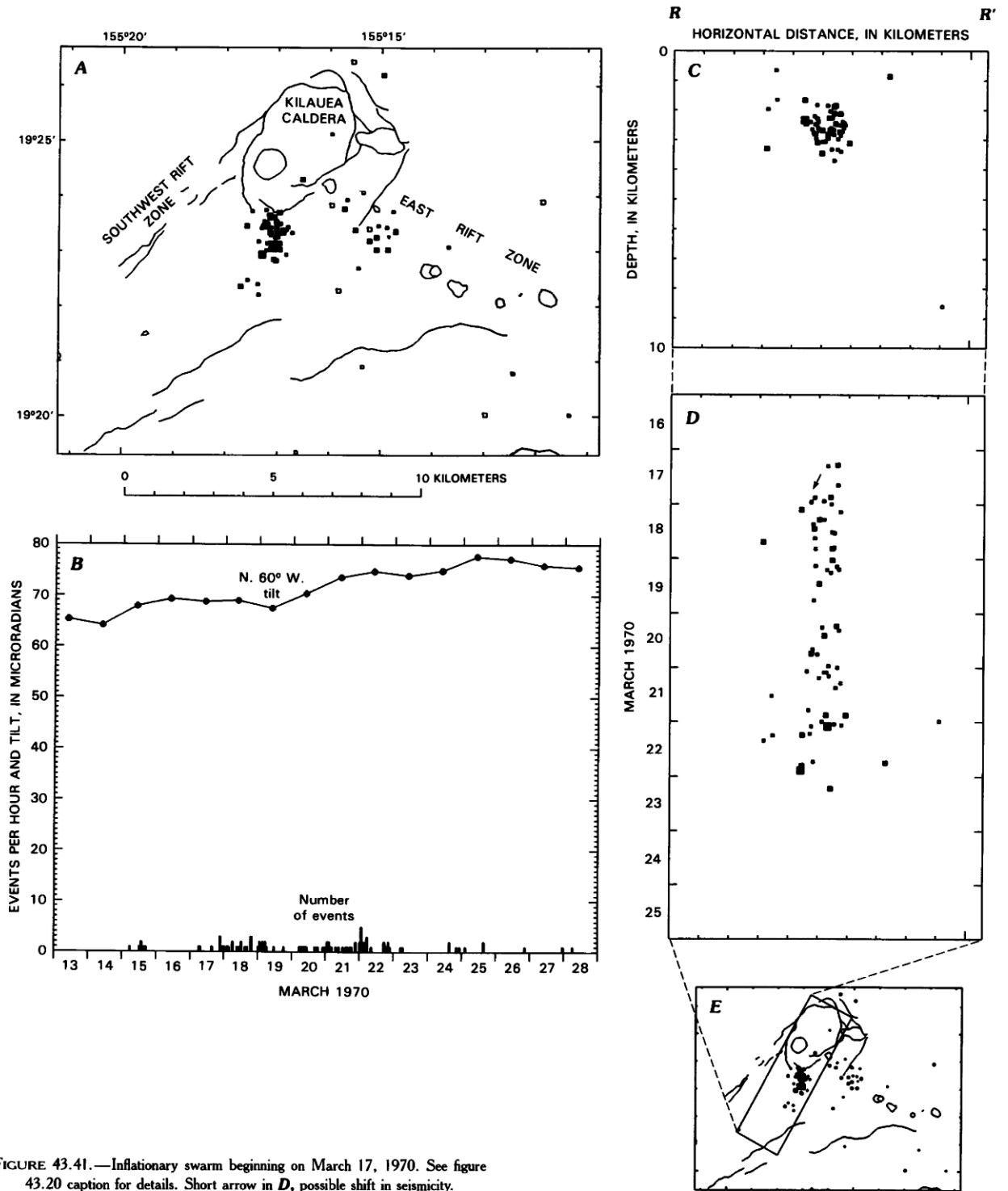


FIGURE 43.41.—Inflationary swarm beginning on March 17, 1970. See figure 43.20 caption for details. Short arrow in *D*, possible shift in seismicity.

#### INFLATIONARY SWARMS AND ERUPTIONS, JUNE 1971 THROUGH JANUARY 1972

Rapid inflation and high seismicity returned in the June–September 1971 period (figs. 43.46*D*, 43.47). Earthquakes were primarily close to the caldera, but to a lesser extent within the rift zones. Eight individual swarms from this interval will be discussed below, but there was also a high background of activity.

The activity of early June 1971 continued at a relatively low but continuous level throughout the south caldera and was accompanied by slowly rising tilt (figs. 43.48, 43.49*B*). The June 1–10 seismicity was thus caused by steady inflation. On June 11 the seismicity intensified and concentrated into a small finger that extended south of the caldera (fig. 43.49*A*). Earthquakes migrated southward at a rate that slowed when seismicity crossed the caldera boundary (fig. 43.49*D*). Following the most intense seismicity, continuing but sparse activity began near Mauna Iki (fig. 43.47). The gradual deflation, slow migration, and later downrift seismicity indicate this was a slow intrusion.

Another episode of elevated summit seismicity commenced in July 1971. It was preceded by about one month of increasing activity in the caldera (figs. 43.46*D*, 43.47). The south caldera activity continued, but on July 19 the ERZ near Kokoolou came alive (fig. 43.50*A*). The swarm moved into the ERZ at about 0.17 km/h, but its rate of advance soon slowed considerably to only 8 m/h (0.2 km/d, fig. 43.50*D*). There was also a hint of migration into the SWRZ (fig. 43.50*C*). The HVO staff expected an eruption very soon because of the high tilt and summit seismicity, but with magma apparently leaking into both rift zones, there was no strong indication of where the eruption would be.

The tilt and rate of seismicity were very high prior to the eruption of August 14, 1971 (fig. 43.51*B*). Earthquakes continued in the south caldera and adjacent 3 km of both rifts (fig. 43.51*A*). The summit inflated as simultaneous slow intrusions penetrated into both rifts (fig. 43.51*D*, *G*). What appeared to be moving trends of earthquakes into the ERZ may have been caused by pulses of magma leaking into the rift. The eruption occurred in the southern part of the caldera on August 14 (Duffield and others, 1982). The lack of earthquakes in the hours following the onset of the eruption (fig. 43.51*D*, *G*) was a result of saturation of the seismic network by high tremor. Both tilt and seismicity dropped rapidly, however, indicating that some of the pressure built up during inflation had been relieved. The few earthquakes that could be timed and located after the eruption began were very close to the eruptive vent in the southern part of the caldera (fig. 43.52).

Another prominent episode of inflation and summit seismicity preceded the SWRZ eruption of September 24, 1971. We divided it into two periods beginning on September 6 (fig. 43.53) and on September 17 (fig. 43.54). The distribution of epicenters matched that of the previous inflationary swarms. Thus the August eruption in the caldera did not change the pattern of magma accumulation. Premonitory seismicity did not seem to favor either rift zone for the impending eruption, although there was a suggestion of earthquake migration into the SWRZ (fig. 43.54*G*).

The earthquakes accompanying the September 24 SWRZ eruption did not follow a continuous linear trend below the eruptive fissure (fig. 43.55*A*). Instead, four main clusters of earthquakes occurred along the rift. The first three roughly coincided with the three main zones of eruptive vents, and the fourth was in the south flank adjacent to the intrusion terminus near Puu Kou. We interpret each cluster as a blockage of the rift conduit, which magma forcefully broke through to continue downrift. Earthquakes were triggered as the dike penetrated and wedged apart each barrier. Earthquake clusters and vents would then coincide because the blockages that produced seismicity also diverted the dike upward before the barrier rifted open. Note also that one barrier is directly beneath Mauna Iki (fig. 43.55*A*), which may have been responsible for its formation in 1919–20. This barrier is probably a major one, as it appears to be responsible for much of the seismicity induced adjacent to it on both sides of the rift, including as much as 12 km into the Kaoiki seismic zone (fig. 43.55*A*).

The earthquakes clearly do not form a linear trend that coincides with the main seismic conduit active during 1970–83 (fig. 43.3*C*, *D*). The September 1971 eruption chose a more northwesterly path. Note also that the eruption earthquakes in the south caldera are displaced west of the inflationary swarms prior to the eruption. Thus, two main SWRZ conduits were active during recent decades: the northerly one which was seismically active during the December 1970 inflationary swarm, the September 1971 eruption, and perhaps the November 1967 eruption; and the southerly one, active during the intrusions of December 1974 and August 1981, as well as most periods of inflation. Using deformation data, Duffield and others (1982) concluded that the September 1971 eruption was fed by shallow parts of the summit reservoir, and the observed range of earthquake depths is consistent with this interpenetration (fig. 43.55*B*). The main rift zone conduits, however, tap the summit reservoir at about 3 km depth.

The September 1971 eruptive vents and earthquakes both progressed downrift (fig. 43.55*C*), indicating that both were caused by the same propagating dike. The times of first eruption from the various vent segments and approximate rates of opening of individual fissures from Duffield and others (1982) are plotted with earthquakes in figure 43.55*C*. The apparent downrift movement of vents is about 0.31 km/h. This speed is a little slower than the initial earthquake migration speed of about 0.53 km/h, but a second wave of earthquakes accompanies the progression of migrating vents. Another way to view the slower speed of the vents relative to the initial earthquake wave is that the time delay between passage of earthquakes and the start of eruption at a given place increased with distance down the rift. The delay ranged from 4 hours in the caldera to about 18 hours at the most distant vent. If the first earthquakes at a given spot mark the initial penetration of magma within the main conduit, the time delay of the eruption occurs while magma moves upward from the conduit to the surface. The increase of these delay times may then be a result of the plunge of the conduit to greater depths away from the caldera and the greater upward distance magma had to travel. The pattern of delay times could also be a

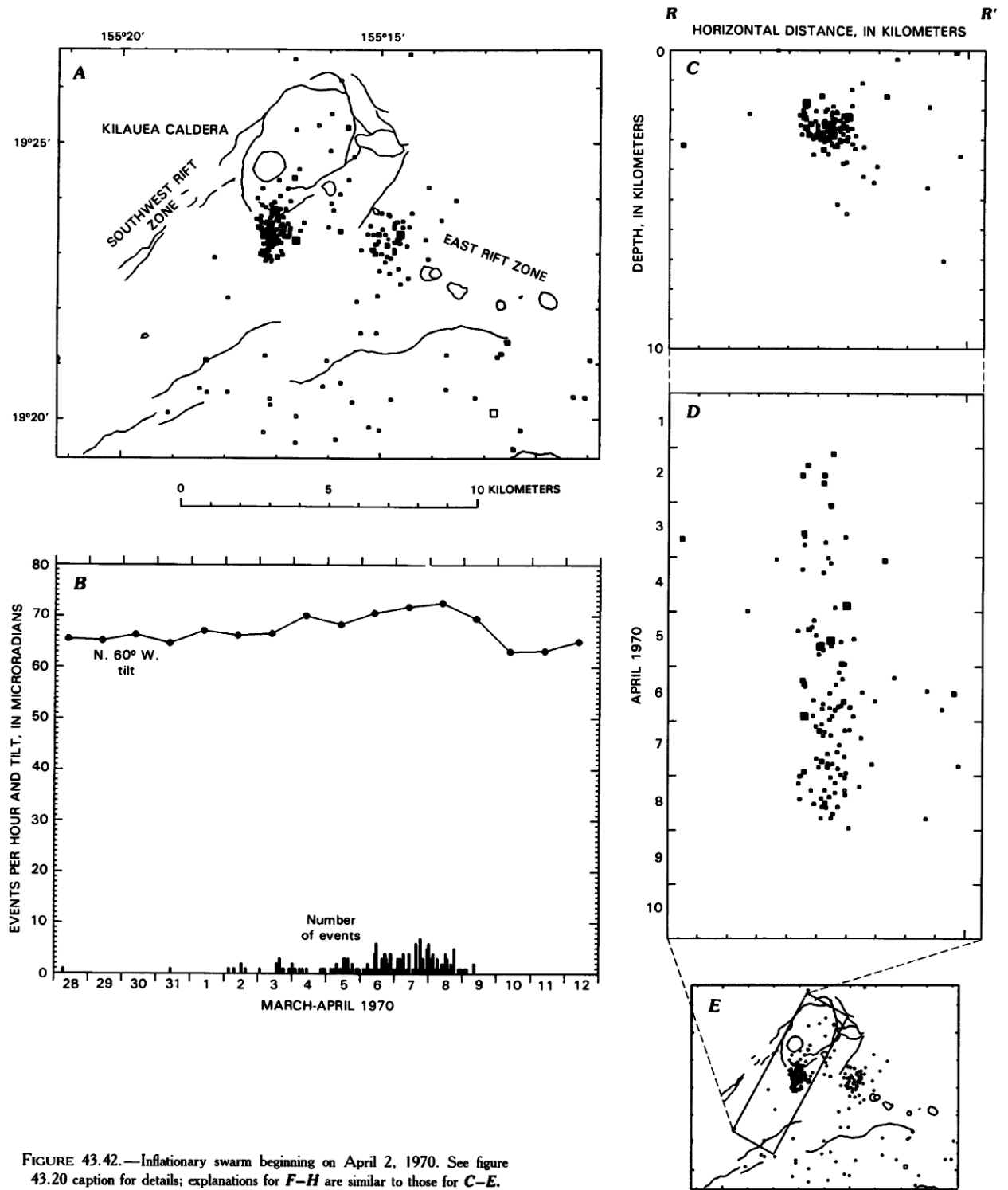


FIGURE 43.42.—Inflationary swarm beginning on April 2, 1970. See figure 43.20 caption for details; explanations for *F–H* are similar to those for *C–E*.

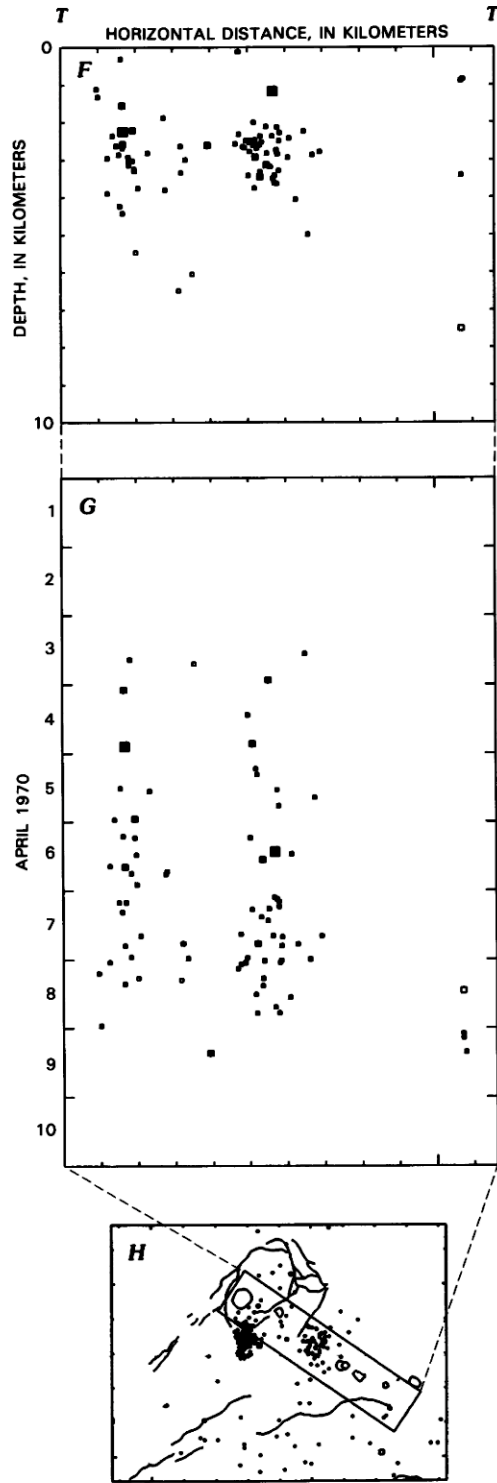


FIGURE 43.42.—Continued.

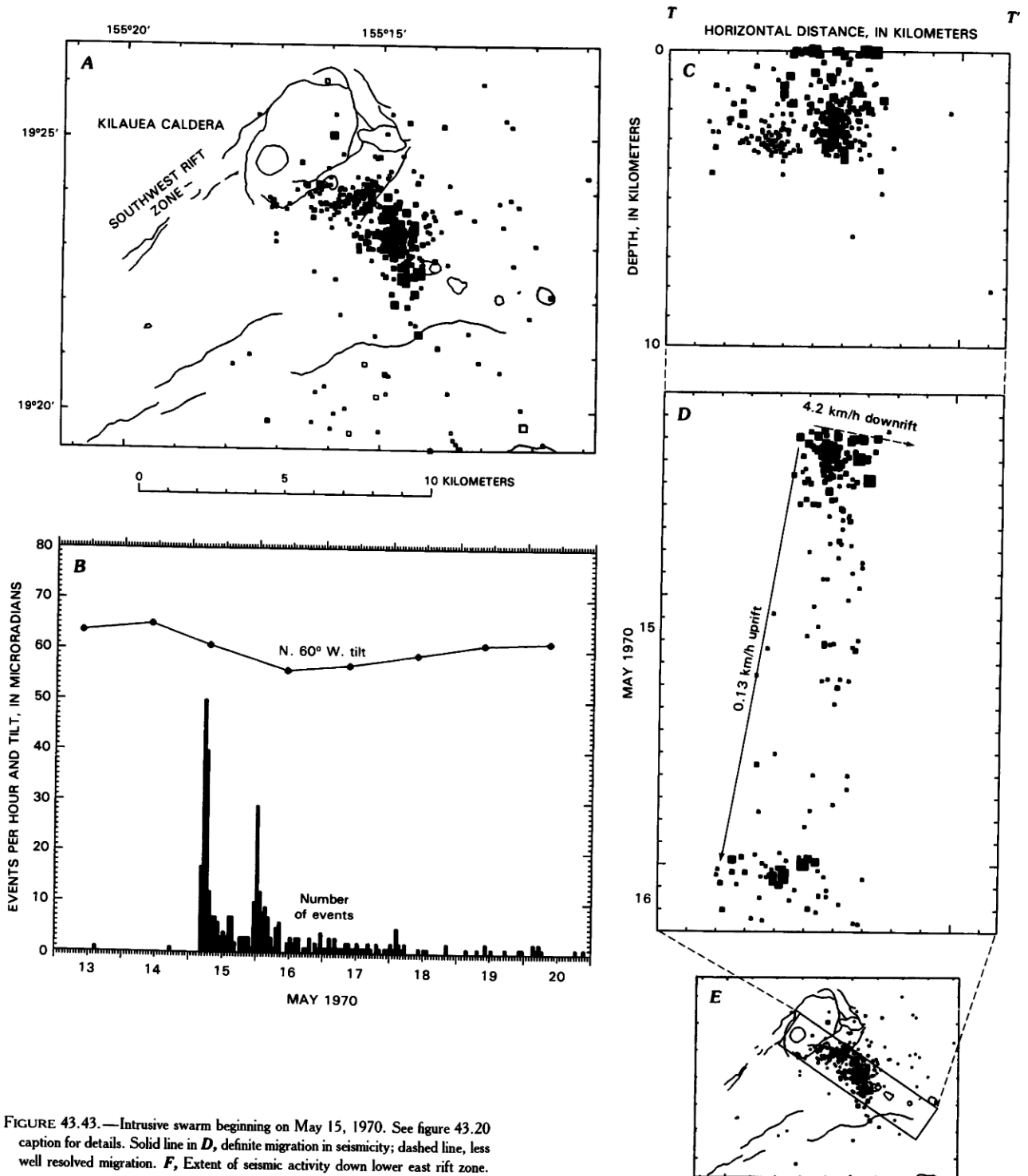


FIGURE 43.43.—Intrusive swarm beginning on May 15, 1970. See figure 43.20 caption for details. Solid line in *D*, definite migration in seismicity; dashed line, less well resolved migration. *F*, Extent of seismic activity down lower east rift zone.

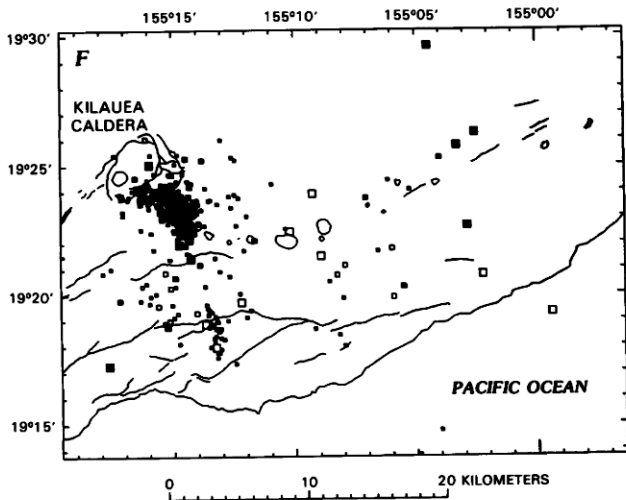


FIGURE 43.43.—Continued.

result of reduced magma pressure and slower upward speed farther down the rift, or a combination of both factors.

The September 1971 eruption is a good example of equating earthquake migration with magma movement and dike propagation. Irregularities in speed do occur, but the leading edge can move at a constant average speed for long segments of the rift. A few scattered earthquakes occur before the magma front passes their location (such as events above the solid line in fig. 43.55C). These events are apparently triggered by small stress increases that move ahead of the growing dike at the much faster speed of elastic waves.

Seismicity declined dramatically following the September eruption (figs. 43.46D, 43.47). The rift widened by perhaps 1–2 m (Duffield and others, 1982), so a significant volume of magma was intruded from the summit reservoir in addition to that erupted. Tilt and survey line changes around the caldera were dominated by the effects of the dike. Subsidence of the magma reservoir was difficult to document geodetically, although part of the floor of Halemaumau

did fall 45 m (Duffield and others, 1982). The drop in seismicity indicates that a drop in magma pressure took place, however, similar to that during caldera subsidence of other eruptions. Kilauea reinflated rapidly after the eruption, and earthquakes increased and gradually penetrated farther into the ERZ (fig. 43.46D).

Another SWRZ swarm three months after the September eruption was probably related to it. The swarm began on December 23, 1971, and lasted about 7 days (fig. 43.56B). Most activity was in the south flank adjacent to the terminus of the September intrusion (fig. 43.56E). The flank probably received an increment of stress from the recently intruded SWRZ. Some earthquakes did occur uprift (fig. 43.56A, F) and they preceded the main part of the swarm in a way suggestive of downrift migration (fig. 43.56H). Little or no change occurred in summit tilt, however, so apparently magma (or stress) was redistributed within the rift complex without much new magma from the summit. As noted above, considerable newly intruded magma was available within the SWRZ conduit. Seismicity in the ERZ was concurrent with the central SWRZ earthquakes and generally progressed uprift (fig. 43.56A, D). The seismicity pattern and lack of a tilt change thus do not suggest a replay of the September event, but rather a readjustment of the two rifts and perhaps the south flank.

Kilauea refocused her attention to the ERZ with an inflation-related swarm there in January 1972. As with similar swarms of the previous two years, seismicity and magma only accumulated above the rift blockage near Pauahi (fig. 43.57A). The swarm was accompanied by rising tilt (fig. 43.57B). The first swarm episode saw events slowly penetrate the rift (fig. 43.57D) but two periods of uprift migration appeared to characterize the second episode (fig. 43.57F). The possible causes of uprift earthquake migration will be discussed in more detail later, but the phenomenon is probably related to the complex system of multiple conduits in the ERZ above Mauna Ulu and their close magmatic communication with the summit reservoir. If the entire uprift part of the ERZ slowly receives and stores magma from the summit supply, then a propagating episode of rifting and accompanying seismicity could go in either direction, because the magma to drive it is present along the whole rift segment. The January swarm was followed by a major eruptive phase at Mauna Ulu on February 4, 1972 (Tilling and others, chapter 16). The eruption was marked by only minor earthquake activity in the Pauahai to Mauna Ulu area and by a halt to the slow inflation (fig. 43.58). The few earthquakes occurred both before and after the eruption, whose onset time was only approximately known due to lack of direct observations (fig. 43.58D).

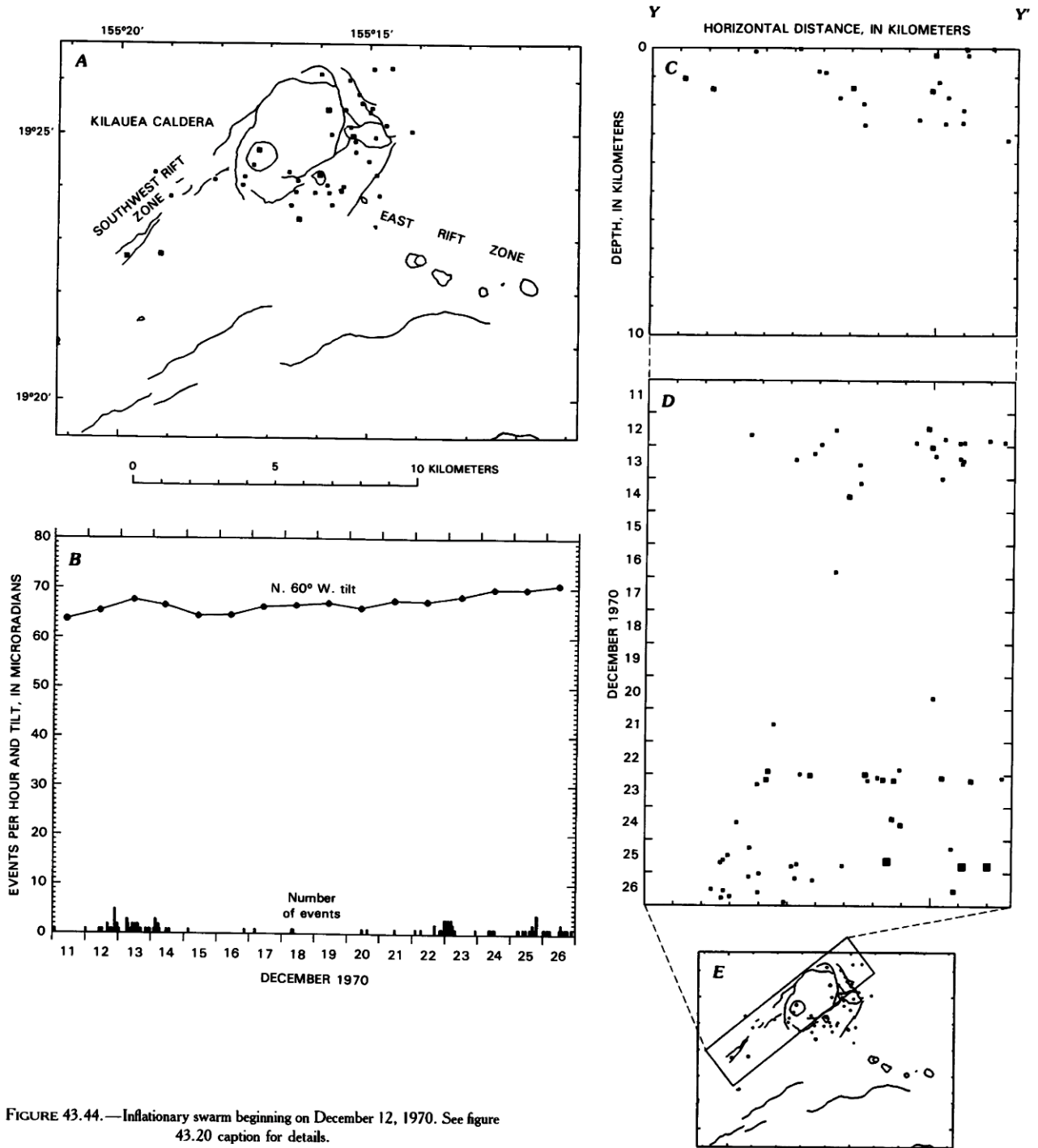


FIGURE 43.44.—Inflationary swarm beginning on December 12, 1970. See figure 43.20 caption for details.

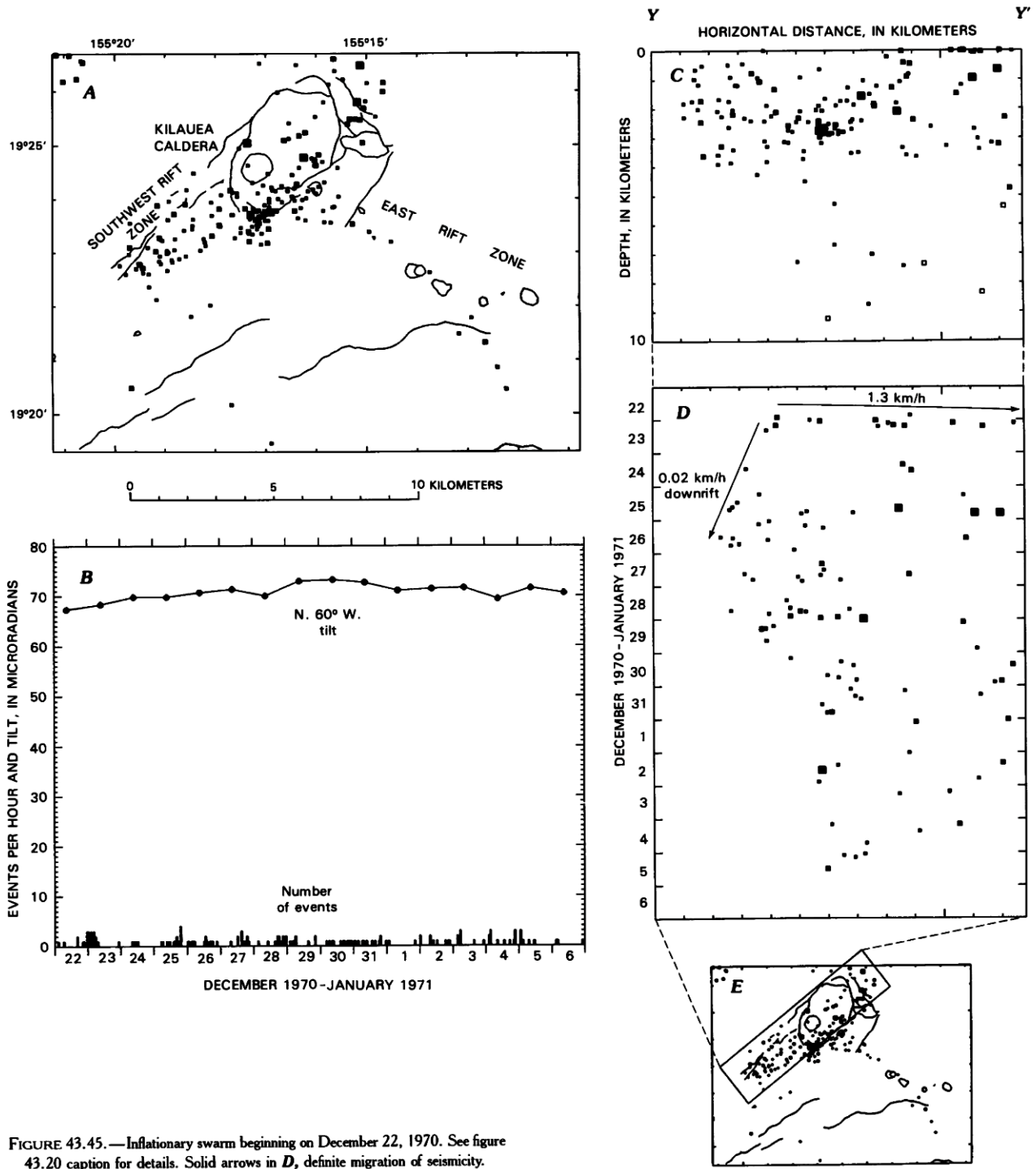


FIGURE 43.45.—Inflationary swarm beginning on December 22, 1970. See figure 43.20 caption for details. Solid arrows in *D*, definite migration of seismicity.

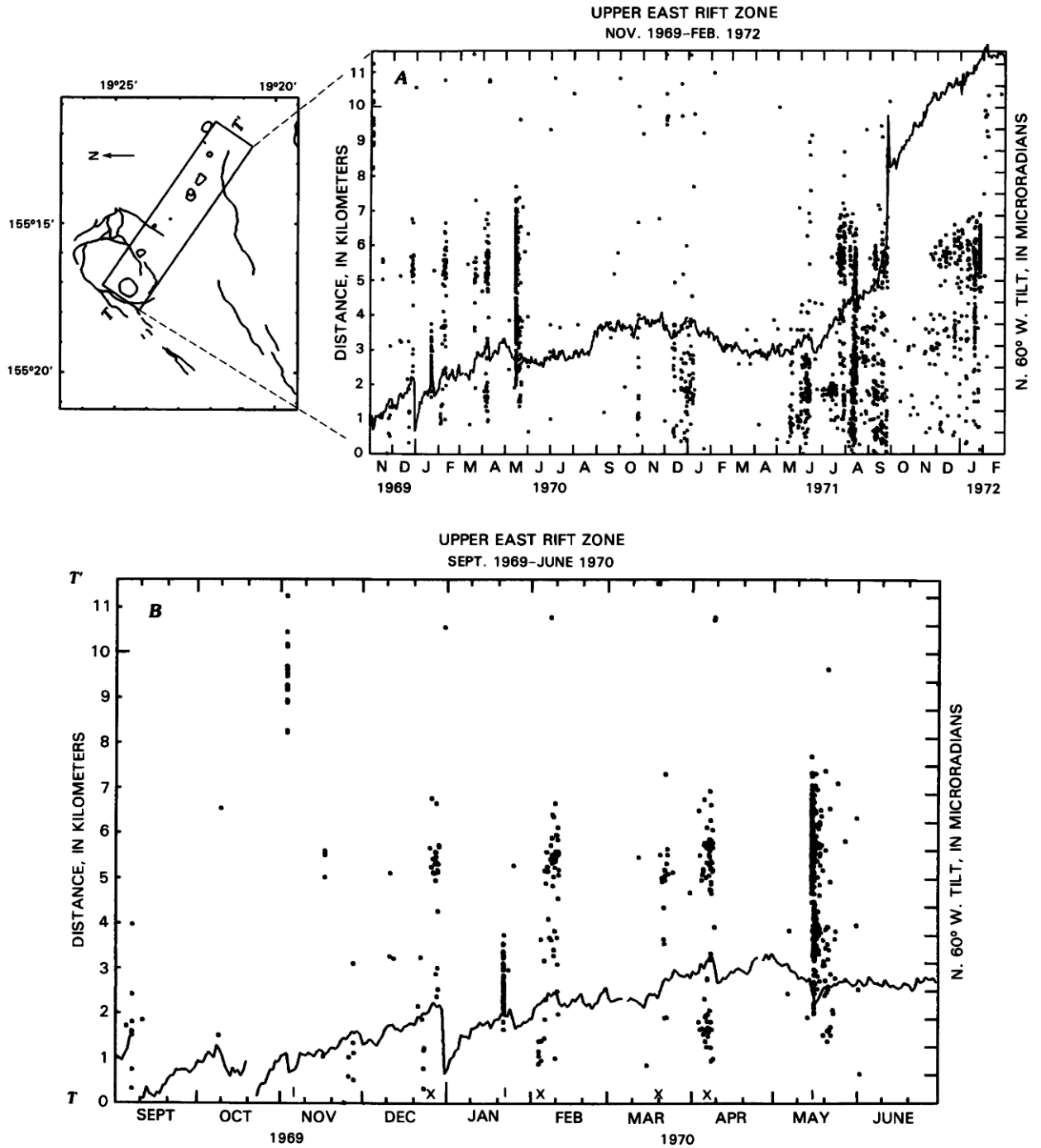


FIGURE 43.46.—Plot of earthquakes along upper east rift zone and N. 60° W. water-tube tilt at Uwekahuna versus time. Tilt axes marked in 10- $\mu$ rad divisions. All earthquakes shallower than 5 km and within geographic box shown are plotted. Endpoints for  $T-T'$  are given in table 43.2. **A**, Plot for entire 28-month period. **B-D**, Same plot as in **A**, but on an expanded time scale. Halemaumau is near endpoint  $T$  and Alae crater is near  $T'$ . Notations along time axis refer to specific swarms detailed in other figures: E, eruption; I, intrusion; X, swarm accompanying inflation.

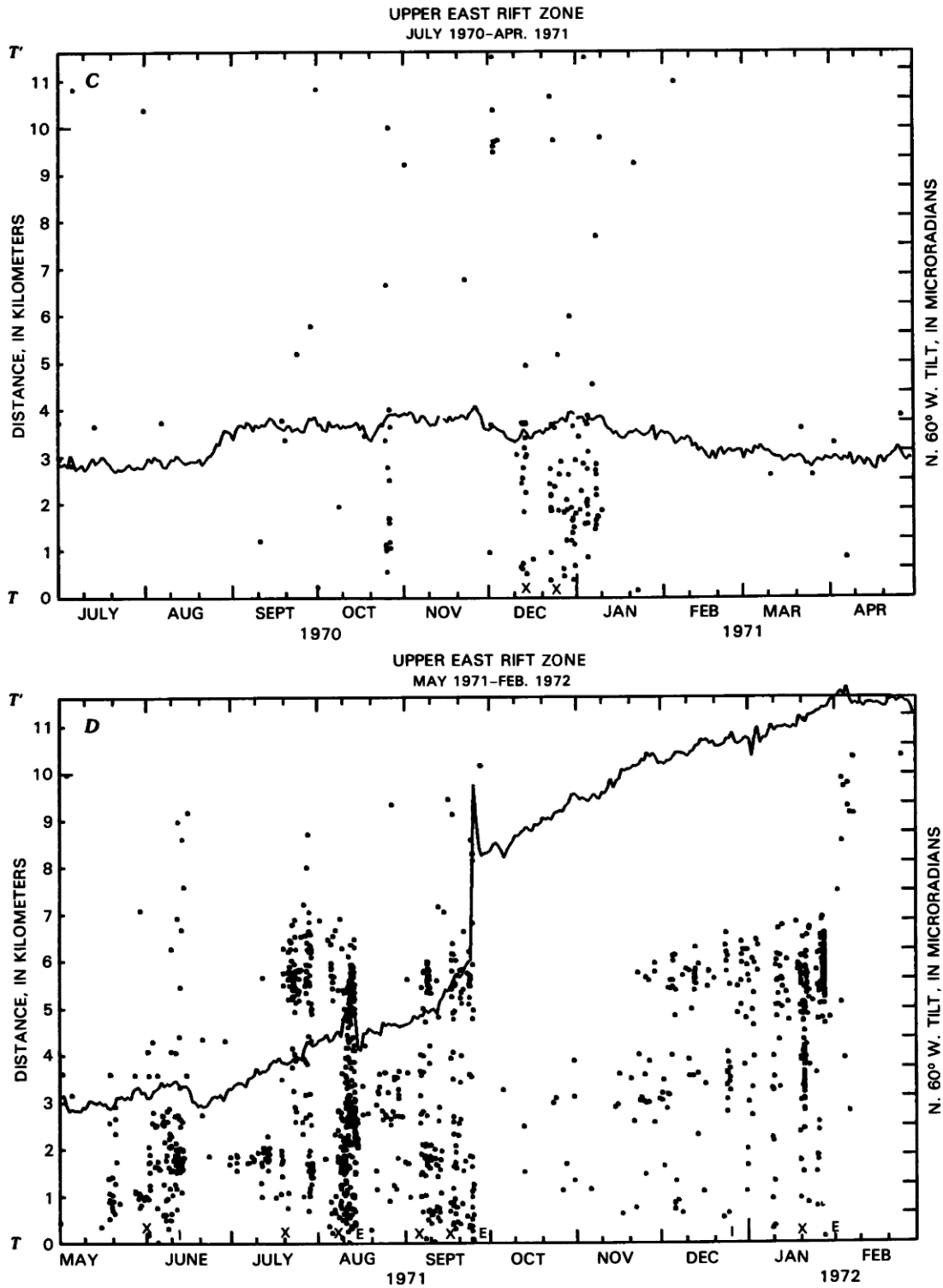


FIGURE 43.46.—Continued.

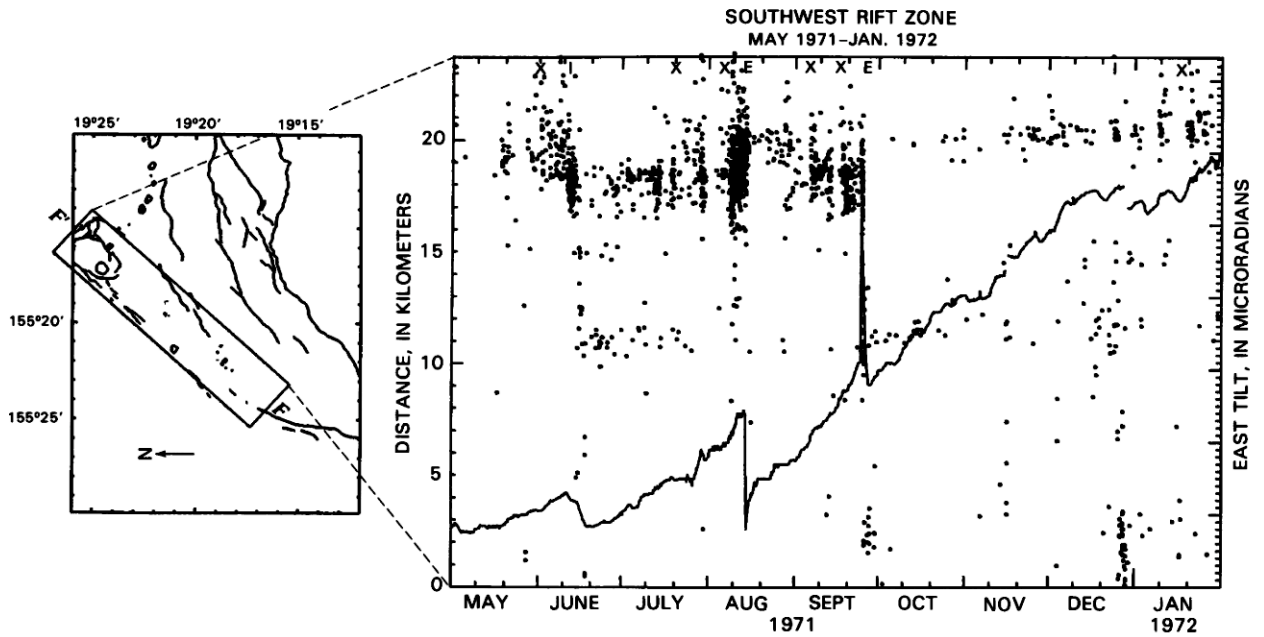


FIGURE 43.47.—Plot of earthquakes along the southwest rift zone and east tilt at Uwekahuna versus time. Endpoints for distance axis  $F-F'$  are given in table 43.2. Tilt is from east-west Ideal Aeromsmith tiltmeter, where east-down tilt is down on plot and generally indicates deflation of summit caldera. Large divisions on tilt scale are 10  $\mu$ rad. Notations along time axis refer to specific swarms detailed in other figures: E, eruption; I, intrusion; X, swarm accompanying inflation.

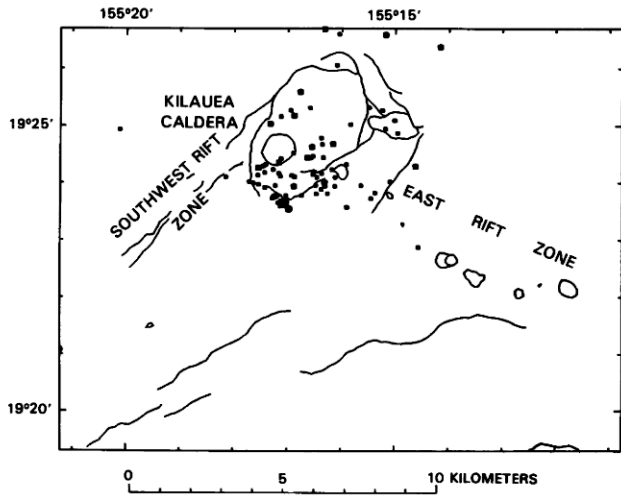


FIGURE 43.48.—Inflationary swarm beginning on June 6, 1971. See figure 43.20 caption for details and figure 43.49B for tilt and hourly earthquake rate.

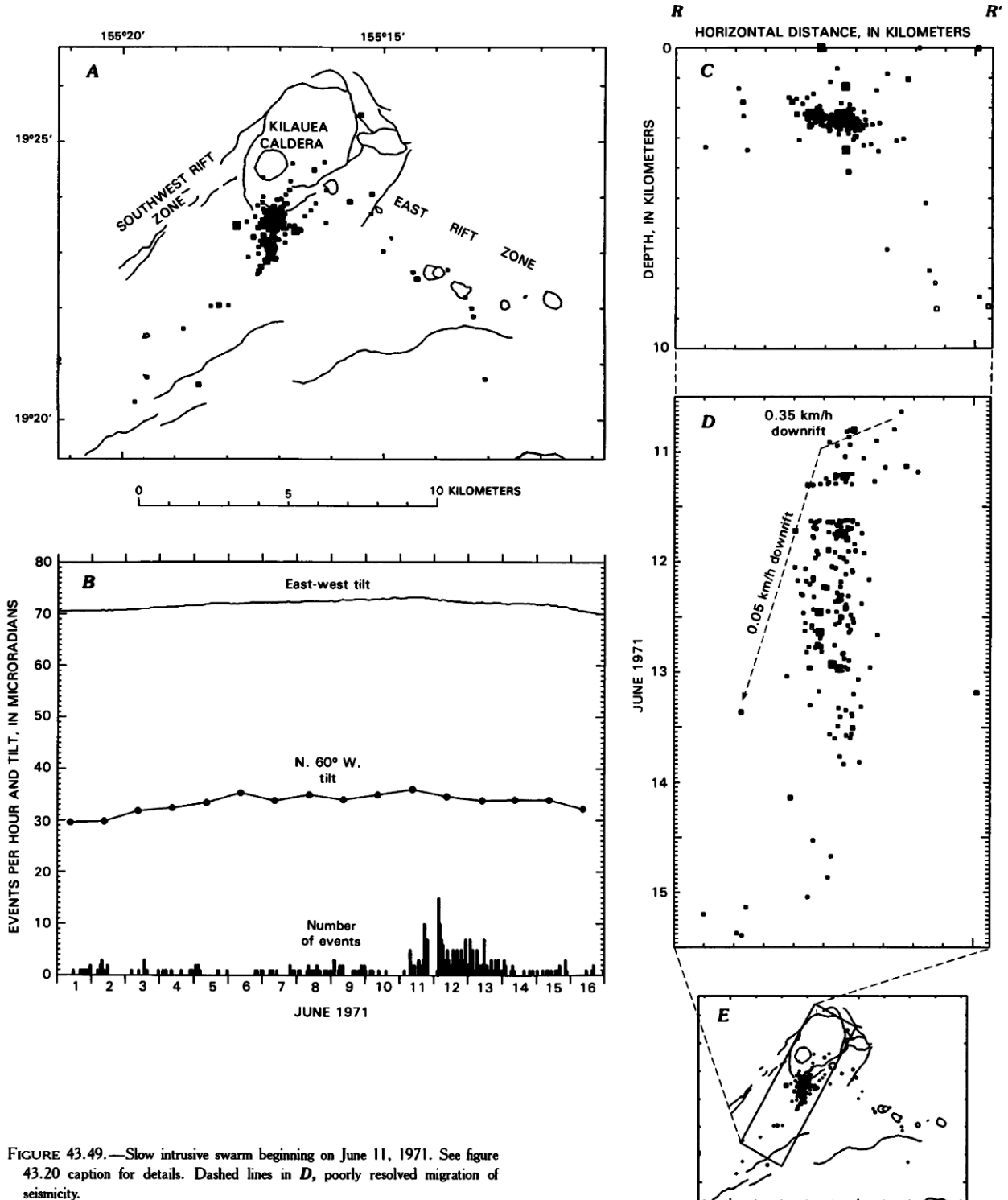


FIGURE 43.49.—Slow intrusive swarm beginning on June 11, 1971. See figure 43.20 caption for details. Dashed lines in *D*, poorly resolved migration of seismicity.

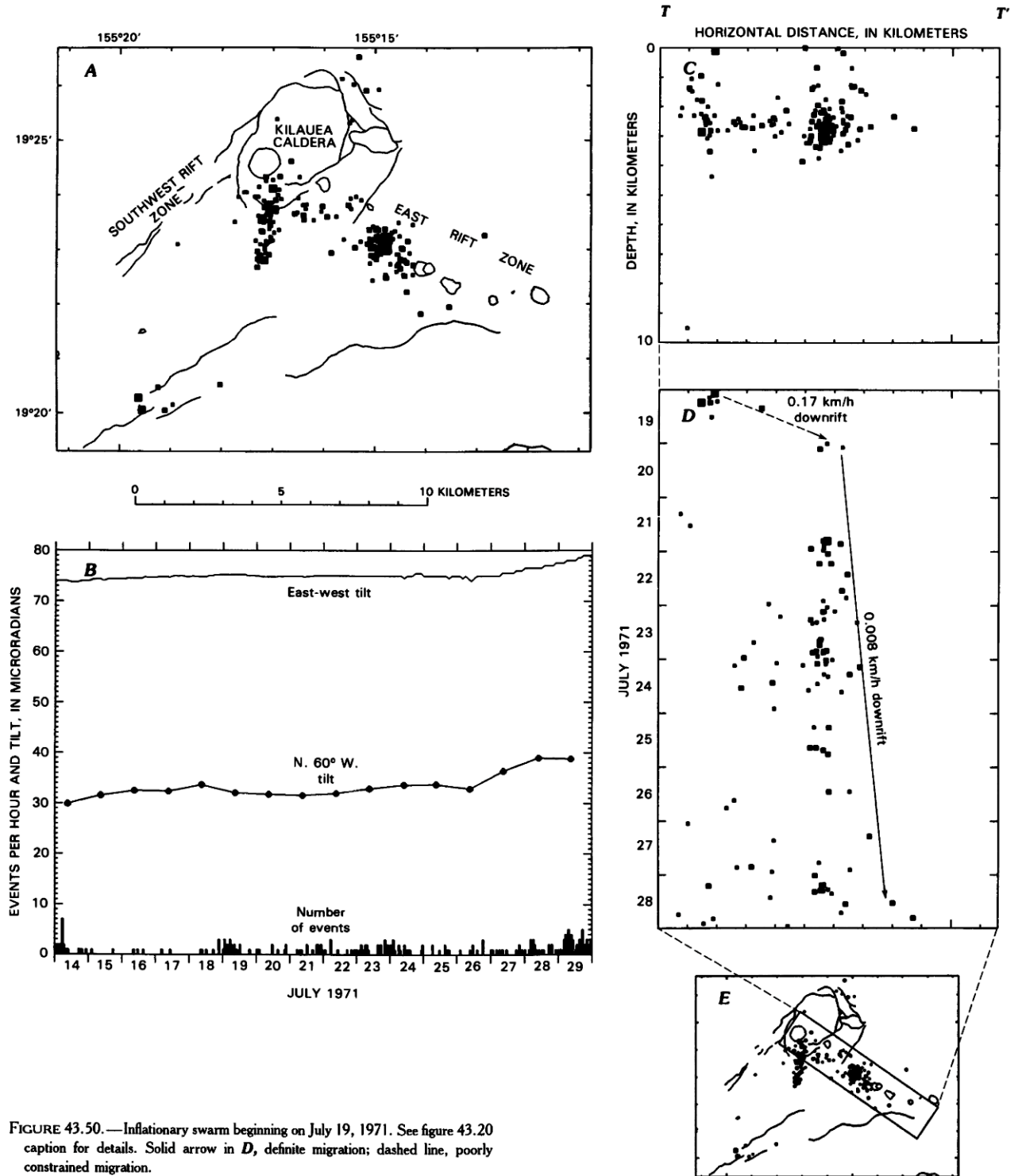


FIGURE 43.50.—Inflationary swarm beginning on July 19, 1971. See figure 43.20 caption for details. Solid arrow in *D*, definite migration; dashed line, poorly constrained migration.

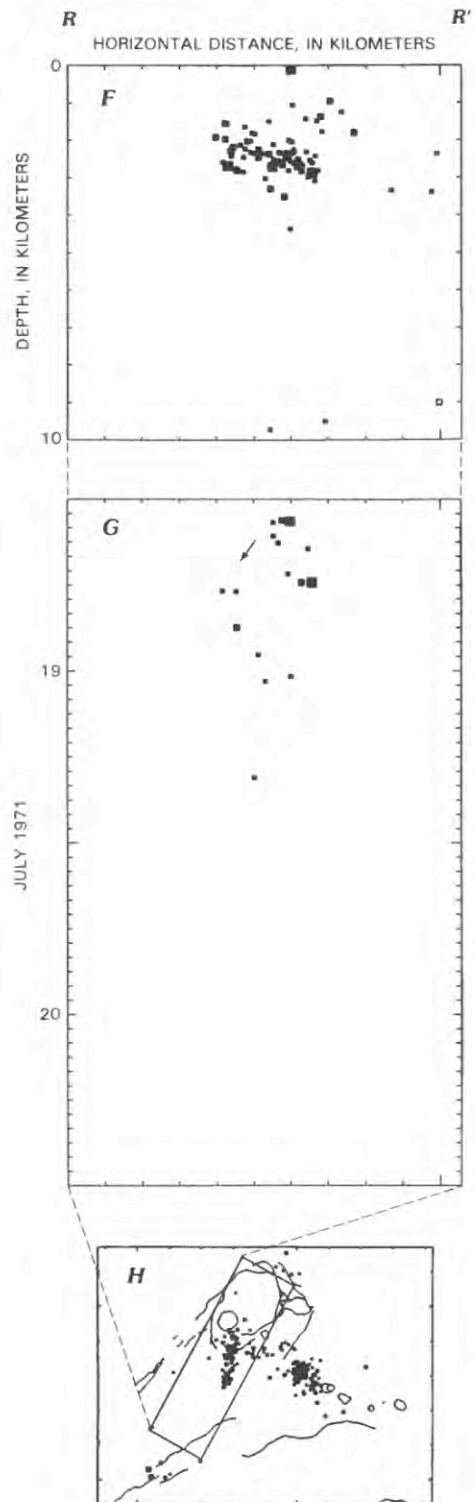


FIGURE 43.50.—Continued.

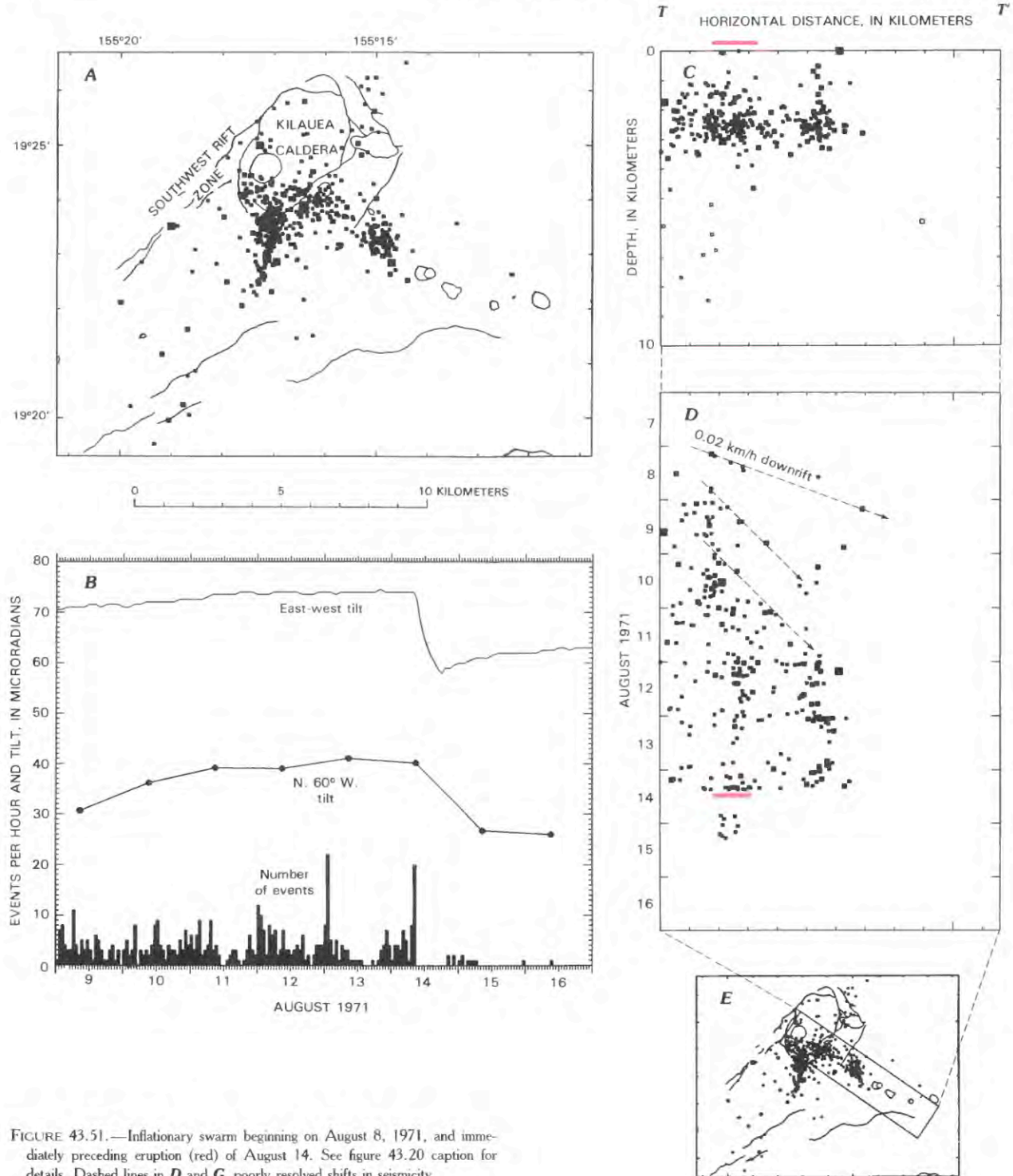


FIGURE 43.51.—Inflationary swarm beginning on August 8, 1971, and immediately preceding eruption (red) of August 14. See figure 43.20 caption for details. Dashed lines in *D* and *G*, poorly resolved shifts in seismicity.

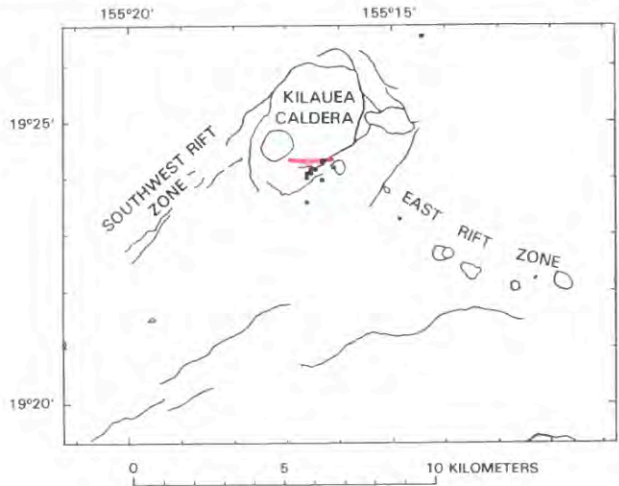
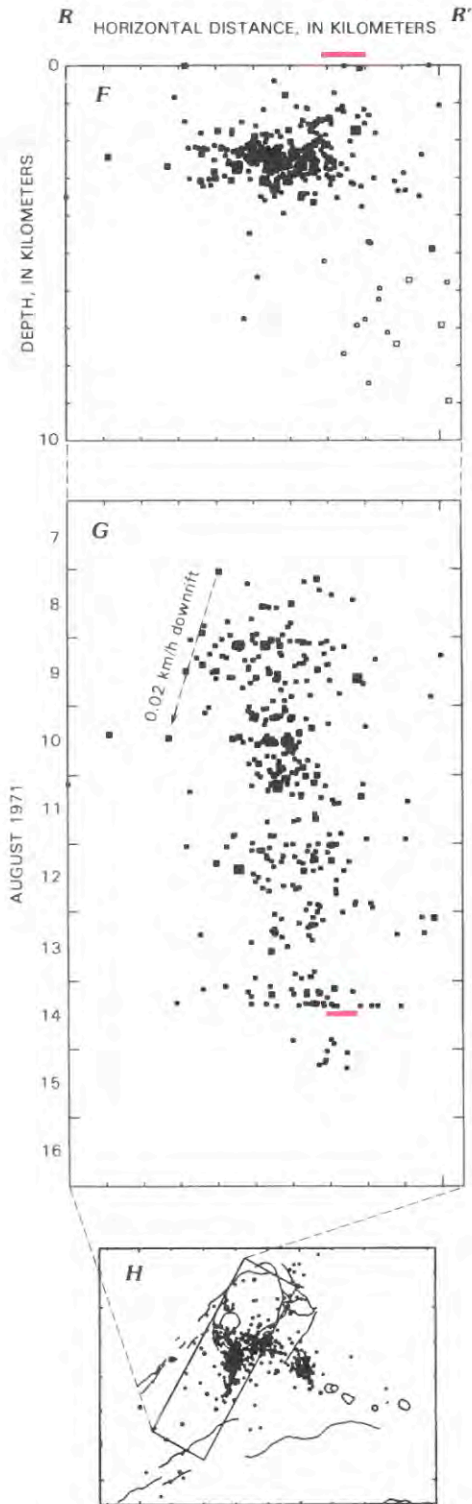


FIGURE 43.52.—Eruptive swarm beginning on August 14, 1971. See figure 43.20 caption for details. Red, location of eruptive vent. See figure 43.51B for tilt and earthquake counts, and figure 43.51D for relation of eruptive swarm to prior seismicity and onset time of eruptive vent (red).

FIGURE 43.51.—Continued.

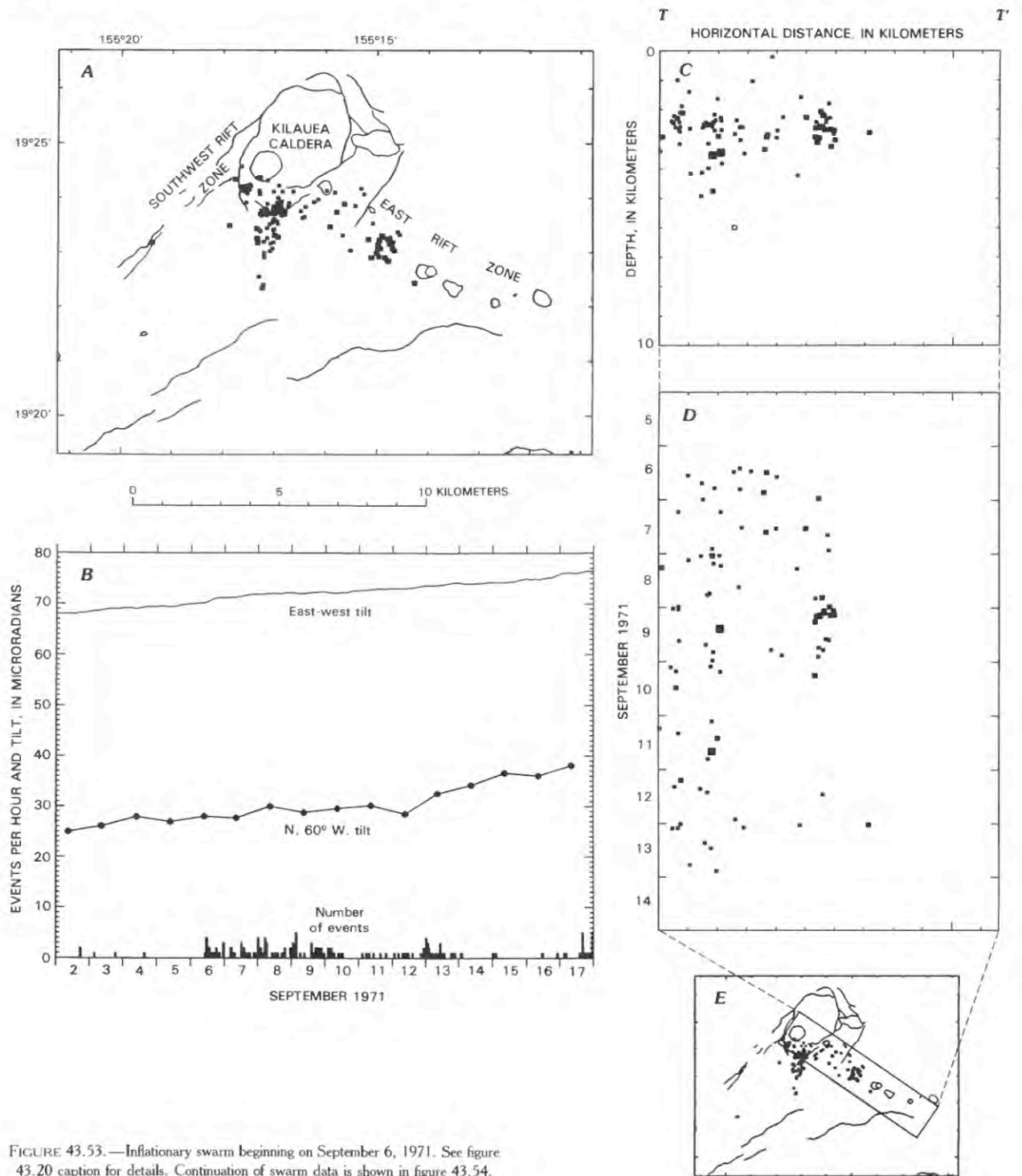


FIGURE 43.53.—Inflationary swarm beginning on September 6, 1971. See figure 43.20 caption for details. Continuation of swarm data is shown in figure 43.54.

#### THE MAY AND JUNE 1973 INTRUSIONS OF THE KOAE FAULT ZONE

More than one year after the resumption of Mauna Ulu volcanism, activity shifted briefly to an eruption at Pauahi on May 5, 1973. The eruption was accompanied by an intense swarm in the adjacent Koae fault zone (fig. 43.59A; Unger and Koyanagi, 1979). The earthquake swarm formed a linear zone extending westward into the Koae from Pauahi (fig. 43.59A), lasted for almost 24 hours, produced many surface cracks and saw rapid deflation of the summit caldera (fig. 43.59B). The shift of eruptive activity from Mauna Ulu to Pauahi was possibly related to the magnitude-6.2 Honouliuli earthquake north of Hilo on April 26, 1973. This earthquake did disturb Kilauea caldera enough to trigger rockfalls and small earthquakes. The May 5, 1973, eruption was immediately preceded by draining of the Mauna Ulu and Alae lava lakes. Therefore, the eruption was likely fed by Mauna Ulu lava or at least diverted its magma supply from under the Pauahi-Mauna Ulu region. The time history of earthquakes supports this inference.

The May 5 swarm began under Mauna Ulu, and seismicity rapidly spread up the ERZ to Hiiaka. The lateral speed of this initial migration was 3.6 km/h (fig. 43.59C), which reduces to an apparent 3.2 km/h when foreshortened by looking from the south-southeast (fig. 43.59D). This initial migration was also from 2–4 km depth below Mauna Ulu to 0–2 km depth below Hiiaka, as seen on the cross sections (fig. 43.59C, F). An upward movement of earthquakes thus took place, as is evident on a depth versus time plot (fig. 43.59I). The initial vertical rate of 3 km/h slowed to 1 km/h within 1.5 km of the surface. These speeds should be regarded as very approximate, because both lateral and vertical migration occurred simultaneously and because they are defined by only a few earthquakes. The observed eruption time requires that vertical migration slowed near the surface, as might be expected for a dike that of 0.36 km/h westward into the Koae for the next 16 hours (fig. 43.59D). Note that earthquakes ceased about 2 km or 6 hours behind their point of inception, so that the point at which earthquakes stopped also migrated into the Koae.

We interpret this swarm as the result of a dike propagating from below Mauna Ulu to Pauahi and then into the Koae fault zone. The dike spread from the active pocket of magma presumably feeding Mauna Ulu. The dike initially found an easy and fast path in the ERZ, probably because of the frequency of intrusions and

consequent high temperatures there. The advance of the dike slowed in the noneruptive Koae, however, perhaps because of more rapid cooling of the dike. Cooling could slow the dike either by increasing magma viscosity or by chilling dike margins and constricting flow to a narrower space. The constant speed of advance and continuous earthquake migration without halting or jerky movement are suggestive of viscous flow under relatively uniform stress conditions.

The initial activity at the eruptive vents migrated from east to west at about the same 0.3 km/h speed as the earthquakes (fig. 43.59D). As noted with other intrusions, vents opened about 3–6 hours after the initial seismic front passed their location. At a particular vent, the time of eruption coincides with the cessation of earthquakes. Thus the earthquakes are not simply being masked by tremor, because events continued to the west. The start of eruption thus relieves some of the stress that caused the earthquakes, probably at the time the dike reaches its maximum width. We then associate the seismicity with the time and place where the dike is growing in width and under increasing pressure, and the moving point at which earthquakes cease is where the dike has reached its maximum width and magma flow is stable.

With the association of earthquakes and dike growth in mind, a very low confining stress in the Koae explains two observations: (1) the dike widens easily, accommodating all the magma it is given without building enough hydrostatic head to reach the surface and erupt, and (2) the dike encounters little resistance from compressive stress normal to itself, and once opened to a width permitting stable and sustained flow, the dike exerts little stress on its walls so that earthquakes cease. The migration speed and width of the earthquake zone during Koae intrusions would then be determined by the mechanical and thermal properties of magma in a cold, dry crack under relatively little stress.

About one month after the May 5 eruption, a second Koae intrusion occurred (fig. 43.60). The June 9, 1973 intrusion was parallel to and about 1 km north of the prior intrusion, but was only about 3 km long (fig. 43.60A). It was also smaller than the May event in the sense of a shorter swarm and smaller deflation (fig. 43.60B). This intrusion apparently did not involve Mauna Ulu directly, because it began from a point just uprift of Hiiaka on the ERZ. The migration speed was about 1 km/h (fig. 43.58D), three times faster than in May. The pairing of these two Koae intrusions is probably not coincidental, and they probably interacted in some way.

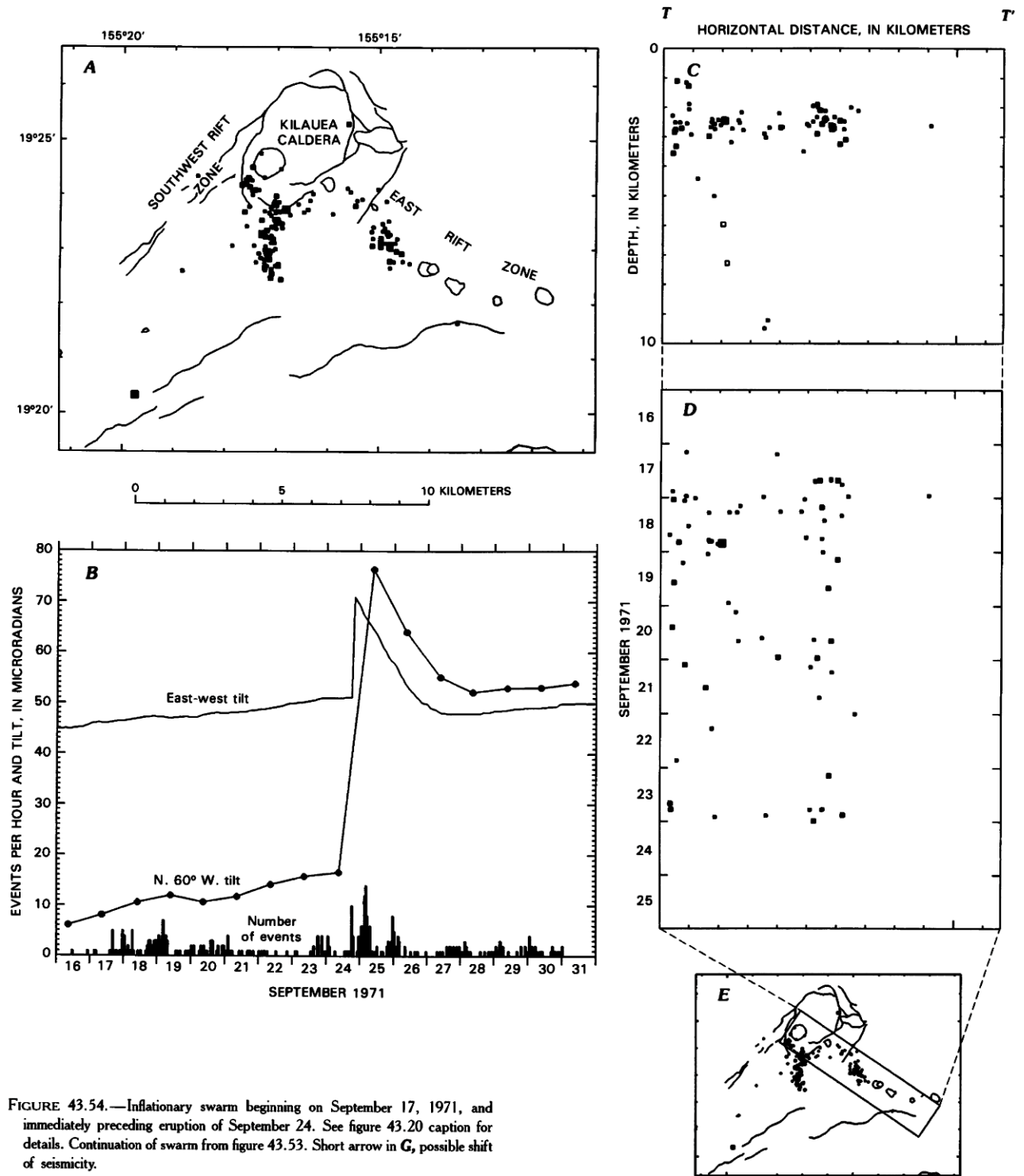


FIGURE 43.54.—Inflationary swarm beginning on September 17, 1971, and immediately preceding eruption of September 24. See figure 43.20 caption for details. Continuation of swarm from figure 43.53. Short arrow in G, possible shift of seismicity.

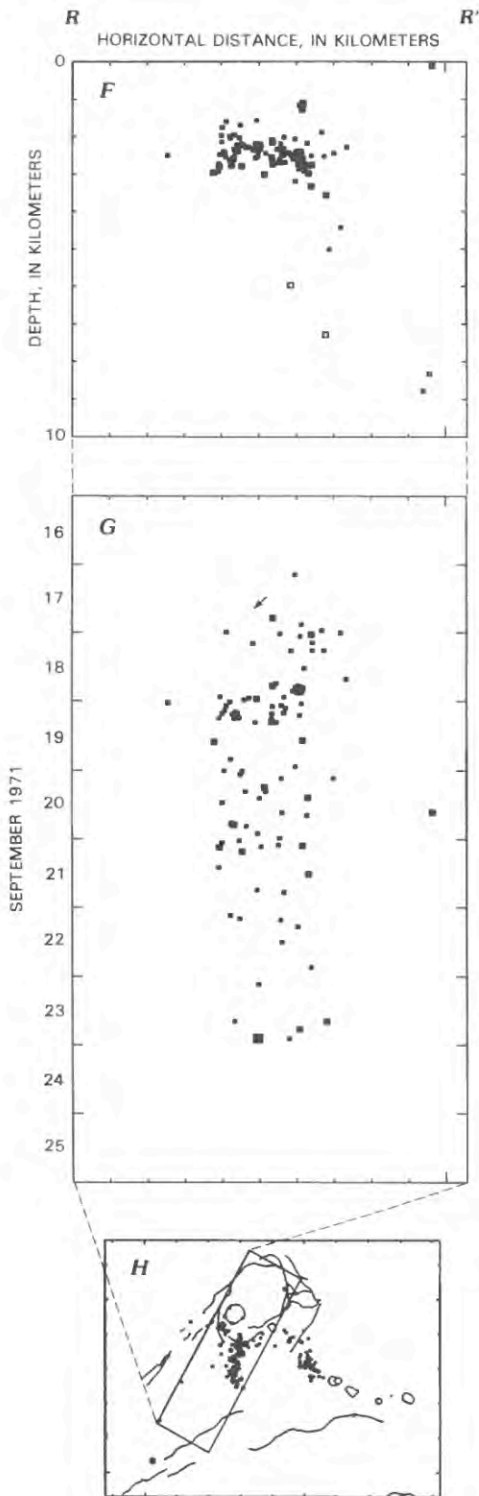


FIGURE 43.54.—Continued.

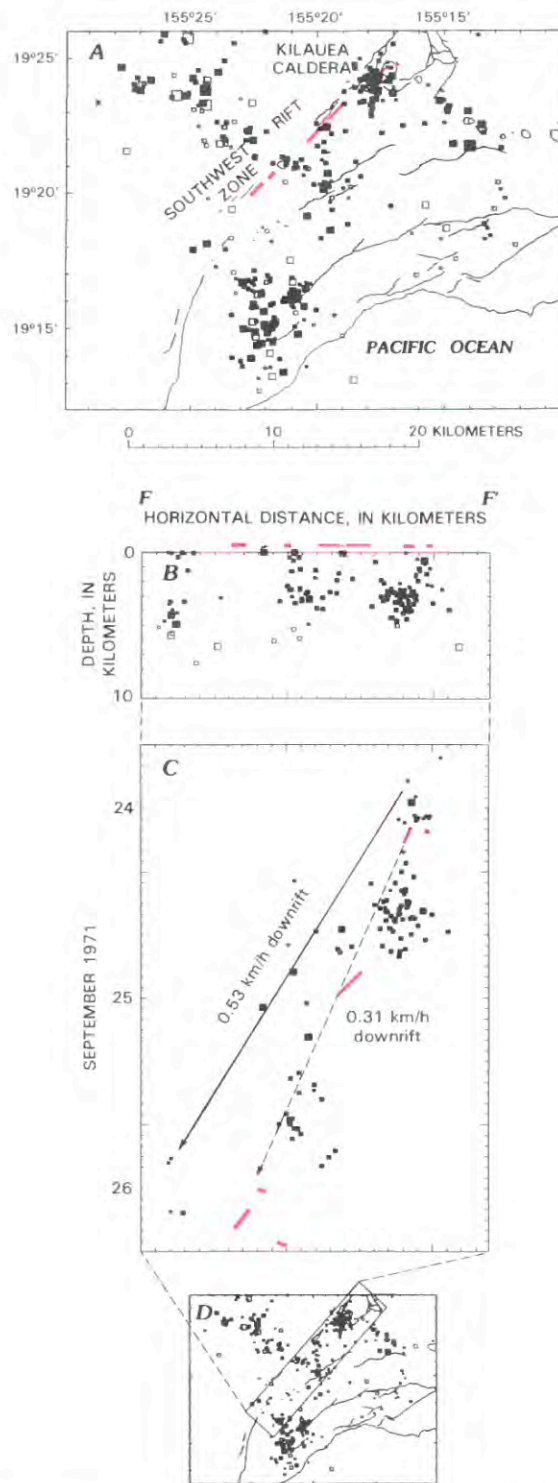


FIGURE 43.55.—Eruptive swarm beginning on September 24, 1971. See figure 43.20 caption for details and figure 43.54 for tilt and earthquake rate. Red, approximate location (A, B) and onset time (C) of eruptive vents; solid arrow in C, definite migration; dashed arrow, poorly resolved migration of seismicity.

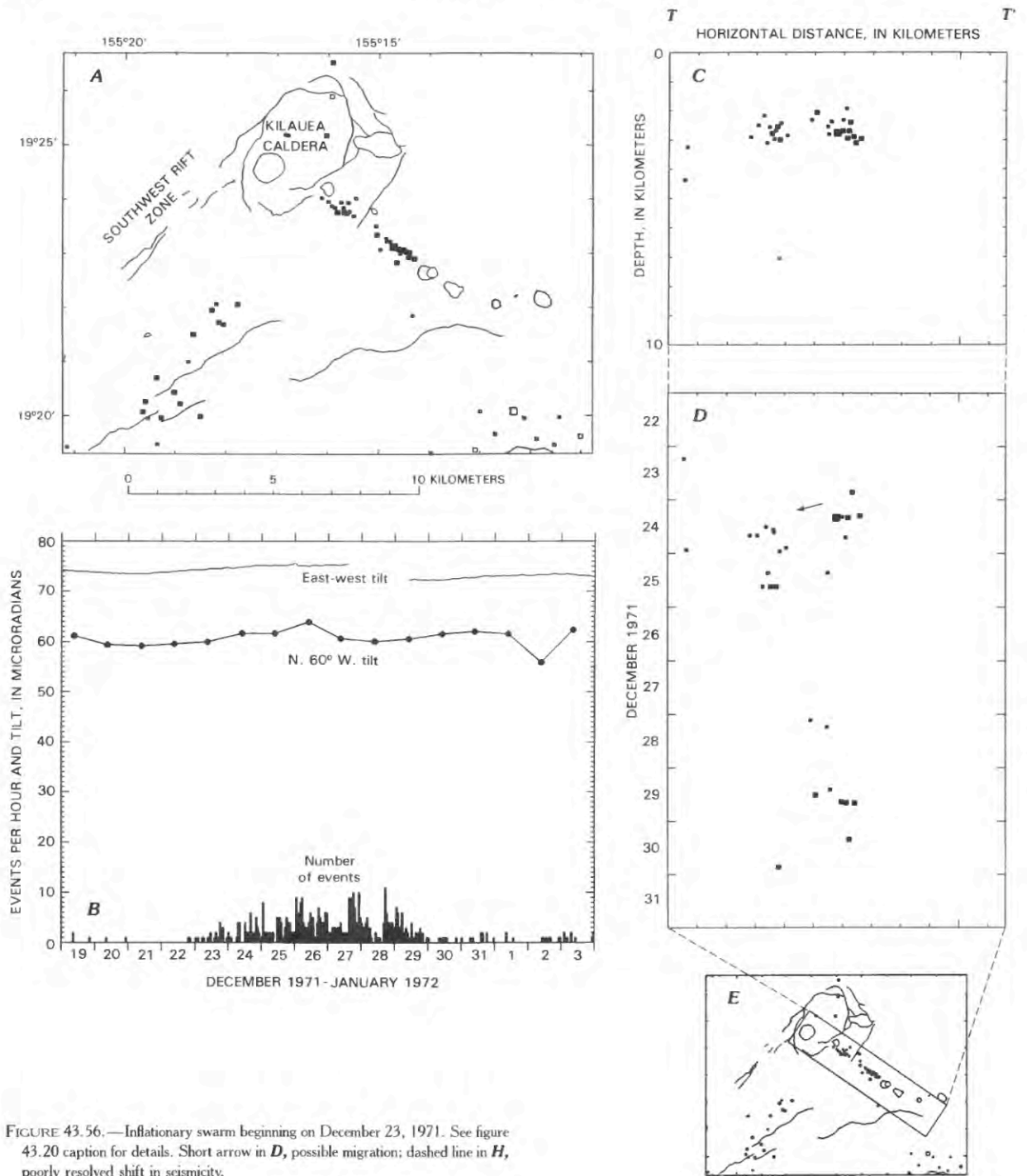


FIGURE 43.56.—Inflationary swarm beginning on December 23, 1971. See figure 43.20 caption for details. Short arrow in *D*, possible migration; dashed line in *H*, poorly resolved shift in seismicity.

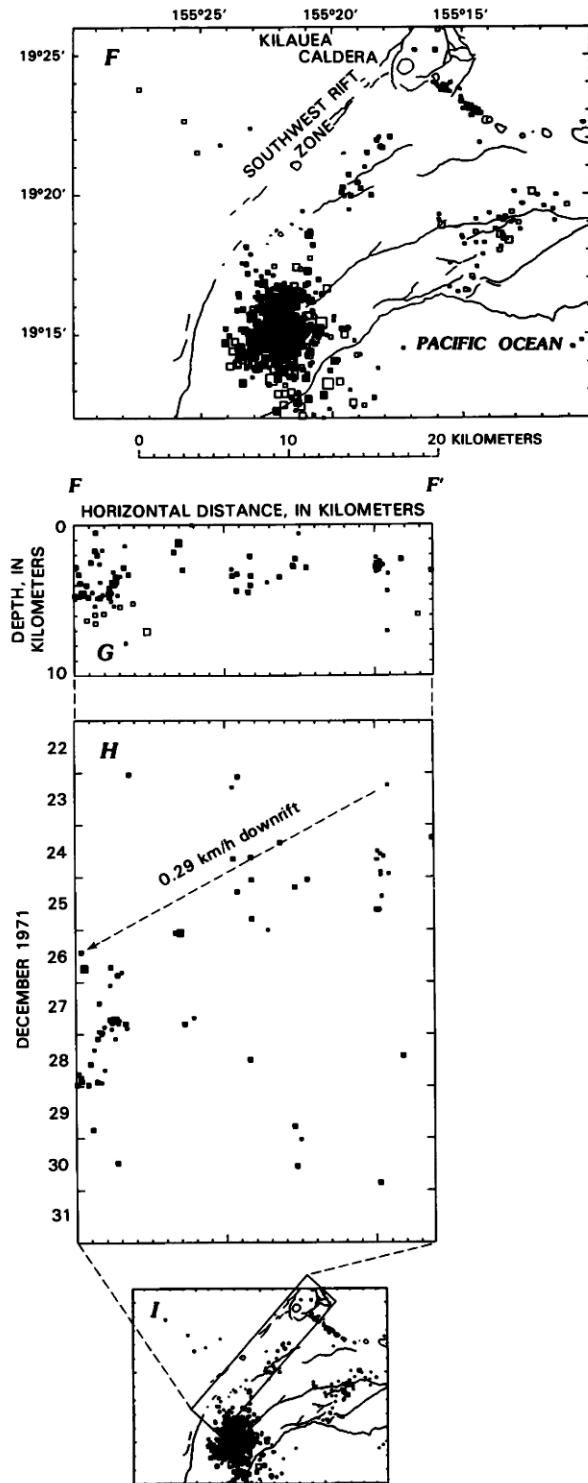


FIGURE 43.56.—Continued.

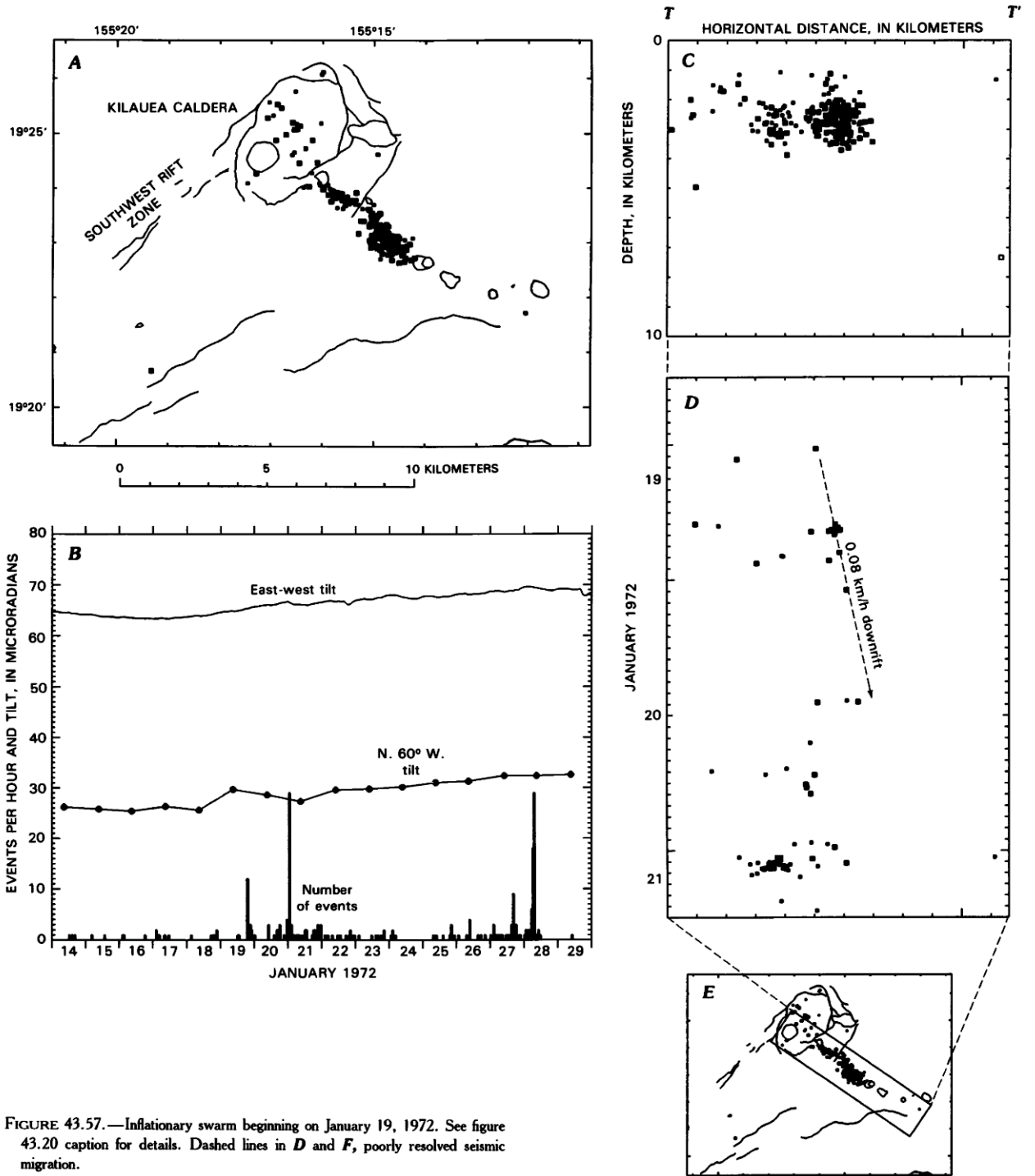


FIGURE 43.57.—Inflationary swarm beginning on January 19, 1972. See figure 43.20 caption for details. Dashed lines in *D* and *F*, poorly resolved seismic migration.

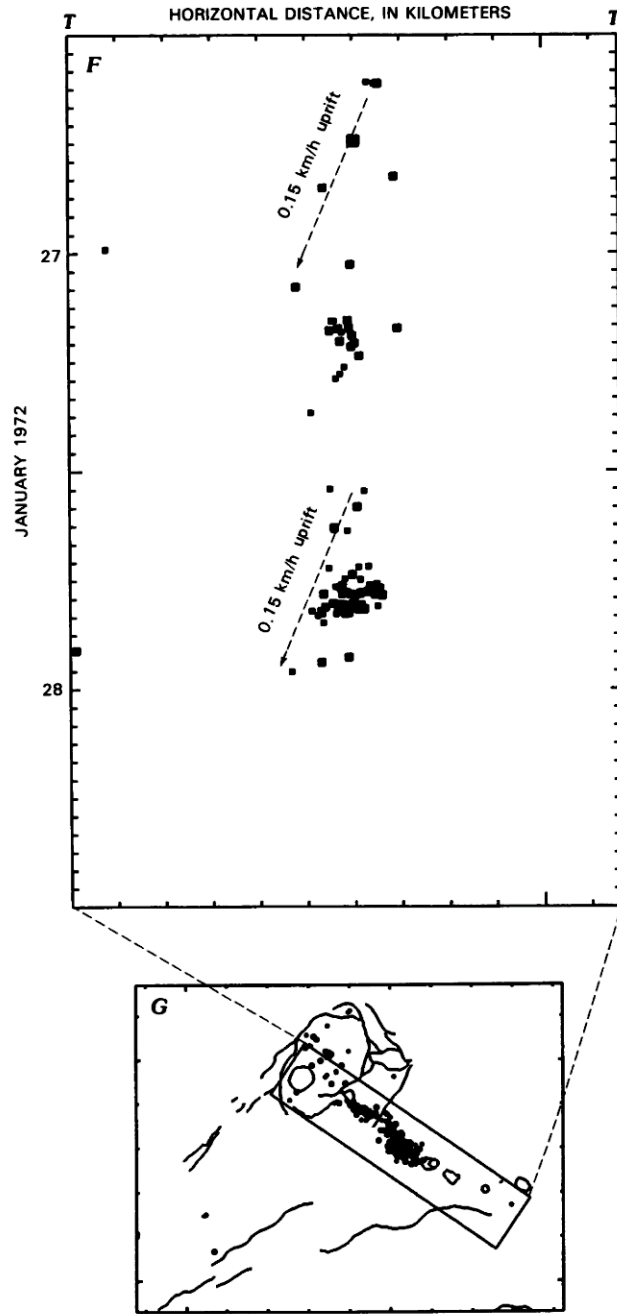


FIGURE 43.57.—Continued.

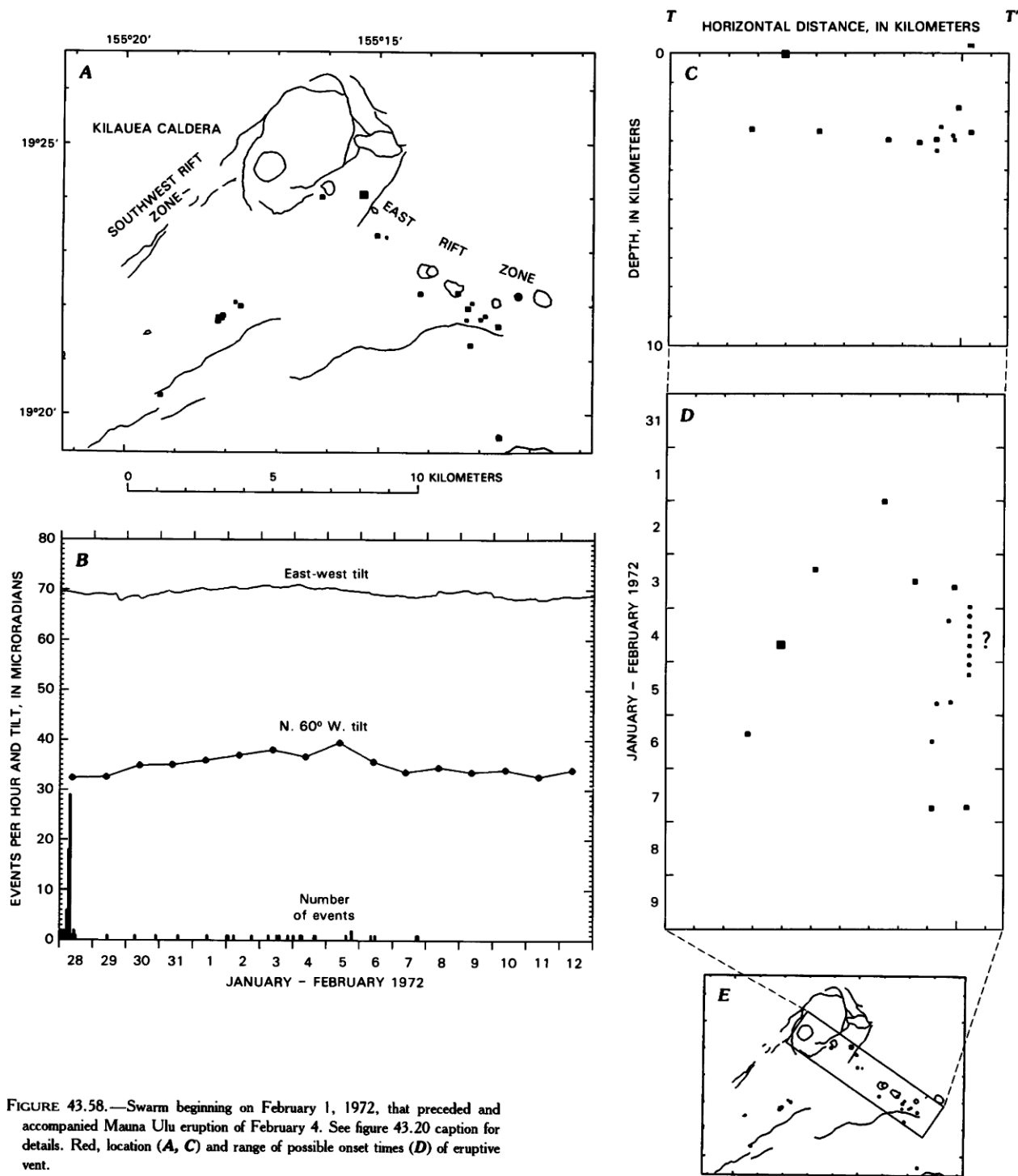


FIGURE 43.58.—Swarm beginning on February 1, 1972, that preceded and accompanied Mauna Ulu eruption of February 4. See figure 43.20 caption for details. Red, location (A, C) and range of possible onset times (D) of eruptive vent.

## ERUPTIONS AND INTRUSIONS, NOVEMBER 1973 THROUGH SEPTEMBER 1974

The next three swarms took place in the ERZ within 8 km of the caldera. The swarm of November 10–11, 1973, preceded and accompanied an eruption near Pauahi. In addition to the main seismic zone parallel to the rift, a few small events extended to the northeast beneath the eruptive vents (fig. 43.61A). The absence of earthquakes in the middle of the swarm (fig. 43.61B, D) is a result of masking of earthquakes by intense tremor. Uprift earthquake migration is suggested, and fountaining spread both east and west along the vent (fig. 43.61D). A definite shallowing of earthquakes, however, preceded the eruption (fig. 43.61F). The apparent vertical speed was about 1.6 km/h interrupted by a break of about 3 hours, but this pattern is based only on a few earthquakes. Figure 43.61E also shows that the depths of events after the start of the eruption averaged about 2 km shallower than those before.

An earthquake swarm lasting less than three hours occurred on March 24 in the Pauahi-Mauna Ulu section of the ERZ (fig. 43.62A). This section is a common place for earthquake swarms to begin, as did 3 of the 4 previous swarms. Three microradians of summit deflation accompanied the swarm, as seen on the Uwekahuna tiltmeter (fig. 43.62B). The event was accompanied by harmonic tremor and a short-lived increase of lava and gas production in the ongoing Mauna Ulu eruptive activity. We therefore interpret this event as a minor intrusion in which some sort of localized magma adjustment occurred, thus feeding the Mauna Ulu system. The episode caused a small volume of magma to drain from the summit complex through the aseismic section of rift above Pauahi.

The earthquake swarm immediately preceding the July 19, 1974 eruption was very intense and lasted only 9 hours (fig. 43.63B). It was in the same Keanakakoi-Kokoolau region active during the preceding 3 months of inflationary seismicity. The summit deflated about 3 microradians, after which tilt nearly leveled off. A larger and more rapid summit deflation followed at 1030 H.s.t., high amplitude tremor began, and the number of earthquakes that could be timed and located sharply diminished. Magma reached the surface about 2 hours later.

The seismic zone is slightly elongate and extends from about 3.5 km beneath Kokoolau to within 1 km or less of the surface near Puhimau (fig. 43.63C). The active zone thus plunges steeply to the southeast. The absence of events between 0 and 1 km depth may result from the poor depth control of the very shallowest earthquakes

or from the fact that the low-rigidity and low-stress surface layer may be too weak to generate earthquakes of locatable magnitude.

Earthquakes migrated uprift at a well-determined rate of about 0.16 km/h (fig. 43.63D). Earthquakes also moved upward at roughly 0.55 km/h (fig. 43.63F), which slowed to about 0.18 km/h within 1 km of the surface, assuming the dike moved at constant speed to the surface. A slowing near the surface is typical of most dikes for which upward movement can be seen. The observed migration patterns and vent location are explained by a plunging zone growing first at about 0.6 km/h then 0.24 km/h. This event was apparently a forceful intrusion of a dike leading from the ERZ conduit below Kokoolau up to the surface. The intense seismicity and tilt rate patterns show that rock was initially breaking under high magma pressure and relatively low volume flow. When the dike reached the surface, pressure and seismicity decreased, and flow volume, tremor and tilt rate increased.

The caldera eruption of September 19, 1974, was seismically unlike the others during the year and did not generate an intense earthquake swarm. It was instead preceded by three days of slightly elevated seismicity just south of the caldera under the SWRZ (fig. 43.64A) and a slowly inflating caldera (fig. 43.64B). The activity of September 16–19 is not distinguishable from other inflationary seismicity during the rest of 1974, although the probability of an eruption is measurably higher when such summit seismicity increases (Klein, 1984).

The pre-eruption earthquakes may have accompanied a slow and low-volume intrusion into the SWRZ. Although the swarm was a weak one, there is a hint of a downrift earthquake migration (fig. 43.64D). The absence of an intense swarm indicates that magma came to the surface without having to create a new dike in a high stress environment. When the eruption began, earthquakes abruptly ceased. This relation is expected if magma pressure induces the earthquakes and suddenly drops when flow and pressure are redirected to an active vent.

A pattern of increasing seismicity in the SWRZ during 1974 suggests that the rift participated in Kilauea's continuing inflation and slowly received magma. The seismic and tilt changes can be seen in figure 43.65, which plots earthquake positions and tilt from May 1974 through February 1975. In May and June most earthquakes were confined to the inflating summit area, but the July–December period saw increasing seismicity as far downrift as Mauna Iki. The rapid inflation of September through December produced the highest tilt values yet recorded. Kilauea appeared to be preparing for a SWRZ event, which came in December and dramatically shifted the active area from the upper to the lower SWRZ.

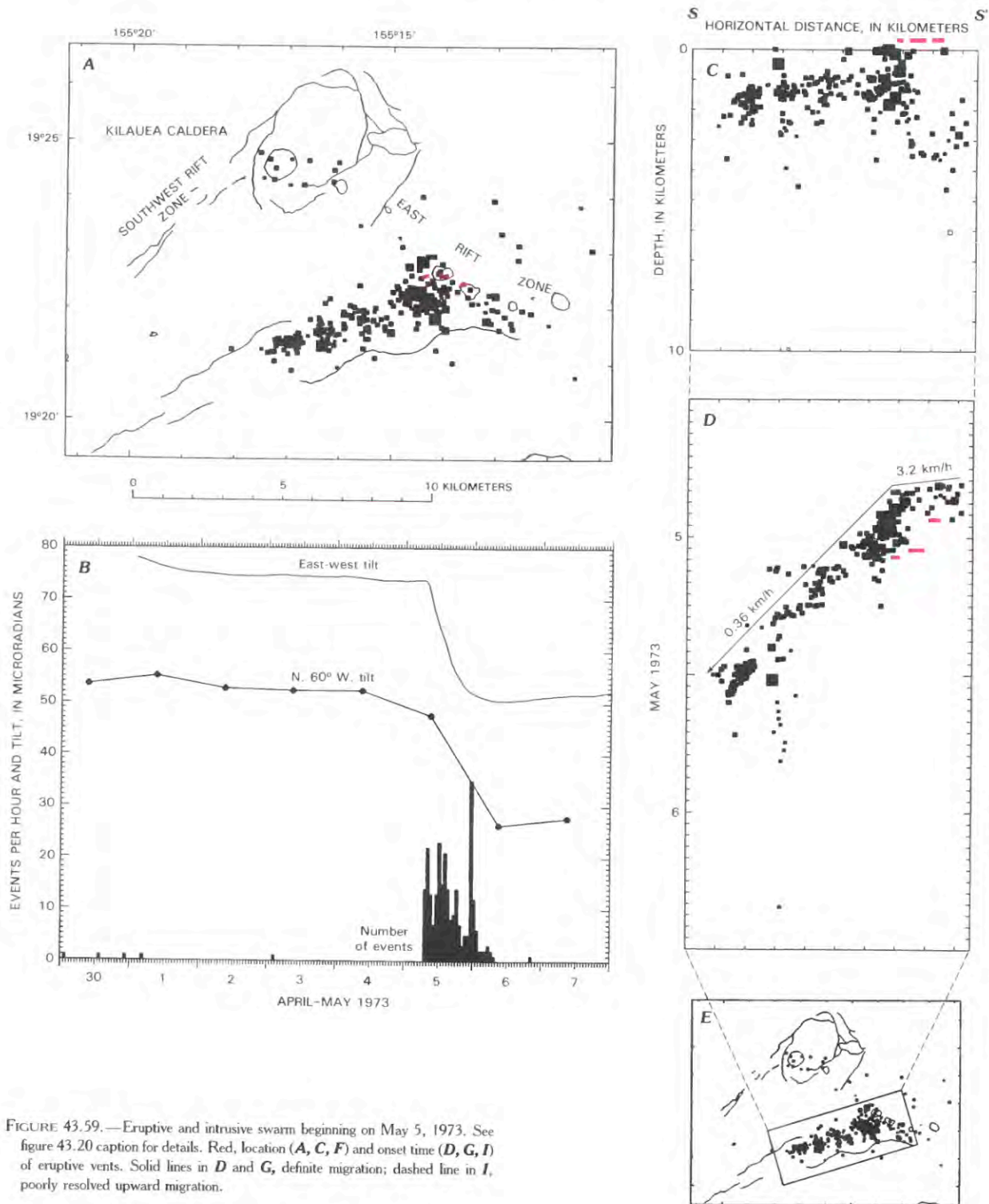


FIGURE 43.59.—Eruptive and intrusive swarm beginning on May 5, 1973. See figure 43.20 caption for details. Red, location (*A, C, F*) and onset time (*D, G, I*) of eruptive vents. Solid lines in *D* and *G*, definite migration; dashed line in *I*, poorly resolved upward migration.

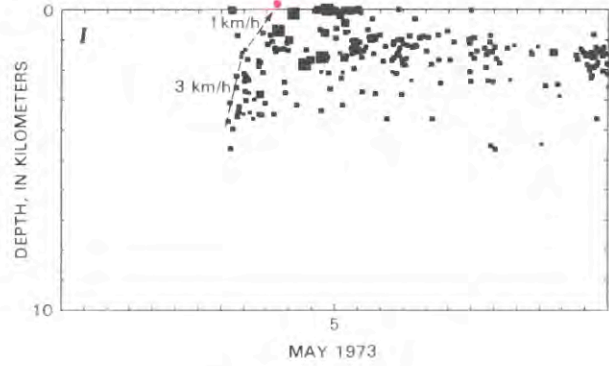
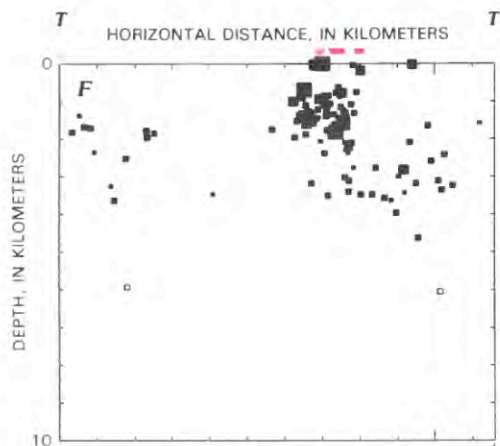


FIGURE 43.59.—Continued.

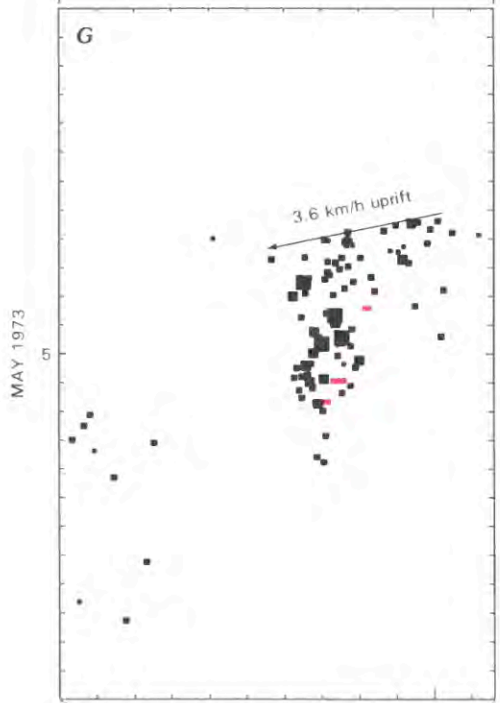


FIGURE 43.59.—Continued.

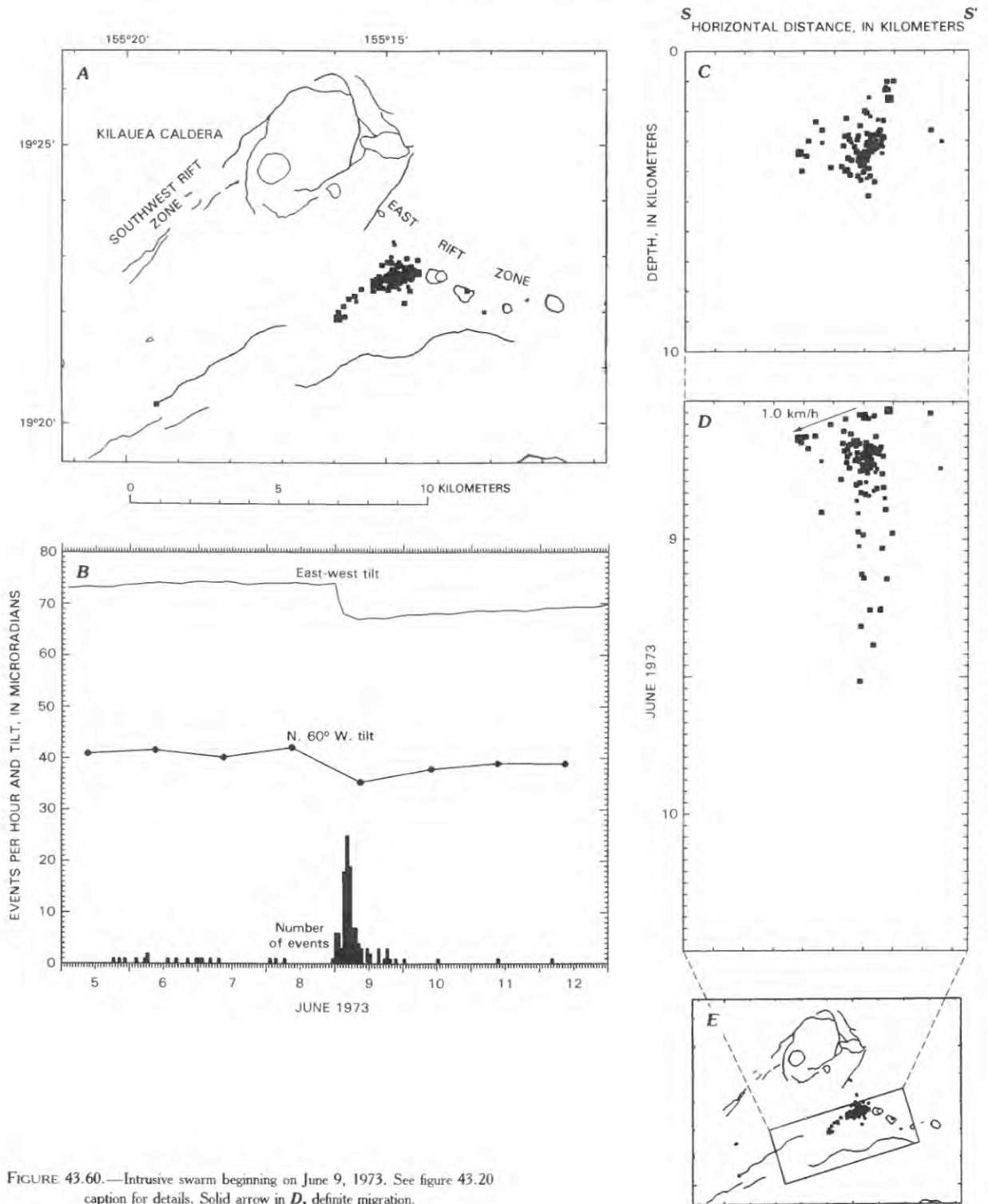


FIGURE 43.60.—Intrusive swarm beginning on June 9, 1973. See figure 43.20 caption for details. Solid arrow in *D*, definite migration.

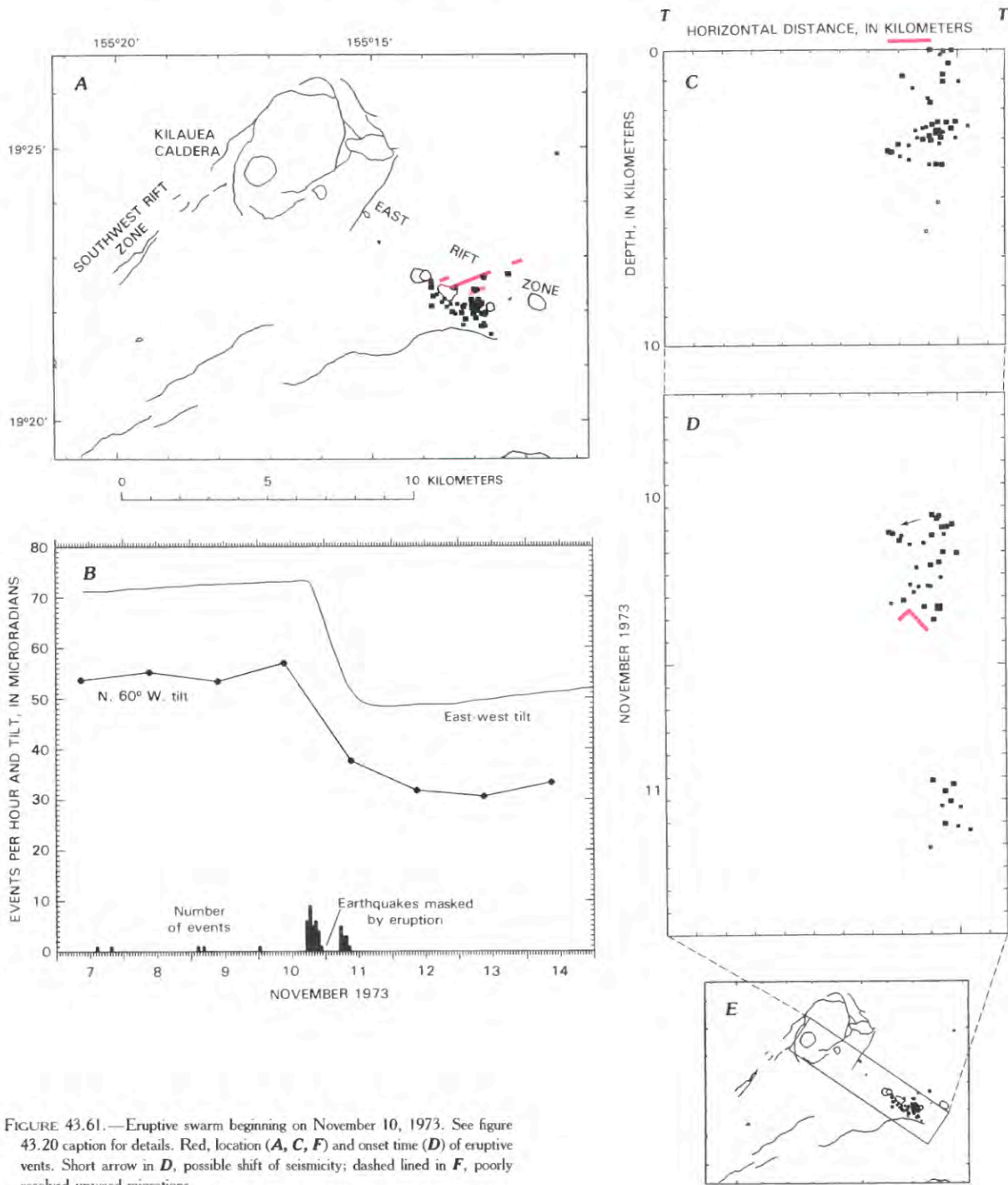


FIGURE 43.61.—Eruptive swarm beginning on November 10, 1973. See figure 43.20 caption for details. Red, location (**A**, **C**, **F**) and onset time (**D**) of eruptive vents. Short arrow in **D**, possible shift of seismicity; dashed line in **F**, poorly resolved upward migrations.

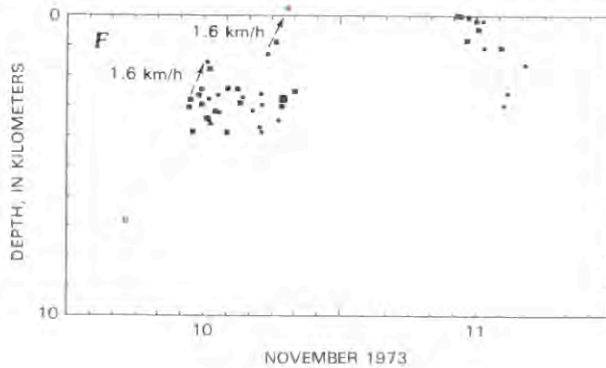


FIGURE 43.61.—Continued.

#### THE DECEMBER 1974 SOUTHWEST RIFT ZONE ERUPTION

Summit seismicity in the parts of both rift zones adjacent to the caldera intensified during the week prior to the December 31 eruption (fig. 43.66). Beginning on December 24, this heightened activity apparently migrated very slowly into both rifts at roughly one kilometer per day (fig. 43.66D, G). These slow intrusions of magma into both rifts simultaneously were another indication of abundant supply in the summit reservoir.

Seismic patterns divide the eruption into two different phases: an intense but short swarm just south of the caldera related to the dike that fed the eruption, and a subsequent intrusion into an additional 18 km of the SWRZ.

The small cluster of earthquakes about 3 km south of Halemaumau occurred beneath the eruptive vent (fig. 43.67A). Earthquakes began in the middle of this cloud around 1600 H.s.t. on December 30 (fig. 43.67D), and were about 2.5 km deep. The seismic zone slowly grew in size until 0100 H.s.t. on December 31, when it was about 2 km in diameter and the swarm reached maximum intensity. The events then ranged between 1 and 4 km depth. Earthquakes migrated upward at about 5 km/h during this intense period, but the dike grew aseismically upward at about 0.3 km/h during the last 3 hours of its journey to the surface (fig. 43.67K). Earthquakes then diminished and tremor intensity grew prior to lava breakout shortly before 0300 H.s.t. As in July, an intense swarm accompanied the lateral and vertical growth of the dike that fed the eruption.

About the time this first swarm reached maximum intensity, additional earthquakes began migrating downrift. The seismically active dike grew about 1.3 km/h for about 14 km, then slowed to one-half that speed as it grew an additional 4 km (fig. 43.67G). Earthquakes not only occurred near the shallow rift conduit at 3 km depth, but also well southeast of the rift near the terminus of the new dike (fig. 43.67B). The events within Kilauea's mobile south flank are typical of those induced by other large SWRZ intrusions and large tectonic earthquakes. The effects of the intrusion (though probably not magma itself) thus reached at least 10 km from the rift axis.

Compressional stress generated by the new dike acting on a weak zone already close to seismic failure apparently caused the south flank earthquakes, including one of magnitude 5.5. Both rift and flank seismicity lasted for several days after the eruption and deflation ceased (figs. 43.66B, 43.67I). Thus either magma continued draining down the rift after its source at the summit was cut off, or the whole system displays a relaxation time of several days, or both. The seismic response of the section of rift adjacent to the caldera was rapid, and earthquakes diminished when the dike reached the surface and the pressure dropped. The lower rift, however, accommodates magma pressure by seismic slip and deformation in the mobile south flank, a process that takes several days because of its mechanical lag time (Dvorak and others, 1985).

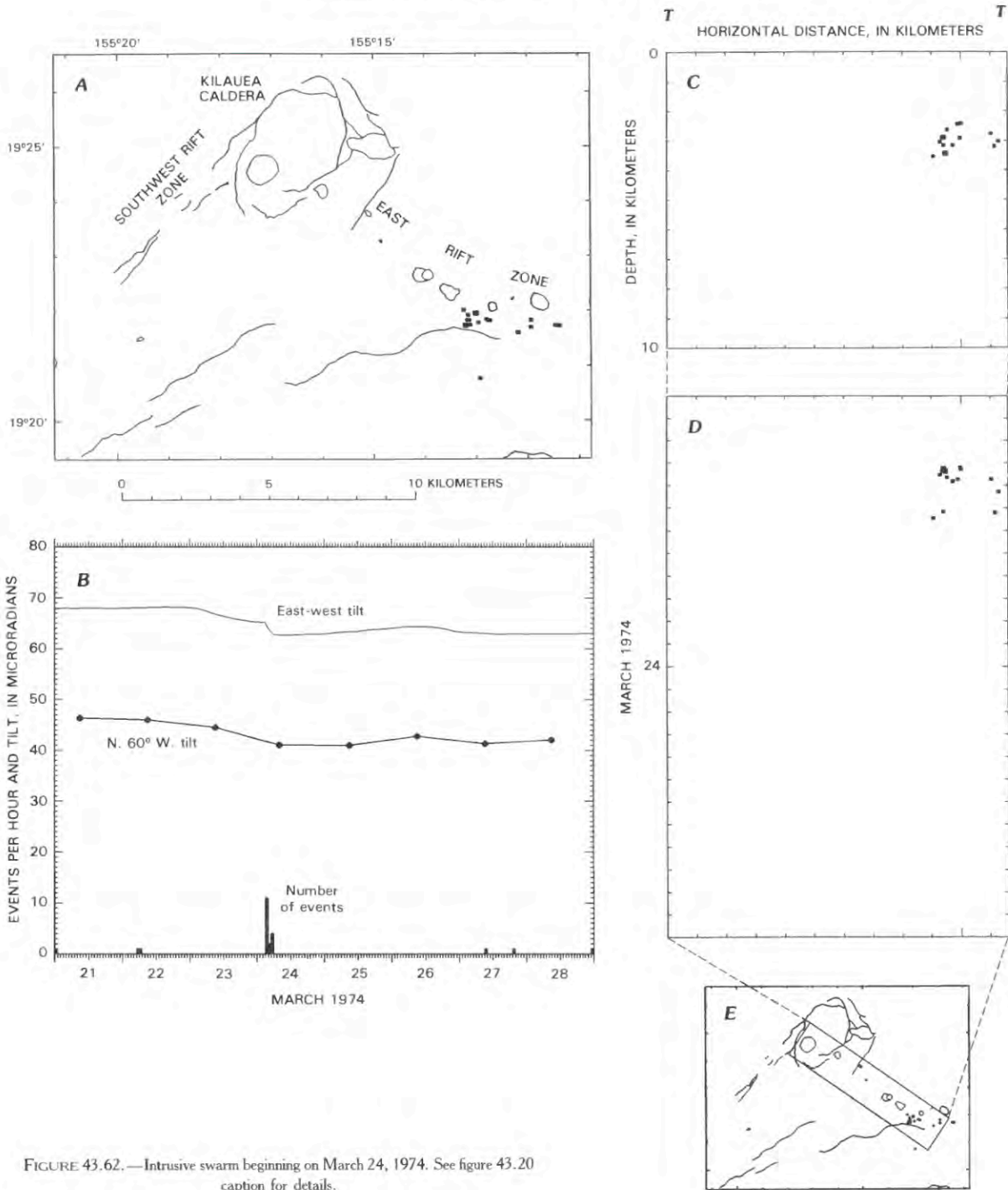


FIGURE 43.62.—Intrusive swarm beginning on March 24, 1974. See figure 43.20 caption for details.

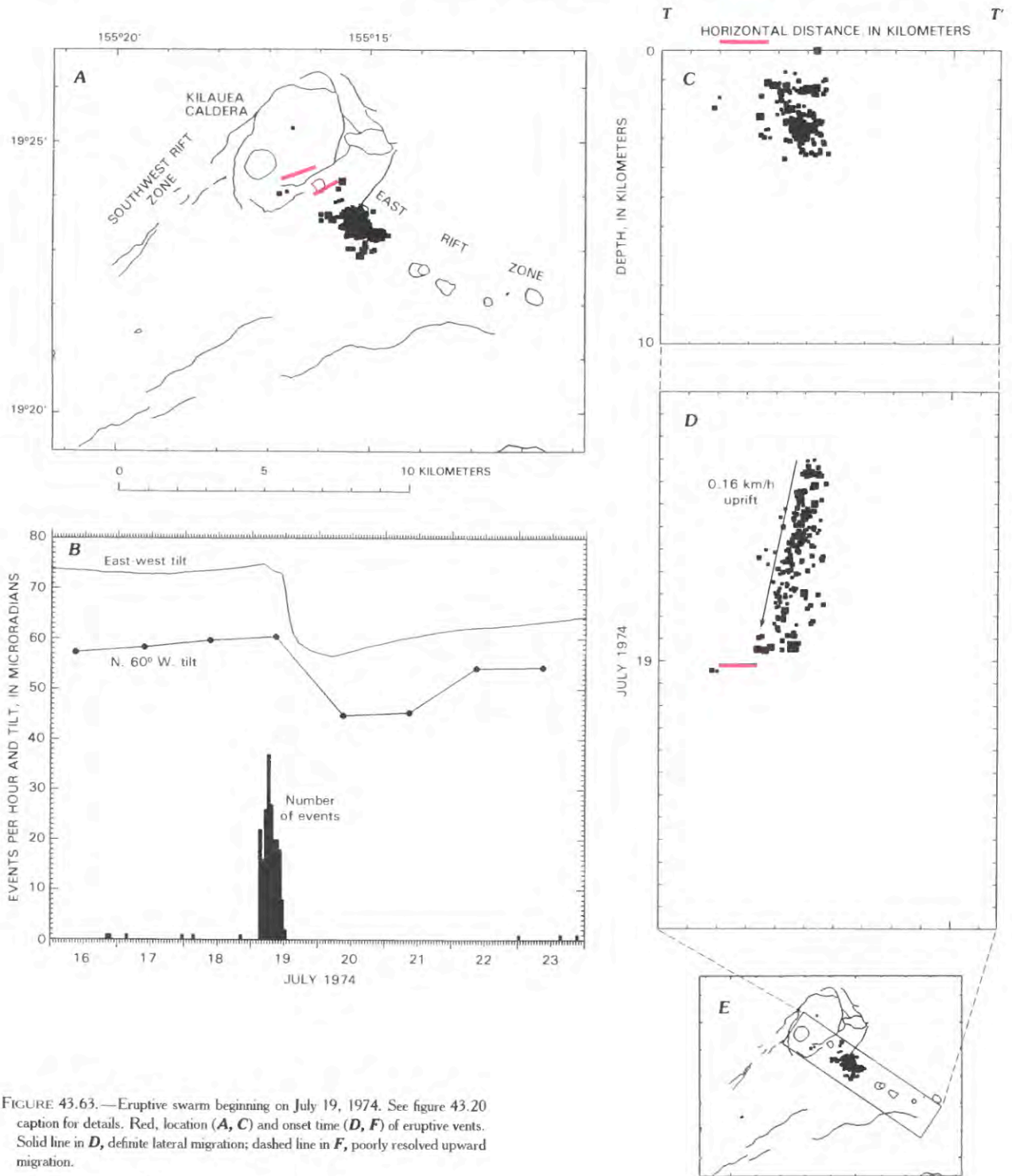


FIGURE 43.63.—Eruptive swarm beginning on July 19, 1974. See figure 43.20 caption for details. Red, location (**A**, **C**) and onset time (**D**, **F**) of eruptive vents. Solid line in **D**, definite lateral migration; dashed line in **F**, poorly resolved upward migration.

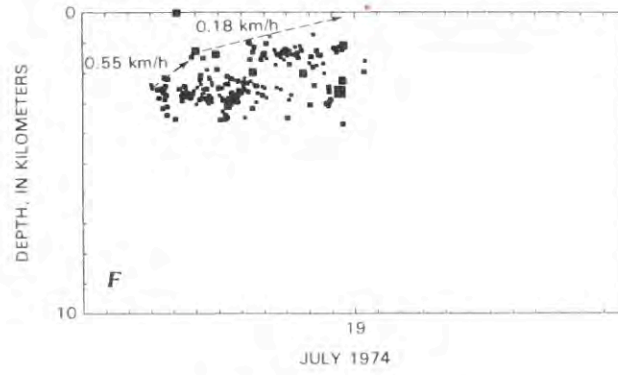


FIGURE 43.63.—Continued.

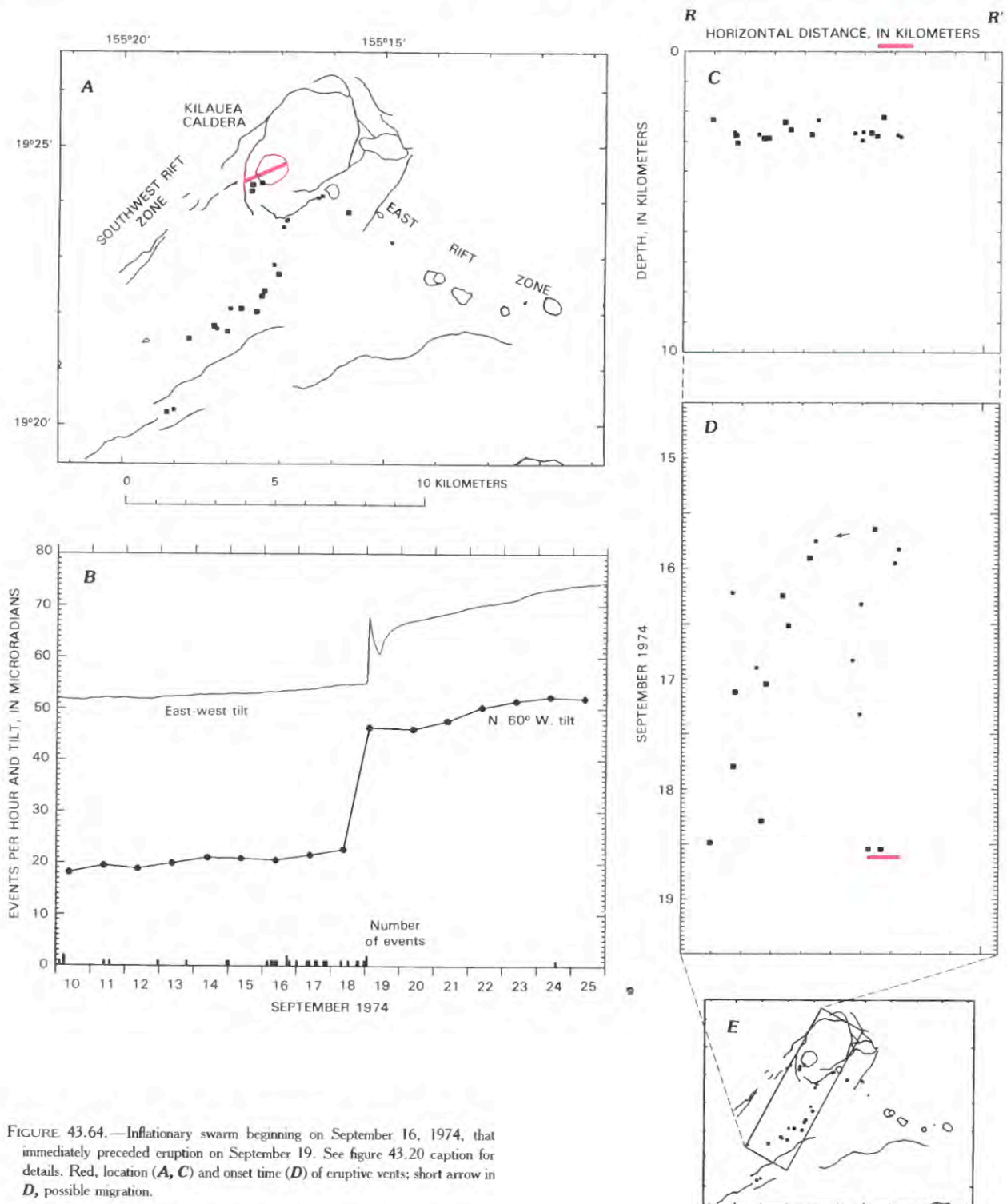


FIGURE 43.64.—Inflationary swarm beginning on September 16, 1974, that immediately preceded eruption on September 19. See figure 43.20 caption for details. Red, location (A, C) and onset time (D) of eruptive vents; short arrow in D, possible migration.

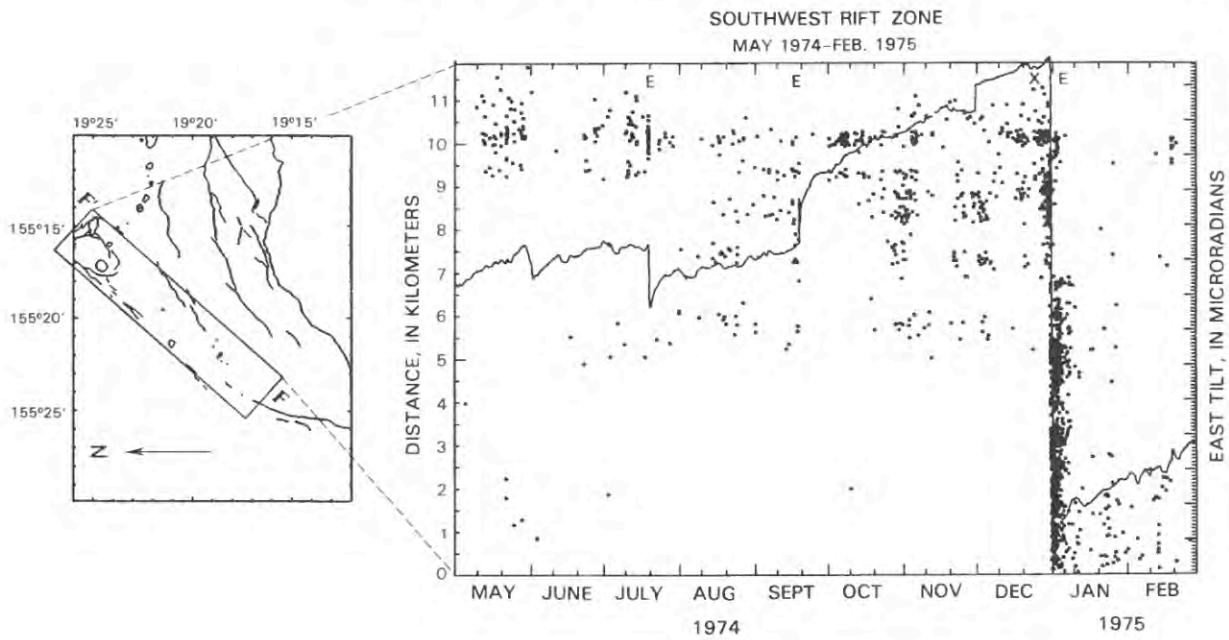


FIGURE 43.65.—Plot of earthquakes along southwest rift zone and east tilt at Uwekahuna versus time. Endpoints for distance axis  $F-F'$  are given in table 43.2. Tilt is from east-west Ideal Aerosmith tiltmeter, where east-down tilt is down on plot and generally indicates deflation of summit caldera. Notations along time axis refer to specific swarms detailed in other figures: E, eruption; X, swarm accompanying inflation. Small tick marks on tilt scale are  $1 \mu\text{rad}$ .

VOLCANISM IN HAWAII

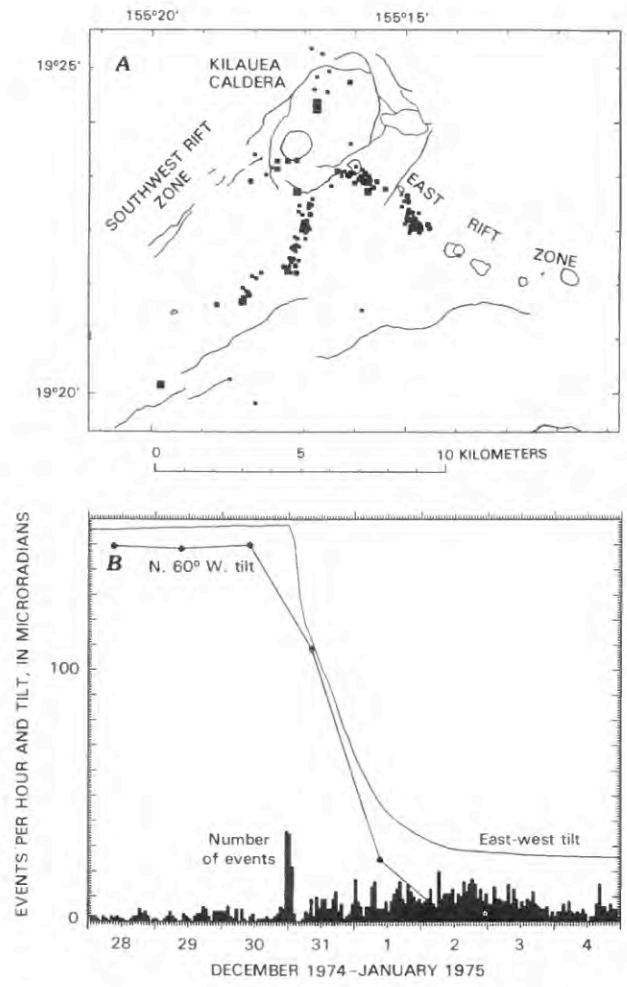


FIGURE 43.66.—Inflationary swarm beginning on December 24, 1974, that immediately preceded the eruption on December 31. See figure 43.20 caption for details. Dashed lines in **D** and **G**, poorly defined migration of seismicity.

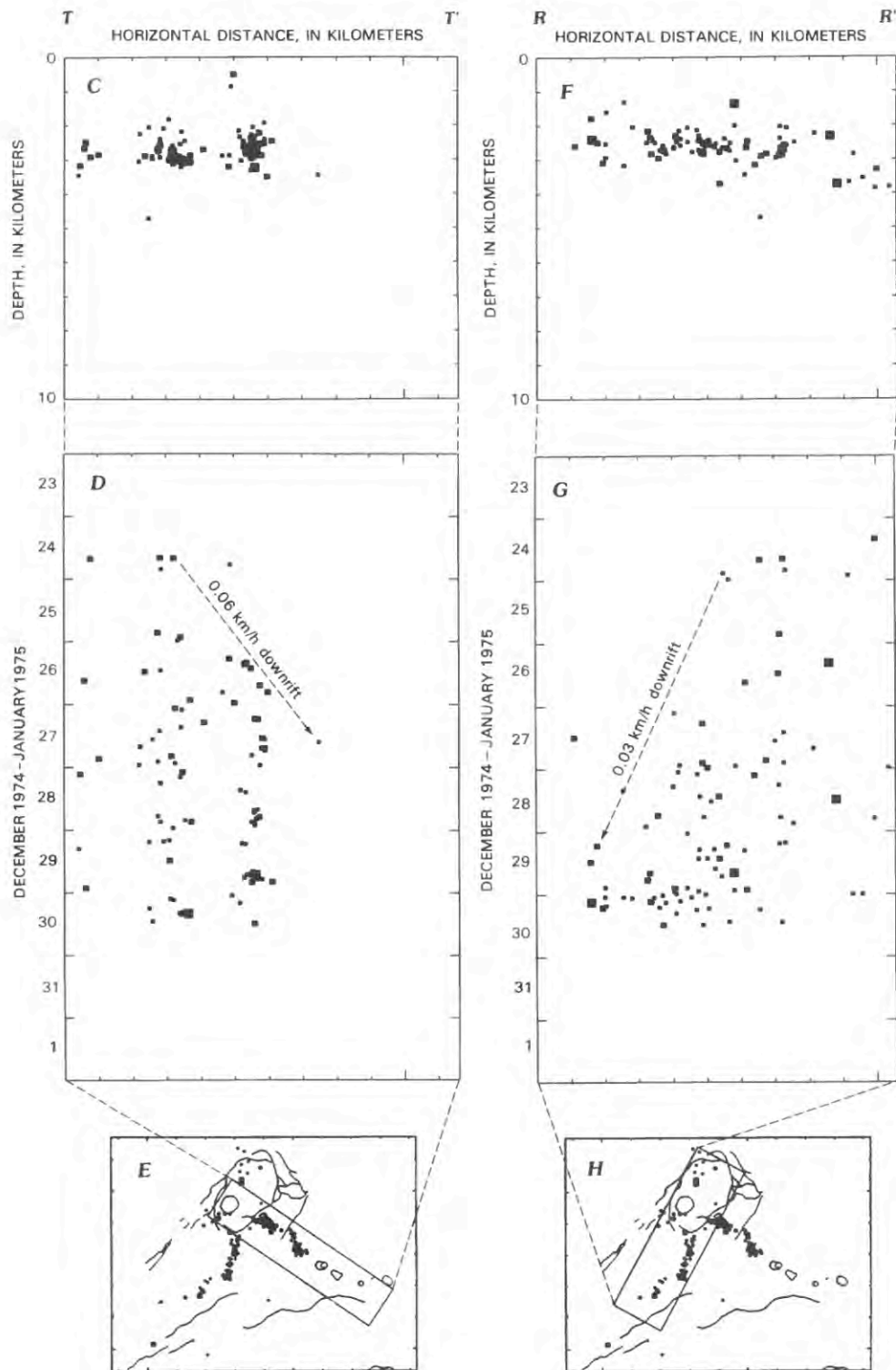


FIGURE 43.66.—Continued.

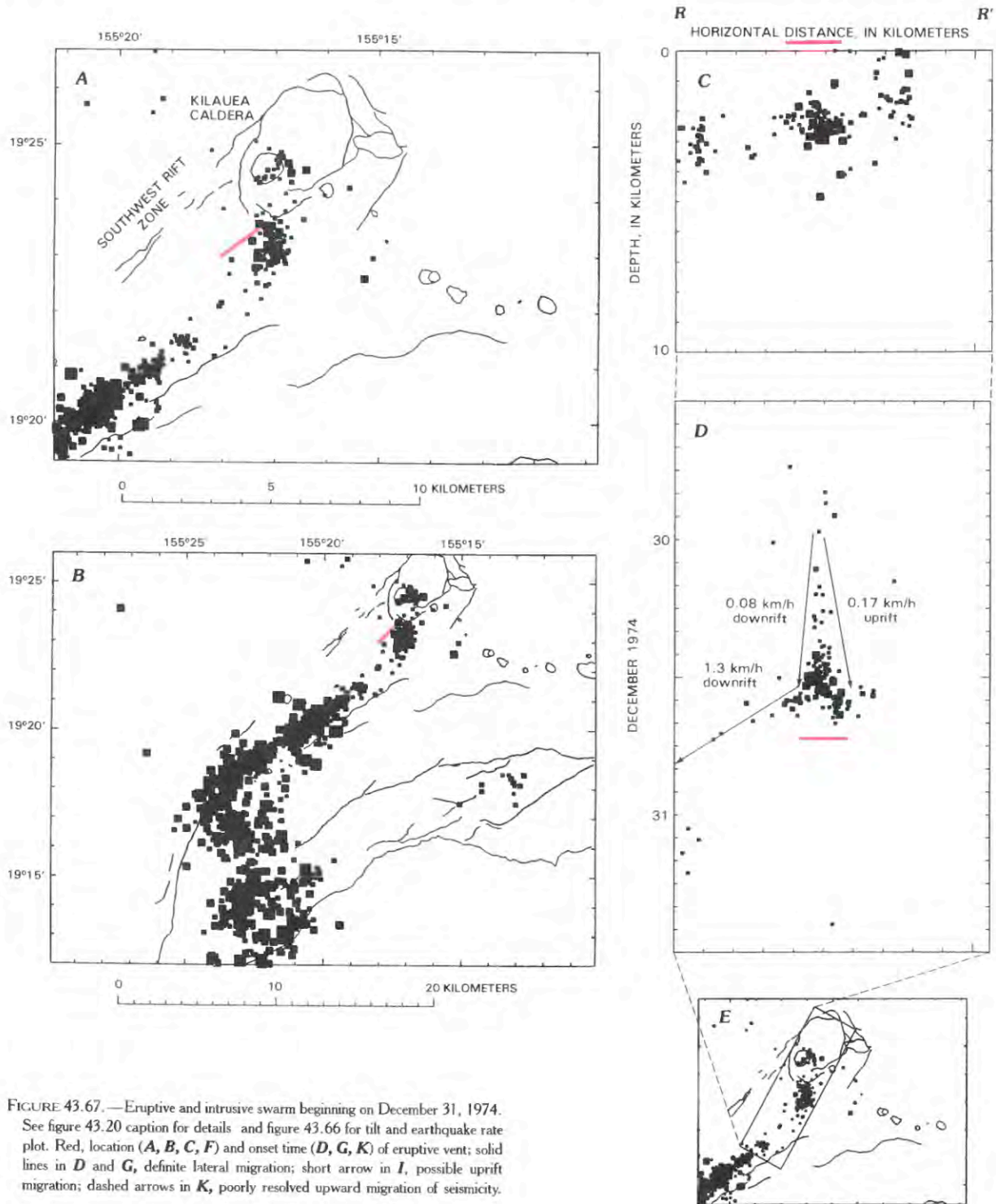


FIGURE 43.67.—Eruptive and intrusive swarm beginning on December 31, 1974. See figure 43.20 caption for details and figure 43.66 for tilt and earthquake rate plot. Red, location (*A*, *B*, *C*, *F*) and onset time (*D*, *G*, *K*) of eruptive vent; solid lines in *D* and *G*, definite lateral migration; short arrow in *I*, possible uprift migration; dashed arrows in *K*, poorly resolved upward migration of seismicity.

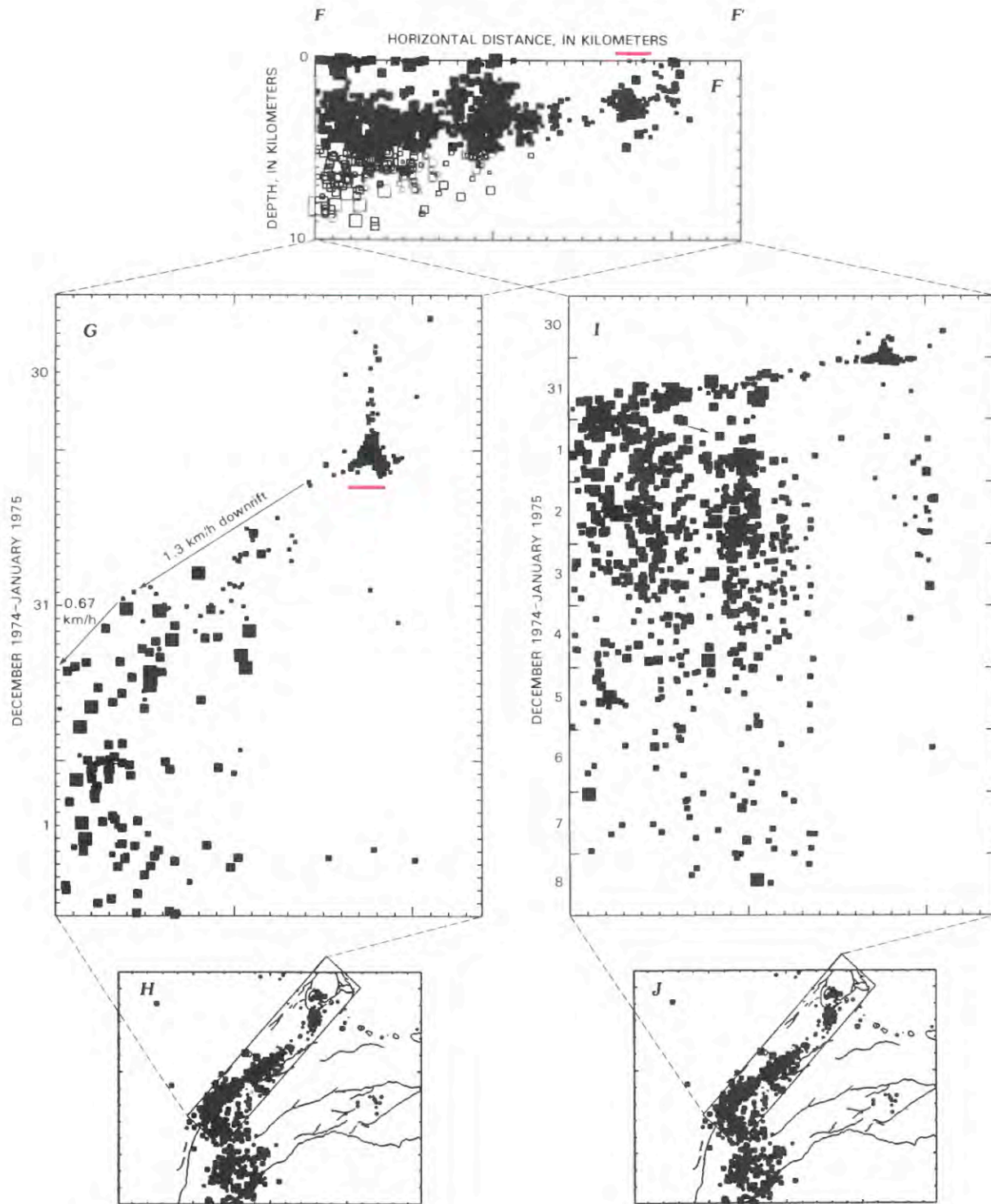


FIGURE 43.67.—Continued.

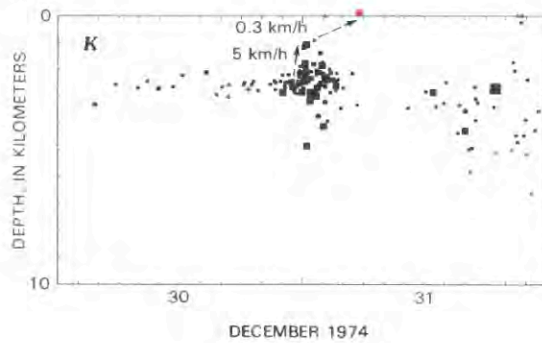


FIGURE 43.67.—Continued.

#### 1976-77 EAST RIFT ZONE INTRUSIONS AND ERUPTION

The next major event at Kilauea was the magnitude-7.2 Kalapana earthquake on November 29, 1975. The south flank's accumulated elastic compression was partly released, and it slipped seaward as much as 8 m (Lipman and others, 1985). The ERZ dilated and accommodated roughly 100 million cubic meters of magma as the summit deflated (Dzurisin and others, 1980). A small summit eruption was triggered by the earthquake, but no ERZ eruption occurred and its magma remained below the surface. We do not consider the November 29, 1975 eruption here because of its atypical origin and because any intrusion seismicity was completely masked by the large earthquake and its aftershocks.

A major change in the short-term volcanic behavior of Kilauea resulted from the Kalapana earthquake. Whereas most swarms immediately prior to the earthquake culminated in eruptions, intrusions outnumbered eruptions during 1976-81. This change in behavior is statistically significant and can be attributed to lowered confining stress on the ERZ and its ease of rifting to accommodate new magma without sustaining pressures necessary for it to reach the surface (Ando, 1979; Klein, 1982b). A second change associated with the Kalapana earthquake was a shift of activity from the SWRZ to the ERZ. Following the December 1974 eruption, the SWRZ did not experience another intrusion until 1981.

The ERZ intrusions of June 21 and July 14, 1976, occurred while aftershocks of the Kalapana earthquake continued. The swarms were very similar. Both extended from Kokoolau to Mauna Ulu (figs. 43.68A, 43.69A). Each swarm lasted less than 24 hours and experienced 10-15 microradians of deflation coincident with the swarm (figs. 43.68B, 43.69B). Both swarms began between Pauahi and Mauna Ulu and migrated uprift. Migration was more

recognizable during the June 21 swarm where the speed was about 1.3 km/h (fig. 43.68D). About the time the June earthquakes ceased moving uprift they veered upward to within 1 km of the surface (fig. 43.68F). The upward speed was about 0.5 km/h. The July earthquakes also displayed an upward migration (at 0.7 km/h, fig. 43.69F). The upward movement in June was between Kokoolau and Hiiaka, but that in July was near the former Aloi Crater.

Both of the 1976 intrusions originated from a point 3 km beneath the surface and just downrift of Pauahi. We interpret the immediate source of these intrusions as a secondary magma pocket below Pauahi. This Pauahi magma reservoir was suggested in an earlier section as the cause of the gap in seismicity below Pauahi, also seen in the 1976 swarms. A barrier containing this reservoir and just downrift of it is then a possible place for magma pressure to initiate earthquake swarms and intrusions. Whatever its cause, a concentration of stress beneath the Pauahi-Mauna Ulu region apparently initiates earthquake swarms that can move along the rift and upward. The magma supplying these intrusions is ultimately from the summit reservoir, but may have been stored within the rift. The summit reservoir must be in close hydraulic communication with the propagating dike, as evidenced by the simultaneity of rift swarm and summit deflation. Intrusions such as these are not simple downrift growth of dikes, and the possible relations of uprift earthquake migration and magma pockets within the rift will be discussed in more detail in the next section.

The ERZ between the caldera and Hiiaka was the site of two brief swarms on January 22 and February 8, 1977. The January swarm began at Keanakakoi, but soon moved to Kokoolau (fig. 43.70A, D). The fact that the summit did not rapidly deflate, but instead experienced slowly rising tilt (fig. 43.70B), and that the swarm's occurrence adjacent to the caldera might lead one to relate this sequence to summit inflation. The brevity of the intense part of the swarm (1 day) and relatively rapid though not precisely determined downrift migration rate (0.7 km/h) were more indicative of a rapid intrusion. This small swarm falls somewhere between the typical event types we have called slow, inflationary swarms and rapid, intrusive swarms.

The January swarm terminated near Kokoolau, where a more intense intrusion began 17 days later on February 8 (fig. 43.71A). The February intrusion lasted for about 11 hours and produced a rapid deflation (fig. 43.71B). The disturbance spread both uprift and downrift, though the continuity of migration is not well developed (fig. 43.71D). The initial 5 earthquakes were followed by an aseismic period, then a more intense episode that coincided with rapid summit deflation. The significant growth in dike volume

thus coincided with the most intense seismicity. At the beginning of the intense part of the swarm, an area of about 3 km by 3 km was active simultaneously (fig. 43.71A, *D*), and it did not grow in area. The disturbed zone thus seems to have aseismically enlarged in surface area before it seismically grew in thickness and volume. We therefore generally associate earthquakes primarily with growth of dike thickness and the compression of adjacent brittle rock. The enlargement of the disturbed zone alone does not then generate intense seismicity in these intrusions unless the dike also grows significantly in width.

The early 1977 swarms suggest that an initial low-volume intrusion propagated from the caldera to Kokoolou on January 22, where it encountered a blockage in the magma conduit. The blockage broke on February 8 when a greater magma volume became involved.

The September 1977 swarm and eruption penetrated farther along the ERZ than any other during 1962–83. A detailed eruption chronology is given by Moore and others, (1980). Four disconnected seismic zones were active during the eruption: the southern part of the caldera and central Koae fault zone (fig. 43.72A), and the ERZ at Makaopuhi and near Kalalua (fig. 43.72F). The deflation of Kilauea summit exceeded 90 microradians and continued for about four days (fig. 43.72B). The start of the rapid deflation, the beginning of the swarm in the southern part of the caldera, and four earthquakes south of the former Aloi Crater were all nearly simultaneous (fig. 43.72D). Seismicity at Makaopuhi and later at Kalalua shows that the part of the intrusion downrift of Mauna Ulu propagated at 1.2 km/h, then slowed to about 0.23 km/h downrift of Kalalua (fig. 43.72H). The absence of earthquakes between the caldera and Aloi and the simultaneity of seismicity at each place indicate that the intrusions of the previous two years left much of the magma conduit open and fluid, and no new dike intrusion or earthquakes were required to transport magma through this area.

The shallow conduit between Makaopuhi and Puu Kamoamo was aseismic, but deeper earthquakes were induced in the south flank immediately adjacent to the gap in shallow earthquakes (fig. 43.72F). This pattern indicates that rifting did occur here, but was probably deeper than elsewhere on the rift. The eruption induced considerable seismicity in the south flank 5–13 km from the vents (fig. 43.69F; Dvorak and others, 1985). Considerably more and larger flank earthquakes were induced as a result of the September 1977 eruption than the somewhat similar January 1983 eruption. The induced seismicity is testimony both to the stress caused by the large intrusion and to the sensitivity of the south flank; these

earthquakes can be partly considered aftershocks of the Kalapana earthquake less than two years earlier. The south flank was left with residual but local stresses, and these caused both aftershocks and the abundance of seismicity triggered by the 1977 intrusion.

The eruptive vents spanned a length of rift equal to that of the Kalalua seismic zone, but were displaced about 2–3 km downrift from the earthquakes (fig. 43.72F). This seismic pattern suggests that the dike intruded at 2–3 km depth and fed the eruption through feeders angled upward and downrift. The vents near Kalalua began erupting 5–10 h after the conduit 2–3 km beneath them became seismically active (fig. 43.72H). The time of opening of the easternmost vent was not observed directly, but the end of the uncertain period seems more likely: vent opening would then follow earthquakes as it does elsewhere. The last vent to open (uprift of Kalalua) does not follow the progression, but seems to accompany a new episode of seismic activity.

The earthquakes in the caldera and Koae are related to the large subsidence and deformation in the summit area. Earthquakes in the central Koae began about 12 hours after the intrusion and slowly progressed eastward at about 0.09 km/h (fig. 43.72K). This earthquake migration was also upward, owing to the dip of the seismic zone (fig. 43.72J). The migration of earthquakes is much slower and of opposite direction to that seen during intrusions of the Koae in 1973, and the seismic zone does not abut either rift. Tectonic movement on Koae faults is thus more likely than an intrusion, because summit subsidence would produce the correct sense of offset on the north-facing fault scarps. The caldera earthquakes began as soon as the intrusion started and slowly diminished during the next 6 days.

Caldera and Koae seismicity resumed on September 27 (fig. 43.73A) and accompanied the major eruptive phase that built the Puu Kiai spatter cone. The ERZ was nearly aseismic during this episode. The earthquakes below Halemaumau spread to the south very slowly at about 10 m/h (fig. 43.73D) and were apparently caused by the slow deflation. The caldera seismicity during the whole eruption thus generally correlates with deflation rate and is probably caused by compressive stresses in the summit area produced as the caldera contracted. These deflation earthquakes are in a similar location but appear to be the reverse of the slow swarms accompanying summit inflation and extension. The September 1977 eruption, the first following the  $M=7.2$  Kalapana earthquake, was thus seismically complex. This complexity arose not only from the length of rift and volume of magma involved, but also from the probable disequilibrium of stresses following the Kalapana earthquake.

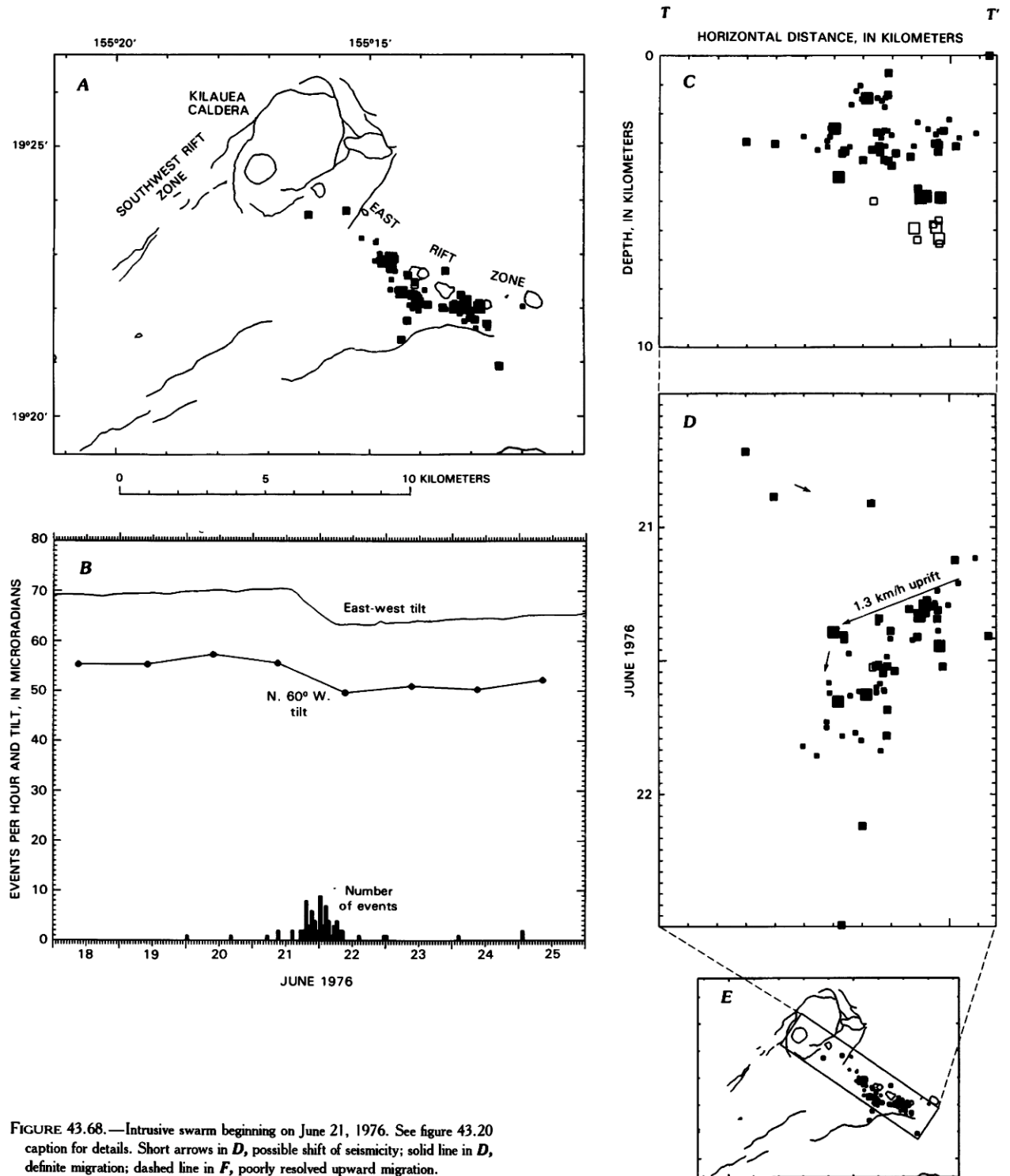


FIGURE 43.68.—Intrusive swarm beginning on June 21, 1976. See figure 43.20 caption for details. Short arrows in *D*, possible shift of seismicity; solid line in *D*, definite migration; dashed line in *F*, poorly resolved upward migration.

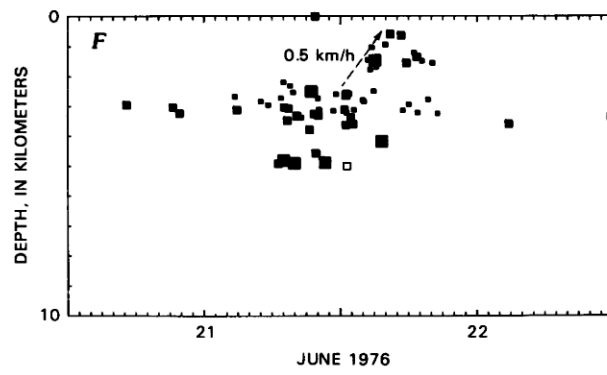


FIGURE 43.68.—Continued.

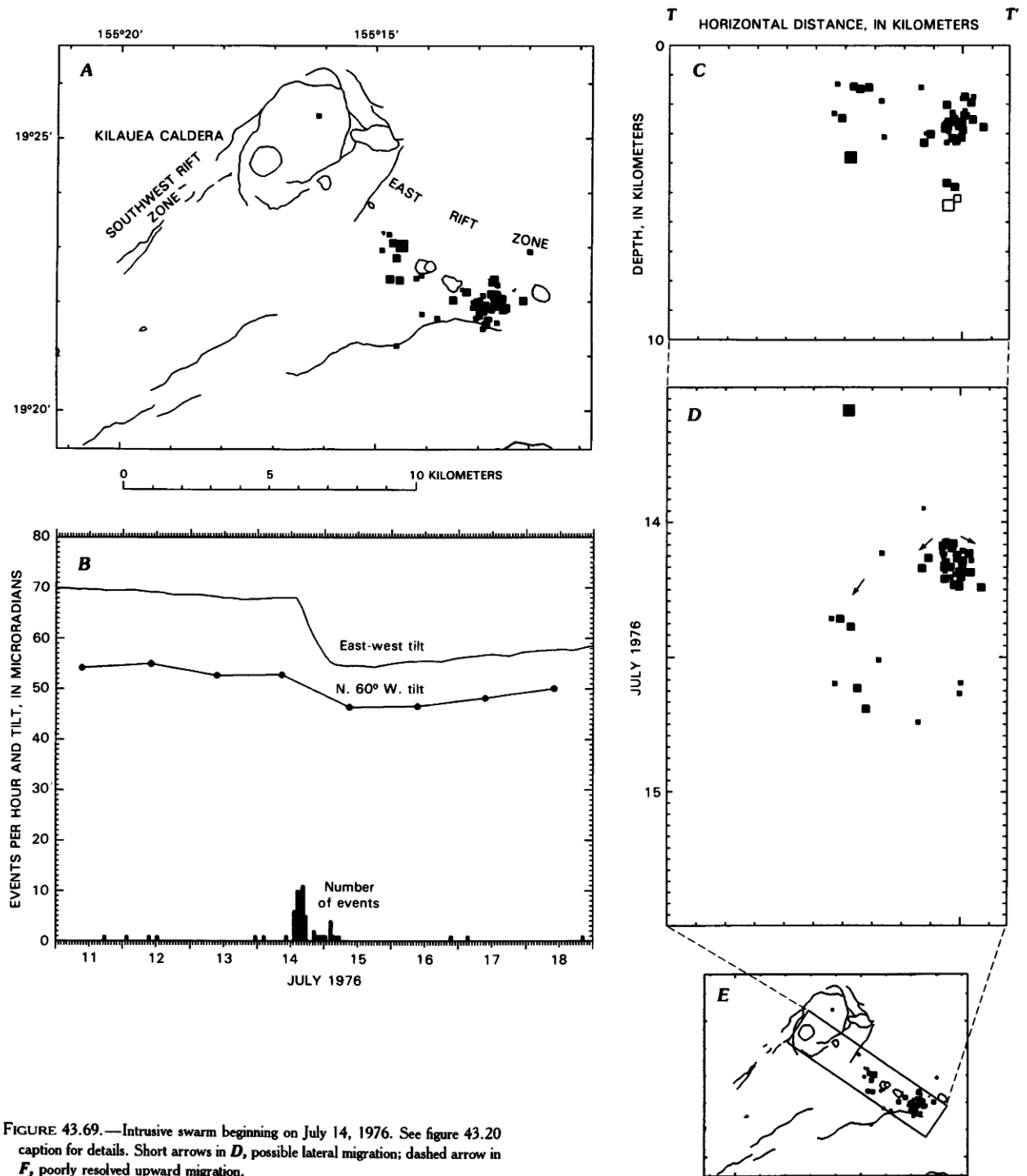


FIGURE 43.69.—Intrusive swarm beginning on July 14, 1976. See figure 43.20 caption for details. Short arrows in *D*, possible lateral migration; dashed arrow in *F*, poorly resolved upward migration.

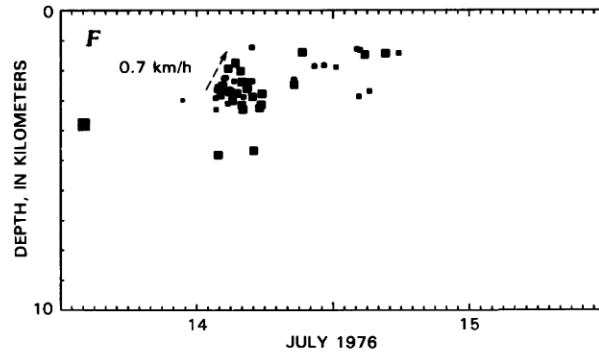


FIGURE 43.69.—Continued.

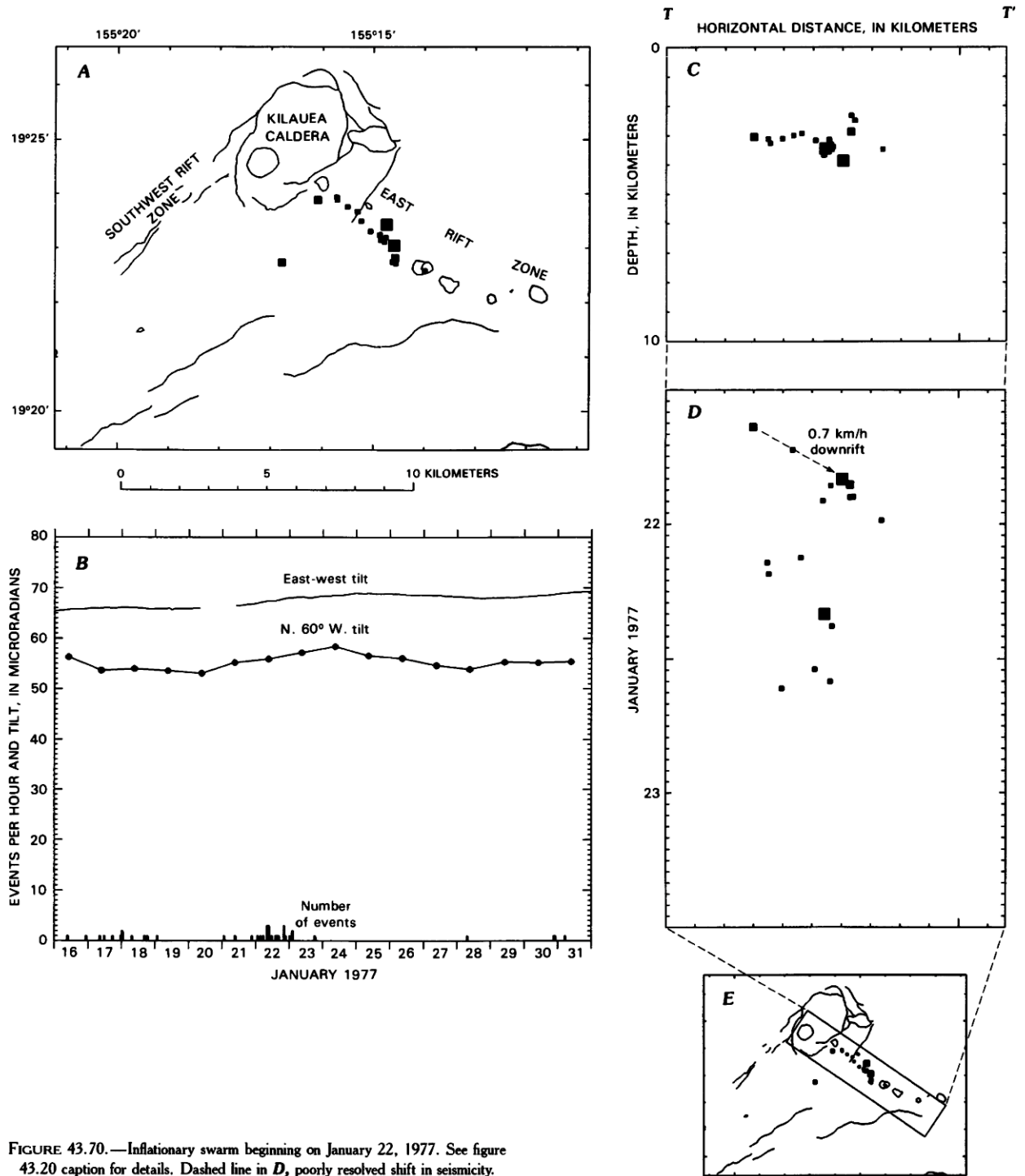


FIGURE 43.70.—Inflationary swarm beginning on January 22, 1977. See figure 43.20 caption for details. Dashed line in *D*, poorly resolved shift in seismicity.

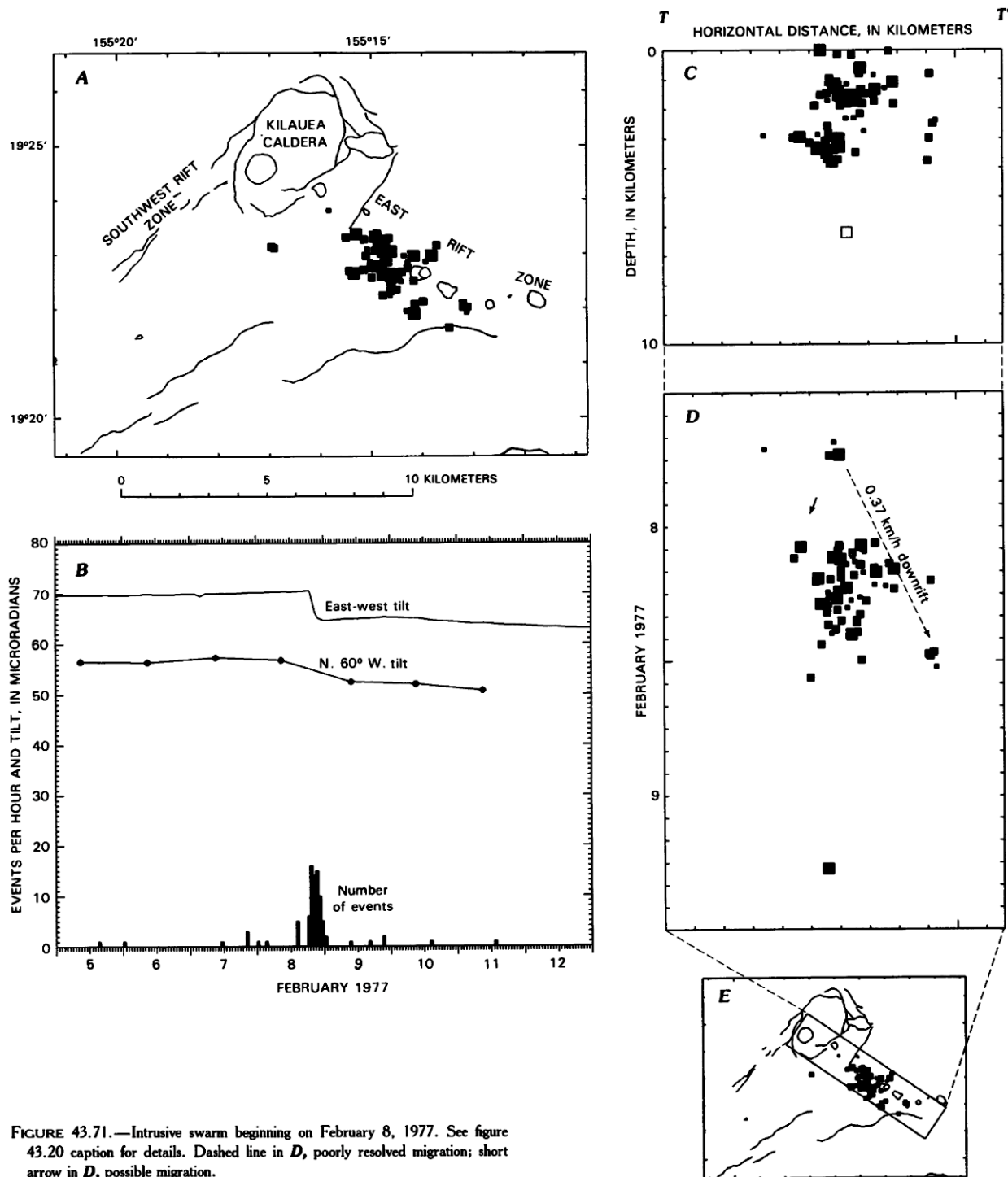


FIGURE 43.71.—Intrusive swarm beginning on February 8, 1977. See figure 43.20 caption for details. Dashed line in *D*, poorly resolved migration; short arrow in *D*, possible migration.

VOLCANISM IN HAWAII

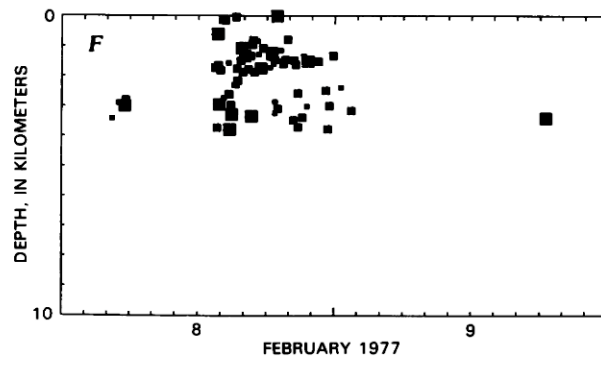


FIGURE 43.71.—Continued.

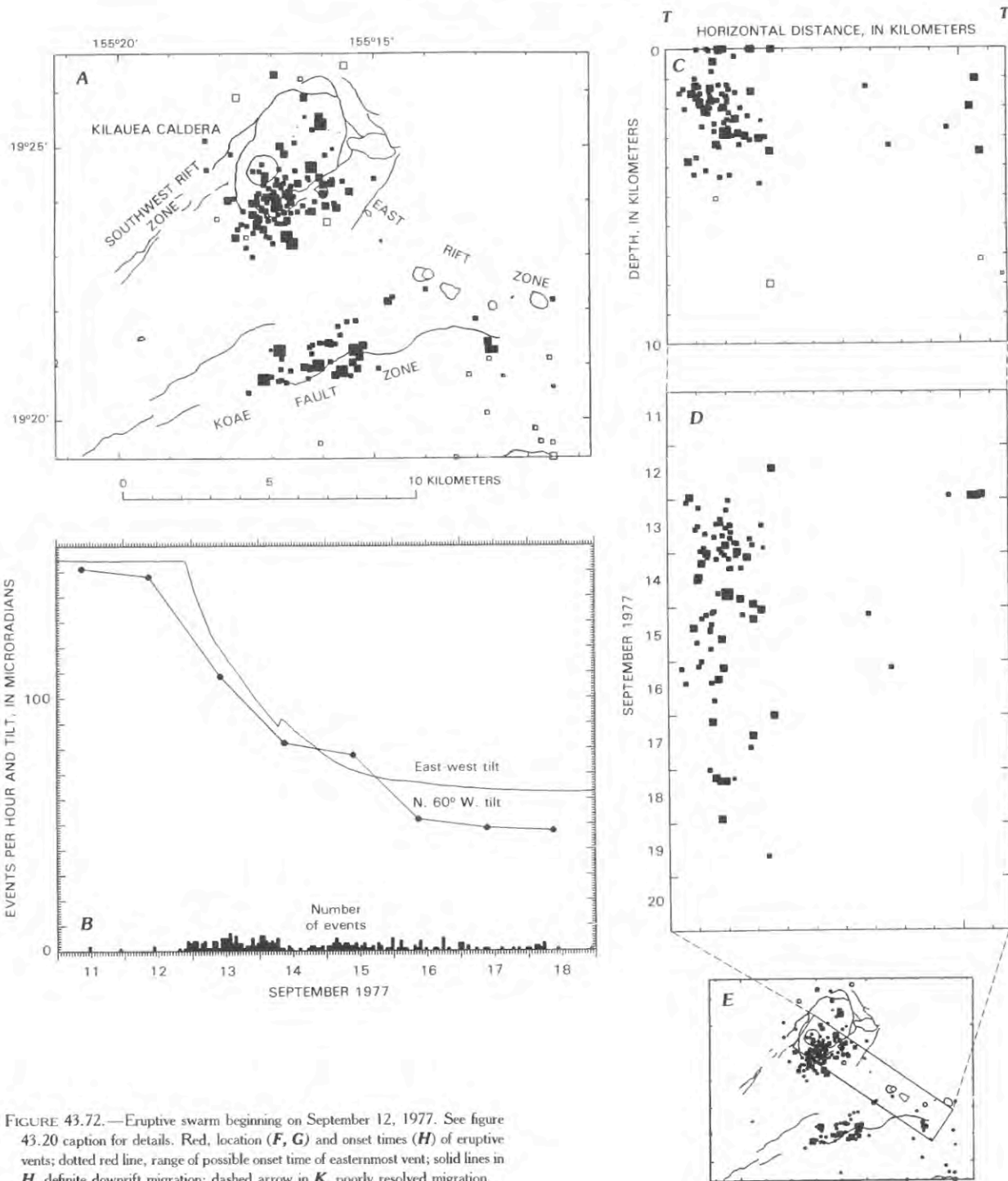


FIGURE 43.72.—Eruptive swarm beginning on September 12, 1977. See figure 43.20 caption for details. Red, location (*F*, *G*) and onset times (*H*) of eruptive vents; dotted red line, range of possible onset time of easternmost vent; solid lines in *H*, definite downrift migration; dashed arrow in *K*, poorly resolved migration.

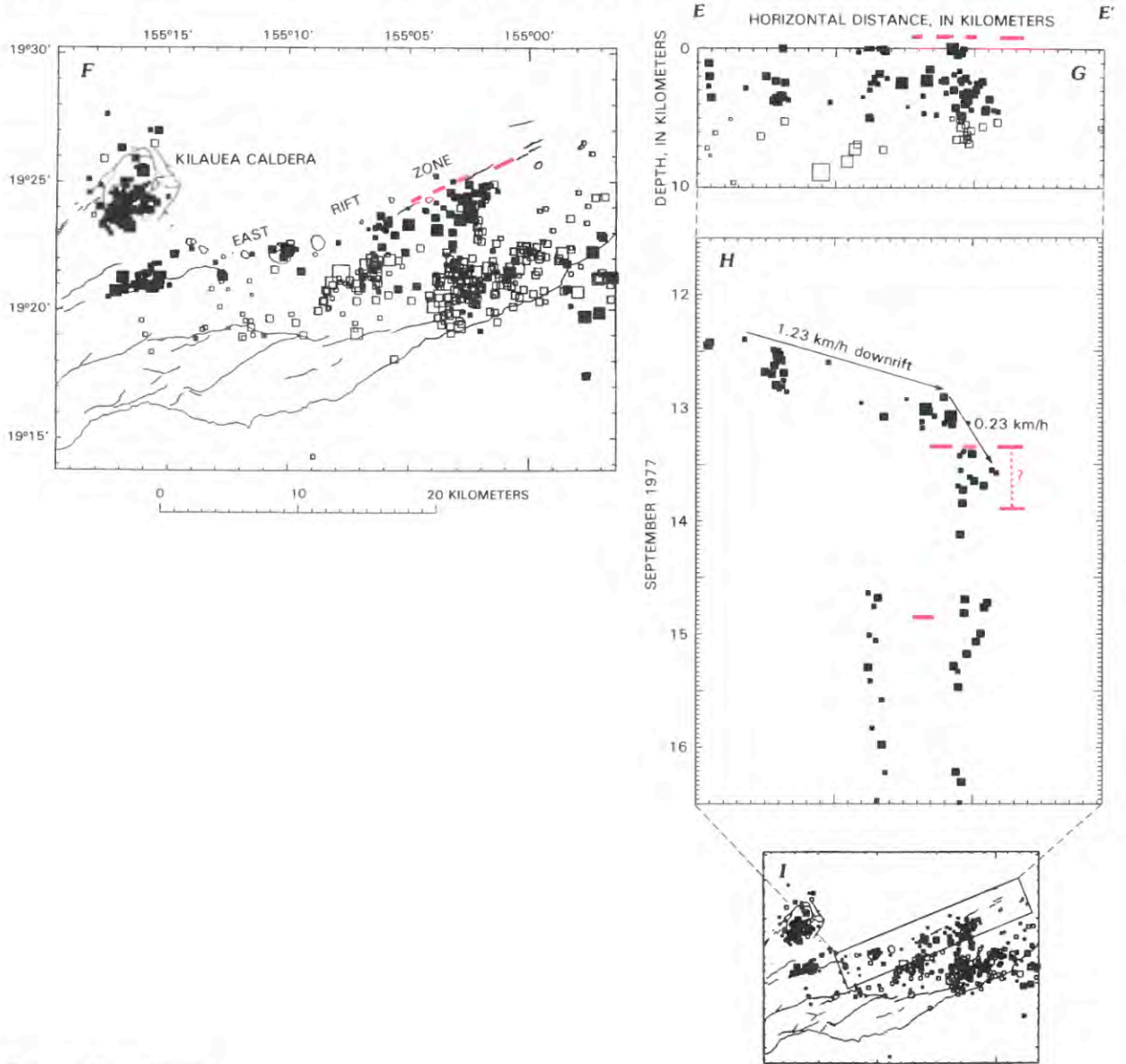


FIGURE 43.72.—Continued.

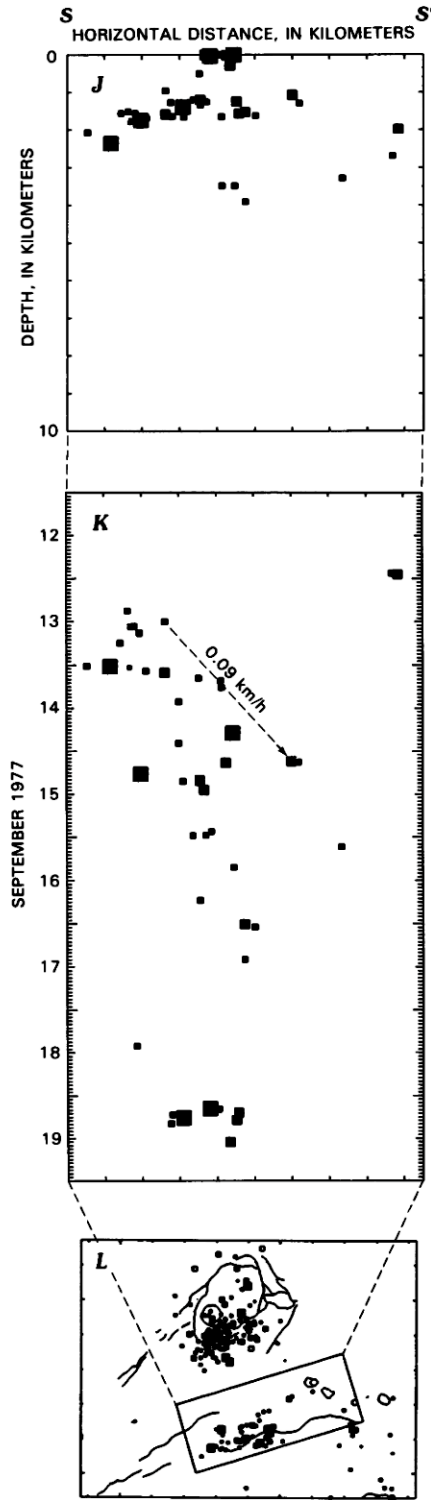


FIGURE 43.72.—Continued.

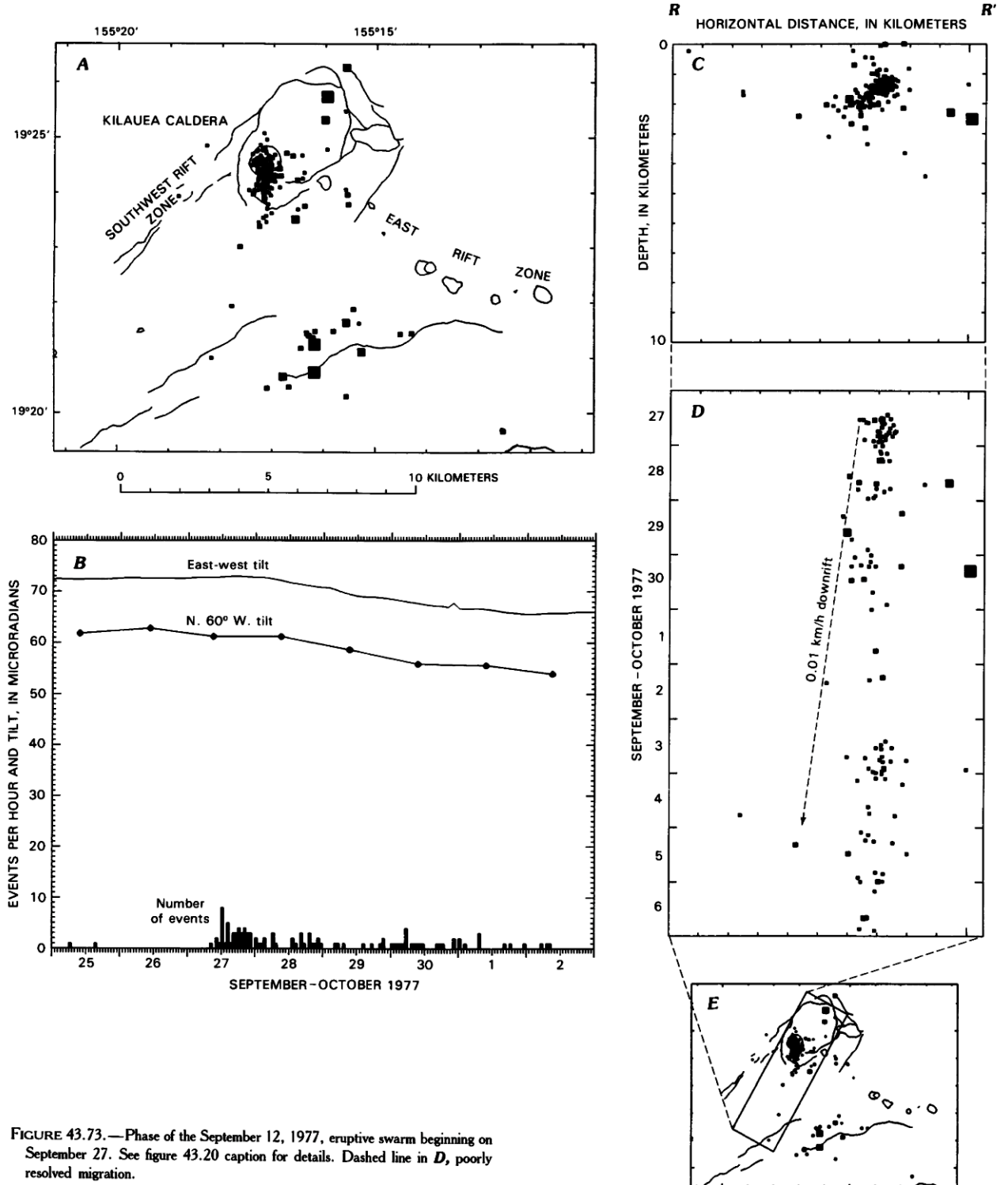


FIGURE 43.73.—Phase of the September 12, 1977, eruptive swarm beginning on September 27. See figure 43.20 caption for details. Dashed line in *D*, poorly resolved migration.

#### EAST RIFT INTRUSIONS AND ERUPTION, NOVEMBER 1978 TO NOVEMBER 1979

The ERZ continued to overshadow the SWRZ during 1978–80 with a variety of eruptions and intrusions. An overview of the summit tilt and position of caldera and ERZ seismicity for the November 1978 through November 1980 interval is shown in figure 43.74. Prior to the first intense swarm on May 29, 1979, both tilt and caldera seismicity increased gradually as the summit inflated slowly (fig. 43.74A). Episodes of shallow earthquakes in the ERZ near Puu Kamoamoia also appeared during this period. These events were generally in slow swarms lasting several days and coincided with episodes of gradual summit deflation. The Puu Kamoamoia swarms were therefore slow intrusions. Because this activity was most prominent in mid-1980, it will be discussed in more detail below, following the March 1980 intrusions.

The ERZ generated two short but intense intrusive swarms on May 29 and August 12, 1979. Both seismic zones were about 4.5 km long (figs. 43.75A, 43.76A), but the May swarm was a little larger in terms of maximum magnitudes, swarm duration, and amount of deflation (figs. 43.75B, 43.76B). The May swarm began under Mauna Ulu and spread simultaneously both uprift to Pauahi and downrift to Makaopuhi (fig. 43.75D). It also started at about 3 km depth but spread rapidly both upward and downward (fig. 43.75F). The vertical migration speeds of 4–6 km/h were an order of magnitude faster than the lateral speeds of 0.6–0.7 km/h. Since the vertical propagation was much faster than for other intrusions, it may have been by a mechanism other than formation of a new dike, such as transmission of a pressure increase in a still-fluid dike.

A vertical column of earthquakes below 5 km depth was observed after 1200 H.s.t. on May 30, more than 12 hours after the intrusion (fig. 43.75C, D). The deeper events thus were induced by the intrusion and probably caused by continuation of rifting to depth or a downward moving dike. Growth of the rifts by intrusion must continue to about 10 km depth where the mobile south flank decouples from the pre-Hawaiian sea floor (Crosson and Endo, 1982). The rifting between 5 and 10 km depths is normally aseismic, and its timing is unknown. Only under Mauna Ulu and in the central section of the SWRZ (see the section "The Southwest Rift Zone Intrusions and Caldera Eruption of March through June 1982") are significant numbers of earthquakes below 5 km depth seen during intrusions.

The August 12 intrusion originated near Keanakakoi adjacent to the caldera and moved rapidly downrift at 1.6 km/h (fig. 43.76D). The intrusion was centered at 3 km depth and was less than 1 km in vertical extent (fig. 43.76C). The swarm continued for a few days in the downrift portion of the intrusion and extended at a very reduced rate (fig. 43.76F). This intrusion is one of the clearest examples of a fairly simple but rapid intrusion originating directly from the summit magma reservoir.

Kilauea continued to inflate and seismicity was nearly continuous in the portions of the SWRZ and ERZ immediately adjacent to the caldera (fig. 43.74B). A short swarm confined to the southern portion of the caldera (fig. 43.77A) punctuated a 30-day period of rapid and nearly continuous inflation. Inflationary swarms are generally not so short and intense. This one may have been associated with some form of dike intrusion caused by the increasing magma pressure, such as the breaking of rock to bridge two chambers of the magma reservoir.

The Pauahi eruption of November 16, 1979, began with a swarm starting abruptly on November 15. Earthquakes eventually engulfed the ERZ from Puhimau to the former Aloi Crater and partly into the Koaie fault zone (fig. 43.78A). Both the main magma conduit at 3 km depth and the shallow 1- to 2-km depth zone were active (fig. 43.78C). The cross section also shows that the shallowest ERZ earthquakes mark a branch of the dike extending upward to Pauahi near the eruptive vents.

The temporal pattern of earthquakes in the November swarm is somewhat complex but shows characteristics common to many intrusions in this part of the ERZ. Earthquakes again underscored the key role played by the hypothesized magma blockage just downrift of Pauahi. The first two earthquakes were uprift of Pauahi. They lie along a front moving at about 3.8 km/h which became seismically intense when it reached Pauahi, and continued for another 1–2 km to the southeast (fig. 43.78D). When projected along the Koaie fault zone, the same migration appears with a foreshortened speed of 1.5 km/h (fig. 43.78G). Earthquakes then moved slowly into the Koaie at a decreasing speed. Summit deflation did not coincide with the first earthquakes, but commenced just minutes after the initial seismic front reached Pauahi and the intense seismicity began. This relation shows that the initial downrift migration did not draw much magma from the summit reservoir, but that the coincidence of intense seismicity and deflation implies a close hydraulic communication between the summit reservoir and Pauahi. Earthquakes then migrated back uprift at about the same speed, almost as if some sort of disturbance was reflected from a barrier just downrift of Pauahi.

After the intense seismicity began, the sense of migration was generally uprift: (1) the western boundaries of the seismic zone moved uprift and into the Koaie, (2) the eastern boundary of the seismic zone moved uprift at about 0.08 km/h, and (3) the eruptive vents opened westward (fig. 43.78D). The possible mechanisms of this uprift migration will be discussed in the section "Discussion of Rift Zone Intrusions." Coincident with the initial uprift movement was an upward migration from 3 km depth that slows and becomes nearly aseismic at a depth of 1 km (fig. 43.78I). These patterns reinforce the earlier suggestion of a secondary magma reservoir about 3 km beneath Pauahi and a blockage of the magma conduit just downrift of Pauahi. The initial downrift migration was not strong enough to penetrate the barrier, where a stress concentration triggered a rifting episode fed by summit magma. Even though possibly triggered by a pulse from the summit, the sequence of events culminating in the eruption at Pauahi were initiated at Pauahi.

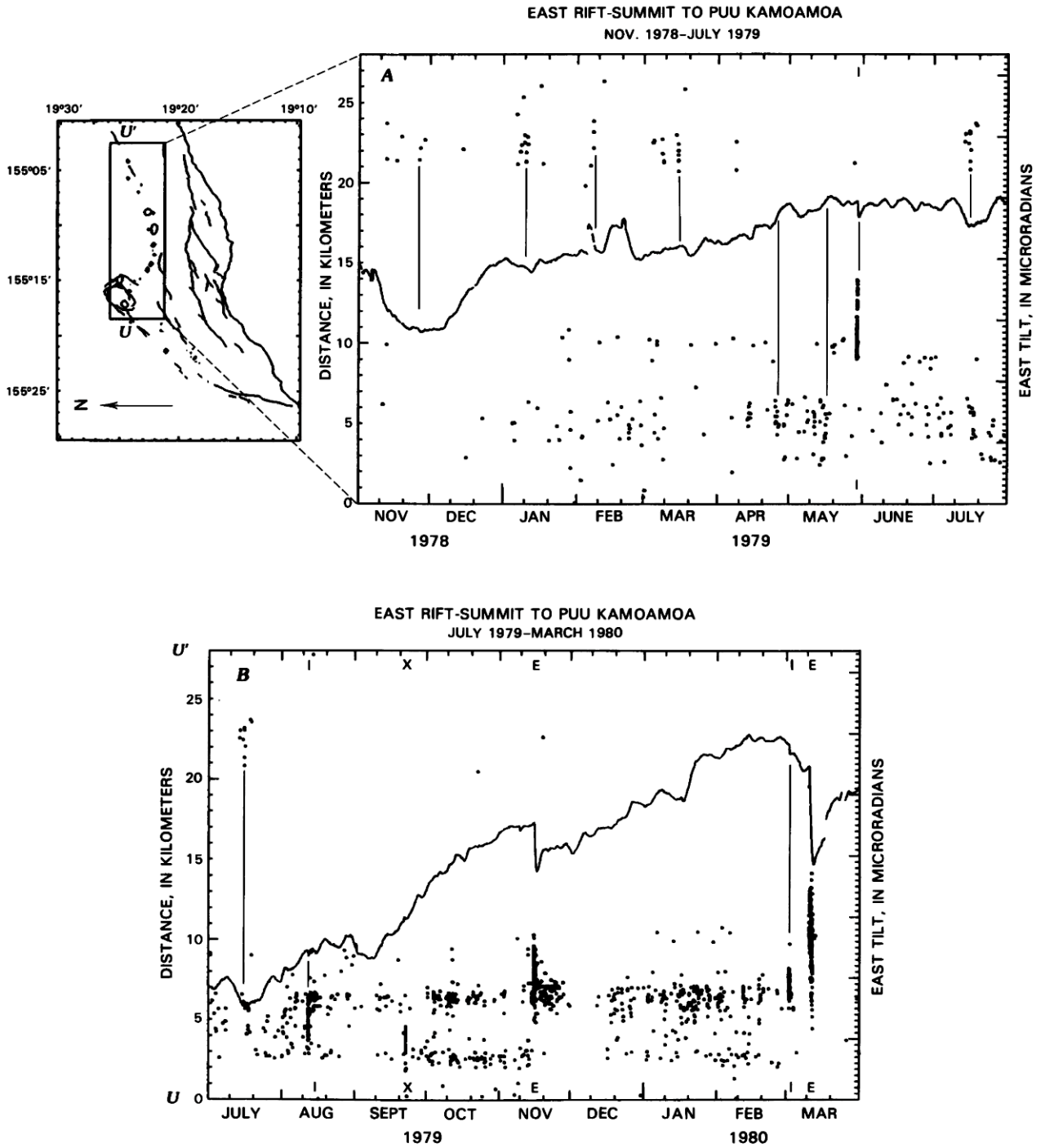


FIGURE 43.74.—Plot of earthquakes along east rift zone and east tilt at Uwekahuna versus time. *A*, November 1978 through July 1979. *B*, July 1979 through March 1980. *C*, March through November 1980. Plot shows changes of position of seismicity with time. Endpoints for distance axis  $U-U'$  are given in table 43.2. Tilt is from east-west Ideal Aeromsmith tiltmeter, where east-down tilt is down on plot and generally indicates deflation of summit caldera. Large divisions on tilt scale are 10  $\mu$ rad. Notations along time axis refer to specific swarms detailed in other figures: E, eruption; I, intrusion; X, swarm accompanying inflation. Vertical lines connect swarms or concentrations of earthquakes with corresponding changes in tilt. Mid-1980 was a period of oscillating tilt and alternating locations of seismicity corresponding to cyclic slow intrusions of the east rift zone.

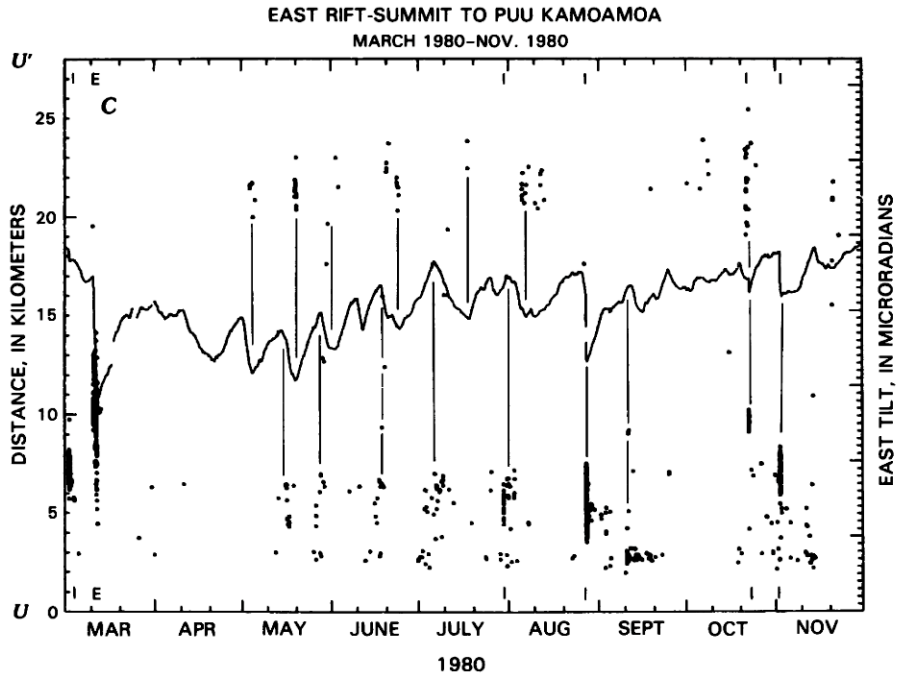


FIGURE 43.74.—Continued.

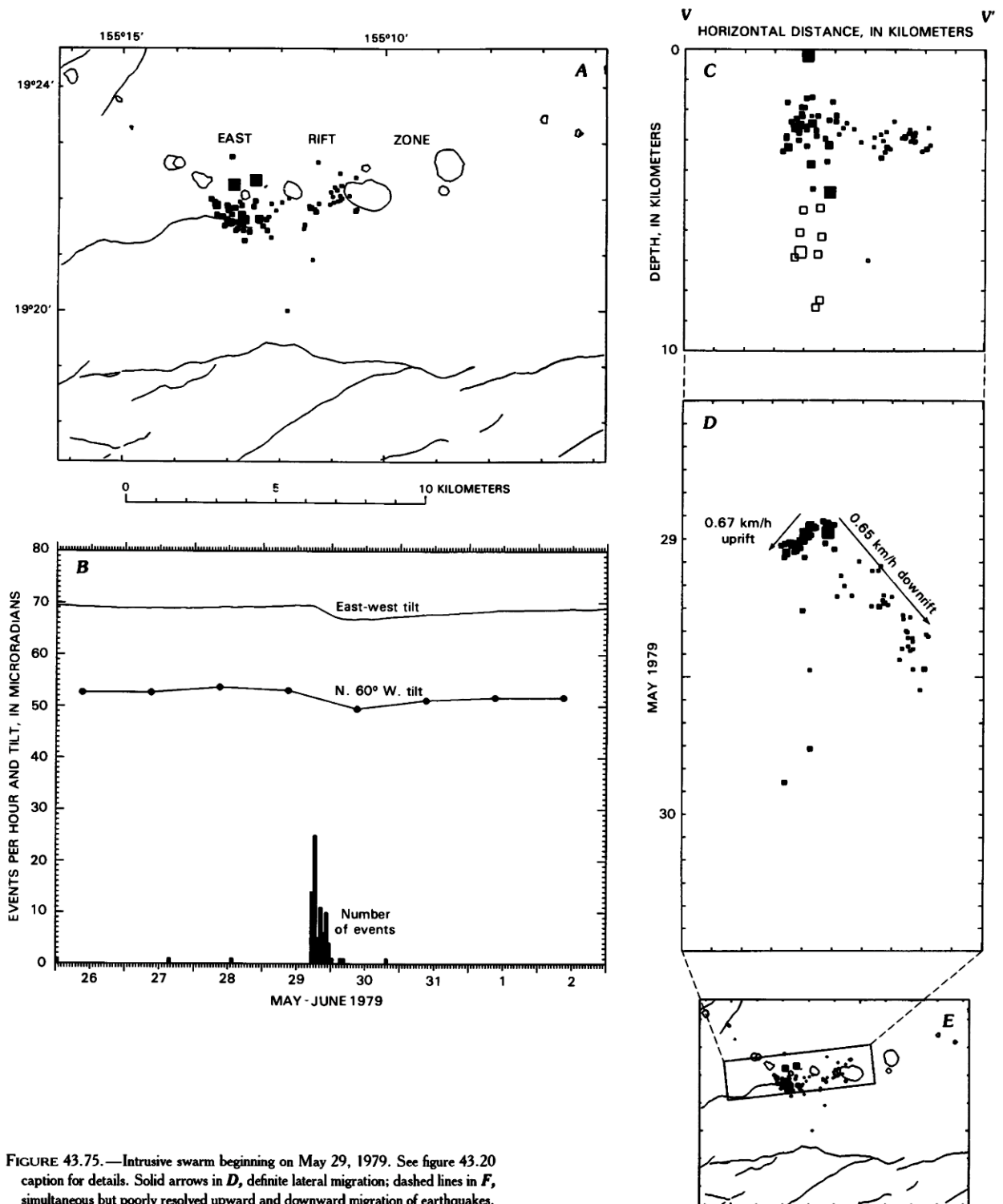


FIGURE 43.75.—Intrusive swarm beginning on May 29, 1979. See figure 43.20 caption for details. Solid arrows in *D*, definite lateral migration; dashed lines in *F*, simultaneous but poorly resolved upward and downward migration of earthquakes.

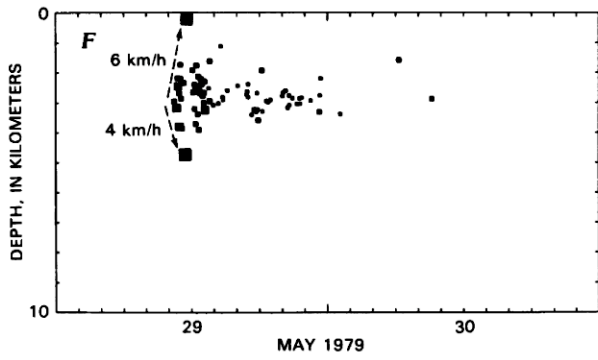


FIGURE 43.75.—Continued.

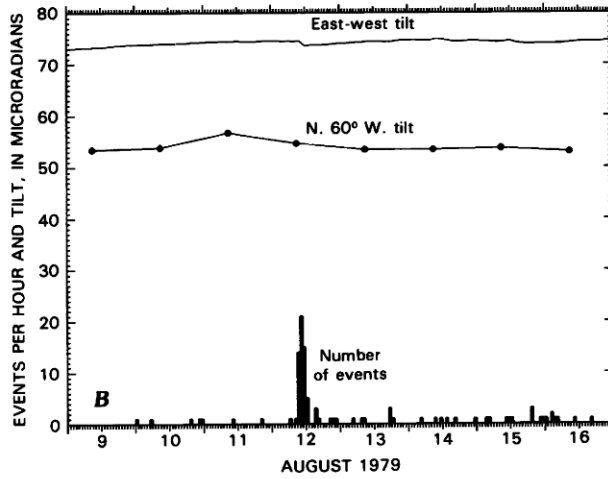
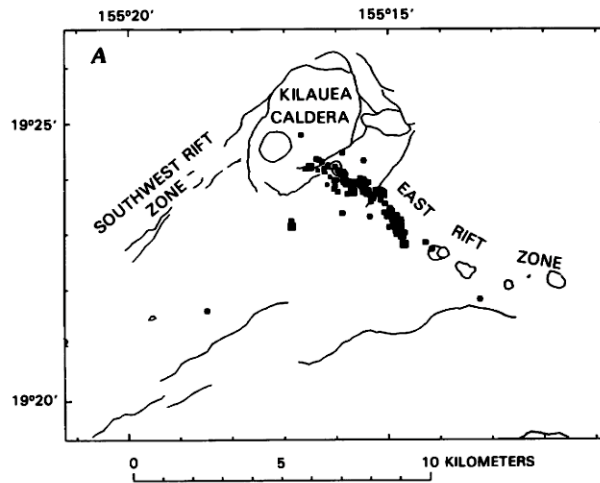


FIGURE 43.76.—Intrusive swarm beginning on August 12, 1979. See figure 43.20 caption for details. Solid line in *D*, definite migration; short arrows in *F*, possible additional downrift migration.

VOLCANISM IN HAWAII

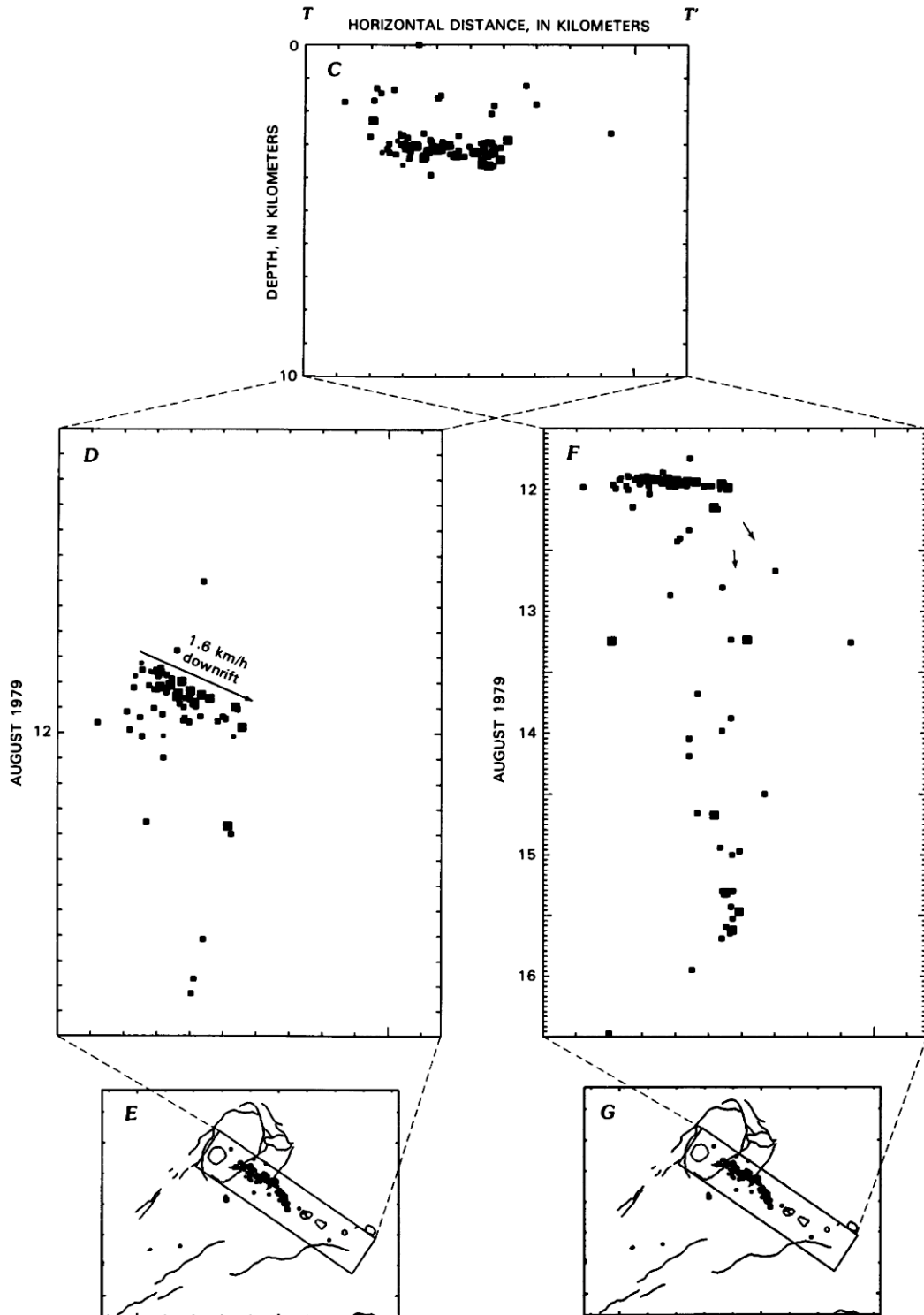


FIGURE 43.76.—Continued.

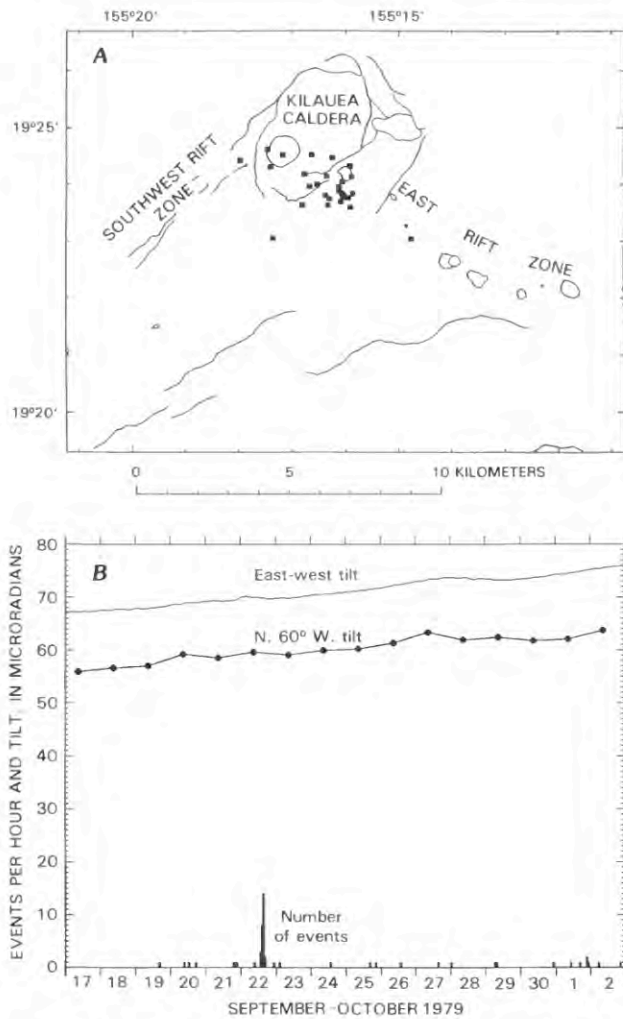


FIGURE 43.77.—Inflationary swarm beginning on September 22, 1979. See figure 43.20 caption for details.

#### EAST RIFT ZONE INTRUSIONS OF MARCH 1980

The ERZ was very busy during 1980 and produced six rapid intrusions, one of which was apparently also a very small eruption. A condensed position versus time summary of the summit and ERZ seismicity is plotted in figure 43.74C. The first two intrusions in March and the last four in the last half of 1980 are readily identified by their intense swarms and sudden deflations in the summit tilt record. The other swarms during May through August were cyclic slow intrusions and will be discussed separately below.

The intrusions of March 1980 were only 8 days apart and successively activated adjacent sections of the ERZ. They appear to be causally related. The March 2 earthquakes were from Kokooloua to Pauahi (fig. 43.79A), and the March 10 swarm

continued downrift from Pauahi nearly to Makaopuhi (fig. 43.80A). The March 2 intrusion was shorter in time, less in deflation, more compact spatially, smaller in earthquake magnitude, and less complex than the March 10 event. The March 2 swarm began about 1 km west of Pauahi where it was most active, but earthquakes soon moved uprift (fig. 43.79D).

The March 10 intrusion produced a complex earthquake pattern and apparently also erupted a few cubic meters of lava that was not noticed until after the event (Norman Banks, written commun., 1981). The intrusion began under Mauna Ulu, and earthquakes rapidly moved uprift at 1.8 km/h for about 2 km (fig. 43.80D) and upward at roughly 4 km/h (fig. 43.80I). The next earthquakes were between the former Alae crater and Makaopuhi, and they probably accompanied the tiny eruption. Next, a relatively slow movement of small earthquakes at 0.2 km/h westward along the rift and into the Koa'e occurred (fig. 43.80D, G). The halo of small earthquakes in the north and south flanks adjacent to the intrusion also diffused outward at this time. Before the swarm ended, a burst of earthquakes just south of the former Aloi crater moved downrift at 3 km/h in the same place as the first part of the swarm.

Clearly, a complex system of dikes and conduits were magnetically active in March 1980. We favor a scenario similar to the following, though many variations and possibilities may exist. During January and February 1980, Kilauea inflated and the accumulating magma produced earthquakes in the ERZ uprift of Pauahi (fig. 43.74B). Magma collected behind a blockage of the conduit, which also forms the uprift side of the magma pocket below Pauahi. The slowly rising magma pressure on the barrier eventually ruptured it, producing the March 2 swarm. This intrusion also drained a small volume of magma from the summit reservoir, which passed through the uppermost section of the ERZ conduit triggering a few earthquakes there.

The summit then deflated slowly and aseismically, sending magma to accumulate behind the next barrier in the conduit near Aloi crater. This second barrier was intruded by a dike on March 10, that moved upward and uprift from a point 3 km beneath Mauna Ulu. The resulting episode of rifting then moved both up and down the ERZ and was fed by summit magma for the 1.5-day duration of the swarm. The rifting and a possible small intrusion also penetrated the Koa'e fault zone. Magma collected on the uprift side of the Aloi blockage faster than it could pass through and thus triggered a second rupture through it, this time in the downrift direction. The amount of dike widening was significant over much of the length of the intrusion and induced small earthquakes as much as 3 km from the rift. The fact that earthquakes migrated in several directions and at different speeds requires rifting by various processes involving shifting stress and moving magma. This complexity also requires more than a single linear magma conduit, a conclusion reinforced by the range of earthquake depths in cross sections of this area.

The ERZ intrusions and eruptions of August and November 1979 and March 1980 each penetrated farther along the rift (fig. 43.74B). They may each have thus opened new sections of the rift conduit and prepared the rift for the passive intrusions of mid-1980.

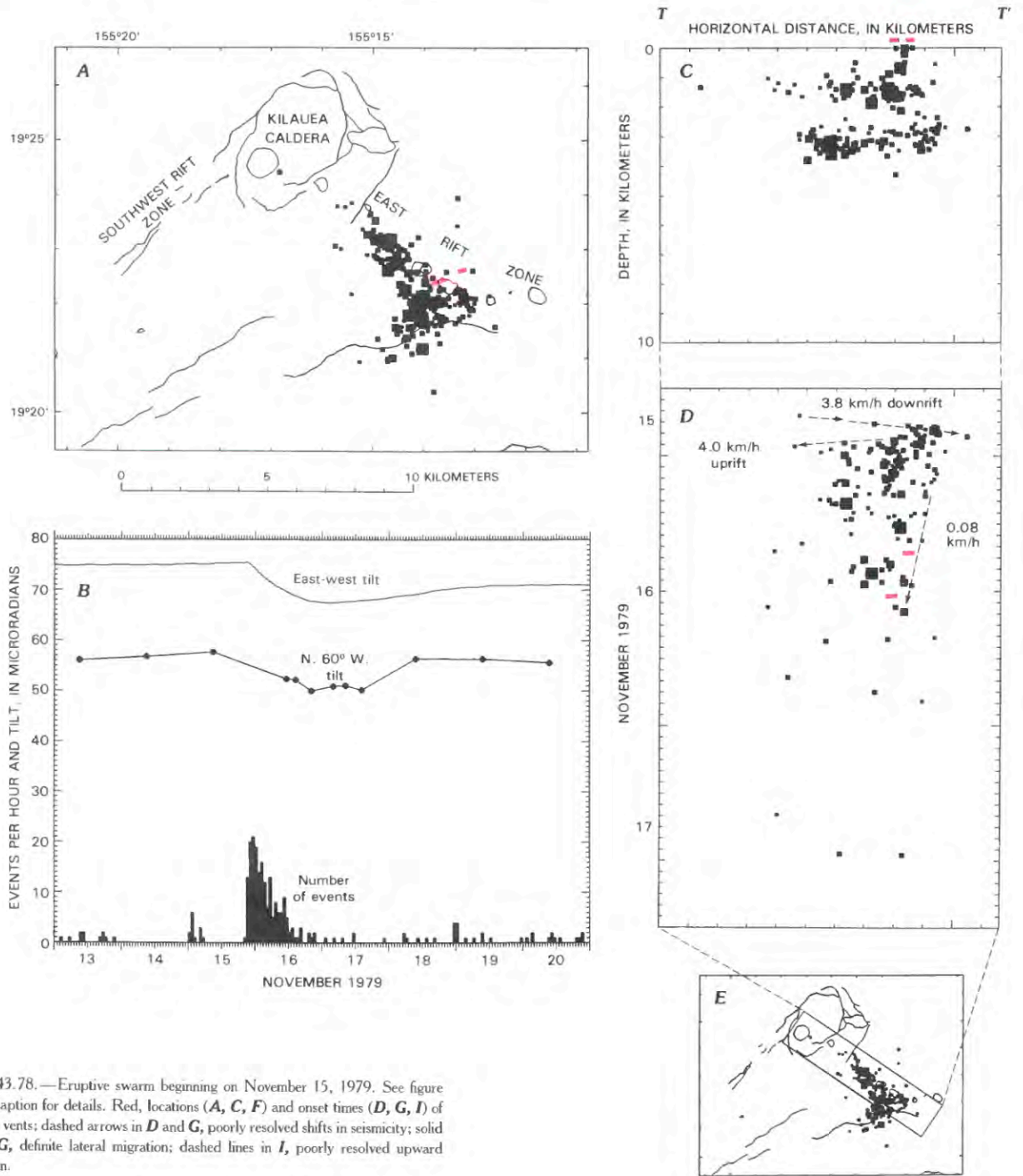


FIGURE 43.78.—Eruptive swarm beginning on November 15, 1979. See figure 43.20 caption for details. Red, locations (*A*, *C*, *F*) and onset times (*D*, *G*, *I*) of eruptive vents; dashed arrows in *D* and *G*, poorly resolved shifts in seismicity; solid line in *G*, definite lateral migration; dashed lines in *I*, poorly resolved upward migration.

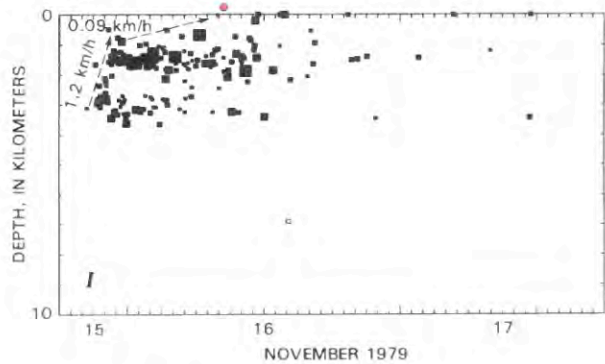
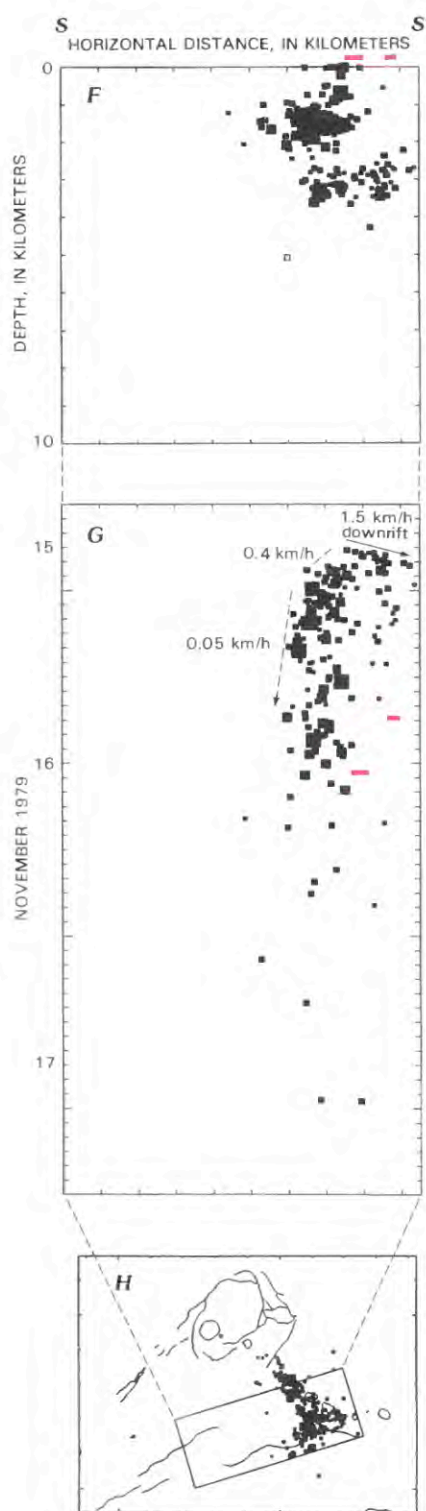


FIGURE 43.78.—Continued.

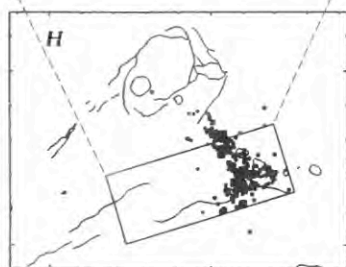
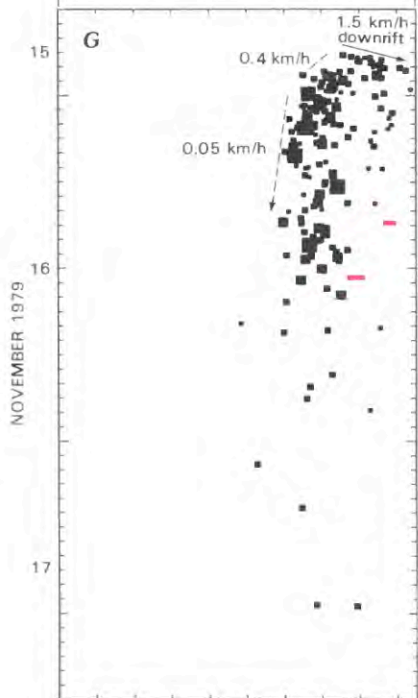


FIGURE 43.78.—Continued.

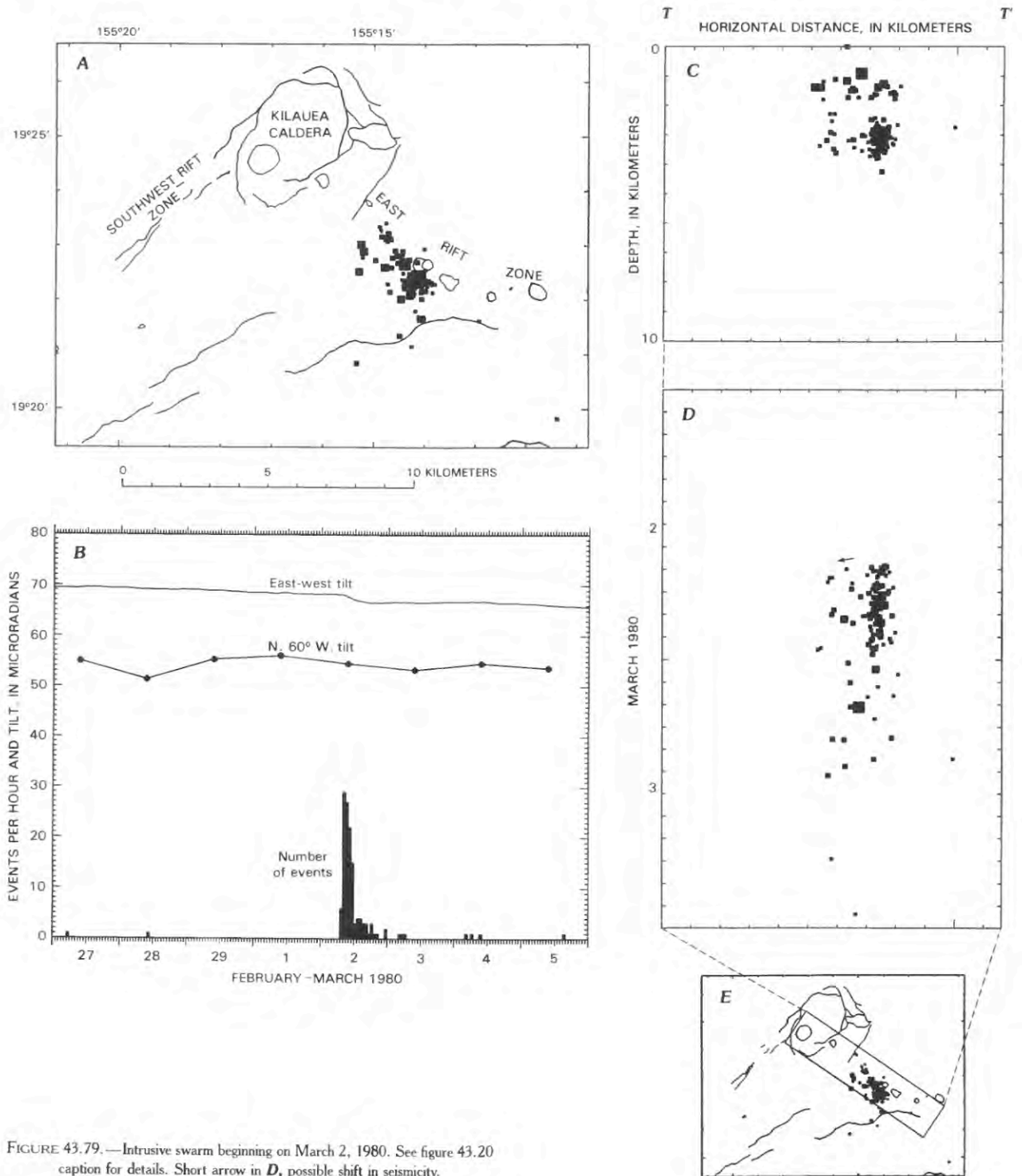


FIGURE 43.79.—Intrusive swarm beginning on March 2, 1980. See figure 43.20 caption for details. Short arrow in *D*, possible shift in seismicity.

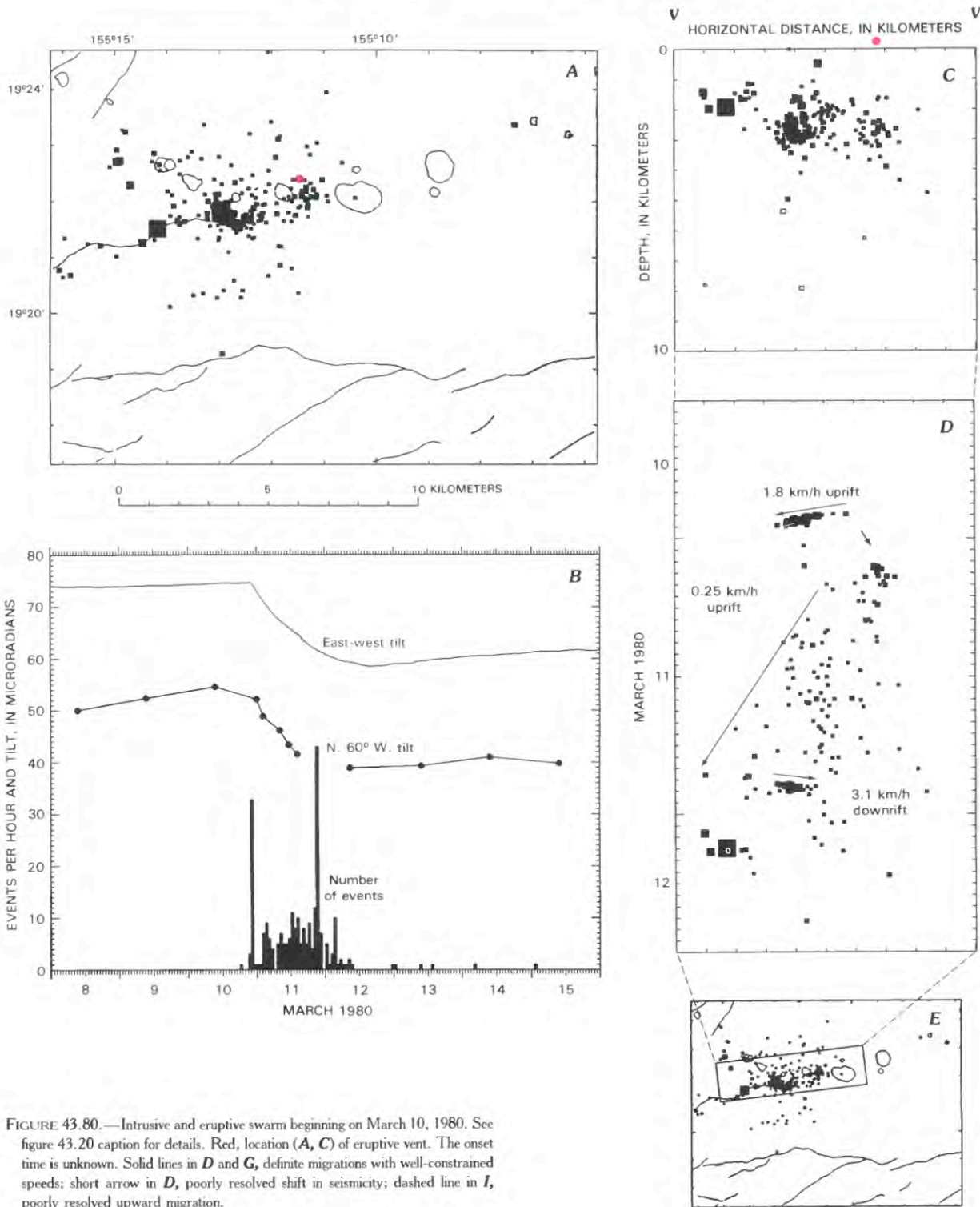


FIGURE 43.80.—Intrusive and eruptive swarm beginning on March 10, 1980. See figure 43.20 caption for details. Red, location (A, C) of eruptive vent. The onset time is unknown. Solid lines in D and G, definite migrations with well-constrained speeds; short arrow in D, poorly resolved shift in seismicity; dashed line in I, poorly resolved upward migration.

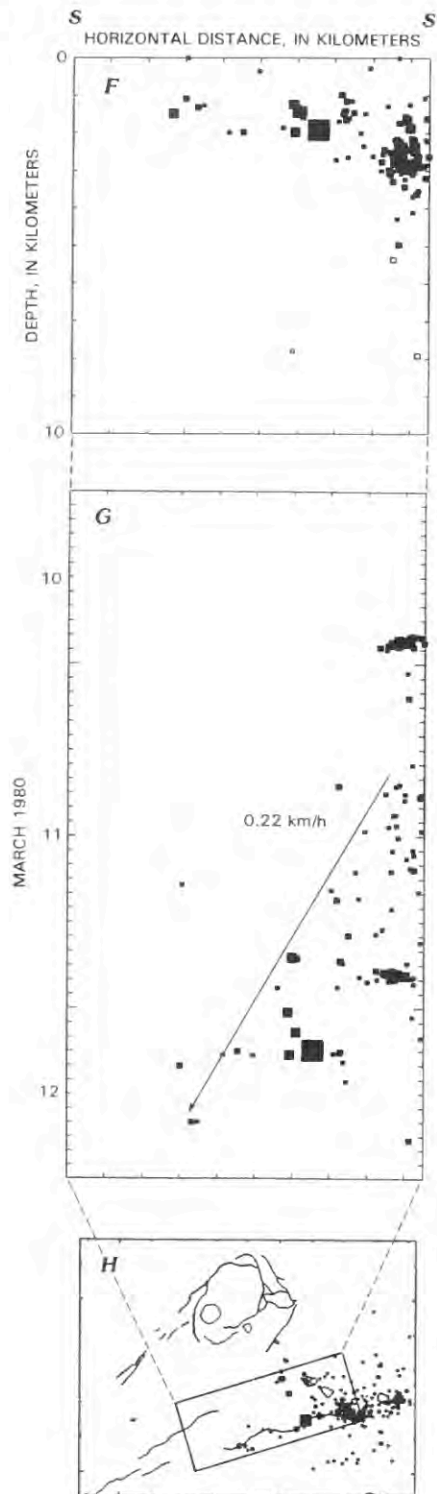


FIGURE 43.80.—Continued.

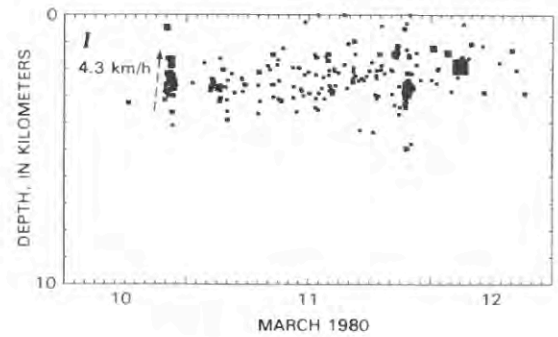


FIGURE 43.80.—Continued.

#### CYCLIC EAST RIFT ZONE INTRUSIONS OF MAY–AUGUST 1980

After the March 1980 intrusions, Kilauea began an unusual mode of transferring magma from the summit reservoir to storage in a section of rift near Puu Kamoamo. The intrusions were cyclic and at intervals more regular than other intrusive swarms. Kilauea inflated gradually for 5–10 days, then deflated at a similar rate for 5–10 days. The accumulating magma in the ERZ during mid-1980 and a similar episode in 1978–79 was measured by outward tilt from a linear zone of inflation (Dzurisin and others, 1984). The largest tilts were near Puu Kamoamo and Kalalua, close to the shallow earthquakes. Dzurisin and others (1984) attributed the rift and summit tilt patterns to a passive and steady transfer of magma from summit to rift. We add the view that earthquake swarms at both summit and rift are variants of the inflationary swarms cataloged in this paper.

A cyclic pattern of magma transfer and oscillatory tilt may also be characteristic of successive episodes of eruption from the same vent, as during the early phases of the Mauna Ulu eruption in 1969–70 or the episodes of the Puu Oo eruption starting in January 1983. Unlike the symmetrical oscillations of tilt during the 1980 cyclic intrusions, the shape of the tilt curve for eruption phases is one of gradual inflation and sudden deflation. Both phenomena accompany a regular delivery of magma to the ERZ.

The cyclic intrusive pattern can easily be seen from the oscillatory tilt in figure 43.74C. The net gain in tilt during this period was very small. A slow swarm of caldera earthquakes generally coincided with peaks in the tilt, and similar swarms near

Puu Kamoamoas were at tilt minima. These swarms are very similar to but smaller than those accompanying inflation and slow intrusions. Caldera earthquakes signaled an inflated summit and ceased as magma drained downrift. Rift earthquakes were caused by local inflation of the rift and occurred while or just after magma was transferred there from the summit. The epicenters of events at the inflating rift can be seen in figure 43.3B as an elongate zone above the main magma conduit. One Puu Kamoamoas swarm (fig. 43.83A) occurred one day before another ERZ intrusion.

Similar episodes of shallow ERZ earthquakes near Puu Kamoamoas were observed from November 1978 to July 1979 (fig. 43.74A). These slow swarms also were generally at or just before minima in summit tilt. Episodes of summit earthquakes similar to those in 1980 were not apparent during this period, except possibly for earthquakes in April and May 1979 that coincided with brief intervals of rapid inflation (fig. 43.74A). The oscillations of tilt and an alternating pattern of earthquake locations did not develop as during the otherwise similar rift inflation of 1980. The rift dilation caused by the 1975 Kalapana earthquake and the ERZ eruption of September 1977 apparently opened most of the ERZ conduit and encouraged the passive magma transfer of 1978–79. Opening of the rift continued with the intrusions and eruptions of August and November 1979 and March 1980. Four additional but rapid ERZ intrusions in the latter half of 1980 apparently disrupted the delicate equilibrium of the magma conduit that permitted the regular cycles of slow intrusion in mid-1980.

#### EAST RIFT ZONE INTRUSIONS OF JULY–NOVEMBER 1980

The ERZ intrusions of July, August and October 1980 successively penetrated farther along the rift, as did the intrusions of August and November 1979 and March 1980. The July 30, 1980 swarm lasted only for about one hour and activated only the 2-km section of rift between Keanakakoi and Puhimau (fig. 43.81). No deflation was detected, apparently because only a small volume of magma was transferred. Earthquakes began nearly instantaneously along the zone. The high speed of swarm growth is probably a result of the presumed high temperatures and lower magma viscosity where the rift conduit adjoins the summit reservoir.

The intrusion of August 27, 1980, reached an additional 3 km downrift to Hiiaka (fig. 43.82A). The swarm began 3 km below Puhimau where the July intrusion terminated. The initial intense seismicity moved downrift at 1.6 km/h and remained at 3 km depth

(fig. 43.82D, F). As the main dike moved downrift, earthquakes also moved upward and uprift (fig. 43.82D). The dike had two horizontal lobes end-to-end at 3 km depth and a connecting vertical lobe (fig. 43.82C). Earthquakes propagated outward along each lobe from the initial center of activity. Summit reservoir deflation and the enlargement of all three seismic lobes were simultaneous. The uprift lobe may have fed magma to the dike system in the downrift direction, with earthquake migration opposite to magma flow. The process by which earthquakes can migrate uprift while magma flows downrift may be complex, but not impossible; for example, widening of an already open dike and the consequent earthquakes may begin from the end toward which magma is flowing and move against the flow direction as the dike fills.

The next intrusion on October 21–22, 1980, may actually have been two unrelated but nearly simultaneous events. The swarm beginning on October 21 near Puu Kamoamoas is apparently one of the last of the slow intrusions recurring from 1978 through 1980. The second intrusion occurred one day later and 14 km uprift of Puu Kamoamoas below the former Alae crater (fig. 43.83A, E). The Puu Kamoamoas swarm happened at a broad minimum in summit tilt typical for these slow intrusions (fig. 43.74C). The rapid deflation and more intense seismicity of the Alae swarm were on a much shorter time scale (fig. 43.83B, D). The second swarm was very compact (1.5-km diameter) and short (3 hours), but movement with time could be resolved. The downrift speed of 2.7 km/h (fig. 43.83H) and upward speed of about 2 km/h (fig. 43.83J) are consistent with the dip of the main finger of earthquakes seen in cross section (fig. 43.83G). The October 22 event appears to be a dike intruded into the rift blockage just downrift of the Pauahi magma pocket. Magma feeding the Puu Kamoamoas inflation probably traveled through a different rift conduit several days earlier, although a local increase in magma pressure could have triggered the second intrusion.

The October intrusion was followed in 11 days by another on November 2, 1980, just 2–3 km uprift (fig. 43.84A). The swarm was very intense but lasted only 4 hours. It began just uprift of Hiiaka and expanded downrift at 0.7 km/h (fig. 43.84D). Earthquakes also moved uprift, but only for about 1 km. No consistent depth migration can be seen, but earthquakes did spread up and down from 3 km depth (fig. 43.84F). Apparently a dike grew outward from a point near the main ERZ magma conduit. This intrusion was the last of a series of ERZ intrusions before Kilauea shifted its magma supply to the SWRZ.

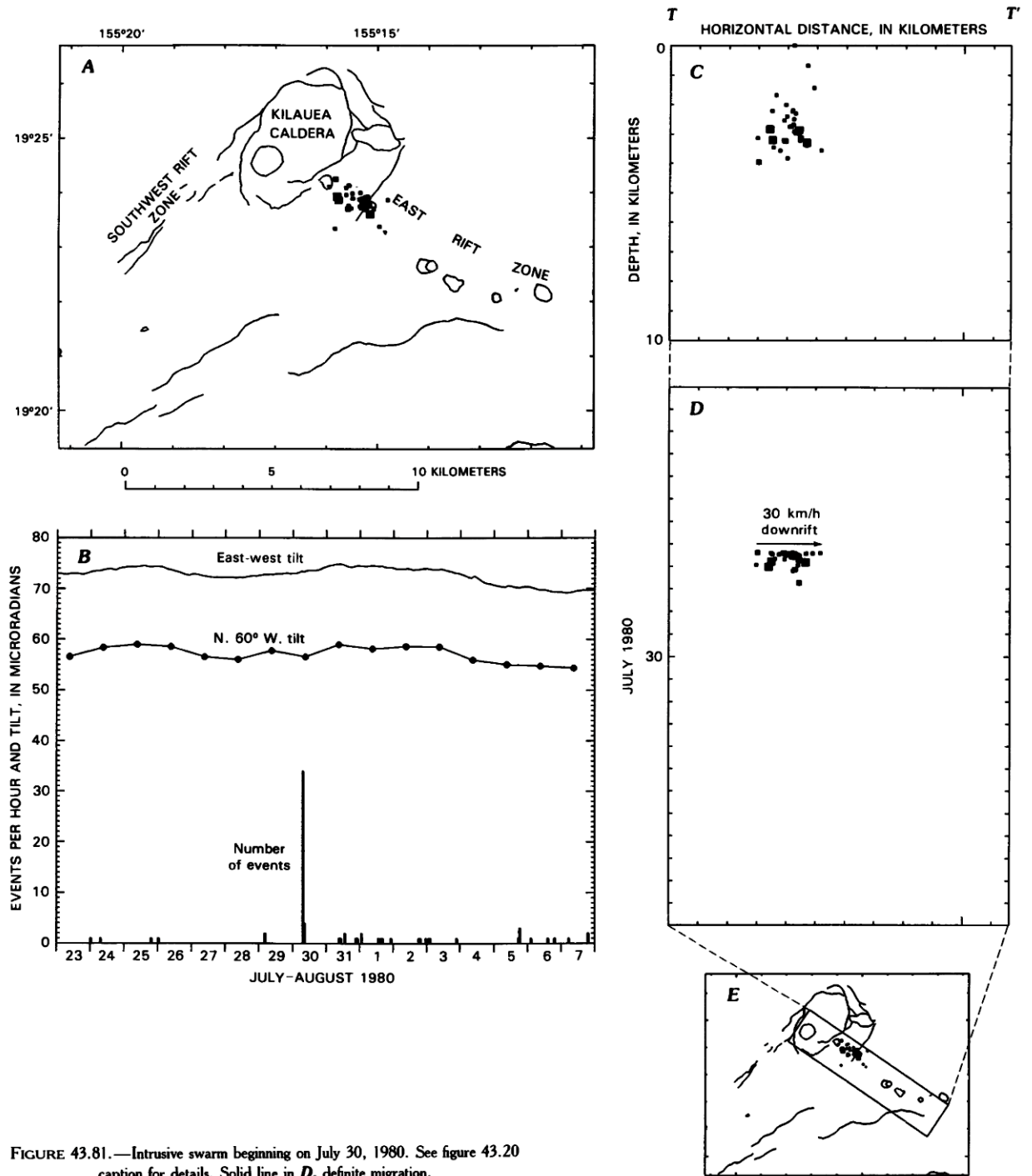


FIGURE 43.81.—Intrusive swarm beginning on July 30, 1980. See figure 43.20 caption for details. Solid line in *D*, definite migration.

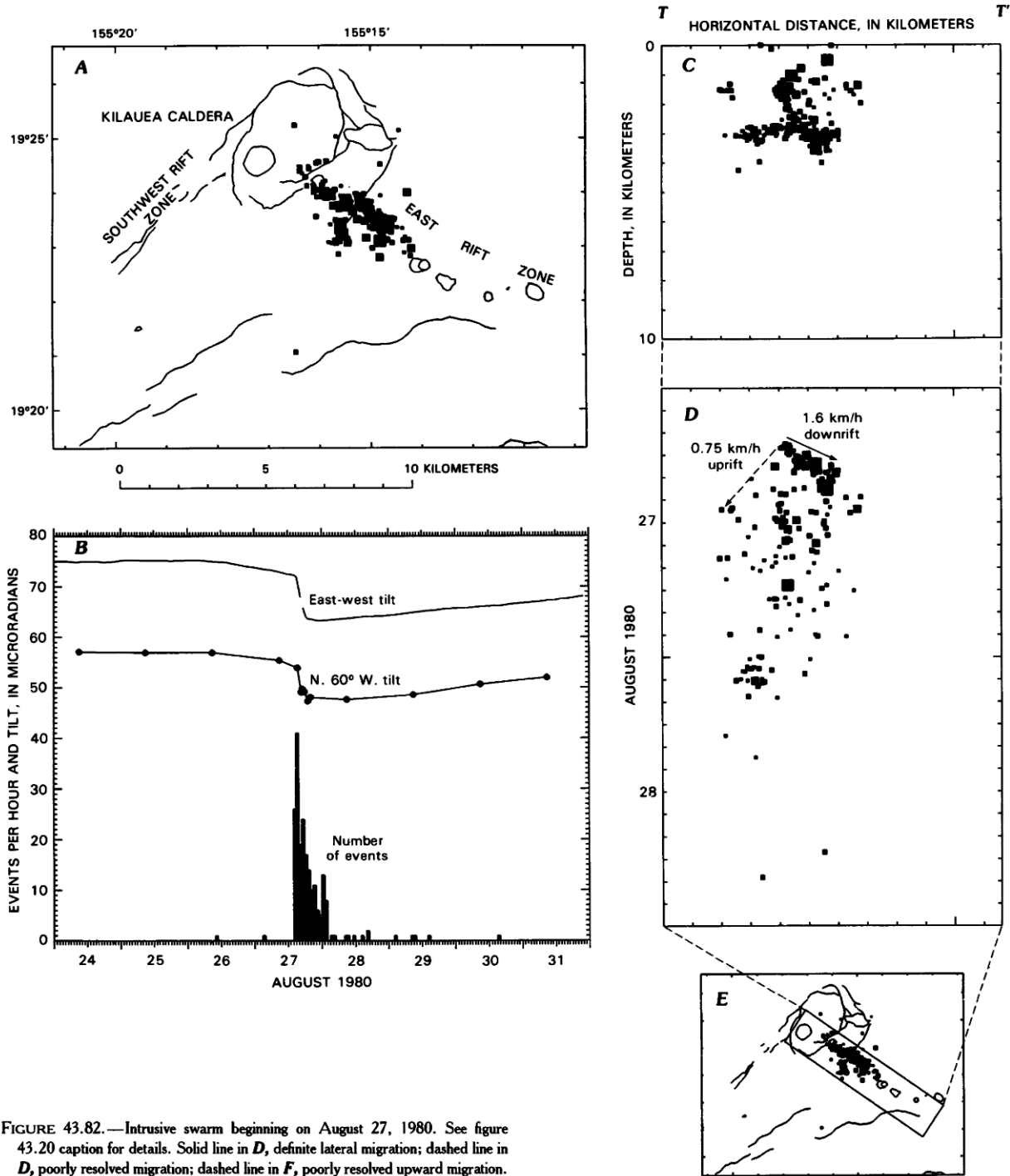


FIGURE 43.82.—Intrusive swarm beginning on August 27, 1980. See figure 43.20 caption for details. Solid line in *D*, definite lateral migration; dashed line in *D*, poorly resolved migration; dashed line in *F*, poorly resolved upward migration.

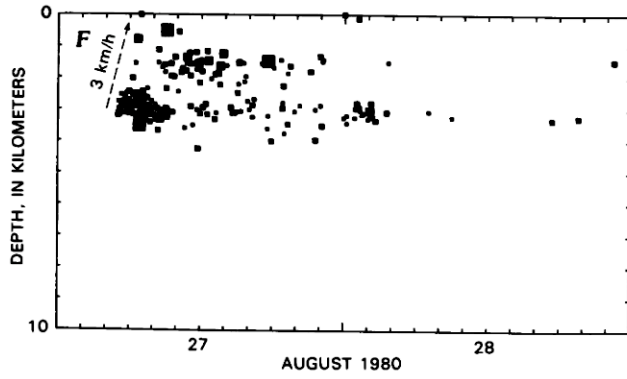


FIGURE 43.82.—Continued.

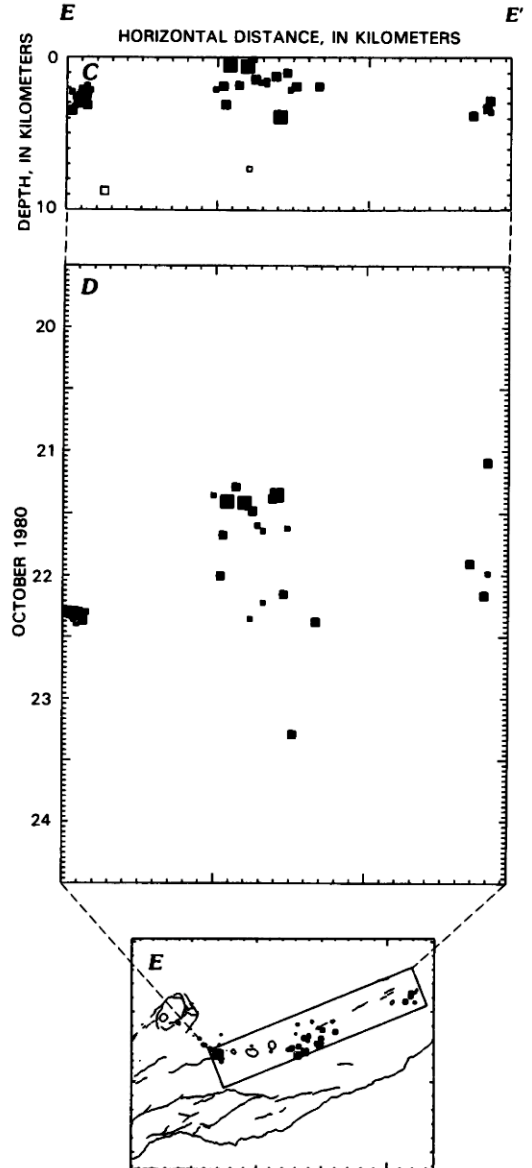
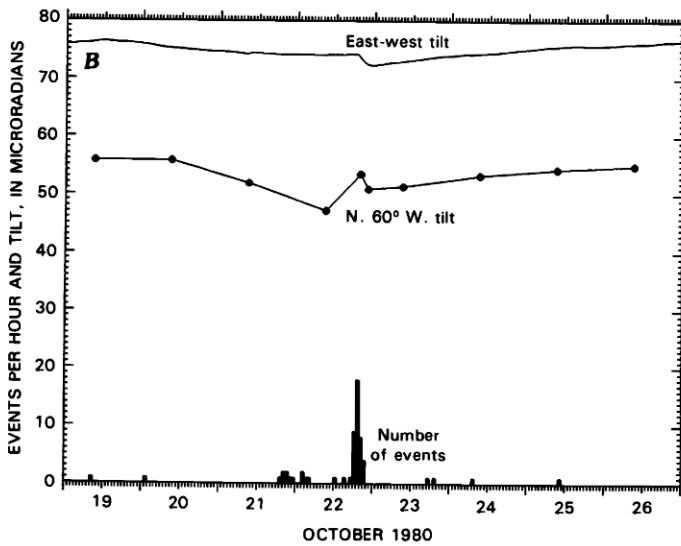
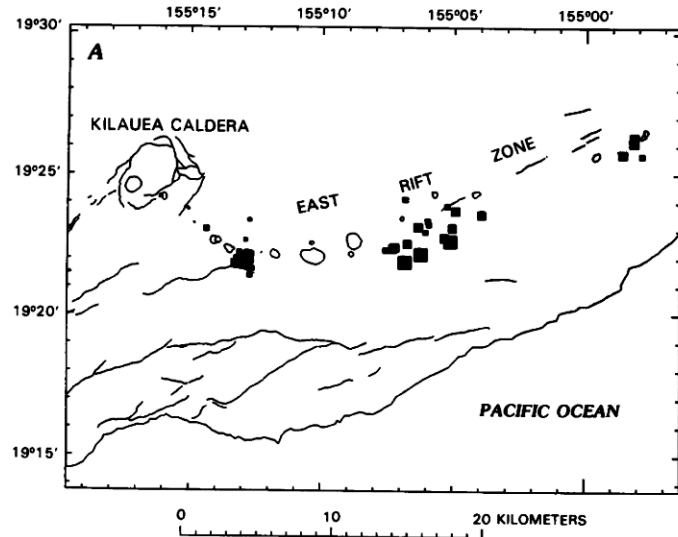


FIGURE 43.83.—Intrusive swarm beginning on October 21, 1980. See figure 43.20 caption for details. Solid line in *H*, definite lateral migration; dashed line in *J*, poorly resolved upward migration.

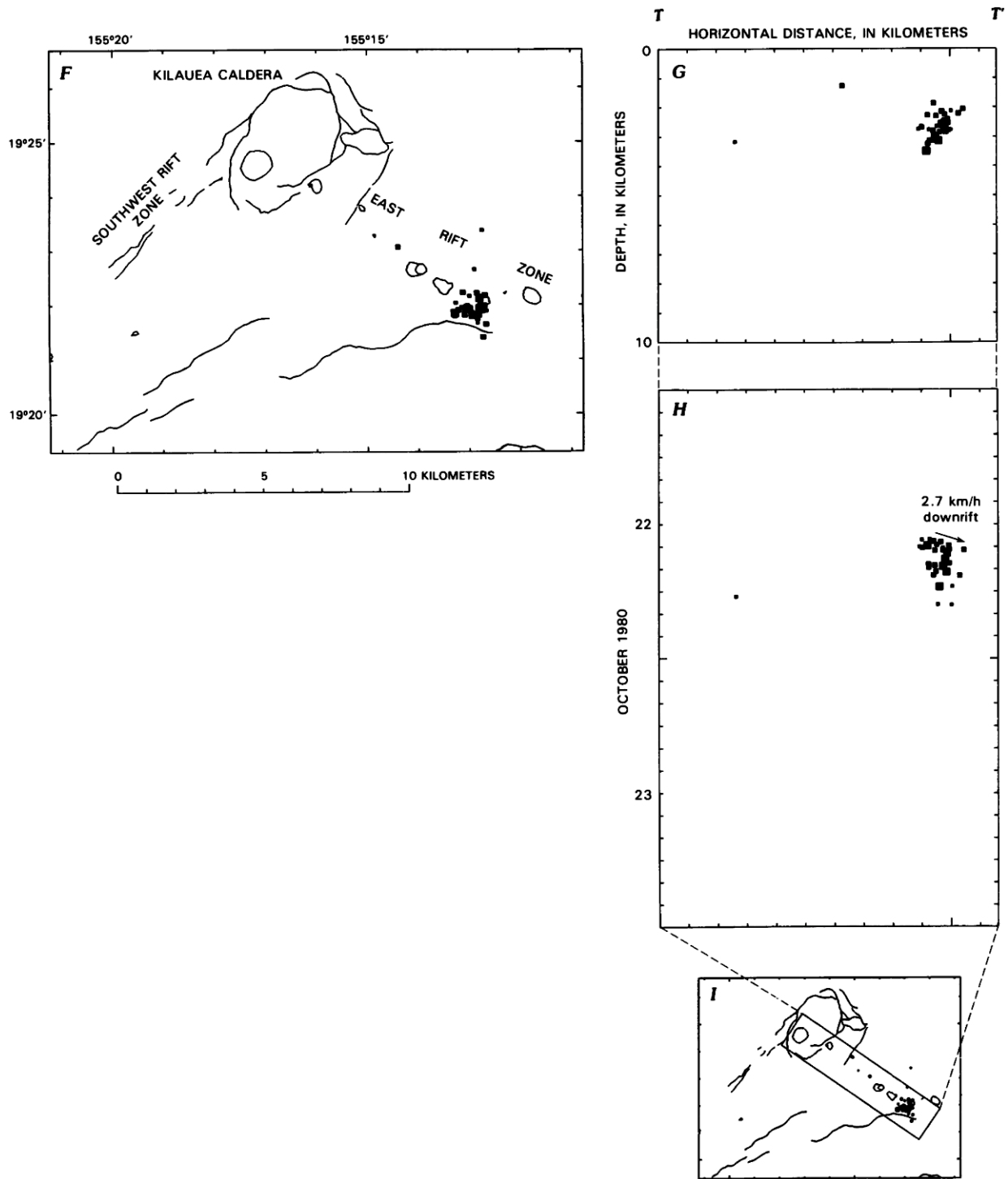


FIGURE 43.83.—Continued.

VOLCANISM IN HAWAII

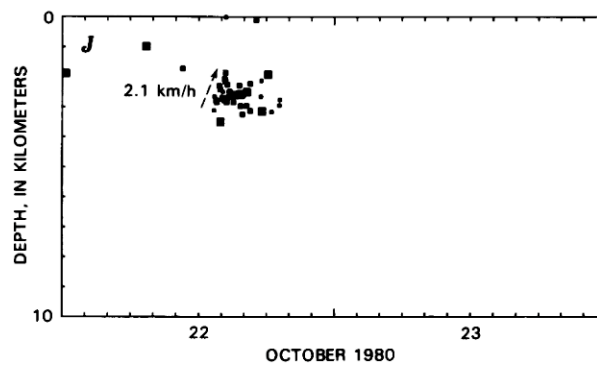


FIGURE 43.83.—Continued.

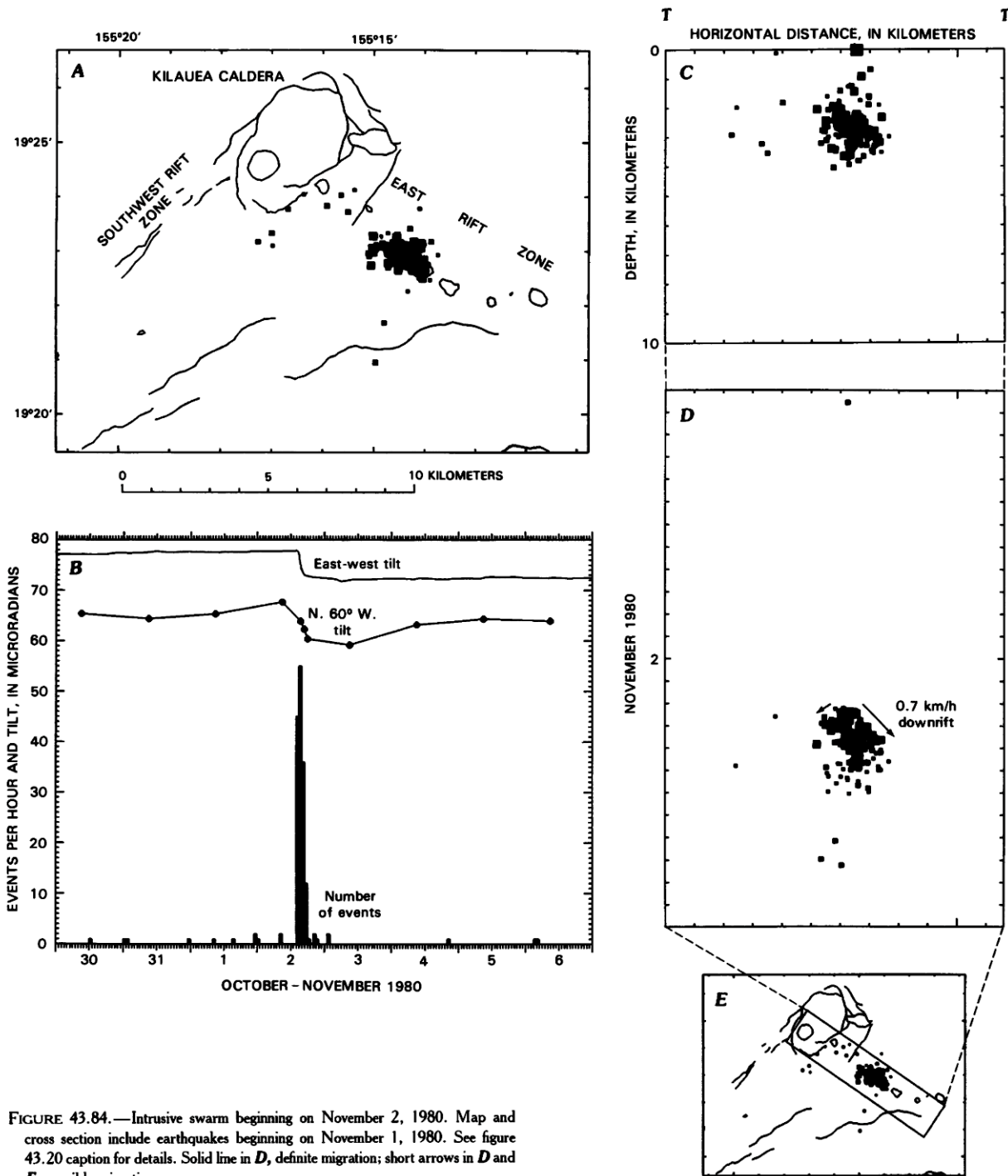


FIGURE 43.84.—Intrusive swarm beginning on November 2, 1980. Map and cross section include earthquakes beginning on November 1, 1980. See figure 43.20 caption for details. Solid line in *D*, definite migration; short arrows in *D* and *F*, possible migration.

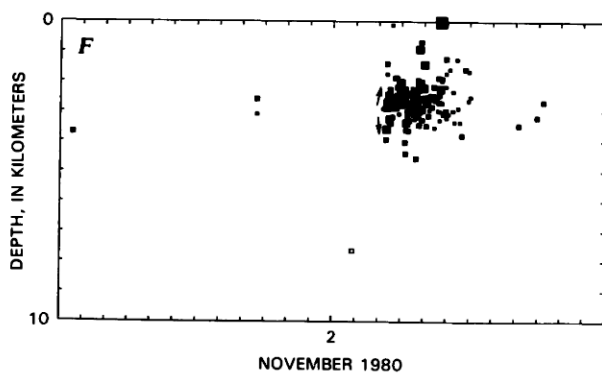


FIGURE 43.84.—Continued.

#### SOUTHWEST RIFT ZONE INTRUSIONS AND CALDERA ERUPTION OF JANUARY–AUGUST 1981

From January 1981 to mid-1982, Kilauea focused most of its magmatic activity on the SWRZ. Figure 43.85 summarizes the positions of shallow SWRZ earthquakes and summit tilt during this 18-month period. Three major intrusions occurred; the first penetrated the SWRZ in three progressive steps in January and February 1981, and continued to slowly pass magma into the SWRZ through June. The prolonged nature of this first intrusion did not require a major summit deflation. The other two intrusions in August 1981 and June 1982 followed a more conventional pattern of rapid summit deflation during a brief earthquake swarm, followed by reinflation of the summit reservoir.

The first phase of the January–February intrusion began on January 20, 1981, with a compact swarm in the main SWRZ magma conduit just south of the caldera (fig. 43.86A). No measurable deflation accompanied this first phase, and in fact Kilauea was inflating at this time (figs. 43.85A, 43.86B). Earthquakes did not migrate downrift, but did spread slowly north into the caldera as the seismic zone enlarged (fig. 43.86D). This phase was apparently the breaking open of a part of the magma passageway in response to inflation of the summit reservoir, but very little magma volume was actually intruded. Had it not been associated with the subsequent SWRZ intrusion and also produced so many earthquakes in a short period of time, this event may have been mistaken for a typical inflationary swarm.

The intrusion's second phase began on January 24 and demonstrated that a slow intrusion was in progress. Earthquakes now extended an additional 3 km along the rift in a zone including the bend in the magma conduit (fig. 43.87A). The deflation and earthquake rates were several times slower than in typical rapid

intrusions (fig. 43.86B). Earthquakes began almost simultaneously along the seismic zone, which remained uniformly active for 3–4 days (fig. 43.87C). This time behavior suggests that a section of the magma conduit filled slowly enough that its expansion was very uniform and without a fast-moving stress concentration such as the tip of a new dike. This pattern is consistent with earlier observations that the sections of rift adjacent to the caldera are often in direct magmatic communication and inflate with the summit reservoir. The January 20 swarm thus accompanied the breaking of a barrier and slow intrusion of the uppermost 5 km of the SWRZ during January 24–27.

The next phase of the intrusion began when magma moved almost aseismically down the SWRZ and generated a swarm near Puu Kou (fig. 43.88A). The sparse seismicity between the caldera and terminus of the intrusion seems to result from the low deflation rate (fig. 43.88B) and probable accommodation of magma flow through an existing conduit without additional rifting. The intrusion apparently stopped at a blockage of the conduit where the rift axis bends just north of the Great Crack. The main seismic zone tilts upward (fig. 43.88C), suggesting that the magma conduit began rising up and over the barrier until it lacked sufficient pressure to overcome it. The slowing expansion of the seismic zone upward and downrift (fig. 43.88D, F) would also be expected if the dike encountered a dipping barrier.

The unusual nature of the January SWRZ intrusion is underscored by the continuing seismicity along the rift through the first half of 1981. After the initial intrusion in January and February, earthquakes persisted in the Puu Koaie, Mauna Iki and Puu Kou areas through June (fig. 43.85A). The positions of earthquakes can be related to summit tilt to infer where magma accumulated during this period. The initial major deflation in February caused caldera earthquakes to stop for about two months, but they returned during the very slow reinflation in April. Their numbers increased as tilt rate accelerated in July. The seismicity of the rift was complementary to that in the caldera, and the pattern paints the following picture. In February and March, all of Kilauea's magma supply was directed into the SWRZ: the summit did not inflate and all earthquakes were downrift and caused by the intruded magma. In April, May and June very slight inflation occurred, a partial shift of seismicity back to the caldera was evident, and a fraction of the magma supply remained in the summit reservoir. The intrusion stopped in July, and typical inflation and earthquakes returned to the summit. This period illustrates the coincidence of falling or level tilt and rift seismicity during intrusions, and rising tilt and caldera earthquakes during inflation.

The passage of magma down the SWRZ was somewhat episodic: migrating pulses of earthquakes and hence magma may be discernable (dashed lines in fig. 43.85A). The speeds of these pulses ranged from about 0.12 km/hr (3 km/d) to 0.024 km/h (0.6

km/d), which are comparable to the speeds of other slow intrusions discussed in this paper. Kilauea's reinflation during July, combined with the opening and heating of the SWRZ magma conduit during the previous six months, apparently combined to permit the rapid intrusion in August 1981.

Just as before the January 1981 intrusion, earthquakes and magma leaked into the rift as a prelude to the August intrusion. Earthquakes slowly expanded into the SWRZ during July as the summit inflated (fig. 43.85A). A pre-intrusion also extended 5 km from the caldera on August 2 (fig. 43.89A). This pre-intrusion was scarcely noticed because no increase in earthquake activity or significant deflation was recognized (fig. 43.89B), only a shift in epicenters down the SWRZ (fig. 43.89D). The slight deflation suggests that some magma did move into the rift, but when this pre-intrusion reached the blockage in the magma conduit 5 km from the caldera, magma backed up and rapid inflation began, triggering the main intrusion on August 10. This pattern is very similar to that in January.

The intrusion on August 10 began with earthquakes just south of the caldera, which rapidly spread both into the caldera and downrift (fig. 43.90D). Some of the initial seismicity moved from the rift conduit at 3 km depth back and up over the magma reservoir (fig. 43.90C, D, F). The swarm soon engulfed the SWRZ from Halemaumau to Puu Kou (fig. 43.90G). The rapid downrift speed of 2.6 km/h slowed near the Kamakaia Hills by a factor of 10 to only 0.28 km/h (fig. 43.90J). The tilt rate slowed dramatically when the dike front reached Puu Kou on August 11 (fig. 43.90B). Earthquakes persisted mainly in the Puu Kou and Mauna Iki areas for about 5 days (fig. 43.90K). The seismicity near Mauna Iki actually spread back uprift. This uprift migration may have resulted from a wave of back pressure in the conduit produced when the downrift migration stopped. Earthquakes also continued in the caldera for about 5 days and were mostly long-period events associated with the subsidence and adjustment of the reservoir and its feeder conduit.

Many earthquakes were in dense clusters along the rift (fig. 43.90G, H). We associate these clusters with constrictions and barriers in the magma conduit. The passage of magma at these places thus required either formation of a new dike or the widening of an existing conduit too narrow to accommodate the magma flow. Either process causes earthquakes. Note that the terminus of the pre-intrusion on August 2 about 3 km east of Puu Koaie was very active then, but nearly aseismic during the August 10 intrusion (compare fig. 43.89A and 43.90A). Apparently this area had already rifted open, allowing the main intrusion to pass through aseismically.

Although the intrusion deepened with distance from the caldera, a cluster of earthquakes at only 1 km depth were seen just southwest of Puu Koaie (fig. 43.90H). These shallow earthquakes

were below the surface cracks produced by the intrusion. Both phenomena were apparently the result of an upward-branching dike from the main conduit that did not quite reach the surface. A plane joining the area of surface cracks and the main seismic conduit dips about 80° SE. This dip matches the shape of the seismic conduit in this area seen in cross section (fig. 43.19E, F) and the dip of the intruded dike deduced from leveling lines crossing the rift (Dvorak and others, 1983).

Comparing the August 1981 intrusion with others in the SWRZ is informative. The August intrusion was much faster and more energetic than the one in January–June, perhaps because the earlier intrusion opened and heated the magma conduit making subsequent intrusions easier. The migration rate in August was double that of the December 1974 intrusion, probably again because of the prior intrusive activity in 1981. Both the 1974 and 1981 intrusions activated the same section of rift, and both produced an apparent reflection from the intrusion terminus of earthquakes migrating back uprift. The 1974 intrusion was about 50 percent larger in magma volume and produced more earthquakes, especially in the flank south of the rift. The reduced flank seismicity in 1981 may have resulted from the intrusion's smaller size, a different distribution of emplaced magma, or release of compressive stress in the flank in 1975 during the intervening Kalapana earthquake.

The geometry of the August 1981 dike can be estimated from the observed rates of deflation and earthquake migration. Using a deflation rate of 11  $\mu$ rad/h at the time of the 2.6-km/h migration yields a cross-sectional area of  $(11/3)/2.6 \times 1000 = 1,500$  m<sup>2</sup>. A dike averaging 1.5 km by 1 m is consistent with earthquake migration speed and depth range and with deflation and geodetic observations. Pollard and others (1983) used a profile of surface displacements to constrain an elastic model of deformation surrounding a new dike. They inferred a dike dipping 82° SE., which is consistent with the dip of the seismically defined conduit of figure 43.14F. Their solution of a 1-m-thick dike extending from 0.25 to 2.75 km depth fits the surface profile everywhere except the central 3 km over the dike, where inelastic deformation occurred. Their cross-sectional area of 2,500 m<sup>2</sup> may include a shallow portion of the rift that grew aseismically and inelastically and that did not participate in the magma flow reflected in our 1,500-m<sup>2</sup> area.

The volume of intruded magma in August 1981 was about 35 million cubic meters, using the observed deflation and the value of 0.3 million cubic meters per microradian of Uwekahuna tilt from Dzurisin and others (1984). The August 1981 volume is comparable to that of the January–June intrusion. The tilt was nearly flat for the earlier period, so Kilauea's magma supply rate of about 9 million cubic meters per month (Swanson, 1972; Dzurisin and others, 1980) was mostly supplied to the SWRZ. Thus about 45 million cubic meters was supplied to the rift during the 5 months of the intrusion, but at a rate 100 times slower than in August.

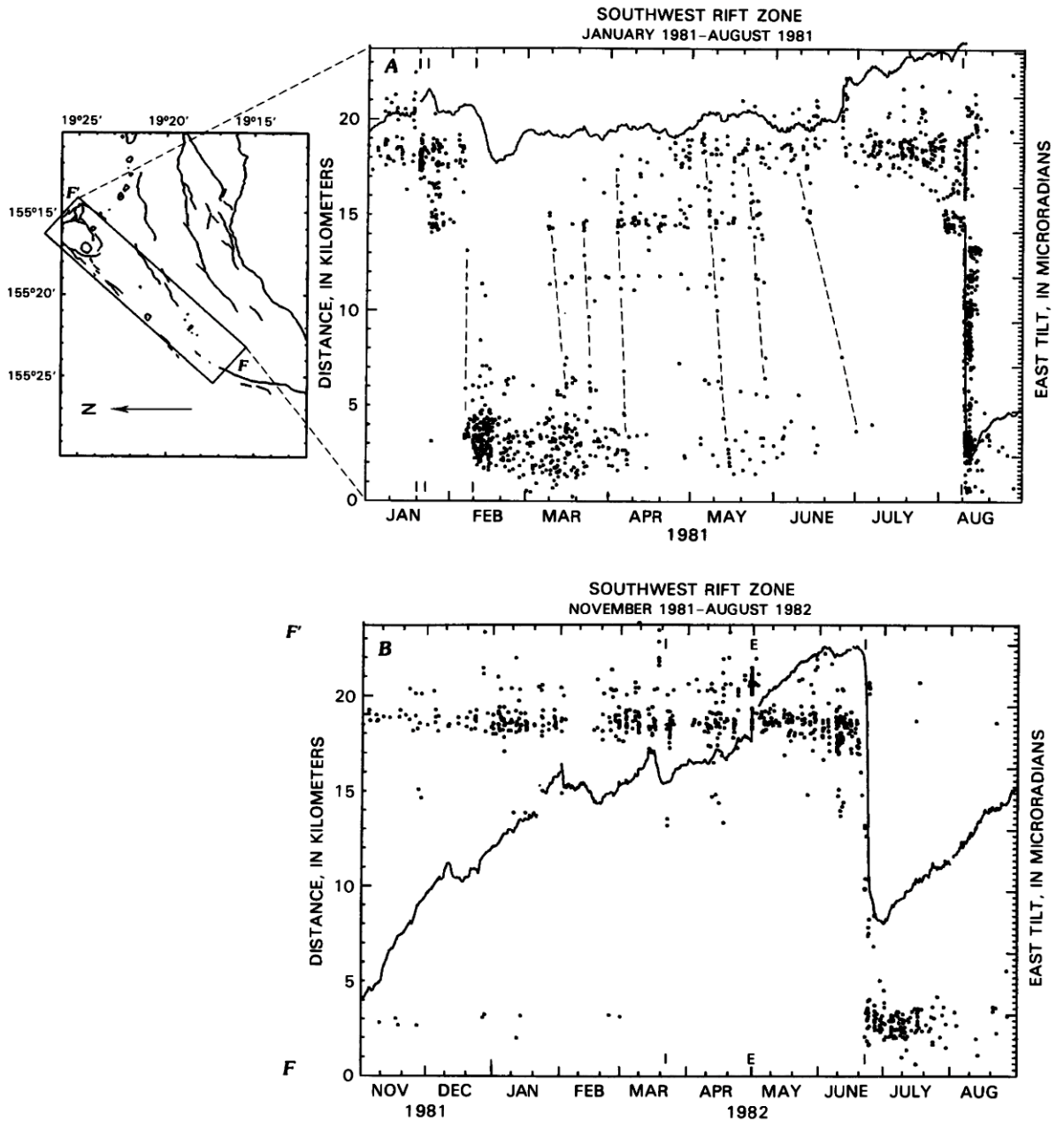


FIGURE 43.85.—Plot of earthquakes along the southwest rift zone and east tilt at Uwekahuna versus time. *A*, January through August 1981. *B*, November 1981 through August 1982. September and October 1981 are omitted and were a seismically quiet time of reflation. All earthquakes shallower than 5 km and within geographic box shown are plotted. Kilauea caldera is at top and Puu Kou is near bottom. Tilt is from Ideal-Aerosmith instrument and down on plot generally indicates deflation of summit caldera. Notations along time axis refer to specific swarms detailed in other figures: E, eruption; I, rapid intrusion. Dashed lines in *A* suggest individual intrusive pulses.

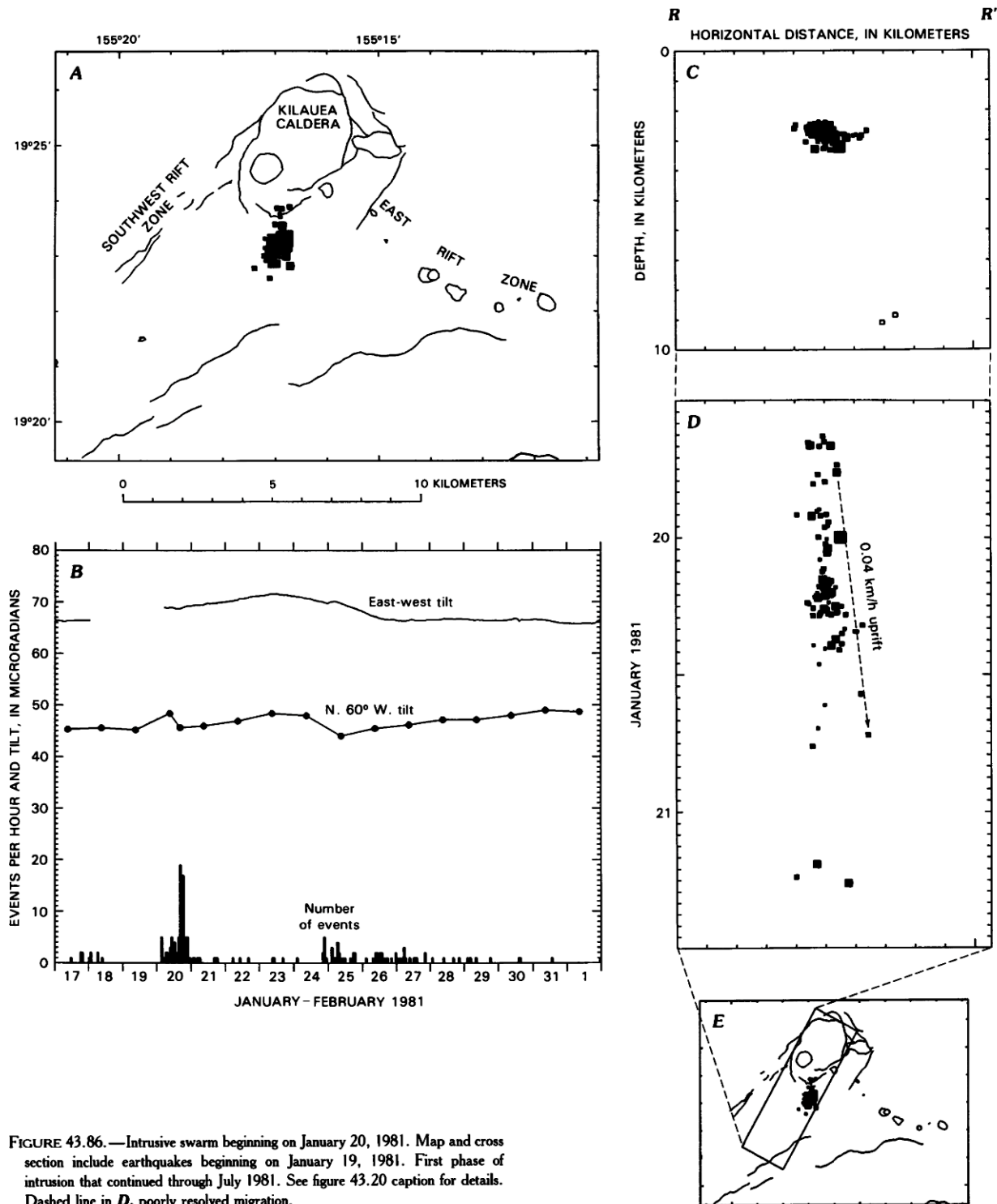


FIGURE 43.86.—Intrusive swarm beginning on January 20, 1981. Map and cross section include earthquakes beginning on January 19, 1981. First phase of intrusion that continued through July 1981. See figure 43.20 caption for details. Dashed line in *D*, poorly resolved migration.

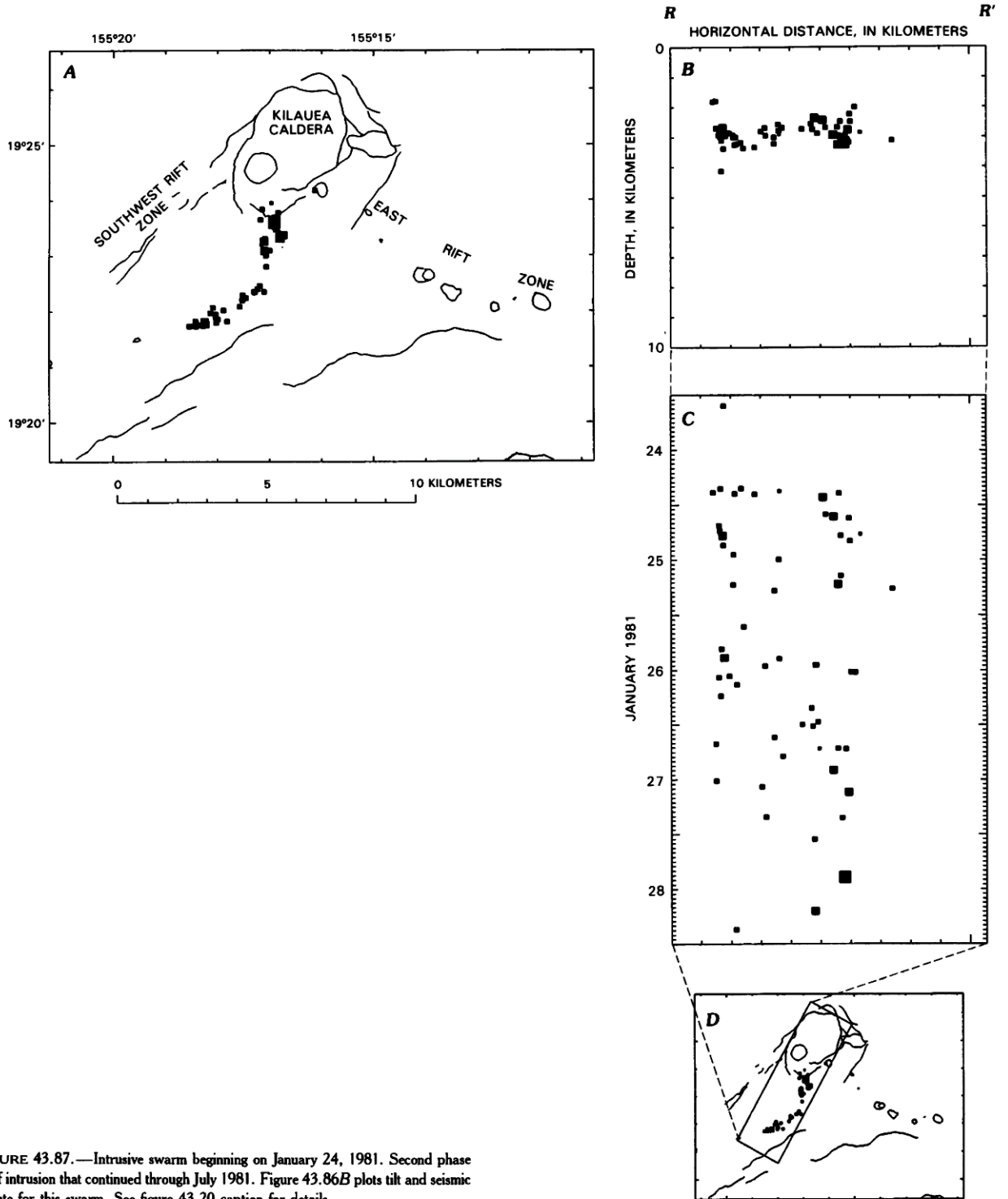


FIGURE 43.87.—Intrusive swarm beginning on January 24, 1981. Second phase of intrusion that continued through July 1981. Figure 43.86B plots tilt and seismic rate for this swarm. See figure 43.20 caption for details.

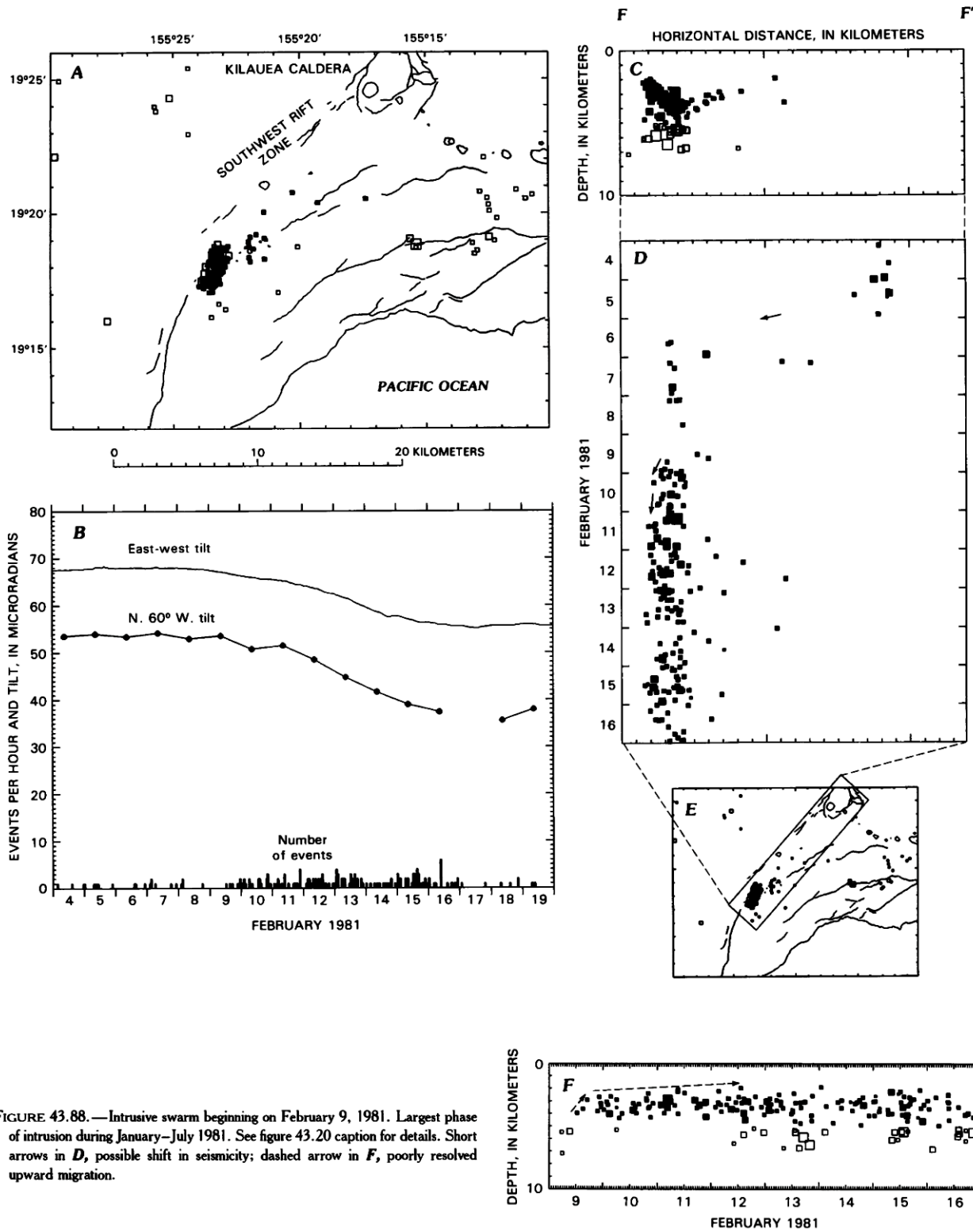


FIGURE 43.88.—Intrusive swarm beginning on February 9, 1981. Largest phase of intrusion during January–July 1981. See figure 43.20 caption for details. Short arrows in *D*, possible shift in seismicity; dashed arrow in *F*, poorly resolved upward migration.

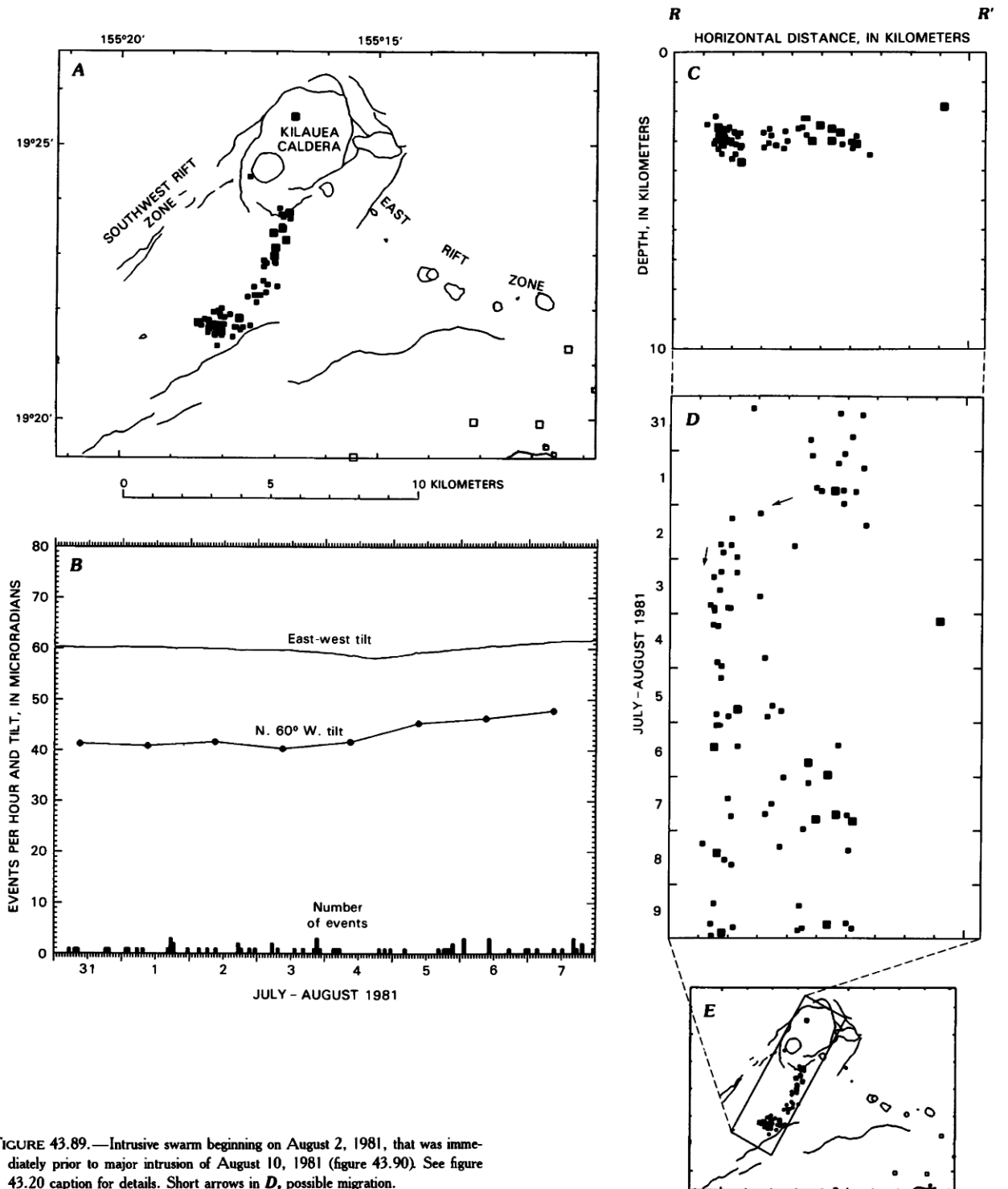


FIGURE 43.89.—Intrusive swarm beginning on August 2, 1981, that was immediately prior to major intrusion of August 10, 1981 (figure 43.90). See figure 43.20 caption for details. Short arrows in *D*, possible migration.

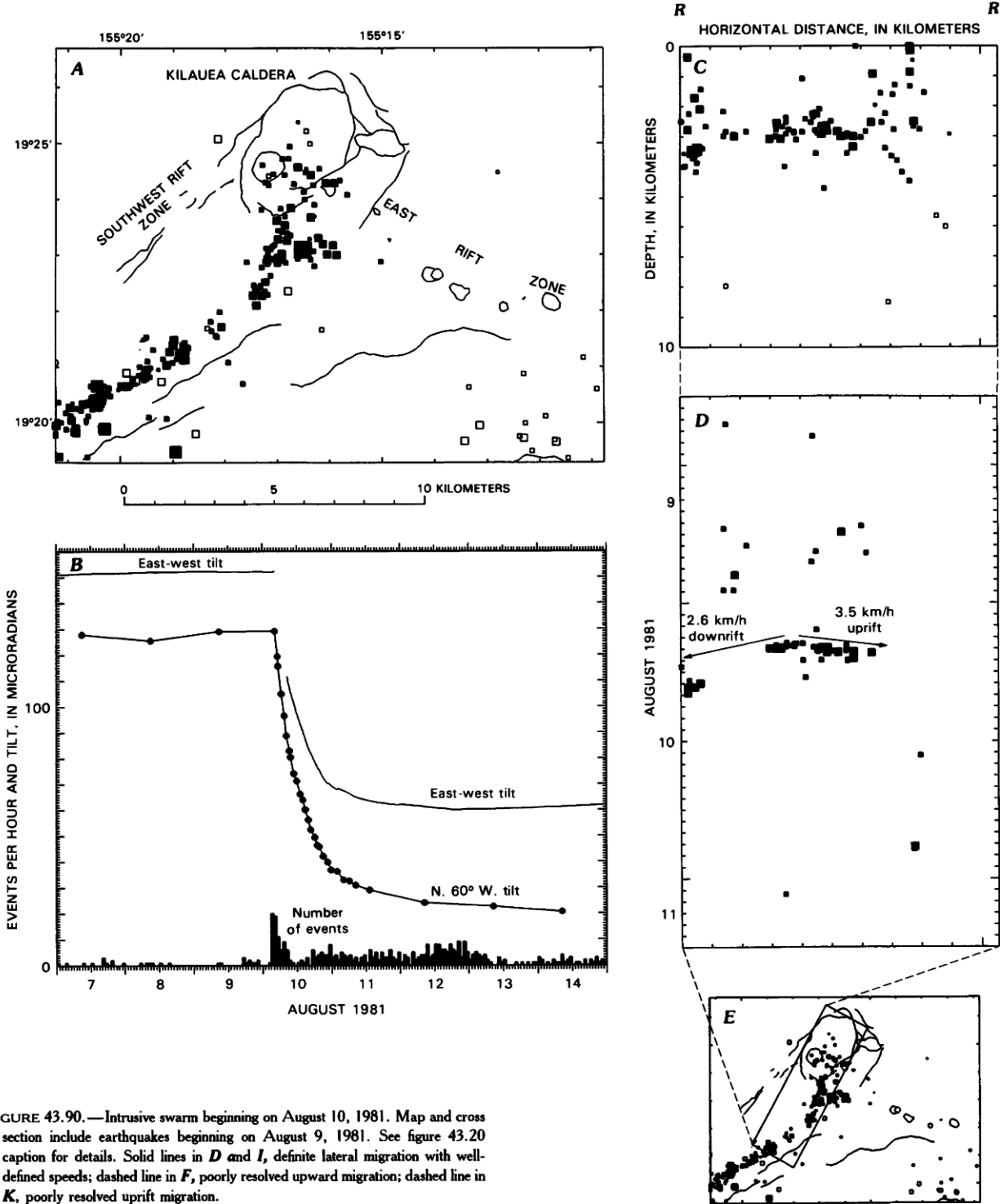


FIGURE 43.90.—Intrusive swarm beginning on August 10, 1981. Map and cross section include earthquakes beginning on August 9, 1981. See figure 43.20 caption for details. Solid lines in *D* and *I*, definite lateral migration with well-defined speeds; dashed line in *F*, poorly resolved upward migration; dashed line in *K*, poorly resolved uprift migration.

## VOLCANISM IN HAWAII

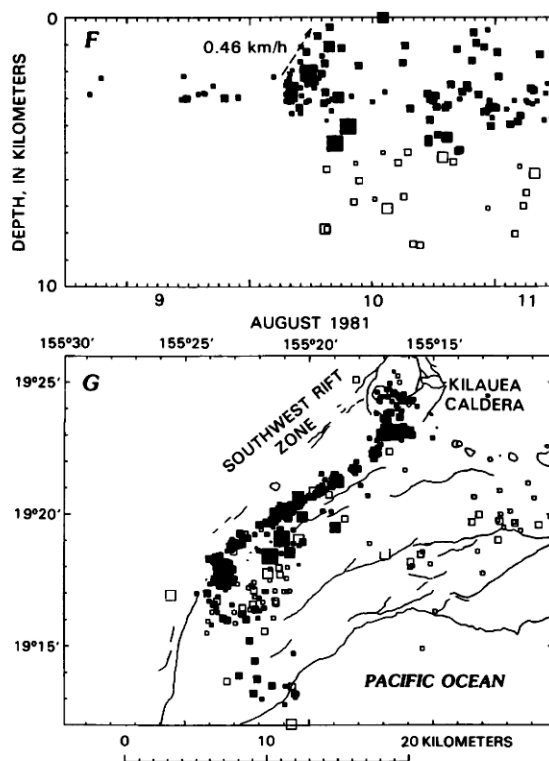


FIGURE 43.90.—Continued.

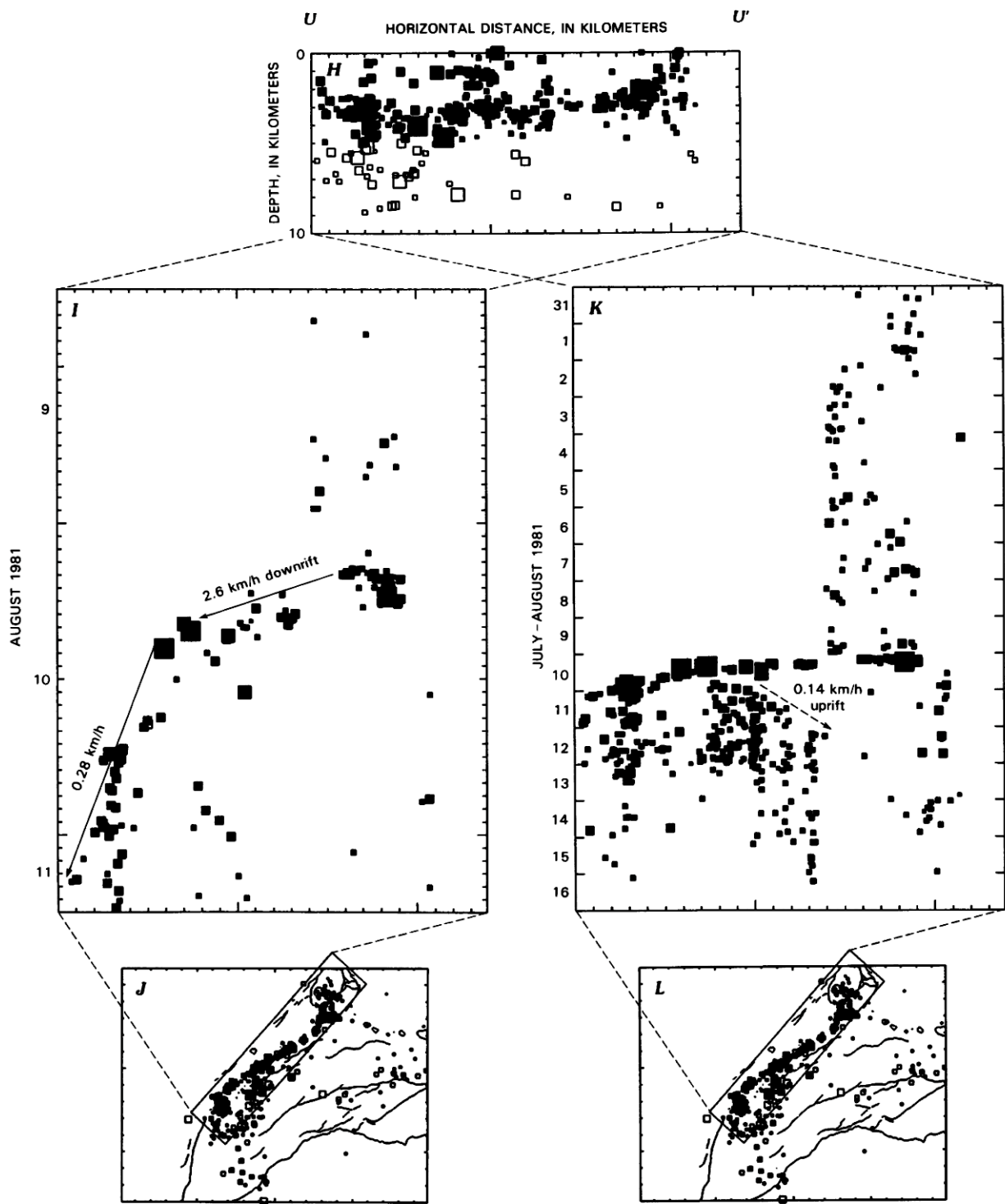


FIGURE 43.90.—Continued.

**THE SOUTHWEST RIFT ZONE INTRUSIONS AND CALDERA ERUPTIONS OF MARCH–JUNE 1982**

In the 10 months following the August 1981 intrusion, Kilauea reinflated rapidly and earthquakes in the south and central caldera steadily increased (fig. 43.85). Very little magma appears to have been intruded into the SWRZ, except possibly for three brief periods of slow deflation. The second deflation in February 1982 temporarily halted the caldera seismicity. The third deflation nearly did the same except for a one-hour swarm on March 23. The swarm may have marked a small intrusion just south of the caldera (fig. 43.91A), but if so the quantity of magma intruded during the swarm itself was so small it was nearly invisible on the tilt record (fig. 43.91B).

Kilauea's reflation was also punctuated by a brief caldera eruption on April 30, 1982. Earthquakes were located in the central caldera between Keanakakoi and the eruptive vent (fig. 43.92A). Earthquake depths primarily 1–2 km beneath the caldera were shallower than the main magma conduit of the adjacent ERZ (fig. 43.92C). The seismic zone was therefore above and to the side of the magma reservoir and did not align with the April vents. The earthquakes may thus have surrounded a set of dikes branching upward from the magma reservoir to the ERZ conduit. The redistribution of magma within the summit complex caused a brief tilt step at Uwekahuna (fig. 43.92B). The onset of the swarm was nearly instantaneous, but appeared to move very rapidly to the northwest (fig. 43.92D). The swarm preceded the eruption by about 2.5 hours, slightly shorter than for typical rift eruptions.

An intrusion in late June 1982 continued the SWRZ activity, but in a pattern very different from the other SWRZ intrusions of the previous 18 months. The June intrusion saw seismicity shift from the summit to the lower SWRZ, as had occurred after the August 1981 intrusion (fig. 43.85). Earthquakes only extended from Puu Koaie to Puu Kou, however, and most of the activity was below 6 km depth (fig. 43.93A, C). The main magma conduit at 3 km depth

scarcely produced any earthquakes, in marked contrast to all other SWRZ intrusions. The pattern of summit deflation was also unusual, having begun very gradually and without reaching the high tilt rates typical of the other SWRZ intrusions (fig. 43.93B). In addition, earthquakes lagged deflation by 1–2 days. Intrusive earthquakes generally begin at the onset of deflation and correlate closely in time with deflation rate, making this an unusual event.

The rates of deflation and earthquake migration suggest that the same uplift section of the magma conduit was involved in the December 1974, August 1981 and June 1982 intrusions. The observed downrift rate of earthquake migration in 1982 was about 0.2 km/h (fig. 43.93D). If the magma front proceeded at the same speed through the aseismic upper 6 km of rift, about 30 hours would have been required, which is close to the observed time delay between the onset of deflation and the first earthquakes seen downrift. We can also repeat the calculation of rift cross-sectional area done for the August intrusion using 0.2 km/h and a deflation rate of 0.83  $\mu$ rad/h. The result is an area of 1,400 m<sup>2</sup> involved in magma flow, which matches the values of 1,500 (1981) and 1,400 (1974) remarkably well.

We interpret the June 1982 intrusion as a relatively passive one into a magma conduit already rifted open by two major intrusions in the previous 1.5 years. The energetic seismicity and rapid deflation characteristic of new dike formation or a highly pressured intrusion were absent. The dike at 3 km depth was aseismic because it was filled with still-liquid magma from the recent intrusions. This older magma could be quietly pushed through the conduit without the wedging apart of wall rock that creates earthquakes. Downrift of Puu Koaie, rifting did extend below the shallow conduit to 10 km, which is the approximate depth of the pre-Hawaiian ocean floor. The intrusion probably represents a downward flow of magma within the SWRZ. The event then completed the cycle of SWRZ intrusions by separating the two flanks down to the base of the volcanic pile at which the south flank is decoupled from the lower crust.

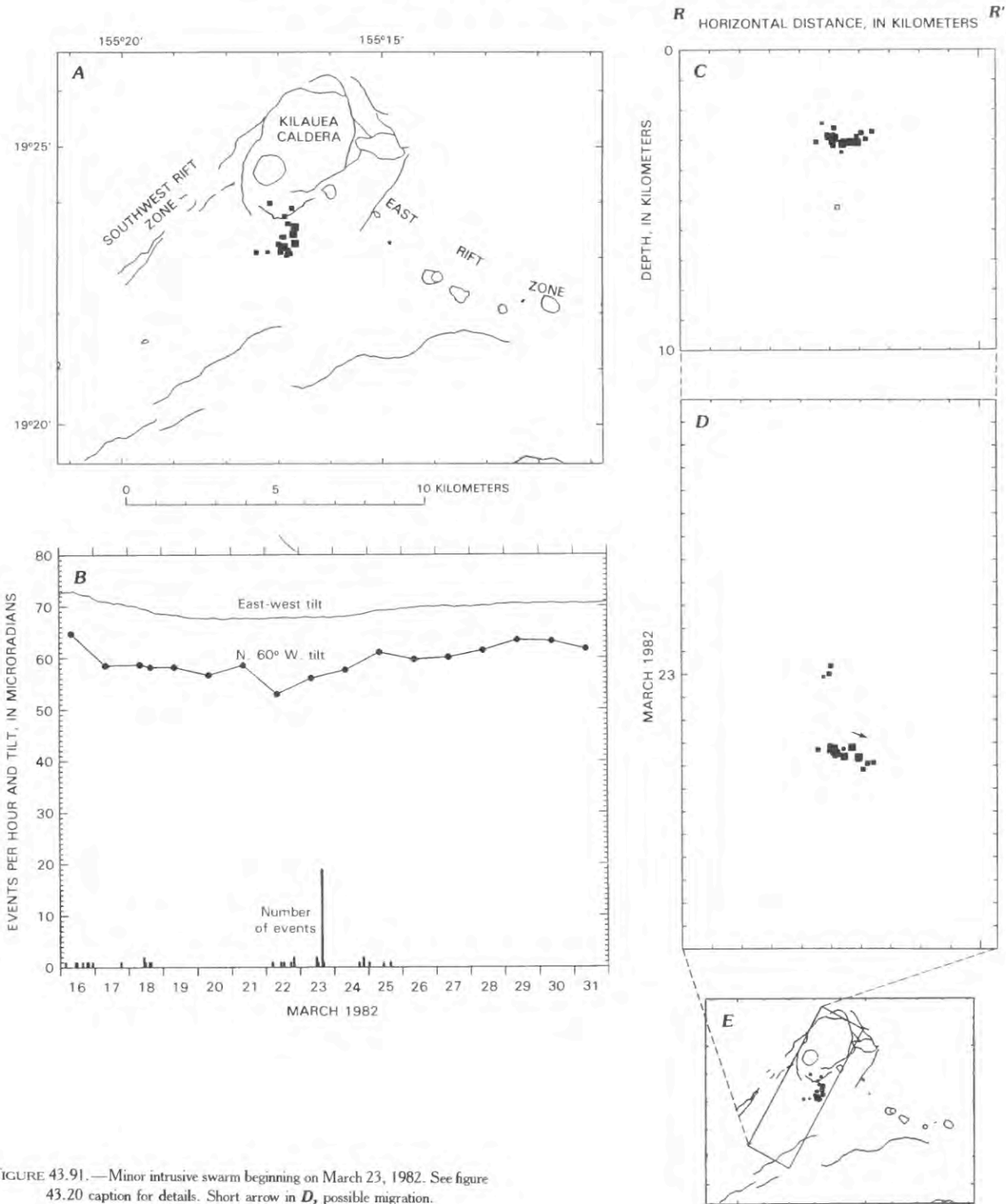


FIGURE 43.91.—Minor intrusive swarm beginning on March 23, 1982. See figure 43.20 caption for details. Short arrow in *D*, possible migration.

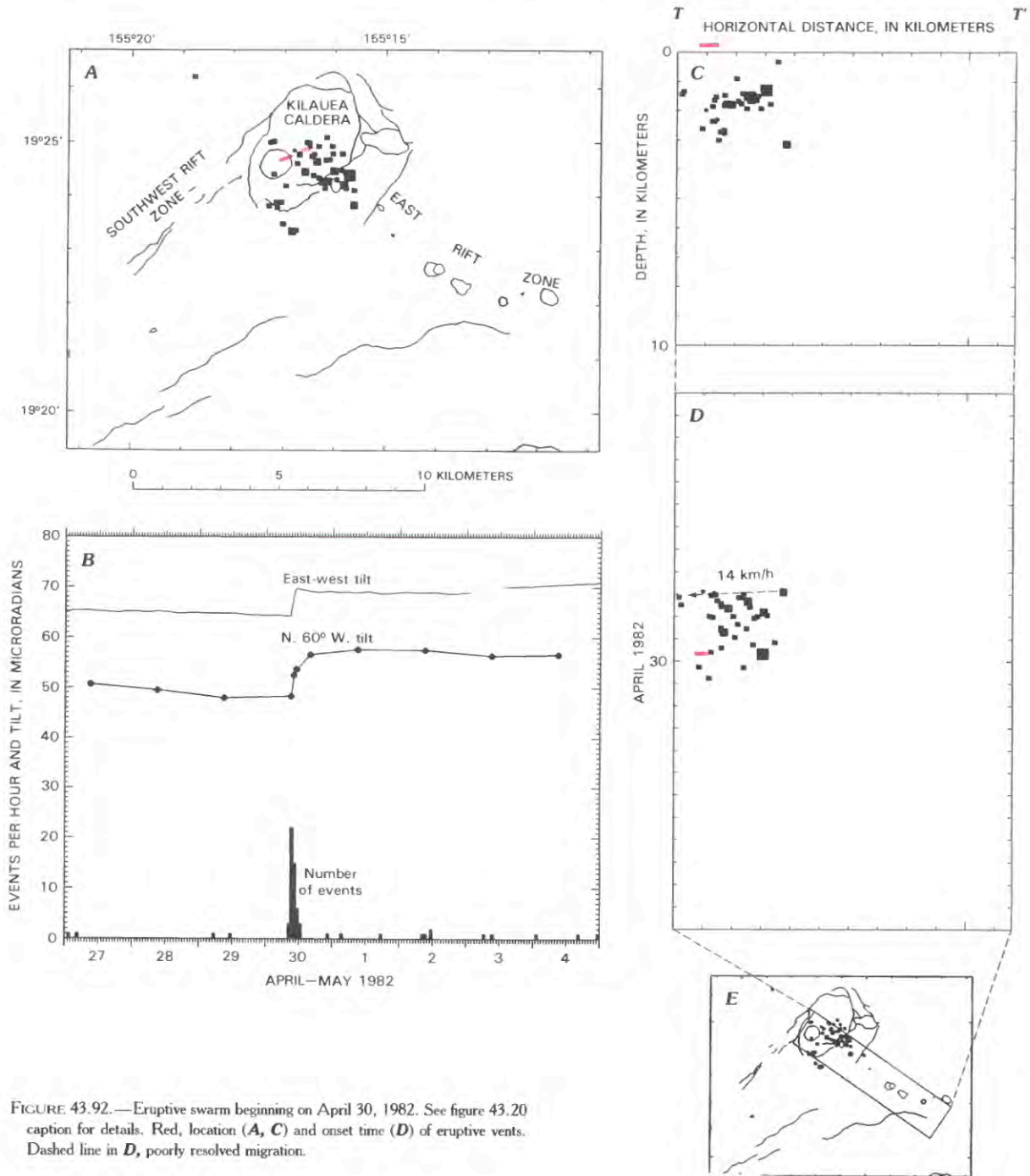


FIGURE 43.92.—Eruptive swarm beginning on April 30, 1982. See figure 43.20 caption for details. Red, location (A, C) and onset time (D) of eruptive vents. Dashed line in D, poorly resolved migration.

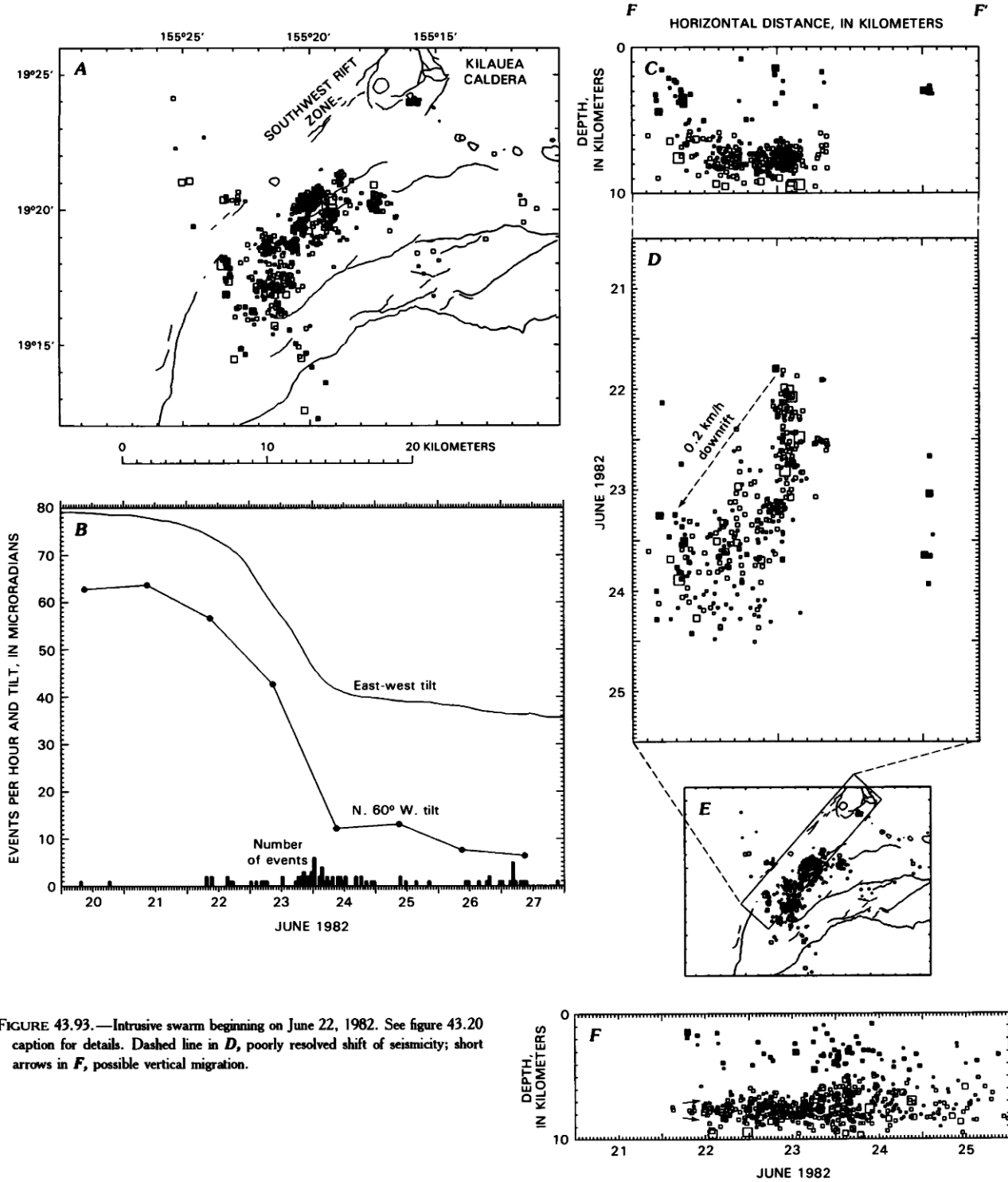


FIGURE 43.93.—Intrusive swarm beginning on June 22, 1982. See figure 43.20 caption for details. Dashed line in *D*, poorly resolved shift of seismicity; short arrows in *F*, possible vertical migration.

**CALDERA AND EAST RIFT ERUPTIONS OF SEPTEMBER 1982 THROUGH JANUARY 1983**

After several SWRZ intrusions, Kilauea began turning her attention back to the ERZ with a caldera eruption on September 25, 1982. The swarm began abruptly and coincided with a rapid step in summit tilt (fig. 43.94B). The intrusion affected portions of both the SWRZ and the ERZ adjacent to the caldera (fig. 43.94A). Earthquakes began under the area of the eventual vent in the south caldera. Seismicity soon spread to the ERZ and moved into both rifts at a speed of roughly 1.4 km/h for a short time (fig. 43.94D, G). A larger but slower wave of earthquakes moved into the ERZ about one hour later, presumably triggered by a major pulse of magma. As the intrusion progressed into the rifts, a dike also moved upward at about 1 km/h producing an eruption only about 2 h after the swarm began (fig. 43.94I).

When the dike reached the surface, earthquakes in the south caldera abruptly ceased (fig. 43.94G). This relation shows that the eruptive and intrusive dikes were hydraulically connected and the erupting dike dropped the magma pressure below the point needed to generate earthquakes. Earthquakes continued in the ERZ, however, which presumably was not as closely connected and did not feel the pressure drop at the time of eruption (fig. 43.94D). The sharp decline in seismicity early in the morning of September 26 is partly a result of masking of the seismograms by high tremor and partly of the real cessation of seismicity caused by magmatic pressure release accompanying the eruption. Conversely, the burst of ERZ seismicity following the eruption at about 0900 H.s.t. on September 26 is a result of timing more earthquakes and the apparent diversion of magma from the eruption to intrusion in the ERZ.

The September 1982 caldera eruption appears to have reactivated the ERZ following its quiescence during the series of SWRZ intrusions. This ERZ activity is partly demonstrated by the multiple pulses of magma intruded at the time of the eruption (fig. 43.94D). The ERZ also appears to have received magma during a slow and continuous intrusion during the month following the erup-

tion. This slow intrusion is revealed by the flat summit tilt, the continuing seismicity in the Kokoolau area and the general tendency of earthquakes to migrate slowly downrift (fig. 43.95). The migration speed was a very slow 6 m/h (0.14 km/d). It was thus not surprising that the next two magmatic events were in the ERZ.

A rapid intrusion of the ERZ on December 9, 1982, extended from the caldera almost to Hiiaka (fig. 43.96A). Earthquakes thus reactivated the same area which was intruded during September and October (fig. 43.95), and the same conduit or dike was likely active at both times. Earthquakes migrated downrift at a rapid 6.4 km/h (fig. 43.96D), one thousand times faster than in October. The earlier slow intrusion, as with the SWRZ in 1981, may have prepared and heated the magma conduit and thus enabled the succeeding intrusion to move very rapidly. The high speed of intrusion may also have been aided by its proximity to the magma reservoir and the frequency of intrusion in this section of the ERZ. Coincident with the most intense seismicity, earthquakes migrated upward at about 0.8 km/h (fig. 43.96F). The upward movement thus followed the downrift migration by 1–2 hours. Magma apparently was deflected upward by the same blockage in the main conduit that halted both this and the October intrusion between Kokoolau and Hiiaka. The three weeks following the December 9 intrusion saw continuing seismicity in the Kokoolau area (fig. 43.95). After December 19, earthquakes began downrift of Pauahi, suggesting that the ERZ was transferring magma downrift in possible preparation for another event.

The ERZ swarm that began on January 1, 1983, was to lead to a major and long-lived eruption. Earthquakes only accompanied the first few eruption phases in early January, however. All succeeding major eruptive episodes were localized to the Puu Oo vent area, a continuous ERZ magma conduit was kept open by the eruption, and essentially no additional volcanic seismicity and probably no new dikes were created. Because this eruption captured most of Kilauea's magma supply, none was left to produce an eruption or intrusion elsewhere. The January 1983 sequence is thus the last

volcanic swarm in this chronology, which is complete through mid-1985.

The earthquake swarm and other studies of the first part of the eruption are treated in detail by Koyanagi and others (in press) and Wolfe and others (in press). The seismic zone extended 17 km from Makaopuhi to just east of Kalalua (fig. 43.97A). Eruptive vents were confined to an 8-km segment from Napau to Puu Kahaualea, so the zone of intrusion was about twice the length of the ERZ experiencing extrusion. Earthquakes were concentrated along the ERZ magma conduit centered at about 2.5 km depth near Makaopuhi, but deepening to 3.5 km beneath Kalalua (fig. 43.97C). Most earthquakes are clustered and are probably at highly stressed areas where magma flow is constricted.

Magma was supplied from the summit reservoir for the 7 days of the swarm, but at a slower average rate than during other intrusions of comparable size. The summit tilt curve (fig. 43.97B) does not show the typical initially rapid subsidence followed by a gradual leveling off: the deflation rate was instead relatively constant except for pauses on January 3, 4 and 6. Seismicity was roughly correlated with deflation rate, both being higher on January 2, 5 and 7.

Both earthquakes and eruptive vents moved successively downrift and in a complex and protracted pattern, eventually localizing near what was to become Puu Oo. The initial seismicity just uprift of Makaopuhi on January 1 broke downrift at 0.6 km/h on January 2 (fig. 43.97D). This first intense seismicity stopped when it reached Napau. The first emission of lava was at Napau about 24 hours after the first earthquakes reached that point. Earthquakes also shallowed with time on January 2 just prior to the first eruption (fig. 43.97F). The vent then opened progressively downrift at the same speed as the downrift earthquake migration, stopping near Puu Kamoamo. The progress of the vent coincided with the cessation of earthquakes at the same point, which thus apparently released the magma pressure that caused the earthquakes. In fact the first phase of the swarm consisted of a zone of earthquakes whose

leading and trailing edges both moved downrift at 0.6 km/h (fig. 43.97D). The last part of the trailing edge of earthquakes coincided with the start of eruption. Earthquakes at any one point lasted for about 24 hours, which probably represents the time for stress to be released either by the growth of the dike to its full width and height or for magma to reach the surface and relieve pressure.

The next phase of the swarm from noon on January 3 through January 6 was marked by somewhat reduced seismicity that expanded slowly both uprift and downrift from near Puu Kamoamo (fig. 43.97D). Both deflation and the eruption had stopped during the first 2 days of this period. A shallowing of earthquakes preceded the resumption of lava emission at noon on January 5 to the east of Puu Kamoamo (fig. 43.97F). For the last phase of the swarm, earthquakes shifted from uprift of the vents (fig. 43.97D). The intrusion then extended an additional 4 km downrift, moving at the same 0.6 km/h speed as the initial intrusion from Makaopuhi to Napau. The intrusion and most earthquakes stopped when the next eruption phase began on the morning of January 7.

The complexity of the swarm in space and time indicates that it was really several successive intrusions that opened the magma conduit from Makaopuhi to the eventual site of the Puu Oo vent. The conduit opened rapidly from Makaopuhi to Puu Kamoamo, then at about 1/25 the initial speed to the lowermost vent, which was established at about the same time as another rapid but short extension of the dike downrift. When the swarm was less than half over at about 1530 H.s.t. on January 3, the eruption stopped, the number of earthquakes diminished and they began moving back uprift, and the summit tilt had leveled off. Apparently the major downrift flow from summit reservoir to vent was momentarily stopped or blocked, and increasing magma pressure and dike growth moved back uprift. This uprift growth originated at the same hypothesized barrier in the magma conduit that initially prevented the vent from opening farther downrift. A variety of these space and time relations are common to many intrusions and will be summarized and discussed in the next section.

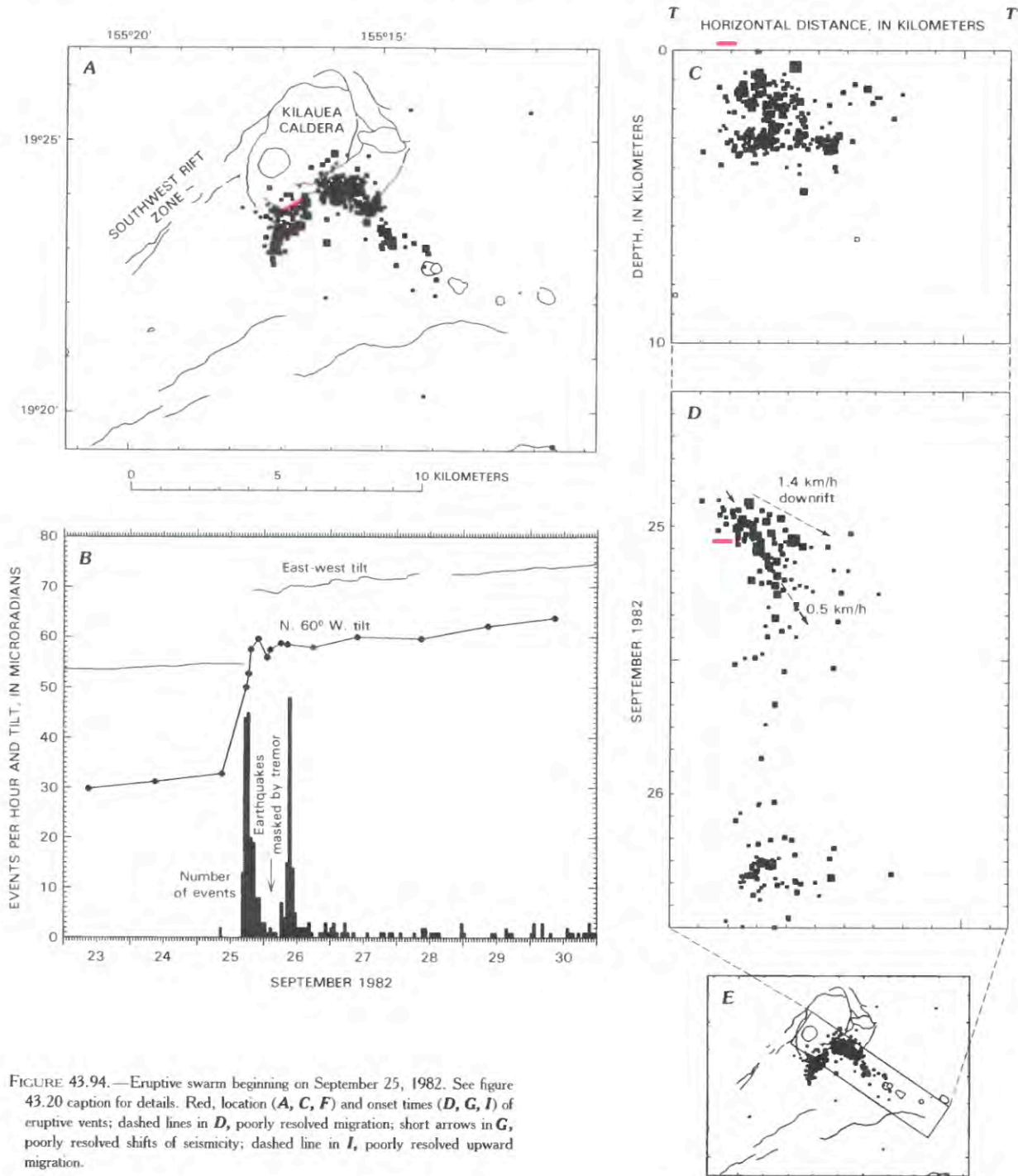


FIGURE 43.94.—Eruptive swarm beginning on September 25, 1982. See figure 43.20 caption for details. Red, location (A, C, F) and onset times (D, G, I) of eruptive vents; dashed lines in D, poorly resolved migration; short arrows in G, poorly resolved shifts of seismicity; dashed line in I, poorly resolved upward migration.

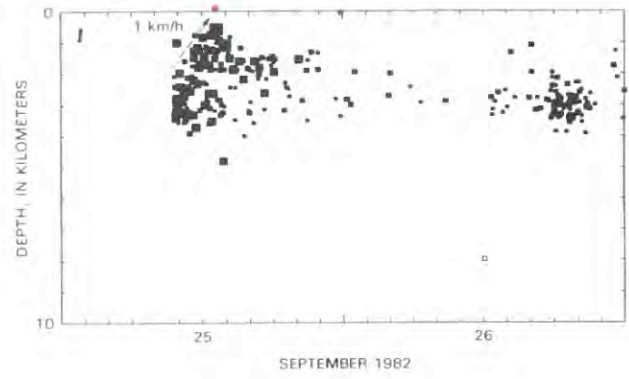
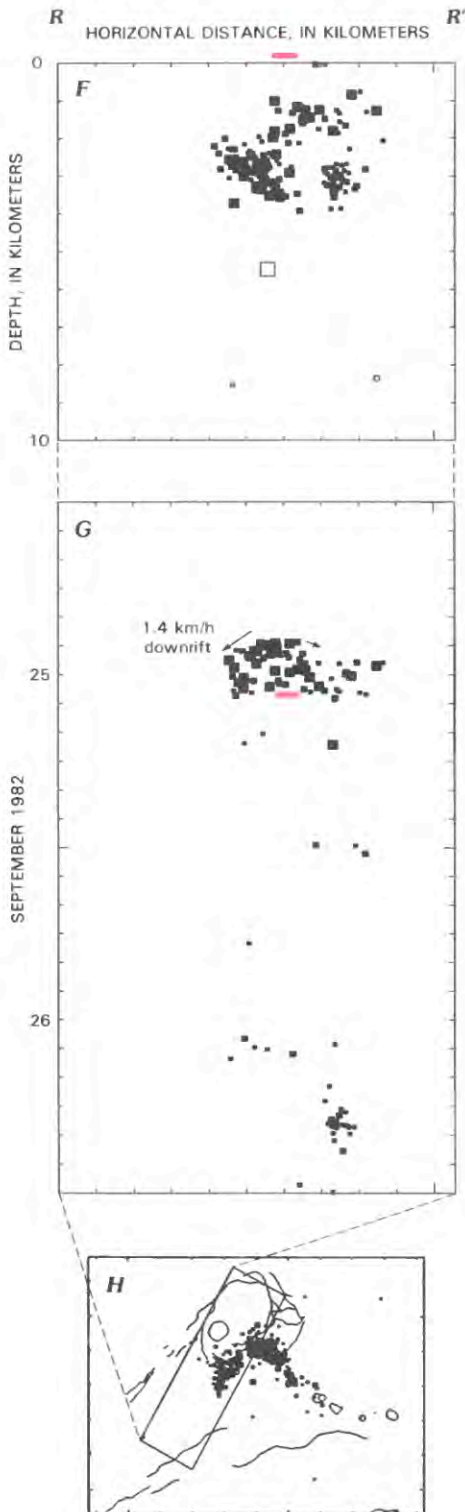


FIGURE 43.94.—Continued.

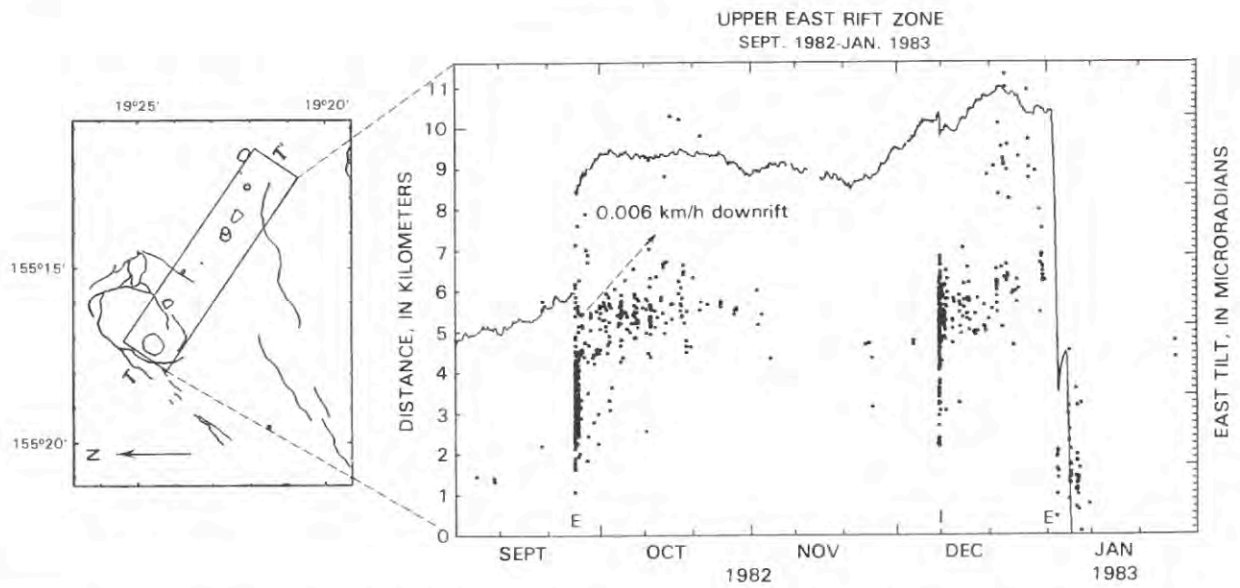


FIGURE 43.95.—Plot of earthquakes along east rift and east tilt at Uwekahuna versus time. All earthquakes shallower than 5 km and within geographic box shown are plotted. Halemaumau is at bottom and Mauna Ulu is near top. Tilt is from Ideal-Aerosmith instrument and down on plot generally indicates deflation of summit caldera. Large divisions on tilt scale are  $10 \mu\text{rad}$ . Notations along time axis refer to specific swarms detailed in other figures: E, eruption; I, rapid intrusion. Dashed line, poorly resolved but very slow migration.

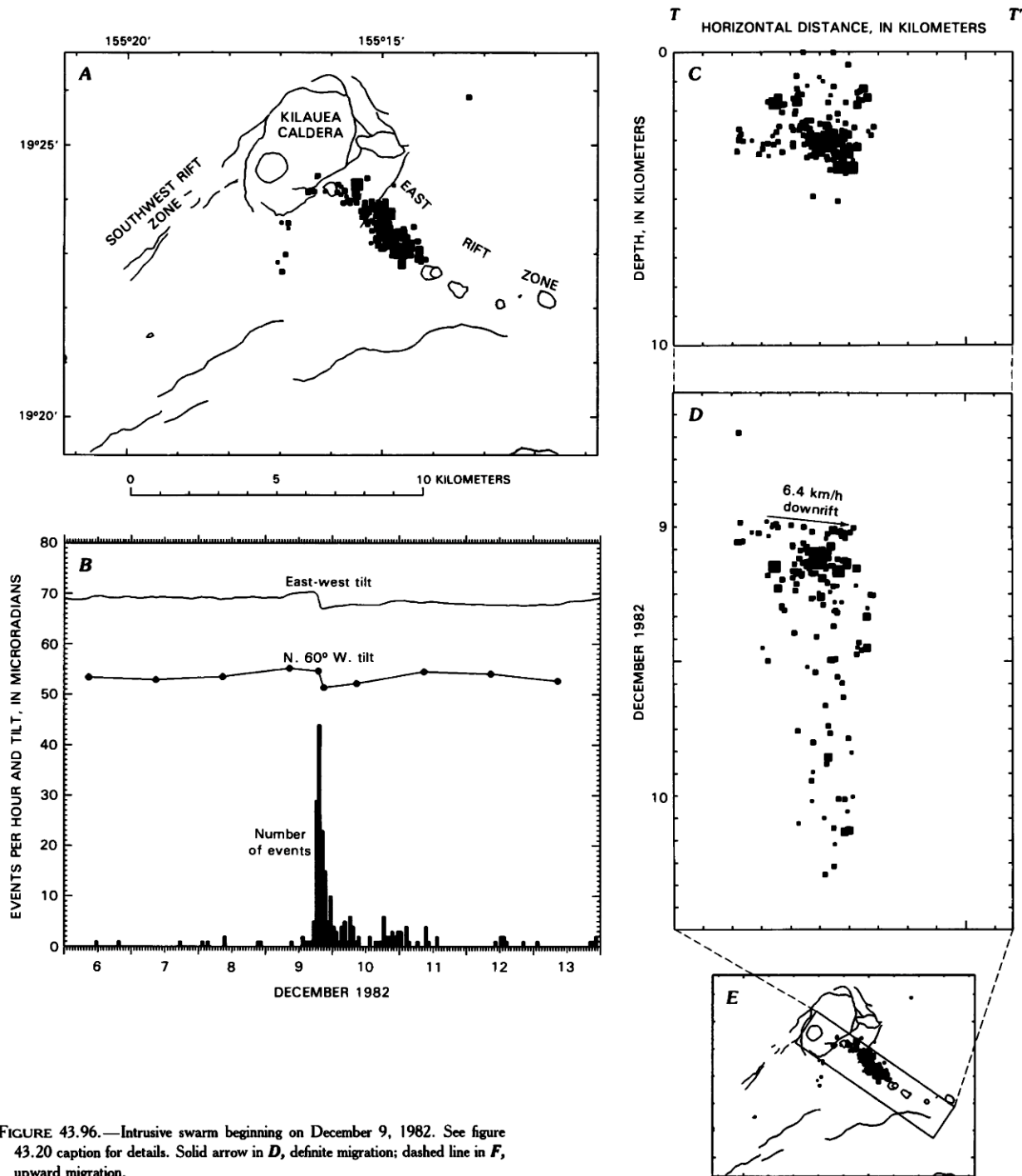


FIGURE 43.96.—Intrusive swarm beginning on December 9, 1982. See figure 43.20 caption for details. Solid arrow in *D*, definite migration; dashed line in *F*, upward migration.

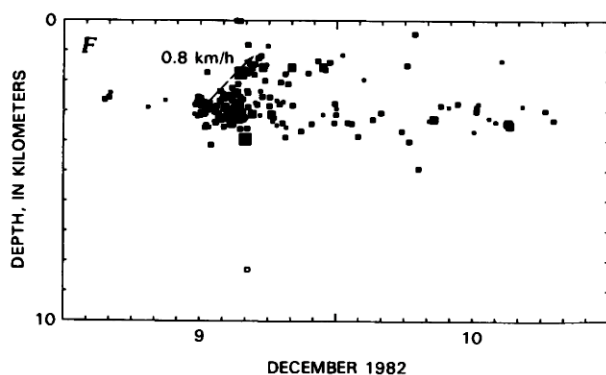


FIGURE 43.96.—Continued.

### DISCUSSION OF RIFT-ZONE INTRUSIONS

This section summarizes and discusses many of the basic seismic patterns seen during intrusions. We will mention processes common to many intrusions and eruptions and discuss their implications for the structure and dynamics of the rifts. We will also point out some relations between different intrusions and how one might affect a later one. Many of these patterns were mentioned in the previous section, but could not be developed in a comparative way because of its chronological format. For detailed descriptions and interpretations of individual swarms, the reader is referred to the previous section. Table 43.1 summarizes the basic data of the individual swarms enumerated in this paper.

Nearly all shallow volcanic earthquakes at Kilauea can be attributed to magma intrusion in some form. We have given different names to different types of swarms based essentially on their location and intensity, but they all result from magma transfer. Swarms accompanying inflation of the summit reservoir are generally of low intensity, in or near the caldera, and are caused by intrusion of the reservoir with magma from below. Slow intrusions may produce a low level of seismicity lasting several days or weeks along the rift zones. Rapid intrusions generally produce an intense, short swarm in the caldera or rift zones and transport magma much faster than Kilauea's magma supply rate. Rapid intrusions either create or enlarge dikes, which produce an eruption if one reaches the surface.

The mechanics of rift intrusions in Hawaii have been treated in many previous studies. Fiske and Jackson (1972) emphasized the large-scale effects of gravitational and edifice stresses on rift-zone development. Dieterich and Decker (1975) and Pollard and others (1983) calculated the deformation and stress field surrounding a dike interacting with the Earth's surface. Duffield and others (1976, 1982) discussed and interpreted deformation measurements for several Kilauea intrusions in terms of forceful magma transport and dike emplacement. Swanson and others (1976a) and Dvorak and

others (1985) discussed ERZ intrusions and their effect on deformation of the adjacent south flank. Shaw (1980) treated magma transport and ascent in terms of fracture mechanics in an applied stress field. Nakamura (1980, 1981) discussed the role of decoupling of the volcanic pile at the buried sediment layer in the formation of long rift zones.

### INFLATIONARY SWARMS AND SLOW INTRUSIONS

Most rapid intrusions are preceded by a period of inflation and consequent slowly increasing seismicity at the summit. A period of inflation lasting several weeks may produce intermittent swarms during that period. The level of swarm seismicity may only be a few times that of the background level and is often accompanied by a brief increase in the rate of rising summit tilt. Seismicity and tilt are highly correlated during inflation, and the caldera seismicity generally ends abruptly if rapid deflation feeds an intrusion downrift. Inflationary swarms are thus caused by increasing magma pressure, uplift and extension in the summit region. The rift zones adjacent to the caldera become active in many inflationary swarms and may receive magma in pulses and slow intrusions. Inflationary swarms were most numerous from December 1969 to January 1972 and during 1974 when tilt and caldera inflation reached the highest values sustained in recent years.

Some inflationary swarms occur immediately before rapid intrusions and are precursory in some sense. Notable examples include February 1969 and September 1974. Other inflationary swarms, such as those of January 22, 1977, and January 20, 1981, may be distinct but precede a rapid intrusion by a few days. These paired inflationary and intrusive swarms are not coincidences, because they are typically adjacent in both space and time. Many inflationary swarms represent periods of accelerated inflation, during which the barriers containing the accumulating magma are more likely to break. Many intrusions may thus be triggered by episodes of rapid inflation.

Some seismic precursors to intrusions are not as obvious as inflationary swarms at the summit. A swarm of shallow ERZ and south flank earthquakes preceded the first Mauna Ulu eruption in May 1969. Although the quality of epicenter locations is poor, the precursory swarm was definitely not at the summit. The Mauna Ulu eruption may have thus been triggered by some south flank instability or downrift magma movement. Some rapid intrusions are immediately preceded by an adjacent intrusion that may also be a precursor or trigger. This pattern will be discussed below in the section "Sequential Relations Between Intrusions Along the Rift Zones."

Slow intrusions have been observed along the active segments of both rifts within 20 km of the caldera, and all share several features in common. Summit tilt may slowly rise, fall or stay level, but the rate is never more than a few microradians per day. Typical rapid intrusions, in contrast, deflate the summit at rates of several microradians per hour. The slow intrusion may be aseismic or weakly seismic, or may produce earthquakes only near the terminus of the intrusion where magma accumulates. As with all intrusions,

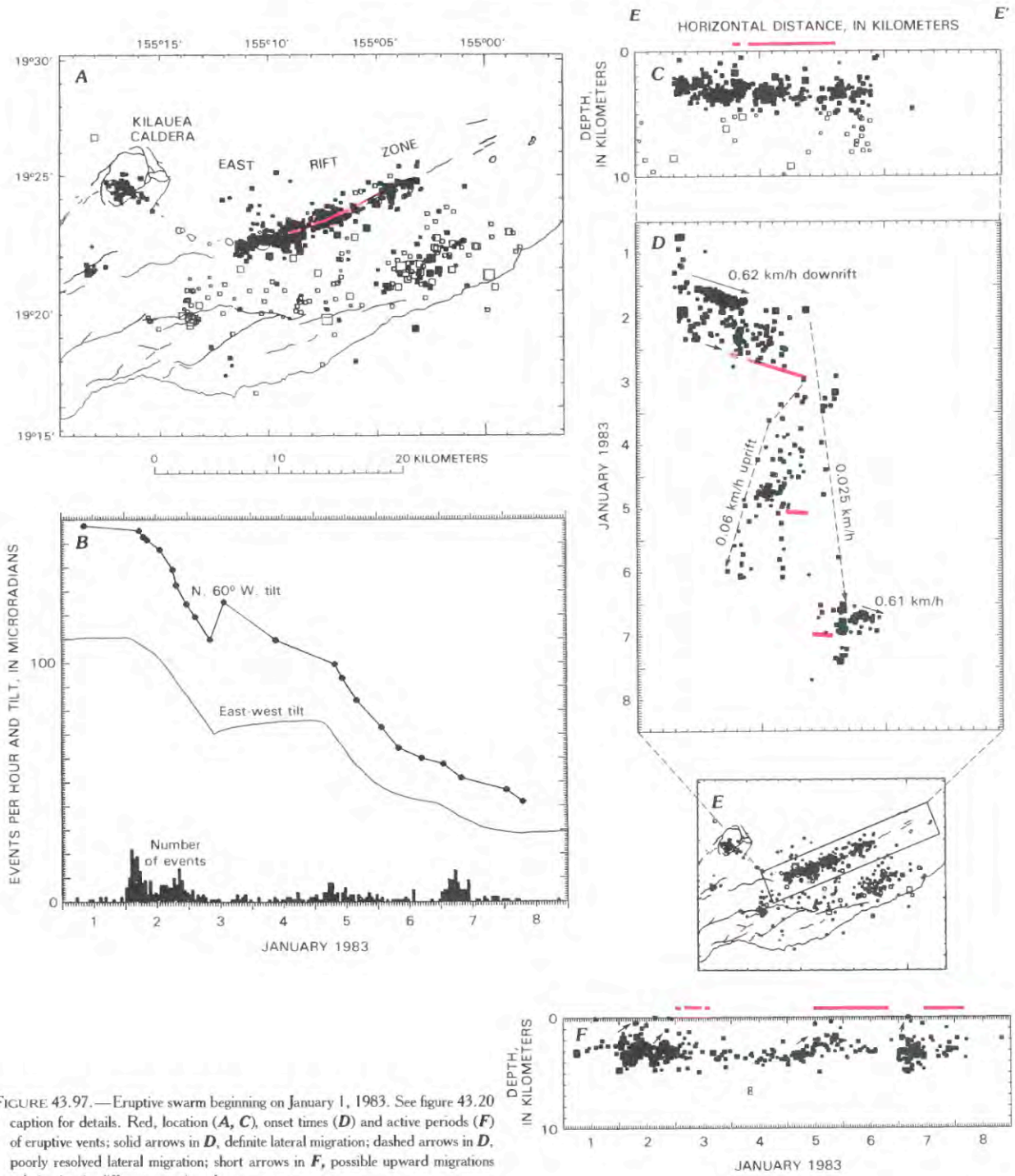


FIGURE 43.97.—Eruptive swarm beginning on January 1, 1983. See figure 43.20 caption for details. Red, location (*A*, *C*), onset times (*D*) and active periods (*F*) of eruptive vents; solid arrows in *D*, definite lateral migration; dashed arrows in *D*, poorly resolved lateral migration; short arrows in *F*, possible upward migrations culminating in different eruptive phases.

aseismic magma passage is presumed to indicate that the rift conduit is unstressed and in equilibrium, and need not widen to accommodate the magma flow. Completely aseismic intrusions are not considered in this paper, but Dzurisin and others (1984) used downward steps in tilt to account for magma transfer into the rifts. We infer that slow intrusions reveal magma leaking passively into the rifts at a rate comparable to that of its accumulation at the summit.

The most common slow intrusions occur from the summit reservoir during periods of inflation. The distinction between steady accumulation and pulsed flow of magma can often only be made if migrations of earthquakes are visible. Pulses of slowly intruding magma are seen in the intrusions of February and December 1970, June and July 1971, January 1972 and December 1974. Migration speeds are typically 0.01–0.05 km/h, which is 1 to 2 orders of magnitude slower than during rapid intrusions. At these speeds, several days are required for magma to traverse a few kilometers of rift. Some intrusions do not fall neatly into a category: the January 1977 event accompanied a short episode of inflation (as might a slow intrusion), but showed a rapid 0.7 km/h speed typical of a rapid intrusion.

Slow intrusions more than 5 km from the caldera have different characteristics on each rift zone. The SWRZ intrusions of October 1969 and February 1981 each generated earthquakes only near Puu Kou, lasted several days, and were accompanied by gradual deflation. Magma thus moved aseismically down 20 km of rift conduit. Pulses of slowly moving magma similar to ones near the summit triggered seismicity along the SWRZ following the June 1971 intrusion, in the 6 months prior to the December 1974 eruption, and during February–June 1981. The ERZ experienced a series of cyclic slow intrusions during November 1978–July 1979 and May–October 1980. The summit tilt oscillated as discrete pulses of magma were dispatched downrift. Episodes of summit seismicity coincided with peaks in tilt, and very shallow swarms near Puu Kamoamo close to minima in tilt were caused by accumulating magma downrift. The rift between the caldera and Puu Kamoamo did not produce migrating earthquakes as magma passed through. The intrusion thus was slow, magma transfer was passive, and seismicity was produced only at places of local inflation.

#### SEQUENCE OF EVENTS WITHIN A RAPID INTRUSION

Most intrusions occur in stages, only some of which may be evident during any one event. Larger and longer intrusions often display the most complexity, such as multiple phases and a variety of earthquake migration patterns.

The seismic zone formed by a rapid intrusion nearly always grows in size or shifts location as magma flows through conduits or fills a dike. In the first tens of minutes an intrusion often produces earthquakes in a small volume 1 km<sup>3</sup> or less in size. Most intrusive swarms begin from the rift-zone magma conduits (and sometimes the summit reservoir itself) near 3 km depth. When shifts in epicenter locations can be resolved, downrift migration of earthquakes and magma is typical of the SWRZ and the ERZ downrift of Mauna Ulu. The caldera and the ERZ between the caldera and Mauna

Ulu are more complex, and swarms may migrate either uprift or downrift with comparable likelihood. A shallowing of earthquakes with time is often observed in swarms where a range of depths can be resolved.

Major intrusions that also produce an eruption often divide into two types of processes, which can be illustrated by the July 1974 eruption. The first phase produced intense seismicity and a moderate deflation rate. Earthquakes migrated laterally (in this case uprift) and also upward from the ERZ magma conduit in a linear fashion toward the vent. We infer a high magma pressure and a growing dike from the intense seismicity, but a relatively low-volume flow from the deflation rate. When the dike reached the surface and the eruption began, tremor and the deflation rate increased dramatically. Earthquakes then ceased, partly because of masking by high tremor on the seismograms and partly because the dike stopped growing. Magma flow through an open-ended dike presumably dropped the magma pressure and did not require a lengthening or widening of the dike. Intense seismicity is therefore associated with a dike that is growing and compressing its walls.

Larger and more complex eruptions may display these seismic dike growth and aseismic magma flow modes simultaneously. If a dike is many kilometers long, eruption from a vertical feeder may start while the dike continues to intrude downrift, as seen in the September 1977 and January 1983 eruptions. Earthquakes at a given place will generally cease when the dike there reaches the surface and magma pressure drops, but seismicity will continue where the dike is still growing. The time between the first earthquakes and eruption at a given location is a measure of the time required for magma to migrate from the conduit at 3 km depth to the surface. This time may be 2–24 hours but is typically 3–6 hours. The deflation rate (and hence the magma volume rate) generally correlates either with the extrusion rate or the intensity of seismicity, depending on the importance of additional dike growth. This correlation of tilt rate and seismicity is easiest to see during large multiphase eruptions such as September 1977 and January 1983.

#### THE GEOMETRY AND DYNAMICS OF INTRUSIVE SWARMS

An intrusion may occur either by the fracturing of rock and emplacement of a new dike or by the opening of an older magma conduit. In either case the pressurized expansion of dike width apparently produces earthquakes in the rock near the dike. How much seismicity if any is produced by tensile fracture at the tip of a dike expanding into fresh rock is presently difficult to say. The recurrence of intrusive swarms in the same rift zone suggests that most intrusions propagate along planes of weakness that are the molten cores or boundaries of older dikes. Thus tensile failure at the crack tip is seismically a minor process compared to shear failure in the compressed rock near the dike. This view is consistent with Hill's (1977) earthquake swarm model, in which earthquakes occur on shear planes joining echelon dike segments.

The mechanics of rapid and slow intrusions determine whether a given event is forceful or passive. The compression and seaward displacement of Kilauea's south flank is a result of forceful intrusions

in the rift zones (Swanson and others, 1976a). We believe that the amount of seismicity and to some degree the speed of migration provide the distinction: rapid and seismically intense intrusions are forceful, and slow intrusions with weak seismicity result from a more passive flow of magma.

Patterns of seismic and aseismic migration of intrusions support the concept of earthquake generation adjacent to an expanding dike. Most Kilauea intrusions produce earthquakes for some distance behind its leading edge, not just at its forward tip. This presumably is the region in which the dike continues to widen after its initial opening. Seismicity then stops at a given place when the dike reaches its full width. Magma-filled conduits are clearly present in the ERZ much of the time, otherwise each intrusion would produce earthquakes along the entire rift between the summit and the intrusion terminus.

Intrusions may alternately migrate both seismically and aseismically. The aseismic migration occurs where the dike is already open and fluid, the adjacent rock is easily and aseismically compressed, or the dike widens only enough to supply magma to its leading tip. One example of aseismic migration through a previously rifted area was seen in the SWRZ intrusions of August 1981. The pre-intrusion of August 2 produced earthquakes out to only 5 km from the caldera before stopping. The main intrusion on August 10 produced no earthquakes where the earlier intrusion stopped because that section was already rifted open. Another type of aseismic dike growth is illustrated by the February 1977 intrusion. An initial and small burst of earthquakes was followed by about 3 hours of seismic quiescence and no deflation. The intense swarm then began simultaneously throughout the seismic zone and was rapidly fed by magma from the deflating summit. We interpret the aseismic period as growth of the dike to its eventual area but only to a small thickness. The dike was then filled at a high volume rate and generated earthquakes as it grew in thickness simultaneously over most of its area.

Earthquakes alone are not adequate to resolve the cross-sectional shape of the conduit, but do constrain its area through which magma flows. The ratio of magma supply rate (deflation rate converted from microradians of summit tilt to magma volume using the value of 0.3 million cubic meters per microradian from Dzurisin and others, 1984) to the earthquake migration rate is equal to the cross-sectional area of the dike. The SWRZ intrusions of December 1974, August 1981 and June 1982 all yield about 1,500 m<sup>2</sup> as the effective area of the main SWRZ conduit (table 43.1). Modeling the August 1981 dike as about 1,500 m by 1 m matches an observed leveling profile (Pollard and others, 1983), so these dimensions are consistent with all seismic and deformation data. The cross-sectional area of the northern SWRZ dike active in September 1971, however, is only about 280 m<sup>2</sup>. The ERZ conduits are also smaller than the main SWRZ conduit and do not exceed 900 m<sup>2</sup> (table 43.1).

Intrusions are most efficient at producing earthquakes between 2 and 4 km depth in most of the rift system, which is apparently the depth of the main magma conduits. The uppermost 2 km of the rifts probably lack sufficient confining stress, and slip occurs aseismically.

Unseen intrusion probably occurs below 4 km, which may be too hot and ductile to deform seismically. Intrusion in some form extends from the surface to at least 10 km depth where the volcanic pile rests on the pre-Hawaiian sea floor. Intrusive volume is ultimately accommodated by seaward slip of the unbuttressed south flank on its base at about 10 km depth.

When intrusive earthquakes do occur above 2 km depth, they often migrate up from the main conduit and follow an upward-branching dike. Many recent examples of upward earthquake migration are apparent, especially in the ERZ from the caldera to Mauna Ulu. Examples of intrusions whose earthquakes display both an upward branching finger and clear shallowing of hypocenters with time are November 1979 and July, August and October 1980. The SWRZ intrusion of August 1981 also contained a vertical branch that produced shallow earthquakes and a zone of surface cracking.

Earthquakes directly beneath the main conduit are less common, but have been recognized under both rifts. The central SWRZ swarm in June 1982 followed 1.5 years of shallow SWRZ intrusions. The swarm appeared to accompany a downward draining of magma to complete the rifting process to the base of the volcanic pile. The most common place that deeper volcanic earthquakes are seen below the ERZ is in a rootless cluster at 5–7 km depth below Mauna Ulu. Activity there (see fig. 43.3F, G) was recognized during the intrusions of June 1976, September 1977, May 1979, and to a lesser extent during many others. Earthquakes during the May 1979 intrusion spread both upward and downward and reached 7 km depth the day after the main swarm. Most of the rifting process below 4 km depth is aseismic, and the study of earthquakes cannot determine the degree to which magma is supplied from the main rift conduit above or through a deeper and lateral system directly from Kilauea's vertical magma conduit.

#### THE MECHANICS OF EARTHQUAKE MIGRATION

As we have seen many times, migrating earthquakes reveal moving magma and the growth of dikes within the rift zones. Earthquakes mostly originate at or just behind the leading edge of the dike, where it is growing in width. Some earthquakes occur ahead of a smoothly advancing front of seismicity. These may be from (1) irregular or jerky dike motion, (2) a stress increase in front of the dike, or (3) triggering by elastic waves radiated by earlier earthquakes.

The direction of migration is generally downrift, except within the caldera and in the ERZ between the caldera and Mauna Ulu. Magma is supplied at the summit, and both its pressure gradient and downslope gravitational flow transport it primarily in the downrift direction. Note that upward movement by buoyancy requires that magma have at least lithostatic pressure. The observed combinations of upward and downrift magma movement thus require the rift to be in a mixture of lithostatic and sublithostatic stress conditions. Sublithostatic pressure might thus prevail in places where downrift magma movement is rapid, continuous or aseismic. Lithostatic pressure probably prevails near blockages of the rift conduit and places where dikes branch upward to form eruptive vents.

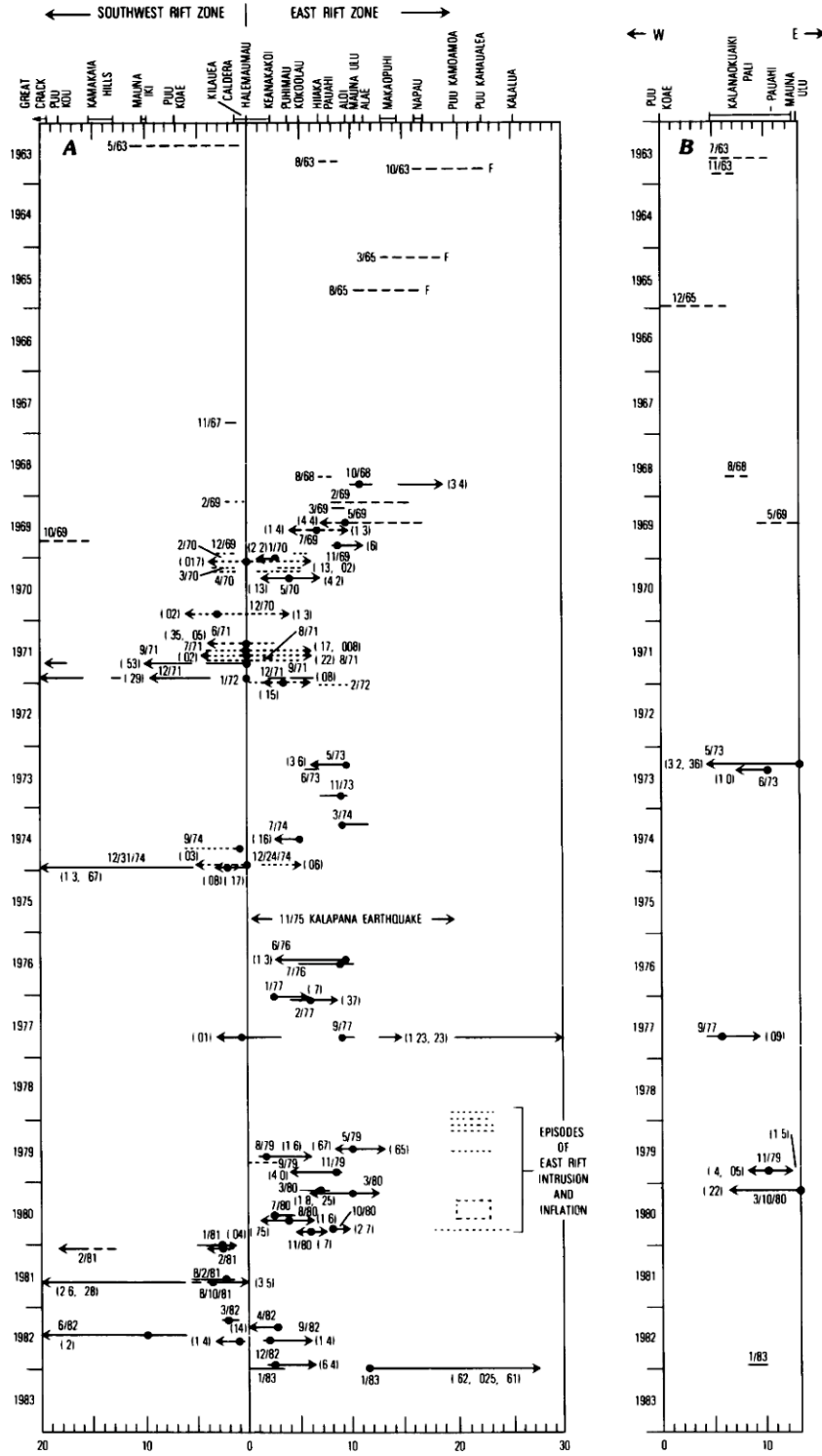
The intrusive patterns for the SWRZ are simpler than for the ERZ. The positions, starting points, migration directions and migration speeds for the earthquake swarms discussed in this paper are summarized in figure 43.98. This distance versus time plot shows what happened where and when. For example, most SWRZ intrusions begin near or just south of the caldera. Within 3 km of Halemaumau, intrusions are about equally likely to migrate into or out of the caldera. The region close to the summit magma reservoir is presumably a complex of conduits that grow as an interconnected network. All intrusions in the SWRZ more than 3 km from the caldera migrate in the downrift direction. The six best observed SWRZ intrusions all reached Puu Kou. Thus, no major barriers capable of stopping an intrusion are present between the south caldera and Puu Kou. The migration speed slowed significantly near the terminus of the major 1974 and 1981 intrusions. This speed decrease could be caused by a drop in temperature or pressure near the end of the intrusion, or the observed upward bend of the seismic conduit over a barrier near Puu Kou.

Intrusions downrift of Mauna Ulu in the ERZ are also relatively simple. For the present discussion we exclude the intrusions of 1963, 1965 and February and May 1969 owing to their diffuse earthquake distributions within the south flank. Each of the seven events that penetrated downrift of Mauna Ulu started within 1 km of that point, and each intruded in the downrift direction. The major September 1977 and January 1983 intrusions slowed with distance from the summit, as did the two largest SWRZ intrusions. Long intrusions apparently cannot sustain a high speed for the entire length of the dike. Unlike the SWRZ, the three ERZ intrusions that passed Makaopuhi each stopped at different places, implying that many barriers capable of stopping intrusions exist in the ERZ. The simplicity of a single, linear magma conduit at 3 km depth appears to exclude complexities such as uprift earthquake migration in the SWRZ and central ERZ.

#### BEHAVIOR OF THE EAST RIFT ZONE FROM THE CALDERA TO MAUNA ULU

Intrusions between the caldera and Mauna Ulu in the ERZ are varied and often complex. This section of rift is distinctly different from the rest of the rift system in several ways: (1) intrusions in recent years were much more frequent than elsewhere; (2) the area often partakes in inflation of the summit magma reservoir and may continuously produce earthquakes during these times; (3) it is the only section of Kilauea's rift system that trends north of west and is therefore most oblique to the greatest principal stress, which controls the strikes of individual vents and the majority of the rift system; (4) the Koaie fault zone meets the ERZ near Mauna Ulu, tectonically separating this section from the simpler ERZ downrift; (5) the only major intrusion to trend oblique to the rift axis was here in July 1969, and some eruptive vents also obliquely extend several kilometers from the rift; (6) earthquakes near 1–2 km depth are numerous—though the main magma conduit at 3 km depth is typical of the whole rift system; (7) magma may supply two events

FIGURE 43.98.—Diagram of position of swarms and intrusions versus time as documented in this paper. Horizontal scale in *A* is in kilometers from center of Halemaumau along the SWRZ (left) and ERZ (right). Solid lines show time and lateral extent of rapid intrusions. Dashed lines, intrusions with diffuse hypocenters; F, swarms in flanks off rift axis; dotted lines, inflationary swarms and slow intrusions; each swarm is labeled with its month and year; solid circles, initiation point of each swarm where earthquakes started; arrowheads and numbers in parentheses, direction, extent, and speed (in kilometers per hour) of earthquake migration. Swarms with a starting point but no arrowhead or speed have speeds that are difficult to measure. *B*, Similar diagram as *A* for the Koaie fault zone.



simultaneously, as with the series of eruptions and intrusions during the 1969–74 Mauna Ulu activity or the two intrusions during October 21–22, 1980; (8) intrusions are equally likely to migrate uprift or downrift and sometimes move outward in both directions from their starting points; (9) intrusions may begin and end at several different places, implying a population of significant blockages within the conduit system; (10) the suspected magma reservoir beneath Pauahi is in this section of rift; and (11) the time between the first seismicity and later eruption at the same point is typically 2–3 h, but is at least 5–6 h elsewhere in the rift system. Though many of these differences are probably interrelated and are consequences of the evolution of the ERZ, we will only discuss a few of them in detail. We interpret differences in the seismicity of the ERZ from the caldera to Mauna Ulu as a result of a complex honeycomb of magma conduits, a high frequency of intrusions and the local trend oblique to the rest of the rift system.

The ERZ as a whole has been seismically and volcanically more active than the SWRZ, both historically and prehistorically. This greater activity is recognized by eruption frequency, higher topography, and larger gravity and magnetic anomalies (Duffield and others, 1982). Of the intrusions and eruptions during 1962–83, about 75 percent have been in the ERZ, and about 75 percent of those primarily involved the section uprift of Mauna Ulu.

The extensive seismicity above 2 km depth uprift of Mauna Ulu probably derives from a complex honeycomb of magma conduits and from a response to frequent slow and fast intrusions of the main magma conduit at 3 km depth. Shallow earthquakes may thus be produced in two ways: (1) The direct intrusion of magma into the shallow parts of the interconnected conduit system produces earthquakes near fingers of dikes that branch upward. These vertical intrusions produce upward earthquake migration and may feed an eruption if they reach the surface. (2) The region above the main magma conduit responds mechanically to intrusions below. A fast intrusion produces earthquakes by frequently extending and uplifting a zone that is highly fractured. A slow intrusion generates the same seismic and deformation patterns as a fast intrusion, but is analogous to the shallow seismicity in the caldera above the main magma reservoir. The occurrence of 0- to 2-km seismicity both above the magma reservoir and within the section of rift that can inflate during slow intrusions suggests that extensional stresses applied for long periods play a part in generating the shallow earthquakes.

The misalignment of the rift axis and greatest principal stress may contribute to the complex seismicity of the ERZ between the caldera and Mauna Ulu. Locally, the shallow stress orientation is defined by eruptive fissures in the rifts and faults in the Koaie fault zone, which trend east-northeast. Evidence of a similar trend at 3 km depth comes from the intrusion of July 1969, which trended east-northeast and crossed the rift near Hiiaka. Earthquakes migrated east and west from the dike's intersection with the main ERZ magma conduit, which thus fed the intrusion. Regionally, the greatest principal stress is also defined as east-northeast by the remainder of Kilauea's rift system. Most intrusions of the ERZ between the caldera and Mauna Ulu, however, follow the southeast trend of the main magma conduit. The magma conduit is self-

sustaining and may have twisted southward with the apparent southward migration of the ERZ (Swanson and others, 1976a). We believe that the rift conduit is now oblique to the greatest principal stress, and this stress direction complicates many of the observed seismic patterns. Stress orientation possibly changes with depth, or the intersecting Koaie fault zone perturbs stresses locally. Additional work including focal mechanisms will be required before stress patterns can be adequately discussed.

#### UPRIFT EARTHQUAKE MIGRATION

A unique characteristic of the ERZ between the caldera and Mauna Ulu is uprift migration of earthquakes during intrusions. Figures 43.98 and 43.99B show that roughly one-half of the migrating intrusions in this section of rift do so in the uprift direction. This observation underscores the fact that intrusions are complex redistributions of magma and stress. Three complicating factors bear on the mechanism of uprift earthquake migration: (1) We interpret the greater vertical extent of earthquakes and the simultaneity of two intrusions or eruptions as indicators of a multitiered honeycomb of magma conduits in the uprift section of the ERZ. (2) Earthquakes appear to be generated by expansion of dike walls under magma pressure. Earthquakes may thus be produced either by rock fracturing near the leading edge of an advancing dike or by a pressure pulse moving within an existing dike. (3) Magma will only flow downward by gravity if confined below hydrostatic pressures, but will flow upward by buoyancy if confined at or above the higher lithostatic pressure. Various intrusion paths are thus possible.

Consider a few examples of how uprift earthquake migration might occur: (1) Over a distance of many kilometers, the magma conduit slopes downward in the downrift direction. Downrift flow might then accompany low stress conditions, and later uprift or buoyant flow might result from high stress conditions. The opening and closing of the connections between conduits in the honeycomb only complicates the possible flow directions. (2) While magma flows downrift, a pulse of pressure causing dike widening and earthquakes might travel uprift. This pulse could occur, for example, after a downrift-moving intrusion reaches a barrier that stops it and creates a back wave of pressure against the flow of magma. Such reversals from downrift to uprift migration accompanied the intrusions of January 1972, December 1974, June 1976, November 1979 and January 1983. (3) The entire intrusion and rifting process may begin at one of the conduit blockages, which serves as a point of stress concentration within the rift. The intrusion may then grow outward from this point in several directions, as did the August 1980 event. The fact that summit deflation begins within minutes of the first intense seismicity argues that a magma storage pocket within the rift, such as suspected at Pauahi, acts only as an initiating stress concentration rather than a major source of magma feeding nearby intrusions. We conclude that the variety of earthquake migration directions in the upper ERZ indicates a complex interaction of varying stresses and pressure gradients on a multiplicity of magma conduits.

### THE STARTING POINTS OF INTRUSIONS

An examination of the places where intrusions begin producing earthquakes reveals likely blockages within the rift conduit where magmatic stresses are concentrated. These blockages probably occur where dikes are squeezed shut or have completely solidified. Magma then accumulates at these barriers, which are the first to break under rising magma pressure. Figure 43.99A shows where well-resolved swarms have begun. Five inferred blockages are near the southern part of the caldera, Keanakakoi, Puhimau, Hiiaka and Pauahi-Mauna Ulu. The Keanakakoi zone is adjacent to the summit magma reservoir. The southern part of the caldera initiates nearly all SWRZ intrusions and also surrounds the summit reservoir. These two barriers are the most intuitive, because they regulate inflating magma and are stressed directly by the inflating reservoir. The barriers identified here in seismicity patterns are larger scale versions of the barriers linking dike segments proposed as a source of harmonic tremor (Aki and others, 1977; Aki and Koyanagi, 1981).

The Pauahi-Mauna Ulu barrier, however, initiates more intrusions than any other. The ERZ bends there and meets the Koa'e fault zone. Structural stresses thus can concentrate in the Pauahi-Mauna Ulu area, where the conduit appears to be frequently pinched closed. Most central ERZ intrusions begin here, and only the January 1983 swarm was observed to begin downrift of this point. Inflationary earthquakes are not recognized downrift of this point, which is the final barrier containing this process. Swanson and others (1976b) proposed a barrier there to account for the pattern of eruption locations during 1965–69 and the absence of any ERZ activity between the August 1965 and August 1968 events. The Pauahi-Mauna Ulu zone was also a major barrier during the June 1976 and November 1979 intrusions: downrift migration of a few earthquakes were immediately followed by a reflected pulse of intense seismicity moving uprift. A wave of magma pressure may have been reflected from this major barrier, which also prevented the intrusion from penetrating farther downrift.

Other barriers within the rifts are recognized by earthquake clusters and by places where intrusive swarms end. Earthquake clusters apparently are caused by barriers having a high stress concentration. The high density and distribution of earthquakes at Puu Kou in the SWRZ implicate it as a major barrier, and it has stopped every intrusion that reached it since at least 1962. Shallow earthquake clusters beneath Mauna Iki (September 1971) and just southwest of Puu Koa'e (August 1981) also mark significant SWRZ blockages. Another barrier 5 km south of the caldera held the small intrusion of August 2, 1981, before it broke on August 10. Places where the intrusions of September 1977, May 1979, March 1980 and January 1983 started, stopped or paused also suggest five additional barriers in the ERZ. All of these major or suspected barriers are plotted in figure 43.100. The lifetime of these barriers beyond the period of seismic observation is not known.

We summarize the starting points and directions of intrusions in figure 43.99B. Triangles point in the approximate directions taken by intrusions, and thin diamonds are used for swarms that spread in both directions from that point. Swarms in the ERZ uprift of

Mauna Ulu are about equally likely to spread downrift, uprift, or in both directions. Two such intrusions moved primarily into the Koa'e. All moving SWRZ intrusions went downrift except for three that started 1.5 km south of the caldera.

The gap between the Hiiaka and Pauahi-Mauna Ulu blockages is a suspected pocket of magma storage within the ERZ conduit. Magma apparently collects behind the major Pauahi-Mauna Ulu barrier. Like the summit magma reservoir, the Pauahi zone is aseismic and is bordered by barriers that initiate intrusions. This magma pocket apparently fed the November 1979 Pauahi eruption with degassed lava (Norm Banks, written commun., 1979), and its existence and proximity are supported by the short 2-hour interval between the first earthquakes and the start of the eruption. Another rift magma reservoir beneath Puu Kamoamoa inflated during the cyclic and slow intrusions of 1978–80. The two ERZ reservoirs and the main summit reservoir are plotted in figure 43.100. A magma reservoir was proposed beneath Makaopuhi by Swanson and others (1976b) and Jackson and others (1975) that may account for the deformation centers reported by Dvorak and others (1983). Seismicity beneath Makaopuhi, however, is not sufficient to resolve a magma reservoir. Other reservoirs are likely present but are not obvious from seismicity patterns. Parts of the rift system between the barriers plotted in figure 43.100 are probably good places to look for reservoirs.

### UPWARD MIGRATION OF EARTHQUAKES

The vertical extent of earthquakes in the ERZ uprift of Mauna Ulu makes upward earthquake migration recognizable and reveals a shallow conduit system. The vertical speed of a dike is generally not as accurate as its lateral speed owing to the greater depth error and narrower depth range of hypocenters, but are observed between 0.1 and 5 km/h (see table 43.1). The retarding effect of gravity may explain why vertical speeds are typically less than lateral speeds. Upward migration is best determined between 3 km depth, where it typically starts, and about 1 km, where the production of earthquakes diminishes as the dike moves upward. The times of eruptions demonstrate that dikes generally slow to a fraction of their initial speed during the last kilometer of their trip to the surface. The persistence of earthquakes below the upward-moving top of a dike shows that typical growth is like a wedge with expansion continuing after the leading edge passes a given point. Clear vertical migration with a slowing near the surface is seen, for example, in the intrusions and eruptions of May and November 1973, July 1974 and November 1979.

Another view of upward movement is provided by the delay time between a dike first reaching a point below an eventual vent (the first earthquakes) and the moment of eruption. This approach is most useful for intrusions where simultaneous migration in several places masks a simple trend on a plot of earthquake depth versus time. Typical delay times are 2–3 h near the caldera and uprift of Mauna Ulu. Short times of dike migration to the surface are reasonable here owing to the vertical extent and shallowness of the conduit system, and the high frequency of intrusive activity. Longer

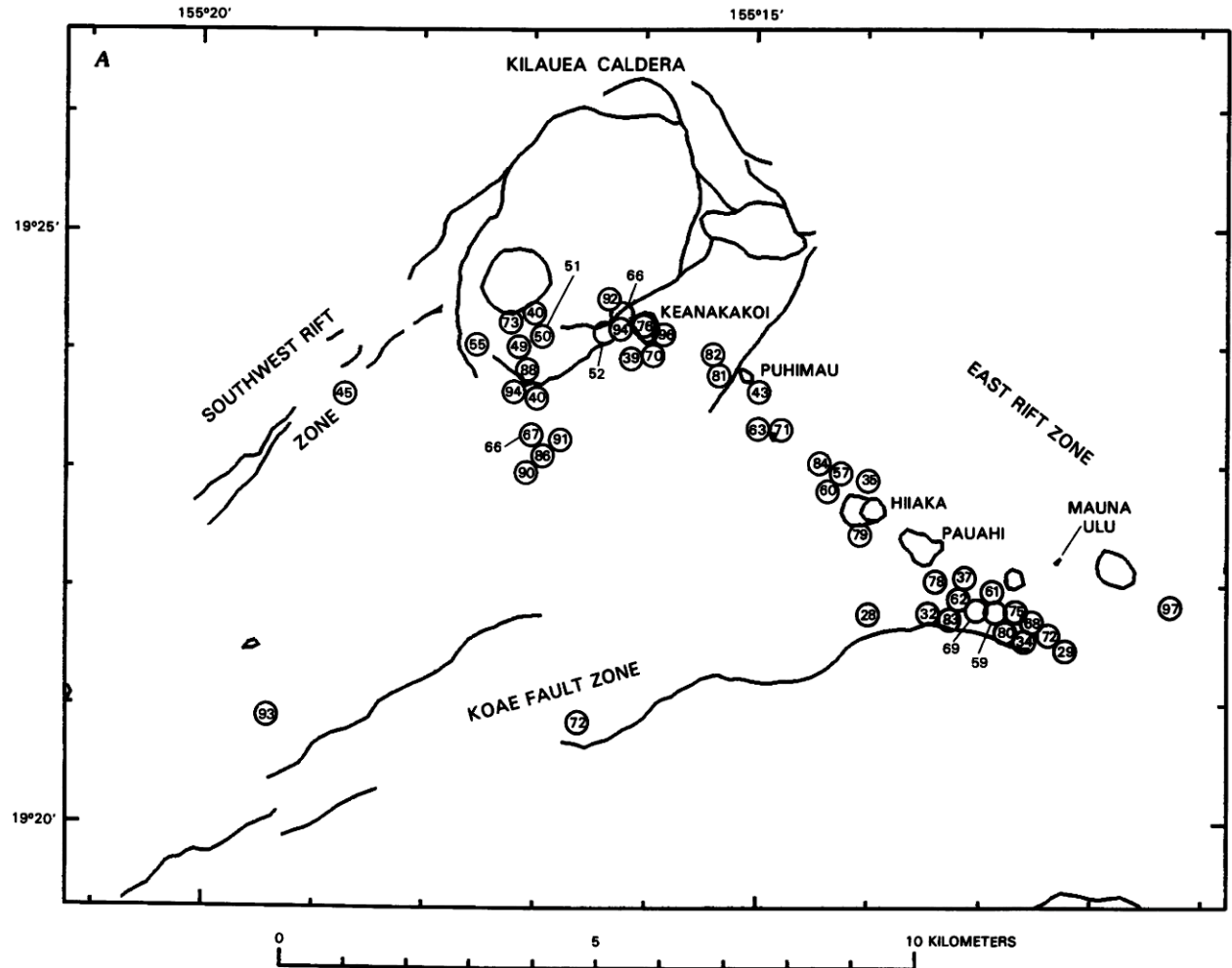


FIGURE 43.99.—Locations of starting points of intrusions. *A*, Those that can be determined from locations of first earthquakes. Circled numbers are figure numbers and are listed in table 43.1. Starting points cluster into five stress points or rift zone barriers. *B*, Locations of starting points and directions of intrusions. Thin triangles show general direction of migration (uprift, downrift, or into the Koa'e fault zone). Thin diamonds indicate earthquakes moved out in both directions.

10- to 12-h delay times are occasionally observed in the caldera-Mauna Ulu area, namely from the December 1974 and November 1979 eruptions, but may be as short as the 1-h delay of the May 1969 Mauna Ulu eruption. The times required for magma to reach the surface characteristically increase with distance from the caldera. A good example is the September 1971 SWRZ eruption, where the delay ranged from about 4 h near the caldera to about 18 h downrift of Mauna Iki. Delays observed in the ERZ are 5 h near Makaopuhi (February 1969), 21 h at Napau (January 1983) and 11 h near Kalalua (September 1977). The infrequency of intrusion, the increased distance from magma conduit to the surface and the reduced magma pressure and temperature downrift presumably all contribute to lengthened transit times of magma to the surface.

#### SEQUENTIAL RELATIONS BETWEEN INTRUSIONS ALONG THE RIFT ZONES

Intrusions clearly tend to occur near their predecessors (fig. 43.98), and activity shifts between the ERZ and the SWRZ. For the moment we exclude the 1963–67 period from discussion because of the reduced sensitivity and resolution of the seismic network.

Many intrusions occur in groups of two or three, and may retrace nearly the same path, as in September and December 1971, May and June 1973, June and July 1976, and February and August 1981. In these cases the first intrusion may weaken and heat a conduit for the second. The second intrusion finds an open conduit and may easily push out magma from the previous event rather than

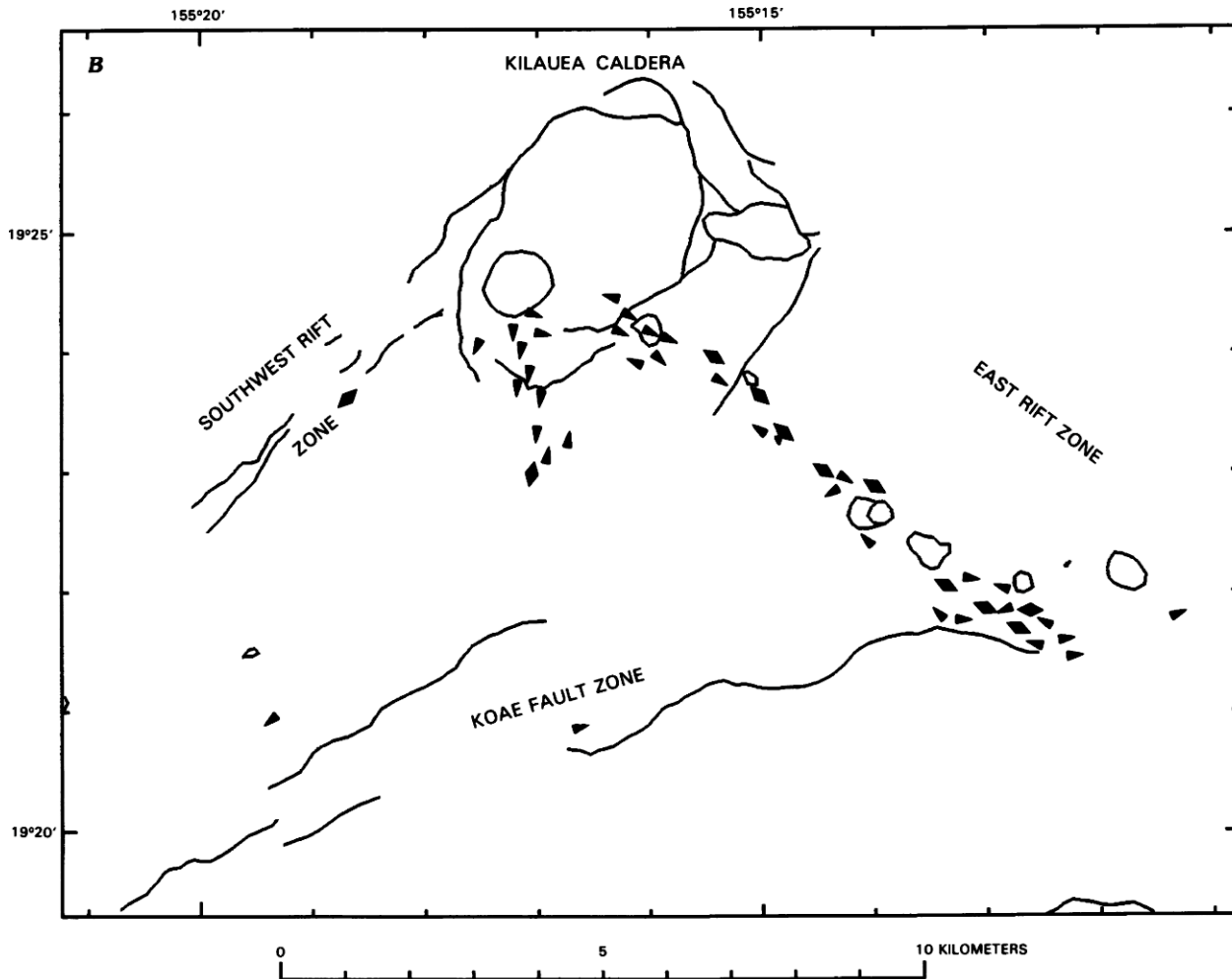


FIGURE 43.99.—Continued.

starting a new one elsewhere. Intrusions may also trigger an adjacent one, as in May, July and November 1969, January and February 1977, May, August and November 1979, March 2 and 10, 1980, July through November 1980, December 1982 and January 1983. These intrusions apparently stressed an adjacent section of rift, which was in turn intruded when magma supply and pressure became sufficient to do so. Alternatively, one intrusion may inhibit a later one if a dike solidifies and increases the compressional stress near it, or locally makes the rift more competent. We prefer the interpretation that a barrier in the magma conduit stops the first intrusion, and this newly stressed barrier becomes the initiation point for the next intrusion.

A shifting pattern of intrusions from the ERZ to the SWRZ and back is also apparent from figure 43.98. Four cycles of activity

occurred during the 1968–83 period, each lasting 3–4 yr. The cycle begins in the ERZ with intrusions originating in the general region of Mauna Ulu, noted above as a major stress point of the rift. Subsequent intrusions in the first part of the cycle are mostly in the Kilauea caldera–Mauna Ulu section of the ERZ. As a whole they may migrate uprift, as during 1968–70. In two of the four cycles, this ERZ activity was followed by a period of inflationary swarms and high summit tilt (1970–71 and 1974). The westward progression of activity continued into the SWRZ for three of the four cycles. Kilauea did not activate the SWRZ in 1977–78. The last stage in the cycle is 1–2 years of quiescence. The quiescent stage was omitted in 1982, when intrusions immediately migrated from the SWRZ back to the ERZ. A distorted and probably incomplete fifth cycle may have occurred during 1963–67. A shift from the

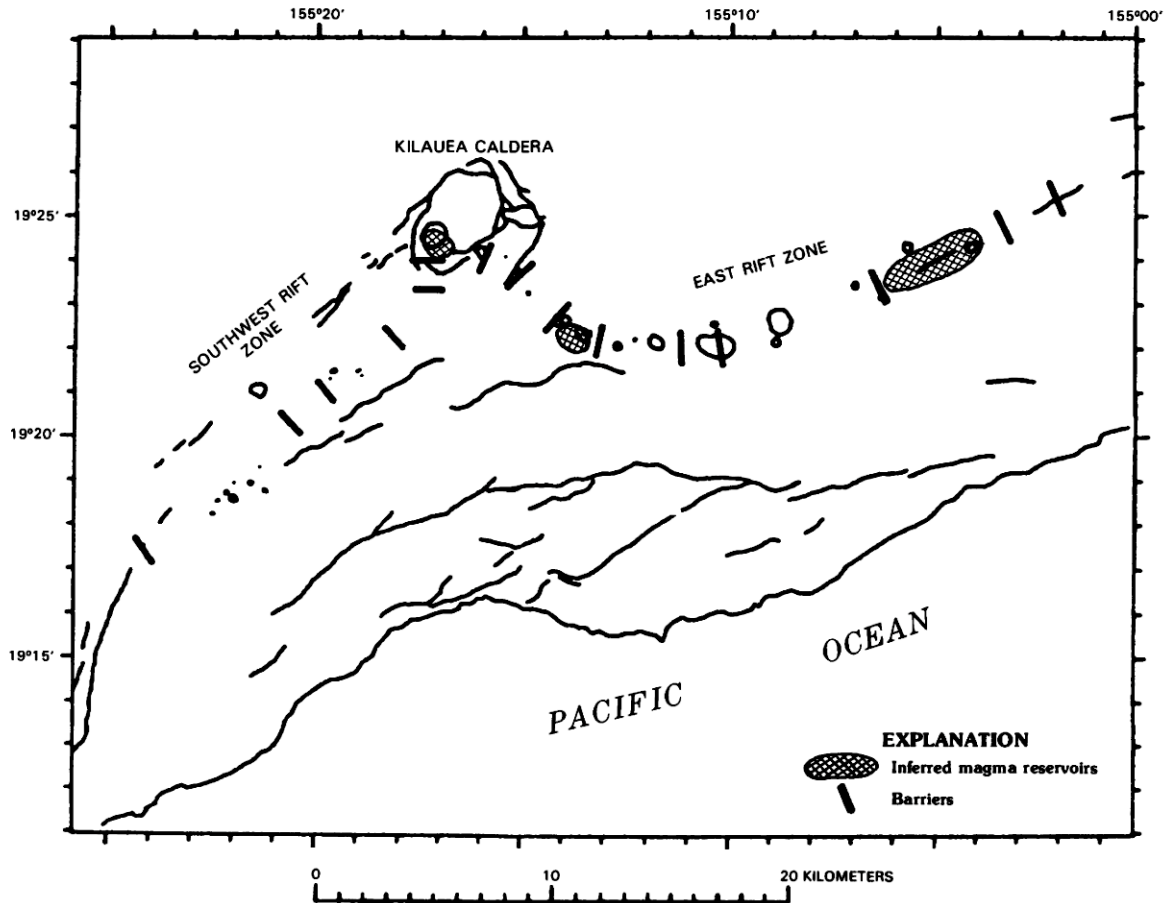


FIGURE 43.100.—Magma reservoirs and barriers within Kilauea caldera and its rift zones. Thick lines transverse to rifts, locations of stress points or barriers within rift zone conduits. Barriers are derived from points at which intrusions frequently start and stop. Three shaded zones mark main magma reservoir beneath caldera and secondary reservoirs in east rift zone inferred from seismicity.

SWRZ to the ERZ occurred in 1963, but without a long pause. Activity moved up the ERZ to the caldera in 1967 but did not then produce a SWRZ intrusion. The overall pattern is then one of intrusions progressing up the ERZ through the summit to the SWRZ, followed by a rest before the cycle starts again.

These large-scale shifts of intrusion location may be aided by the tendency of one intrusion to trigger an adjacent one, but this tendency alone cannot produce such systematic shifts. Some regional and oscillatory tectonic process seems also to be at work. The accumulated compression in the south flank adjacent to one rift may hinge the other rift open, making intrusions there more probable. Once a series of intrusions begins in one rift zone, they tend to trigger each other until compression of the south flank retards intrusion in that rift and favors the other one. Using similar

reasoning, Duffield and others (1982) suggested that a combination of south-flank displacement and a deflated Mauna Loa foster SWRZ intrusions by a reduction of compressional stress there.

Completion of rifting downward to the 10-km depth at which the volcanic pile is decoupled from the prevolcanic sea floor may play a part in the cycle. We interpret the 5- to 10-km depth swarm and intrusion of the SWRZ in June 1982 as extension of rifting to depth following the series of shallow 1981 intrusions. A similar but aseismic process may occur after each cycle or half-cycle, possibly during the seismically quiescent interval between cycles.

If changes in regional stress play a part in the intrusion cycle, then large earthquakes within Kilauea's flanks must also interact with the cycle. The  $M=7.2$  Kalapana earthquake in November 1975 was by far the largest during this period and caused Kilauea's south

flank to slip seaward as much as 8 m. Surprisingly, the earthquake did not disrupt the cycle in a major way: the SWRZ intrusion of December 1974 was followed in 18 months by resumption of intrusions in the ERZ, as if no earthquake had occurred. The Kalapana earthquake, however, may have caused some significant changes. (1) Intrusions outnumbered eruptions in the six years following the earthquake, but the reverse was true prior to the earthquake (Klein, 1982b). This switch may have resulted from a drop in confining stress on the rifts and the inability of magma to develop sufficient pressure to reach the surface. (2) The cycle following the earthquake was disrupted to the extent that no SWRZ intrusion occurred. The greatest coseismic displacements were in the flank south of the ERZ, which may have favored it as the site of intrusions until the end of the following cycle. (3) The two cycles following the earthquake had no period of inflationary swarms. (4) Two major ERZ eruptions penetrated downrift of Kalalua, but no others had since the 1960 eruption. (5) The cyclic slow intrusions and magma accumulation near Puu Kamoamoia may have been made possible by reduced stress across the ERZ. (6) The shift of intrusions from the SWRZ back to the ERZ in 1982 without a quiescent period shows that the ERZ was in some sense favored for intrusion, as in (2) above. (7) The Puu Oo eruption that started in January 1983 captured all of Kilauea's magma supply and prevented any other eruptions or intrusions. The long-lived Mauna Ulu eruption, however, coexisted with other intrusions. The intervening Kalapana earthquake may have permitted the establishment of a major magma path to the exclusion of others.

Another tectonic change may have been coupled with the shift of intrusive activity from the ERZ to the SWRZ during 1974. Significant earthquakes occurred in the Kaoiki seismic zone on June 19, 1974 ( $M=4.8$ ), November 30, 1974 ( $M=5.5$ ) and December 15, 1974 ( $M=4.8$ ). The mechanism of the events was strike-slip (Endo and others, 1978; Endo, 1985), which acted to relieve compressive stress across the SWRZ and permit an easier intrusion path than before. Shaking from the larger earthquake may also have disturbed the delicately balanced equilibrium of the magma system. The Kaoiki earthquakes may have been triggered by the inflation accompanying the seismic reawakening of Mauna Loa (Koyanagi and others, 1975), which would have acted to increase the shear stress on the ultimate fault plane. Thus, shifts in rift activity could be accomplished through mechanical coupling with Kilauea's flanks. Large earthquakes in the flanks apparently play a part, but aseismic deformation and even Mauna Loa may contribute as well. Seismicity and magma movement at Kilauea are clearly linked in a variety of ways, and earthquakes provide many insights into the dynamics of Kilauea Volcano.

## REFERENCES

- Aki, K., Fehler, M., and Das, S., 1977, Source mechanism of volcanic tremor: fluid-driven crack models and their application to the 1963 Kilauea eruption: *Journal of Volcanology and Geothermal Research*, v. 2, 259-287.
- Aki, K., and Koyangi, R.Y., 1981, Deep volcanic tremor and magma ascent mechanism under Kilauea, Hawaii: *Journal of Geophysical Research*, v. 86, p. 7095-7109.
- Ando, M., 1979, The Hawaii earthquake of November 29, 1975: low dip angle faulting due to forceful injection of magma: *Journal of Geophysical Research*, v. 84, p. 7616-7626.
- Bosher, R., and Duennebier, F.K., 1985, Seismicity associated with the Christmas 1965 event at Kilauea Volcano: *Journal of Geophysical Research*, v. 90, p. 4529-4536.
- Crosson, R.S., and Endo, E.T., 1982, Focal mechanisms and locations of earthquakes in the vicinity of the 1975 Kalapana earthquake aftershock zone 1970-1979: implications for tectonics of the south flank of Kilauea Volcano, Island of Hawaii: *Tectonics*, v. 1, p. 495-542.
- Decker, R.W., Koyanagi, R.Y., Dvorak, J.J., Lockwood, J.P., Okamura, A.T., Yamashita, K.M., and Tanigawa, W.R., 1983, Seismicity and surface deformation of Mauna Loa Volcano, Hawaii: *Eos, Transactions, American Geophysical Union*, v. 64, p. 545-547.
- Dieterich, J.H., and Decker, R.W., 1975, Finite element modelling of surface deformation associated with volcanism: *Journal of Geophysical Research*, v. 80, p. 4094-4102.
- Duffield, W.A., 1975, Structure and origin of the Koaie fault system, Kilauea Volcano, Hawaii: U.S. Geological Survey Professional Paper 856, 12 p.
- Duffield, W.A., Christiansen, R.L., Koyanagi, R.Y., and Peterson, D.W., 1982, Storage, migration and eruption of magma at Kilauea Volcano, Hawaii, 1971-1972: *Journal of Volcanology and Geothermal Research*, v. 13, p. 273-307.
- Duffield, W.A., Jackson, D.B., and Swanson, D.A., 1976, The shallow, forceful intrusion of magma and related ground deformation at Kilauea Volcano, May 15-16, 1970: *Bulletin Volcanologique*, v. 39, p. 577-597.
- Dvorak, J., Okamura, A.T., and Dieterich, J.H., 1983, Analysis of surface deformation data, Kilauea Volcano, Hawaii, October 1966 to September 1970: *Journal of Geophysical Research*, v. 88, p. 9295-9304.
- Dvorak, J.J., Okamura, A.T., English, T.T., Koyanagi, R.Y., Nakata, J.S., Sako, M.K., Tanigawa, W.R., and Yamashita, K.M., 1986, Mechanical response of the south flank of Kilauea Volcano, Hawaii to intrusive events along the rift zones, *Tectonophysics*, v. 124, p. 193-209.
- Dzurisin, D., Anderson, L.A., Eaton, G.P., Koyanagi, R.Y., Lipman, P.W., Lockwood, J.P., Okamura, R.T., Puniwai, G.S., Sako, M.K., and Yamashita, K.M., 1980, Temporal variations in gravity on Kilauea Volcano, Hawaii: implications for the magma budget, November 1975-September 1977: *Journal of Volcanology and Geothermal Research*, v. 7, p. 241-270.
- Dzurisin, D., Koyanagi, R.Y., and English, T.T., 1984, Magma supply and storage at Kilauea Volcano, Hawaii, 1956-1983: *Journal of Volcanology and Geothermal Research*, v. 21, p. 177-206.
- Eaton, J.P., 1962, Crustal structure and volcanism in Hawaii, in *Crust of the Pacific Basin*: American Geophysical Union Monograph no. 6, p. 13-29.
- Eaton, J.P., and Murata, K.J., 1960, How volcanoes grow: *Science*, 132, p. 925.
- Ellsworth, W.L., and Koyanagi, R.Y., 1977, Three dimensional crust and mantle structure of Kilauea Volcano, Hawaii: *Journal of Geophysical Research*, v. 82, p. 5379-5394.
- Endo, E.T., 1985, Seismotectonic framework for the southeast flank of Mauna Loa Volcano, Hawaii: Seattle, University of Washington, PhD dissertation, 350 p.
- Endo, E.T., Koyanagi, R.Y., and Klein, F.W., 1978, Geologic and seismic evidence for strike-slip faulting between Kilauea and Mauna Loa Volcanoes, Hawaii [abs.]: *Seismological Society of America, annual meeting, Sparks, Nevada*.
- Fiske, R.S., and Jackson, E.D., 1972, Orientation and growth of Hawaiian volcanic rifts: the effect of regional structure and gravitational stresses: *Proceedings of Royal Society of London, series A*, v. 329, p. 299-326.
- Fiske, R.S., Kinoshita, W.T., 1969, Inflation of Kilauea Volcano prior to its 1967-68 eruption: *Science*, v. 165, p. 341-349.
- Fiske, R.S., and Koyanagi, R.Y., 1968, The December 1965 eruption of Kilauea Volcano, Hawaii: U.S. Geological Survey Professional Paper, 607, 21 p.
- Furumoto, A.S., and Kovach, R.L., 1979, The Kalapana earthquake of November 29, 1975: an intraplate earthquake and its relation to geothermal processes: *Physics of the Earth and Planet Interiors*, v. 18, p. 197-208.
- Hill, D.P., 1977, A model for earthquake swarms: *Journal of Geophysical Research*, v. 82, p. 1347-1352.

- Jackson, D.B., Swanson, D.A., Koyanagi, R.Y., and Wright, T.L., 1975, The August and October 1968 east rift eruptions of Kilauea Volcano, Hawaii: U.S. Geological Survey Professional Paper 890, 33 p.
- Kinoshita, W.T., 1967, May 1963 earthquakes and deformation in the Koa'e fault zone, Kilauea Volcano, Hawaii: U.S. Geological Survey Professional Paper 575-C, p. C173-C176.
- Kinoshita, W.T., Koyanagi, R.Y., Wright, T.L., and Fiske, R.S., 1969, Kilauea Volcano: the 1967-1968 summit eruption: *Science*, v. 166, p. 459-468.
- Klein, F.W., 1978, Hypocenter location program HYPOINVERSE: U.S. Geological Survey Open-File Report 78-694, 113 p.
- 1981, A linear gradient crustal model for south Hawaii: *Bulletin of the Seismological Society of America*, v. 71, p. 1503-1510.
- 1982a, Earthquakes at Loihi submarine volcano, and the Hawaiian hot spot: *Journal of Geophysical Research*, v. 87, p. 7719-7726.
- 1982b, Patterns of historical eruptions at Hawaiian volcanoes: *Journal of Volcanology and Geothermal Research*, v. 12, p. 1-35.
- 1983, Users guide to QPLOT, an interactive computer plotting program for earthquake and geophysical data: U.S. Geological Survey Open-File Report 83-621, 40 p.
- 1984, Eruption forecasting at Kilauea Volcano, Hawaii: *Journal of Geophysical Research*, v. 89, p. 3059-3073.
- Klein, F.W., and Koyanagi, R.Y., 1980, Hawaiian volcano observatory seismic network history 1950-79: U.S. Geological Survey Open-File Report 80-302, 84 p.
- 1985, Earthquake map of south Hawaii 1968-1981: U.S. Geological Survey Miscellaneous Field Investigations Map I-1611, scale, 1:100,000.
- Koyanagi, R.Y., and Endo, E.T., 1971, Hawaiian seismic events during 1969: U.S. Geological Survey Professional Paper 750-C, p. C158-C164.
- Koyanagi, R.Y., Endo, E.T., and Ebisu, J.S., 1975, Reawakening of Mauna Loa Volcano, Hawaii: a preliminary evaluation of seismic evidence: *Geophysical Research Letters*, v. 2, p. 405-408.
- Koyanagi, R.Y., Endo, E.T., Tanigawa, W.R., Nakata, J.S., Tomori, A.H., and Tamura, P.N., 1984, Kaoiki, Hawaii earthquake of November 16, 1983: a preliminary compilation of seismographic data at the Hawaiian Volcano Observatory: U.S. Geological Survey Open-File Report 84-798, 6 p.
- Koyanagi, R.Y., Endo, E.T., and Ward, P.L., 1976b, Seismic activity on the Island of Hawaii, 1970-1973, in *The geophysics of the Pacific Ocean basin and its margin: American Geophysical Union Monograph 19*, p. 169-173.
- Koyanagi, R.Y., Nakata, J.S., and Tanigawa, W.R., 1981, Seismicity of the lower east rift zone of Kilauea Volcano, Hawaii, 1960-1980: U.S. Geological Survey Open-File Report 81-984, 15 p.
- Koyanagi, R.Y., Swanson, D.A., and Endo, E.T., 1972, Distribution of earthquakes related to mobility of the south flank of Kilauea Volcano, Hawaii: U.S. Geological Survey Professional Paper 800-D, p. D89-D97.
- Koyanagi, R.Y., Tanigawa, W.R., and Nakata, J.S., in press, Seismicity associated with the eruption of Kilauea Volcano from January 1983 to July 1984, in Wolfe, E.W., ed., *The Puu Oo eruption of Kilauea Volcano, Hawaii: the first 1 1/2 years*: U.S. Geological Survey Professional Paper.
- Koyanagi, R.Y., Unger, J.D., Endo, E.T., and Okamura, A.T., 1976a, Shallow earthquakes associated with inflation episodes at the summit of Kilauea Volcano, Hawaii: *Bulletin Volcanologique*, v. 39, p. 621-631.
- Liu, H-P., and Kosloff, D., 1978, Elastic-plastic bending of the lithosphere incorporating rock deformation data, with application to the structure of the Hawaiian Archipelago: *Tectonophysics*, v. 50, p. 249-274.
- Lipman, P.W., Lockwood, J.P., Okamura, R.T., Swanson, D.A., and Yamashita, K.M., 1985, Ground deformation associated with the 1975 magnitude-7.2 earthquake and resulting changes in activity of Kilauea Volcano, Hawaii: U.S. Geological Survey Professional Paper 1276, 45 p.
- Macdonald, G.A., 1956, The structure of Hawaiian volcanoes, *Koninklijk Nederlandsch Geologisch Mijnbouwkundig Geheeschap*, v. 16, p. 274-295.
- Mogi, K., 1962, Study of the elastic shocks caused by the fracture of heterogeneous materials and its relation to earthquake phenomena: *Bulletin of the Earthquake Research Institute of Tokyo University*, v. 40, p. 125-173.
- 1963, Some discussions on aftershocks, foreshocks, and earthquake swarms—the fracture of a semi-infinite body caused by an inner stress origin and its relation to the earthquake phenomena, 3: *Bulletin of the Earthquake Research Institute of Tokyo University*, v. 41, p. 615-658.
- Moore, J.G., and Koyanagi, R.Y., 1969, The October 1963 eruption of Kilauea Volcano, Hawaii: U.S. Geological Survey Professional Paper 614-C, p. C1-C14.
- Moore, R.B., Helz, R.T., Dzurisin, D., Eaton, G.P., Koyanagi, R.Y., Lipman, P.W., Lockwood, J.P., and Puniwai, G.S., 1980, The 1977 eruption of Kilauea Volcano, Hawaii: *Journal of Volcanology and Geothermal Research*, v. 7, p. 189-210.
- Nakamura, K., 1980, Why do long rift zones develop in Hawaiian volcanoes: a possible role of thick oceanic sediments (in Japanese with English abstract): *Bulletin of the Volcanological Society of Japan*, v. 25, no. 4, p. 255-269.
- 1981, Why do long rift zones develop better in Hawaiian volcanoes: a possible role of thick oceanic sediments: *Symposium on Oceanic Volcanism, International Association of Volcanology and Chemistry of the Earth's Interior, Azores University, 1980, Proceedings*.
- Nakata, J.S., Tanigawa, W.R., Klein, F.W., and Decker, R.W., 1982, Hawaiian Volcano Observatory Summary 81, Seismic data, January to December 1981: U.S. Geological Survey Hawaiian Volcano Observatory, Hawaii National Park.
- Pollard, D.D., Delaney, P.T., Duffield, W.A., Endo, E.T., and Okamura, A.T., 1983, Surface deformation in volcanic rift zones: *Tectonophysics*, v. 94, p. 541-584.
- Richter, C.F., 1958, *Elementary seismology*: W.H. Freeman, San Francisco, 768 p.
- Ryan, M.P., Blevins, J.Y.K., Okamura, A.T., and Koyanagi, R.Y., 1983, Magma reservoir subsidence mechanics: theoretical summary and application to Kilauea Volcano, Hawaii: *Journal of Geophysical Research*, v. 88, p. 4147-4181.
- Ryan, M.P., Koyanagi, R.Y., and Fiske, R.S., 1981, Modelling the three-dimensional structure of macroscopic magma transport systems: application to Kilauea Volcano, Hawaii: *Journal of Geophysical Research*, v. 86, p. 7111-7129.
- Shaw, H.R., 1980, The fracture mechanisms of magma transport from the mantle to the surface, in Hargraves, R.B., ed., *Physics of magmatic processes*: Princeton, Princeton University Press, p. 201-264.
- Swanson, D.A., 1972, Magma supply rate at Kilauea Volcano, 1952-1971: *Science*, v. 175, pp. 169-170.
- Swanson, D.A., Duffield, W.A., and Fiske, R.S., 1976a, Displacement of the south flank of Kilauea Volcano: the result of forceful intrusion of magma into the rift zones: U.S. Geological Survey Professional Paper 963, 39 p.
- Swanson, D.A., Duffield, W.A., Jackson, D.B., and Peterson, D.W., 1979, Chronological narrative of the 1969-71 Mauna Ulu eruption of Kilauea Volcano, Hawaii: U.S. Geological Survey Professional Paper 1056, 55p.
- Swanson, D.A., Jackson, D.B., Koyanagi, R.Y., and Wright, T.L., 1976b, The February 1969 east rift eruption of Kilauea Volcano, Hawaii: U.S. Geological Survey Professional Paper 891, 30 p.
- Thurber, C.H., Um, J.H., and Das, S., 1983, New ideas in seismic ray tracing and velocity inversion: applications to Kilauea Volcano, Hawaii [abs.]: *Eos, Transactions, American Geophysical Union*, v. 64, p. 901.
- Thurber, C.H., Karpin, T., and Um, J.H., 1984, Focal mechanisms of earthquakes at Kilauea Volcano: a detailed study [abs.]: *Eos, Transactions, American Geophysical Union*, v. 65, p. 1001.
- Thurber, C.H., 1984, Seismic detection of the summit magma complex of Kilauea Volcano, Hawaii: *Science*, v. 223, p. 165-167.
- Unger, J.D., and Koyanagi, R.Y., 1979, Evidence of the effects of shallow magma intrusion on Kilauea Volcano [abs.]: *Hawaii Symposium on Intraplate Volcanism and Submarine Volcanism, Hilo, Hawaii, July 1979*.
- Unger, J.D., and Ward, P.L., 1979, A large, deep Hawaiian earthquake—the Honoumuli, Hawaii event of April 26, 1973: *Bulletin of the Seismological Society of America*, v. 69, p. 1771-1781.

- Watts, A.B., and Cochran, J.R., 1974, Gravity anomalies and flexure of the lithosphere along the Hawaiian-Emperor Seamount Chain: *Geophysical Journal of the Royal Astronomical Society*, v. 38, pp. 119-141.
- Watts, A.B., ten Brink, U.S., Buhl, P., and Brocher, T.M., 1985, A multichannel seismic study of lithospheric flexure across the Hawaiian-Emperor Seamount Chain: *Nature*, v. 315, pp. 105-111.
- Wolfe, E.W., Neal, C.A., Banks, N.O., Duggan, T., and Ulrich, G., in press. Geologic observations and chronology of the first 20 episodes of the Puu Oo eruption, January 3, 1983 through June 8, 1984, in Wolfe, E. W., ed., *The Puu Oo eruption of Kilauea Volcano, Hawaii: the first 1½ years*: U.S. Geological Survey Professional Paper.
- Wright, T.L., and Kinoshita, W.T., 1968, March 1965 eruption of Kilauea Volcano and the formation of Makaopuhi lava lake: *Journal of Geophysical Research*, v. 73, p. 3181-3205.
- Wys, M., 1973, Towards a physical understanding of the earthquake frequency distribution: *Geophysical Journal of the Royal Astronomical Society*, v. 31, p. 341.
- Wys, M., Klein, F.W., and Johnston, A.C., 1981, Precursors to the Kalapana  $M=7.2$  earthquake: *Journal of Geophysical Research*, v. 86, p. 3881-3900.
- Zucca, J.J., and Hill, D.P., 1980, Crustal structure of the southeast flank of Kilauea volcano, Hawaii, from seismic refraction measurements: *Bulletin of the Seismological Society of America*, v. 70, p. 1149-1159.